Metatech

Meta-R-320

The Early-Time (E1) High-Altitude Electromagnetic Pulse (HEMP) and Its Impact on the U.S. Power Grid

Edward Savage
James Gilbert
William Radasky

Metatech Corporation
358 S. Fairview Ave., Suite E
Goleta, CA 93117

January 2010

Prepared for

Oak Ridge National Laboratory
Attn: Dr. Ben McConnell
1 Bethel Valley Road
P.O. Box 2008
Oak Ridge, Tennessee 37831
Subcontract 6400009137

FOREWORD

This report describes the threat of the early-time (E1) high-altitude electromagnetic pulse (HEMP) produced by nuclear detonations above an altitude of ~30 km. The report describes the mechanisms that create the E1 HEMP, the evidence for concern about this threat, and how it can impact the U.S. power grid. As the late-time (E3) part of the HEMP is considerably different in its frequency content and how it affects the power grid, this aspect will be discussed in another report.

This report is organized to provide an introduction to the report in Section 1, followed by an overview of E1 HEMP in Section 2. Section 3 then provides a brief history of E1 HEMP experience. Section 4 discusses in some detail how the E1 HEMP is generated for those who have more interest in the physics of the problem. Section 5 presents details concerning the coupling of these fields to extended lines, while Section 6 describes vulnerabilities of electronics to this threat. In Section 7 there is a detailed discussion of the main concerns of E1 HEMP on the U.S. power grid, and this section is crucial to set the stage to describe and recommend protection approaches and methods in the future. Section 8 follows with a brief discussion of potential impacts of large-scale power outages on society. Section 9 provides a bibliography highlighting some of the most important papers dealing with the E1 threat, standards to deal with the impacts of the threat, and recent publications produced for the EMP Commission and other groups related to the vulnerability of different aspects of the U.S. power system to electromagnetic threats. Finally, an appendix discusses some common E1 HEMP myths.

Table of Contents

Section **Page**

Section **Page**

Appendix **Page**

List of Figures

Figure **Page**

Figure ..... Page

Figure ..... Page

List of Tables

Table **Page**

Section 1
Introduction

This report discusses the threat and impacts of the early-time (E1) HEMP. This is the earliest part of HEMP (high altitude electromagnetic pulse, generated by an exoatmospheric nuclear burst), encompassing the part of the HEMP that runs out to about a microsecond. It has the highest amplitude in the HEMP waveform, and typically rises to that peak fast, often in a few nanoseconds. It is driven by the burst's gammas – very high energy photons, which are produced by nuclear reactions within the nuclear burst.

This discussion does not assume that the reader already has any EMP experience, so it starts at a very tutorial level. It also continues into more advance discussions, and some physics (engineering, etc.) background might be needed to fully appreciate all the details. Including all details, even simple ones, was done because, especially with the Internet, there is much erroneous EMP information available. Much of the best E1 HEMP material is not readily available, and much of what is easily available has inaccuracies. This is especially true for some of the E1 HEMP information on the Internet. For example, burst "yield" is often considered as the measure of a nuclear device, and correctly so for the blast and shock produced by a surface burst. For E1 HEMP the burst yield has much less significance. Maximum E1 HEMP levels on the ground do not correlate well with device yield.

E1 HEMP work has often been done within the classified environment. Two important reasons for this security are:

1. HEMP generation is intimately connected to significant design details of a nuclear weapon.
2. The work might directly, or indirectly, involve the vulnerability levels of U.S. military systems, and we do not want our enemies to know the HEMP levels to which our security forces are hardened.

E1 HEMP development is reflected in numerous government supported technical reports, and many are classified. However there is also much material in open literature, which is applied in this report.

The initial part of the report deals with E1 HEMP in general, and not exclusively with the effects on the electric power system. Toward the end of the report there are sections specifically dealing with the electric power system. Section 2 is an overview of E1 HEMP - an introduction to many aspects of it. Many of these subjects are then covered in more detail later. Section 3 is a very brief history of E1 HEMP work. Section 4 is a detailed look at the generation of E1 HEMP and the modeling of the process. This deals with the production of the electromagnetic (EM) field that propagates down towards the Earth's surface. Section 5 is about these EM fields "coupling" to conductors – generating voltages and currents. By far, it is these electrical signals that are the main concern for E1 HEMP effects. Section 6 discusses the adverse effects of E1 HEMP – usually from the voltages and currents either temporarily disrupting, or permanently damaging, systems. Section 7 considers possible failures of the electric power system from E1 HEMP. Failures might occur over a very wide area of the U.S., and there undoubtedly

could also be failures to other vital parts of the U.S. infrastructure. Section 8 considers such issues of widespread U.S. infrastructure failures. Section 9 provides a bibliography of E1 HEMP references. Finally, an appendix discusses some common misunderstandings about E1 HEMP.

In the past the Oak Ridge National Laboratory (ORNL) has looked at HEMP effects on the U.S. electric power system. Also, because of special safety concerns, HEMP effects of nuclear power plants were also studied. More recently, the EMP Commission looked into HEMP and the U.S. critical infrastructure, concluding that the electric power system is one of the most significant components that should be worried about. The U.S. military has taken E1 HEMP very seriously for a long time, including hardening and testing efforts. On the civilian side, the problems have not really been addressed. There has been a wide range in the perception of E1 HEMP as a threat. There are skeptics – those that think E1 HEMP does not exist, or that the models are wrong, or the field levels are not as bad as calculated. There are also those who believe we cannot do anything about it – if it happens we will just have to deal with it then. Then there are others that think every electronic device in the country will fail, and we will go back to the Stone Age. There are many such exaggerated scenarios; for example, it is doubtful that more than a very small fraction of vehicles will suddenly stop working – but how long will they be able to run with gasoline supply disruptions from possible electric power grid problems? And much of the open discussions of nuclear burst EM effects deal with E1 HEMP, as it has very large peak fields, and has often been what is meant by the term "HEMP". However, there are also other parts to HEMP, and E3 HEMP effects could be just as disastrous to the power grid, or even more so in some cases, than E1 HEMP.

Many perceptions of E1 HEMP effects, and the feeling that nothing can be done about E1 HEMP vulnerabilities, are also erroneous. Besides accounting for the unlikely chance of a HEMP event, efforts to protect against E1 HEMP effects also tend to have other benefits. There are other intense EM environments, such as lightning, and switching transients in electric substations, for which there is some overlap in protection methods. There is also a growing concern of "IEMI" (intentional electromagnetic interference), in which criminal or terrorist elements purposely generate high electromagnetic levels to cause upset or damage to the operation of electronics in a building or a substation.

It is noted that there are thousands of reports that have been produced in the United States on the topic of E1 HEMP over the past 40 years. It was not possible to reference every possible document of interest. Instead, in Section 9 at the end of this report there is a list of general HEMP references. That section also adds two additional lists of documents. The IEC (International Electrotechnical Commission) has published numerous HEMP related documents, some of which are listed in the first added list. In the second added list there are documents from the congressionally created "Commission to Assess the Threat to the United States from Electromagnetic Pulse (EMP) Attack" (the "EMP Commission") and also other organizations dealing with HEMP effects on power systems.

Section 2
An Overview of E1 HEMP

In this section we will briefly introduce many aspects about E1 HEMP. Some of it will introduce the subjects that are more thoroughly discussed later, while some will not be discussed further. This material should provide a good basic understanding of E1 HEMP, its effects, and possible protection. There are many subsections, some short and dealing with a very specific issue.

2.1 Historical Prospective

It was anticipated that a nuclear burst would generate electromagnetic signals, and possibly cause problems for electronic equipment. This proved to be true, and a whole range of EM effects from nuclear bursts were discovered and studied over many years. For E1 HEMP, initial hypotheses were inadequate, and actual signal levels proved to be much higher than anticipated. Adequate theories for E1 were not developed until after nuclear testing was moved underground. There has been extensive theoretical and experimental work on E1 HEMP, including from underground nuclear tests.

Besides work for critical military systems, there were also some early efforts for the telephone network – as seen by one of the first E1 HEMP specification waveforms coming from Bell Laboratories. However, in the competitive commercial environment it is understandable that such E1 HEMP hardening did not go forward. Studies were also done by ORNL for various aspects of E1 HEMP effects on the electric power system in the 1980's. While over the years interest in E1 HEMP tended to lessen in the U.S., recently it has increased worldwide. The recent efforts of the EMP Commission have shown a renewed sense that E1 HEMP should not be completely ignored by the civil infrastructure.

The only direct experience with E1 HEMP was in 1962, when the U.S. and USSR both experimented with a few high altitude nuclear bursts. For the U.S., the bursts were over the wide expanse of the sparsely populated South Pacific. The only real infrastructure was in Hawaii, very far away, and generally consisted of electronic tubes, and power grid relays that were bulky (and hardy) electromechanical devices. There were some upset and damage effects in Hawaii. The Russian experience, which was over land and more pertinent, was over a vast desert region, also with very antiquated infrastructure equipment. They did have damage associated with long lines (communications and power insulators), and also damage to diesel generators and radar systems. Now, more than half a century later, and after all the technical advances in our modern infrastructure (solid state electronics), it is certainty true to say that E1 HEMP is likely to be a bigger problem than it was in 1962.

2.2 E1 HEMP Environment

The term "environment" is generally used to refer to the basic signal generated by a nuclear explosion, irrespective of any system. Electromagnetic fields may be altered by objects, including a system itself. For E1 HEMP, the "E1 environment" usually also means that the ground reflection is ignored – it is just the incident EM signal (this will become clearer below). Including ground reflections greatly complicates the situation, including the need to specify what ground conductivity to use. (Later time HEMP cannot be discussed as an incident wave – those environments can only be given with reference to some assumed ground conductivity.)

E1 HEMP is an electromagnetic signal that is generated by a nuclear burst that explodes high above the Earth – generally said to be "above the atmosphere". The atmospheric density gradually decreases with altitude, and so often some approximate altitude is given, such as 30 km (18.6 miles). However, E1 HEMP does not really have a firm height-of-burst (HOB) limit, and there is still E1 HEMP generated for lower altitude bursts, although with lower field levels.

E1 HEMP is a fast narrow pulse, typically going up to high electromagnetic field levels not commonly seen from natural events. Figure 2-1 shows a generic waveform for a full HEMP signal – E1 HEMP is the "prompt gamma signal" part that lasts out to about a microsecond. The rest of the signal is much lower, but also much longer in time extent. Very generally, the bigger the system is (including its attached cables), the more that the wider, but lower level, later time HEMP signals could be a concern. The early part of E2 is actually an extension of E1, but at a much lower level, and typically not of much interest compared to E1. The rest of the HEMP signal types involve different mechanisms. These categories also cannot be specified without giving an assumed Earth conductivity.

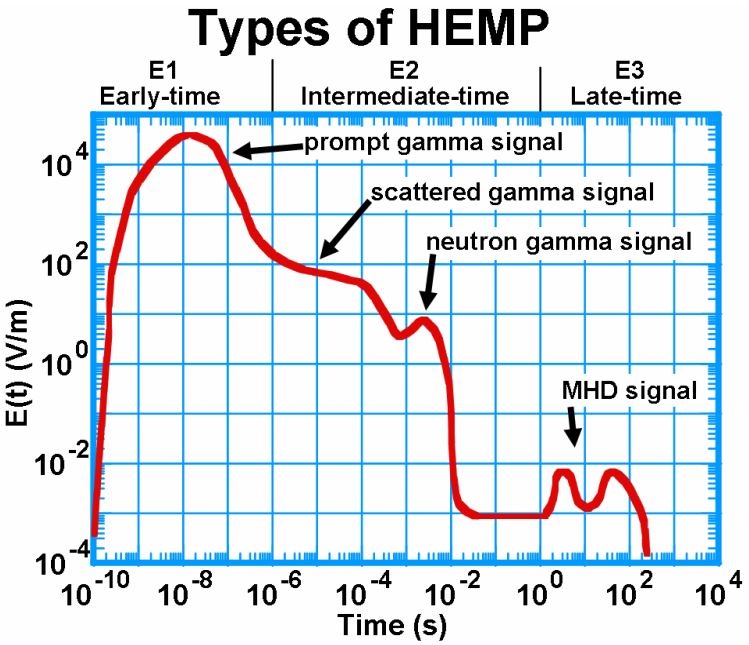

Figure 2-1. The various parts of a generic HEMP signal.

Figure 2-2 shows a general diagram of the E1 HEMP process. A nuclear burst puts out a fast pulse of gamma rays (like x rays, but with higher photon energies – about a few MeV). This thin shell of photons streams outward, including downward toward the Earth and its increasing air density. Once low enough in altitude, the gammas start striking air molecules, knocking electrons off. The Earth's magnetic field causes the electrons to turn coherently, and this constitutes an electric current, which generates an EM signal, much like the currents on a transmitting antenna. This EM field propagates downward as an EM wave – the E1 signal.

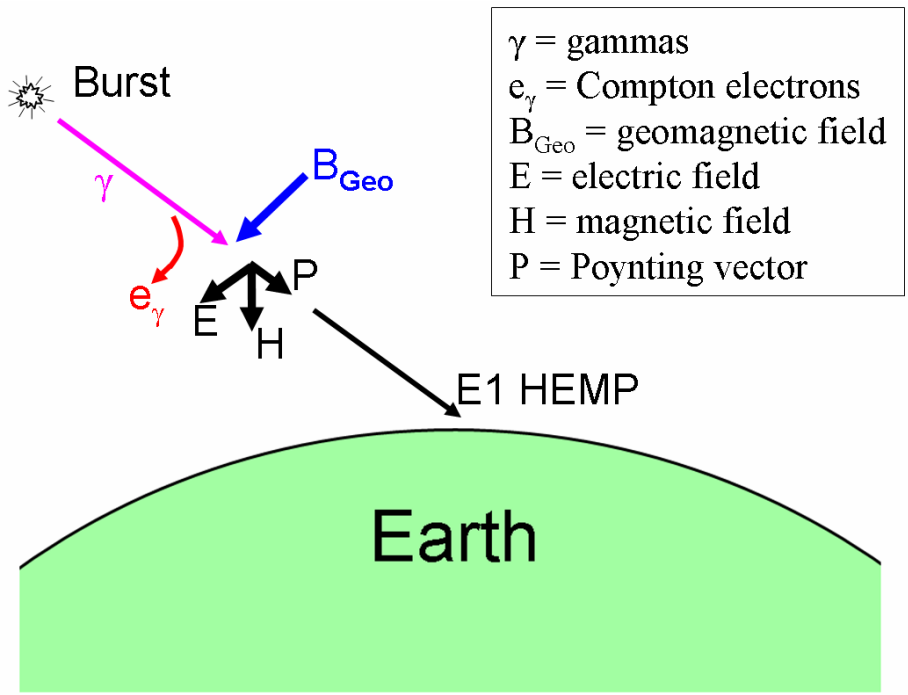

Figure 2-2. General basis of the E1 HEMP generation process. Gammas from the nuclear burst interact with the upper atmosphere – generating Compton electrons, which are turned in the Earth's geomagnetic field, and produce a transverse current that radiates an EM pulse towards the Earth.

The symbols shown in this figure will be seen in other figures in this report. Specifically, the EM wave has an electric field part "E", and a corresponding magnetic field part "H". For an E1 HEMP signal (and EM waves in general), these two terms are perpendicular to each other, and also to the direction of travel (the ray from the burst point to the observer on the Earth). The ray also represents the direction of the "Poynting" vector – giving power (and energy) flow (named after John H. Poynting, but also conveniently "pointing" in the direction of power flow). As shown in the figure, all three vectors are at right angles, and the "right-hand rule" applies: using the right hand, curve fingers in the direction from E to H, and then the thumb points in the direction of P.

The Earth's magnetic field is traditionally identified by a "B" instead of an "H". The symbol B is used for the magnetic flux density, and H is used for magnetic field intensity – these two are related by a material's permeability (which is often about the same as the value for vacuum).

Note that at the ground (Earth's surface), and up into the atmosphere where humans might be present (at least up to about 50,000 feet – 15 km, 9 miles) there is no weapon radiation – no radioactive particles, no gammas, no x rays, no neutrons, no betas (high energy electrons); just an EM signal, such as in our environment from radio, TV, and as produced by our cell phones.

Besides being very strong, the E1 HEMP signal coverage is also very widespread – out to the Earth's horizon as seen from the burst point. However, for a given weapon and burst location, the E1 HEMP that is seen varies with observer position on the Earth within the exposed region. Figure 2-3 shows a sample variation for the northern hemisphere. This plots the peak of the E field waveform at locations on the Earth (as a fraction of the highest peak seen for all locations). For an obvious reason, contour plots of peak E1 HEMP are often called "smile diagrams" (note the red "lips" with the choice of contour colors used in this example). Here the peak is slightly south of the "Ground Zero" (the point directly below the burst), and there is a low field point (centered on the "null point") north of Ground Zero. HEMP is governed by the Earth's magnetic field (geomagnetic field), and so the peak and null points are actually geomagnetically south and north from Ground Zero in the Northern Hemisphere. For E1 HEMP we typically mean geomagnetic, not geographic, directions in our discussions.

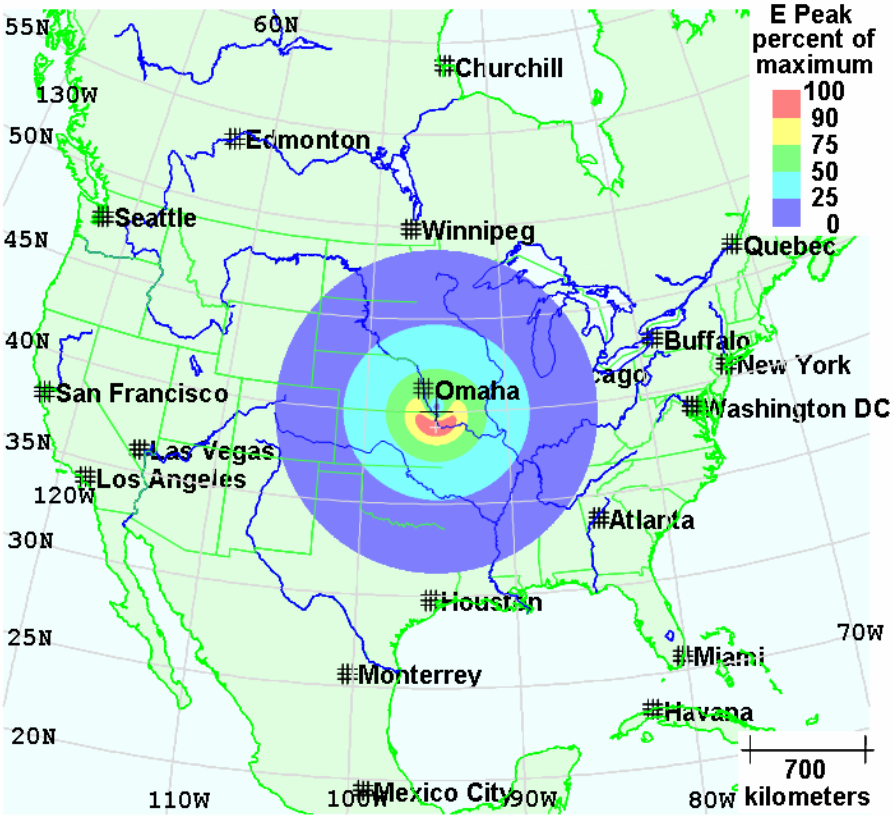

Figure 2-3. A sample E1 HEMP "smile" diagram. Such diagrams show contours of peak incident E levels, for a burst height of 75 km in this example. Here contour levels are shown as fractions of the biggest peak level (which is to the south of the burst point for this northern latitude burst). Over the exposed region, the average value is 10.4% of the maximum (12.4% if we use the square root of the average square of the peak instead).

Some of the variation shown in the smile diagram is due to the way the geomagnetic field comes into play in the E1 HEMP generation process. For example, the null point is were the ray from the burst to the observer is parallel to the geomagnetic field lines, while the maximum E1 HEMP point is near where the ray and geomagnetic field are at right angles. There is also an effect from the angle at which the burst-observer ray goes though the Earth's atmosphere. A ray that enters at a steep angle (the steepest being for GZ – straight down) tends to be higher, faster rising and falling, and possesses more high frequency content, than a ray that enters the atmosphere at a shallower angle (the shallowest being for the outer edges of the exposed region, for rays that are tangent to the Earth's surface).

E1 HEMP is generated by the gamma rays from a nuclear explosion. Table 2-1 shows a sample set of energy distribution for a high altitude nuclear explosion. (This is for the initial explosion of a high altitude burst. Vastly different values might be found for an air burst, in which energies get transferred to other forms over time – even a very short time.) It can be seen that the gammas are actually a very small fraction of the energy emitted. X rays represent most of the energy from the burst. X rays can play a part in E1 HEMP, but usually only as a limiting effect by producing air conductivity, decreasing the field levels; and then only for the small part of the x-ray output that is high-energy photons, while the vast majority of the x-ray energy is in the part of the spectrum with photons of much lower energy.

Table 2-1. Typical distribution of energy from a high altitude nuclear explosion. The gammas, which generate E1 HEMP, are a small fraction of the total energy.

Energy Fractions of Burst			
Type	Typical Percentage	Source	Typical particle energy
X rays (photons)	70	Atomic processes - electrons	10 keV
Kinetic energy	25	Thermal	-
Neutrons	1	Processes in Nucleus	0.01 – 15 MeV
Gammas (photons)	0.1	Nucleus	0.1 - 5 MeV

Energy distribution changes as time evolves, and with differences between surface bursts (in normal air density, such as near the Earth's surface) and exoatmospheric bursts (in the vacuum of space). A nuclear burst, in a very short time, releases energy as photons (gammas and x rays), neutrons (freed from the nucleus of atoms), betas (energetic electrons), and kinetic energy (atoms and molecules {reactions tend to break apart molecules} with very high velocities). These atoms and molecules are often ionized, having been stripped of many of their electrons. For an air burst, for example, the x rays will be absorbed close to the burst point, and the air will get extremely hot, radiating away light – especially much energy as UV.

2.3 Some Similar Effects

There are some other EM effects that have similarities to E1 HEMP, such as shown in Figure 2-4. Drawing "a" shows a radio transmitter. Current flows up and down the vertical antenna, generating an outward-going EM wave that the radio receiver demodulates into the transmitted music. In drawing "b" there is a lightning cloud-to-ground strike, with its vertical currents, which also sends out EM waves – possibly heard as crackling in the radio receiver (although a direct hit on the radio antenna would most likely damage the receiver, unless there was a very good lightning arrestor attached). In drawing "c" we see that E1 HEMP is also an EM wave – picked up by the radio, it might make a crackle or pop, or silence the radio by causing damage. The last EM example, drawing "d", shows IEMI – intentional electromagnetic interference. Here someone, for whatever sinister reason, sends out a strong EM signal, trying to disrupt or destroy some electronic system.

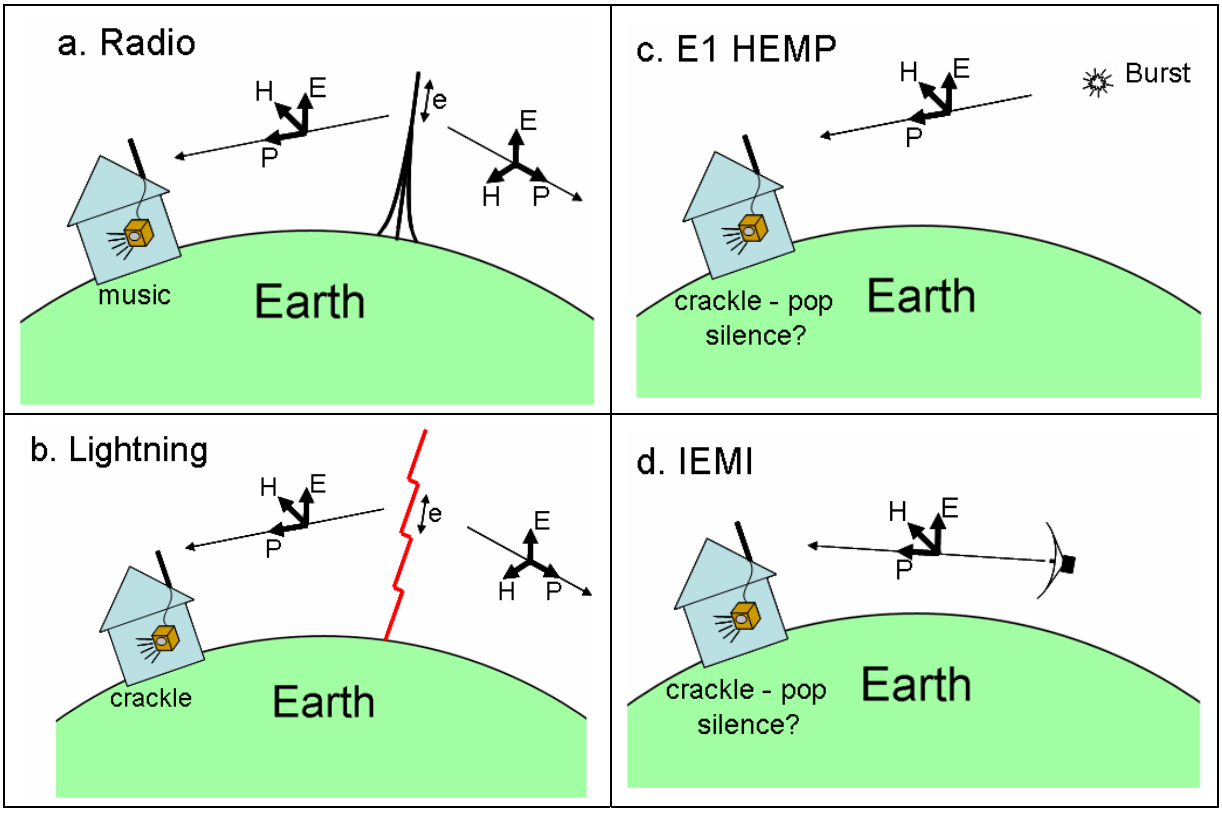

Figure 2-4. Some similar EM situations. In drawing "a" the AM radio antenna, using antenna currents produced by the transmitter, radiates an EM signal, which is picked up and demodulated to the music signal sent by the station. In "b" a lightning strike has vertical currents, which generate an EM interference signal (which also can be called a form of EMP, but not HEMP) that is heard as a crackle in the radio receiver. In drawing "c" an E1 HEMP, generated in the upper atmosphere, propagates down to the radio, where it is heard as some interference (such as a crackle or pop), and possibly silence, if the radio is damaged. In "d" a criminal uses a high power RF generator and antenna to disrupt or destroy electronic equipment, such as security devices in a robbery attempt or vital equipment in an extortion scheme.

Figure 2-5 shows an approximate spectral representation of various high-level EM environments, including lightning, E1 HEMP, and wideband and narrowband signals that include IEMI. We see that E1 HEMP dominates in the middle, from about one megahertz to several hundred megahertz. Normal EM noise ("EMI environments") and radio stations are shown below at the bottom of the chart.

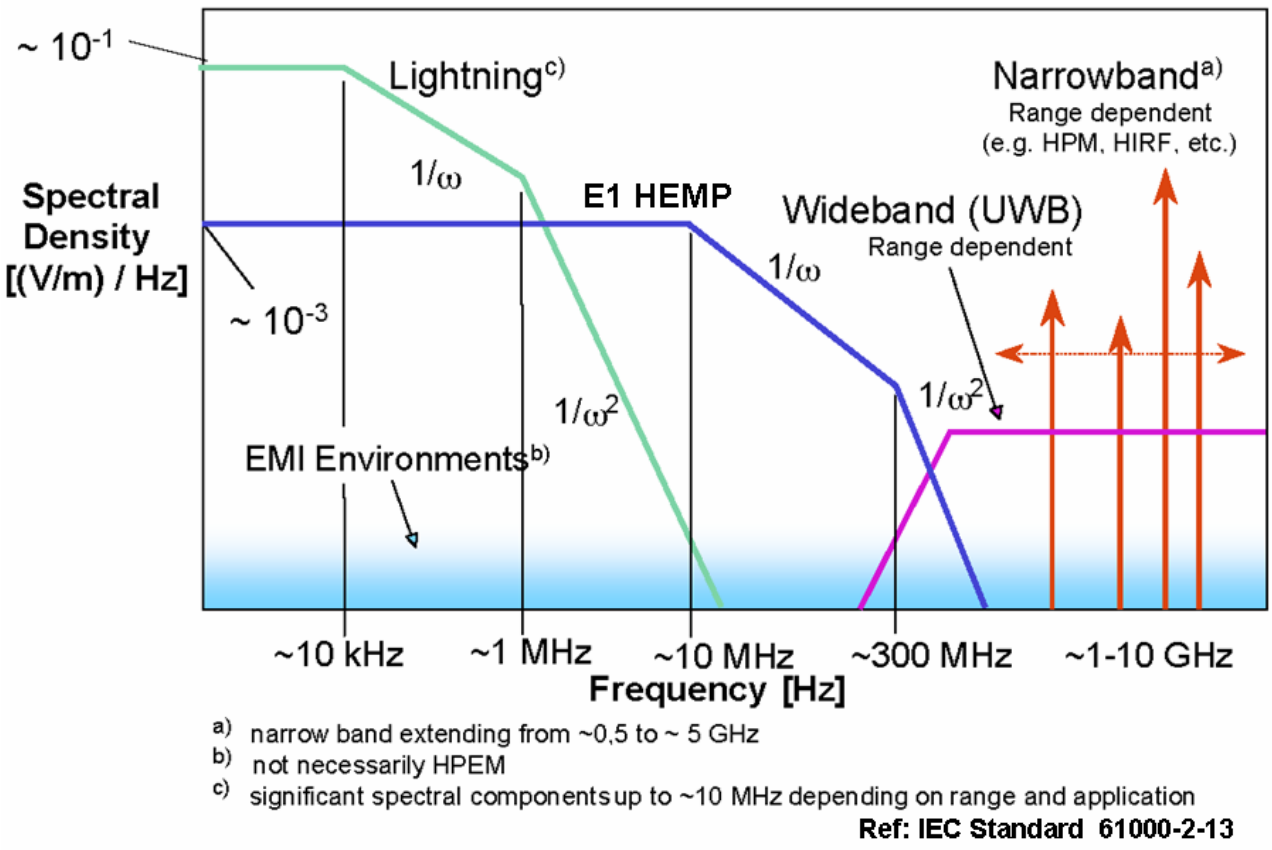

Figure 2-5. Approximate EM spectrums for various EM disturbances. E1 HEMP dominates in the range of about 1 MHz to several hundred MHz. IEMI is represented by the "Wideband" and "Narrowband" signals on the upper frequency (right) side.

2.4 Other Types of EMP

Traditionally "EMP" often refers to E1 HEMP, but it is not the only EM environment produced by a nuclear blast. Table 2-2 lists some other effects that are associated with nuclear blasts or high level EM. The term NEMP (nuclear EMP) is sometimes used to indicate a nuclear burst as the source. HEMP (high-altitude EMP) is also sometimes written with the "a" for "altitude" – HAEMP; or as HABEMP for "high-altitude burst" EMP. HEMP itself has various parts:

E1: early time HEMP; also called prompt gamma HEMP.

E2: intermediate time HEMP, consisting of E2A (scattered gamma HEMP) and E2B (neutron gamma HEMP).

E3: late time HEMP, also called MHD (magnetohydrodynamic) EMP; consisting of the E3A (blast wave) and E3B (heave) MHD.

DEMP (dispersed EMP) is an E1 HEMP signal that propagates back into outer space, either from being above the Earth's horizon, so missing the ground, or by reflecting off the ground. In going into outer space, it goes through the ionosphere, which distorts the HEMP pulse into a ringing signal.

For bursts within the atmosphere (not "high altitude") there would also be EM fields generated, but they tend to be small unless the burst is near the Earth's surface. SREMP is source region EMP, from a burst on or near the Earth's surface. In this case there would be other nuclear effects that might be of more concern, such as blast damage from the burst itself, but EM effects are of concern for hardened (such as buried) military systems.

SGEMP (system generated EMP) and IEMP (internal EMP) deal with EM effects associated with radiation interaction with a system itself. This can be gammas or x rays producing electrons by colliding with the system molecules. IEMP is a subclass of SGEMP, dealing with radiation penetrating into the interior of a system, where it generates EM fields; while SGEMP itself can also include the generation of fields outside the system, by electrons knocked off the outside. This may be taking place in vacuum, air, or some other gas for the "empty" spaces inside and outside (such as for a satellite or a missile outside the atmosphere).

Nuclear induced lightning (NIL) was observed in high-yield nuclear surface burst tests. This "lightning" was at the edge of the fireball, and so its high current would only be an issue for a hardened system – such as for an antenna connected to a buried system.

For all of the nuclear EM effects we have the disadvantage of a lack of real experience – our current infrastructure has not been exposed to nuclear effects, nor can we fully simulate all of the effects. The closest simulations were for SREMP, SGEMP and IEMP, with small systems in underground tests (when such tests were still being done). Also, there are some high-level gamma and x-ray test machines that, to varying degrees, can simulate nuclear environments for SREMP, SGEMP and IEMP. Some high level EM effects occur naturally, and we do experience them occasionally in our every-day environments. LEMP refers to the EM environment associated with standard lightning. Of course lightning is very common, especially so for certain parts of the world, and so there is real experience with the EM signals generated by lightning, and techniques to use to protect against lightning effects. ESD (electrostatic discharge) is a "mini-lightning", and it also has many similarities with lightning, except its target tends to be an internal system and very localized, such as the front panel of some machine, with its manual controls; while lightning environments are typically outside and more widespread. It should be noted that ESD provides much higher frequency content than lightning EM fields and therefore creates a real problem in modern electronic systems.

The last entry in the table is "TREE" – transient radiation effects on electronics. All the other effects involve only electromagnetics, and typically, coupling of voltages and currents to wires, which then might connect to a vulnerable electronic device. TREE instead introduces solid-state physics effects in solid-state electronics, with EM of little

concern. Solid state physics involves how transistors work – the "electronics" so prevalent in our modern lives. TREE is caused by nuclear particles (such as gammas, x rays, neutrons, alphas, or betas) striking the electronic device (usually only just of interest if the active region within the solid state substrate is affected). There can be instantaneous upset or damage, or long-term cumulative damage build-up.

Table 2-2. List of some types of EMP, and other related effects.

Types of EMP and Related Effects		
Acronym	Type	Description
EMP	electromagnetic pulse	Any electromagnetic transient signal, but typically used to refer to nuclear EMP, and often specifically early time high altitude EMP (E1 HEMP). The British used "radioflash" in the early days.
NEMP	nuclear EMP	As opposed to other, common EMPs, such as from lightning or ESD.
HEMP HAEMP	high altitude EMP	The burst is outside of the atmosphere, and the fields of interest are free field (propagating EM wave, with no induced air conductivity).
HABEMP	high altitude burst EMP	
E1	early time HEMP	The prompt gamma part of HEMP.
E2	intermediate time HEMP	The scattered gamma HEMP (E2A) and neutron gamma HEMP (E2B)
E2A	first part of E2	The scattered gamma HEMP; from gammas that have scattered (secondary gammas).
E2B	second part of E2	The neutron scatter gamma HEMP – from gammas created when weapon neutrons scatter from air molecules.
E3	late time HEMP	Also known as MHDEMP.
MHDEMP	magnetohydrodynamic EMP	The late-time, low level, part of HEMP (E3), produced by the deformation of the Earth's magnetic field (blast wave, E3A), and the rise of the hot burst debris in the Earth's magnetic field (heave, E3B).
DEMP	dispersed EMP	E1 HEMP that propagates up through the ionosphere (which distorts the pulse into ringing oscillations).
SREMP	source region EMP	The region of interest is close enough to the burst that the surrounding air becomes significantly conductive. The SREMP electric and magnetic fields do not have the simple impedance relationship of free space.

(Table 2-2 continued)

Types of EMP and Related Effects (continued)		
Acronym	Type	Description
SGEMP	system generated EMP	This EMP is driven by currents produced by the interaction of the burst's radiative particles with the structure of interest itself (as opposed to interactions with the air and ground, which produce SREMP fields). Because SREMP, when present, overshadows it, SGEMP is of most concern in the upper atmosphere (little air) for external fields, and inside systems (see IEMP).
IEMP	internal EMP	This is SGEMP produced inside a structure. Electrons emitted inside the structure, due to its interaction with the nuclear particles, create the currents and conductivity which produce internal electromagnetic energy – which has easier access to vulnerable electrical components.
NIL	nuclear induced lightning	For some surface burst nuclear tests there was lightning around the edge of the nuclear fireball – where only hardened buried structures would be expected to survive the blast anyway.
LEMP	lightning EMP	A direct lightning strike could put very high currents onto a system. Also, a nearby strike produces an EM propagating pulse. However, the spatial region exposed to high fields is limited.
ESD	electrostatic discharge	This is similar to a mini lightning strike – a direct discharge, created by a human, puts current onto the system, and propagating EM fields are generated.
HIRF	high intensity radiated fields	High level EM fields, such as from being close to a strong radar.
IEMI	intentional electromagnetic interference	This is intentional malicious generation of electromagnetic energy, so as to introduce noise or signals into electrical and electronic systems, and thus disrupt, confuse, or damage the systems for terrorist or criminal purposes.
HPM	high power microwave	Concerned with narrowband EM environments that involve high signal levels. This can include IEMI, and HIRF, for example.
TREE	transient radiation effects on electronics	This is generally not an EM field, but involves solid state physics effects of nuclear output particles (gamma, x ray, neutron, etc.) striking the active regions inside electronic devices, and causing upset or damage.

2.5 Parameters That Control E1 HEMP

To help understand E1 HEMP, it is useful to know what parameters have to be assigned values in order to make an E1 EMP calculation. Table 2-3 lists the parameters – the set is fairly short. They include characterization of the gamma and x-ray outputs for the burst. For the x rays it is only the high-energy ones that are important. The other parameters are geometry – placement of the burst and the observer.

Table 2-3. List of E1 HEMP input parameters. These parameters have to be given values in order to make an E1 HEMP environment calculation.

E1 HEMP Calculation Inputs		
Parameter Categories		Parameters
Weapon	Gammas	Time evolution of gamma emission spectrum
	High energy x rays	Time evolution of high-energy x-ray emission spectrum
Geometry	Burst location	Latitude, longitude, altitude
	Observer location	Latitude, longitude (altitude if aircraft)

First consider the geometry factors. The burst location has to be given: latitude, longitude, and altitude; and then the same location information for the observer. As a simplification, traditionally the observer has just been assumed to be at sea level – accounting for topology would typically be more of a complication than it would be worth for the small effect on the magnitude of the incident E1 HEMP. Thus, observer altitude is usually not a required input. However, if one is concerned with aircraft, then altitude could be high enough to be significant – including the fact that the exposed region is larger, because rays above the tangent can expose more air space. For this document on the electric power system, however, the observer altitude can be ignored.

The important aspects of geometry are:

1. Setting the intensity level – the $1/r^2$ spherical fall-off for the gammas to the source region, and for the EM wave power from there to the observer.
2. Setting the air density profile along the burst-observer ray. Shallower angles through the atmosphere (closer to tangent) mean lower, wider (and with less high frequency) pulses.
3. Setting the "source point" position, and so the geomagnetic field intensity and direction. The basic driver for E1 HEMP is given by the relative angle between the geomagnetic field lines and the burst-observer ray line (at the source points).
4. Determining the incident angle and polarization of the incident E1 HEMP at the observer point.

All the geometry calculations involve straight-forward geometry and vector formulas.

Gammas (more correctly, gamma rays) and x rays are both just photons – the same as other electromagnetic radiation (radio waves, visible light, infra-red, ultra-violet, etc.). Formally, gammas come from nuclear reactions (such as fission and fusion), while x rays

come from electron transitions in atoms. Typically, gammas have energies of several MeVs. Most of the burst output energy is in x-ray energy, but concentrated toward lower energies. (For an air burst, these x rays are quickly absorbed by the air, within a short distance, and they help generate the "fireball".) For E1 HEMP the interest is only in the high-energy tail of the x-ray spectrum – tens of keV (but then just to a much less extent than the interest in the gammas).

As noted in the table, for E1 HEMP calculations the gamma spectrum must be given, along with the time waveform of the gamma emission. It is often assumed that the time and spectral variations are independent – the shape of the spectrum is always the same, just the total emission varies with the given time waveform. However, generally the spectrum does change with time, and for the best quality calculations the input data should give a separate time waveform for each gamma energy in its spectrum data.

In the early days of E1 HEMP calculational efforts, the x rays tended to be ignored. Most of the x-ray output is at low energies, and they are easily absorbed by the atmosphere. However, there are some x rays at much higher energies, such as 10 keV or more. For these photons we need the same information as for the gammas – time evolution of the spectrum (a time waveform for each energy in the spectrum data).

Two factors are important for the x rays:

1. X rays contribute little to generating E1 HEMP (they do not add much to the current source); their effect is mostly in generating air conductivity. So they tend to lower the peak of the E1 HEMP.
2. The burst output x rays tend to be delayed relative to the gammas.

Thus, if we ignore the x rays, we could over-predict the E1 HEMP field level. As the E1 HEMP is rising up from the currents produced by the gammas, the air conductivity may suddenly increase from the x rays, and the E1 rise will be halted. Thus the E1 HEMP peak value can be affected by both the gamma rays and the x rays.

It is important to note what is <u>not</u> important for E1 HEMP:

1. Kinetic energy.
2. Neutron output.
3. Low energy x rays (most of the weapon output energy)
4. Device yield.

It should also be noted that device yield cannot even be used indirectly to calculate the E1 HEMP. It is not possible to calculate the needed gamma and x-ray parameters from a given value of yield. There can be variations from one weapon design to the next in terms of the gamma and high energy x-ray parameters that are important for E1 HEMP.

Some EMP calculations, such as source region EMP, need weather parameters – air density and water vapor content (from the humidity and temperature). These, especially considering large possible variations in water vapor content, affect the air chemistry (air conductivity) significantly. However, at very high altitudes these are not very important – there is not as much "weather" variation, and the water vapor content is very low.

2.6 HOB Variation

Note that the burst is described as being exoatmospheric – above the atmosphere. Except for various effects that can occur on satellites and very long range communications, the nuclear burst may not produce any other effects on man except through its HEMP. There is no exact criterion for HOB (height of burst) that qualifies for HEMP; however HEMP varies with HOB, as shown by the sample results in Figure 2-6. The average result (violet line) is averaged over the full exposed region, which is larger for higher HOB. For each weapon there is an optimum burst height to produce the maximum peak HEMP E field – usually somewhat less than 100 km. As one goes lower in HOB, the peak HEMP E eventually falls, and starts falling significantly when the burst locations gets into the atmosphere – typically we might ignore E1 HEMP when the HOB gets below about 20 km (again, an approximate altitude). Going to altitudes above the peak HOB, the peak HEMP E falls gradually, so that there might be some E1 HEMP when the burst is greater than many multiples of 100 km. Again, the exact details of the HOB variation (and other variations, such as with observer position) depend on the burst (the weapon parameters).

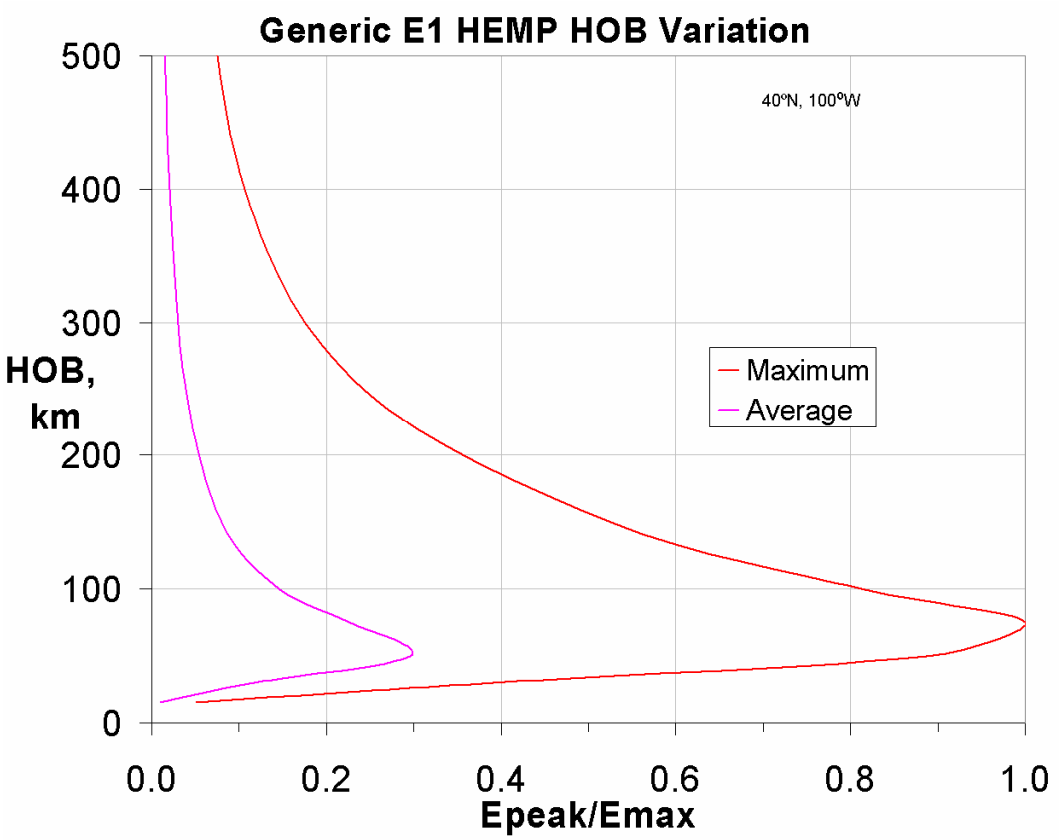

Figure 2-6. Sample E1 HEMP HOB variation. This shows the HOB variation, for a typical device, for the highest E1 peak seen over the full exposed region (red line), and for the average E1 Peak – averaged over all the exposed area. The E1 peak levels are plotted as a fraction of the absolute maximum E1 HEMP for all burst heights (it occurs about HOB=75 km in this case).

2.7 Exposed Region

However, besides the variation of the maximum E peak with HOB, there is also a variation in the area coverage – the amount of the Earth's surface that is exposed to the E1 HEMP. This is simply determined by geometry – a given point on the Earth will be illuminated by E1 HEMP if it is within line-of-sight of the burst location. (For such determinations, for simplicity, the Earth is usually just assumed to be a sphere, ignoring topography and the Earth's slight ellipsoid shape.) Figure 2-7 plots the radius of the exposed region versus burst height, and Figure 2-8 plots the area. Figure 2-9 shows area coverage for a burst over the U.S., for several burst heights.

As can be seen, a very large area is exposed to the E1 HEMP. Going higher (HOB higher) increases the area coverage, however, note that the ground range increase is sub-linear with HOB – the area coverage is approximately linear in burst height. Also, the E1 HEMP strength tends to have its maximum for HOBs below 100 km, and so above that the extra area coverage for higher HOB comes at the expense of lower field levels.

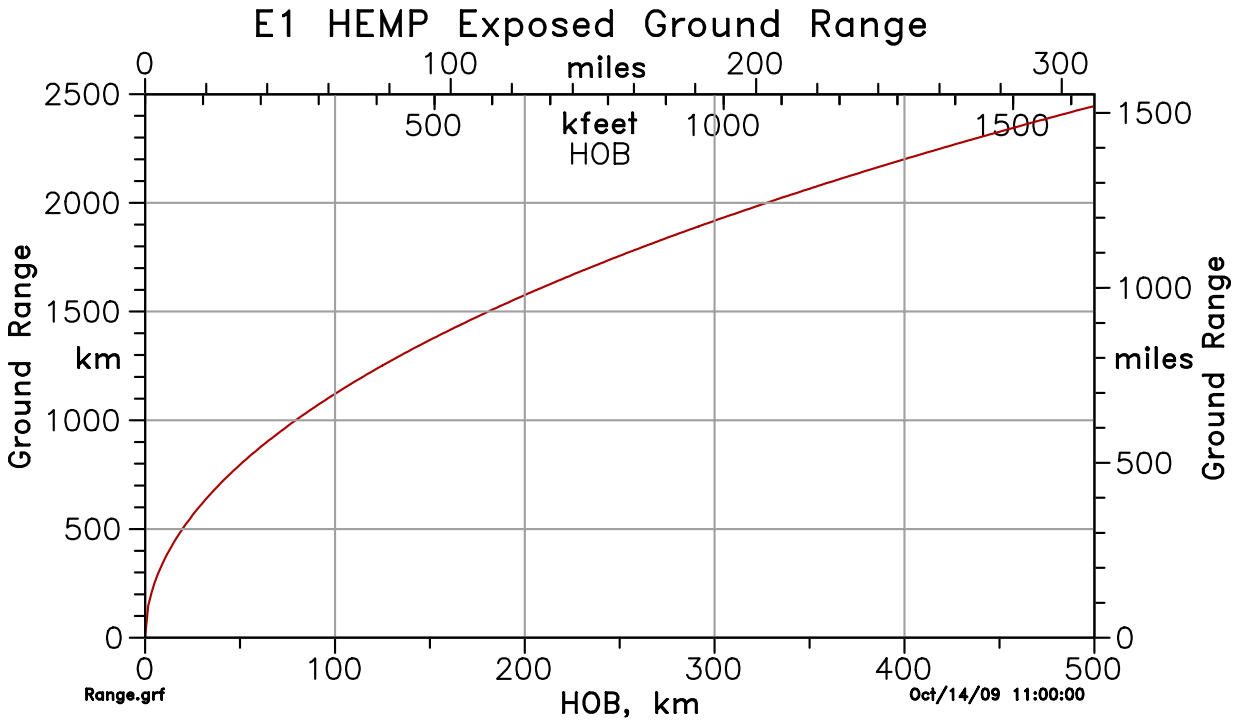

Figure 2-7. Radius of the E1 HEMP exposed region on the Earth versus the burst height.

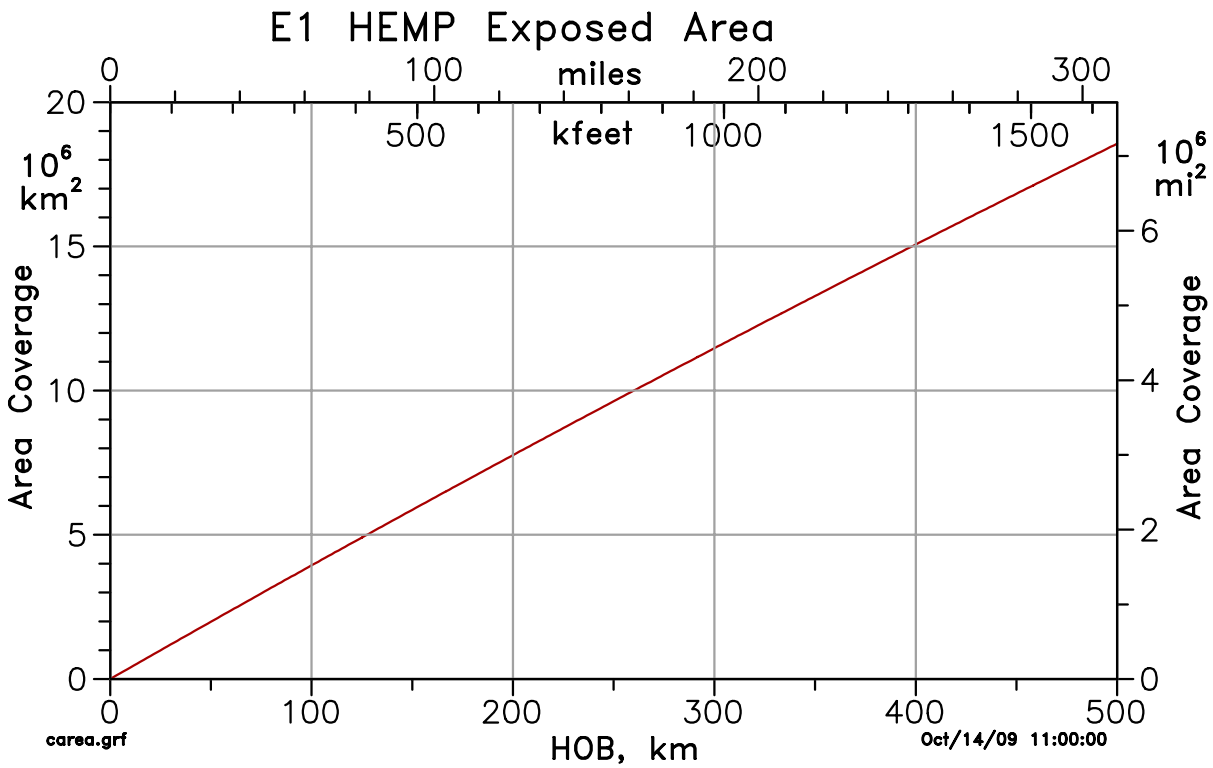

Figure 2-8. E1 HEMP exposed region area versus burst height. The area is given in million of square kilometers (left axis) or square miles (right axis). The continental U.S. has an area of about 8.0 million square kilometers (3.1 million square miles).

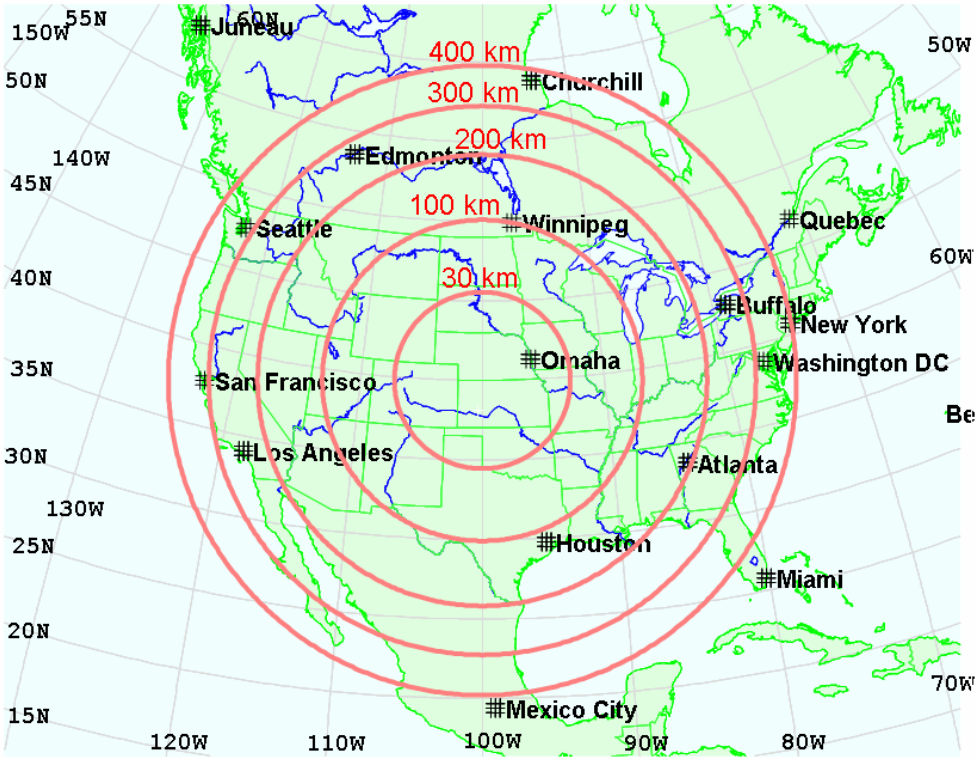

Figure 2-9. Samples of E1 HEMP exposed regions for several heights. The red circles show the exposed regions for the given burst heights, for a nuclear burst over the central U.S.

2.8 E1 HEMP Geometry Features

There are a few common geometric features for a "smile" diagram. Figure 2-10 shows a north-south cut cross-section through a burst point in the northern hemisphere (all results shown in this report are for the northern geomagnetic hemisphere, and many results are shown for a burst over the central U.S.). The view is from the west, looking east, with the north to the left and the south to the right. This figure shows the three special points, and the tangents. The rays originating at the burst and that are tangent to the Earth's surface define the maximum extent of the E1 HEMP exposure region, as discussed in the previous subsection.

Ground Zero (GZ) is the point directly below the burst – the observer ray goes straight down. This is the center of the smile diagram. Also, often observer points are located in terms of "ground range" – this is the distance, along the Earth's surface, from GZ to the observer (a full location determination would then also require the observer's azimuthal angle, such as measured clockwise from the north direction).

The red region in the atmosphere is the "source region" – its boundary depends on how we want to define it, but could be assumed to be, for example, the region between 20 and 40 km in altitude. The GZ ray goes through the source region most directly, and for the tangent point the ray is more oblique, taking a longer path in going through the source region layer. (We can also see that the spherical divergence effect – $1/r^2$ fall off – means the level of the gammas reaching the source region is less as we go out from the GZ point.)

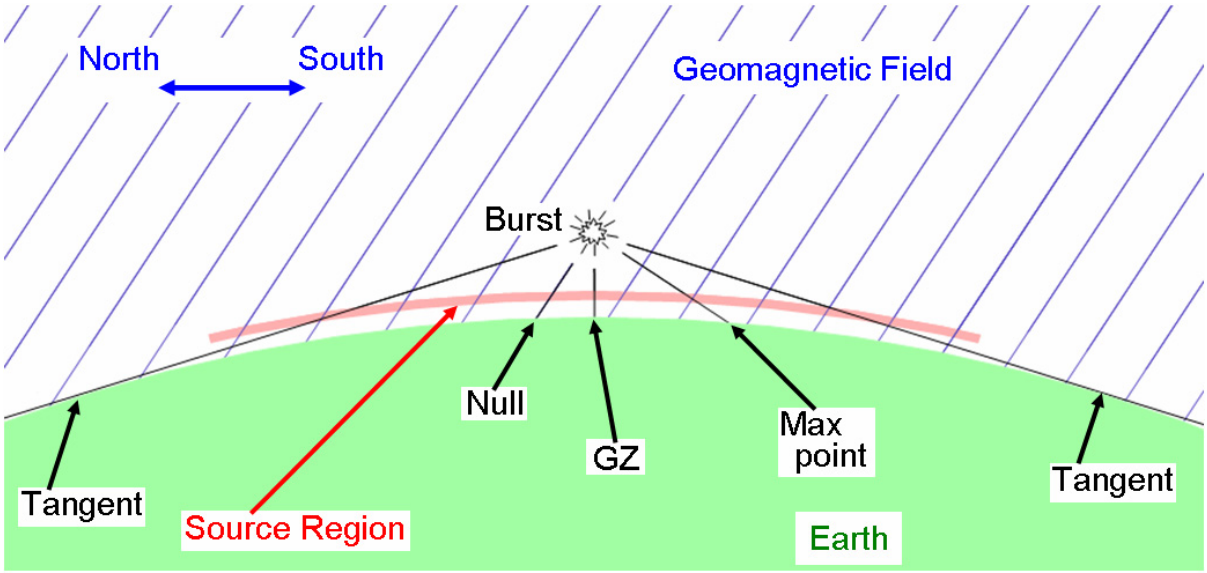

Figure 2-10. Explanation of smile diagram variation along the center north/south line. This is a cut through the center, with north to the left, and south to the right, for a northern hemisphere burst. (For the southern hemisphere the null point is on the south, and the max point to the north.)

The bottom edge of the source region could be defined relative to the "breakaway point". On the ray from the burst to the observer, the level of the gammas decrease along its path through the source region, and the level of the E1 HEMP increases. At some point the gammas are too weak to contribute much more to increasing the level of the E1 HEMP, nor to generated high enough air conductivity to erode away much of the E1 HEMP field. This is essentially the bottom edge of the source region. This is called the breakaway point – for points further down the ray the E1 HEMP is now a free wave, with no more effects from the sources and conductivities of the source region. This is really an arbitrary point, because the gamma effects do not suddenly stop at any point, but decrease smoothly (but sharply) with increasing air density. Often some criterion is used to define breakaway, such as the condition

$$\frac{\sigma}{d\sigma/dz} < \frac{2}{Z_o \sigma} \qquad \left(\text{the right hand side is an approximation to } \frac{E}{dE/dz} \text{ in conductive air} \right)$$

where σ is the air conductivity, E is the electric field (both vary with time), and Z_o is the impedance of free space (about 376.7 ohms). (The right hand side is the attenuation distance of EM waves for $\sigma \ll \omega\varepsilon_o$.) This condition says that the conductivity is falling faster (relatively) with lower altitude than the relative fall in the E field due to conductivity. Generally we would want to take any E1 HEMP calculations to slightly lower altitudes. (Although often a simpler lower altitude criterion is used – assuming the bottom of the source region has been hit when the calculated rE product, E times distance from the burst, did not change significantly from the previous calculational position.)

The other two special positions in Figure 2-10 are related to the geomagnetic field. The "null point" is where the observer ray and geomagnetic field lines are parallel. For this point the E1 HEMP is very low (ideally it would be zero). On the opposite side of GZ is the "max field point" (or "max point" for short). This term has been used to name the location on the smile diagram where the E1 HEMP has its maximum peak level. There are two effects involved in this – one is that the most direct rays through the atmosphere generally produce the highest E1 levels, and so this would favor the GZ ray. However, the second effect is the angle at which the observer ray crosses the geomagnetic field lines – favoring the point at which they are at right angles. This point could be called the "geomagnetic max point". Note that the max field point depends on both the device and geometry, while the geomagnetic max point only depends on geometry.

For the northern hemisphere, generally the max field point is a little north of the geomagnetic max point – pulled away from the point of being at right angle to B_{Geo} by the better angle through the atmosphere nearer to GZ. However, there is a third effect that also sometimes comes into play. This involves the breakaway point. For very large gamma outputs and very lower burst heights, the breakaway altitude may be pushed very low, especially for straight down rays. At such low altitudes the Compton electrons have shorter life times, thus less turning in the geomagnetic field and so less total source current to generate the E1 HEMP. Thus, for such cases (large gamma output, very low HOB), the atmosphere angle variation might not be best straight down – there it might actually be significantly suppressed. In that case the max field point might vary from the

usual position of being a little north of the geomagnetic max point, and actually be south of the geomagnetic max point, especially for lower geomagnetic latitudes.

Note that for this report we will often mean "geomagnetic max point" when we use the "max point" term. The geomagnetic max point depends only on the geometry – the burst location (latitude, longitude, and height) – while the actual maximum field point, typically slightly to the south of GZ for a northern hemisphere burst, also depends on the characteristics of the nuclear explosion, and so varies from weapon to weapon.

Figure 2-11 shows two plots – it gives the ground range from GZ to the null point (on the left) and geomagnetic max point (on the right) versus HOB (burst height), for various geomagnetic latitudes. (For example the position 40°N, 100°W, in the central U.S., has a geomagnetic dip angle of 67.55°, and geomagnetic latitude of about 50.43°N.) Different horizontal axis scalings are used for the two sides of the figure. The solid green line (to the left on both sides of the plot) is for the 10°N geomagnetic latitude positions, and then higher latitudes (closer to the geomagnetic poles) lines are to the right, up to the dashed red line for 80°N. The null point is always near GZ – the farthest it is away is for a burst near the equator. As seen, it is about 700 km away from GZ, out of the maximum E1 radius of about 2400 km, for a 500 km HOB. (The blue line on the right side gives the tangent ground range.) For the geomagnetic max point the variation is the opposite – the maximum range from GZ is for the higher latitudes; and it gets so far out that for the 75°N and 80°N cases the max point gets out to the tangent point and beyond for higher burst heights (the red lines go out to the blue line).

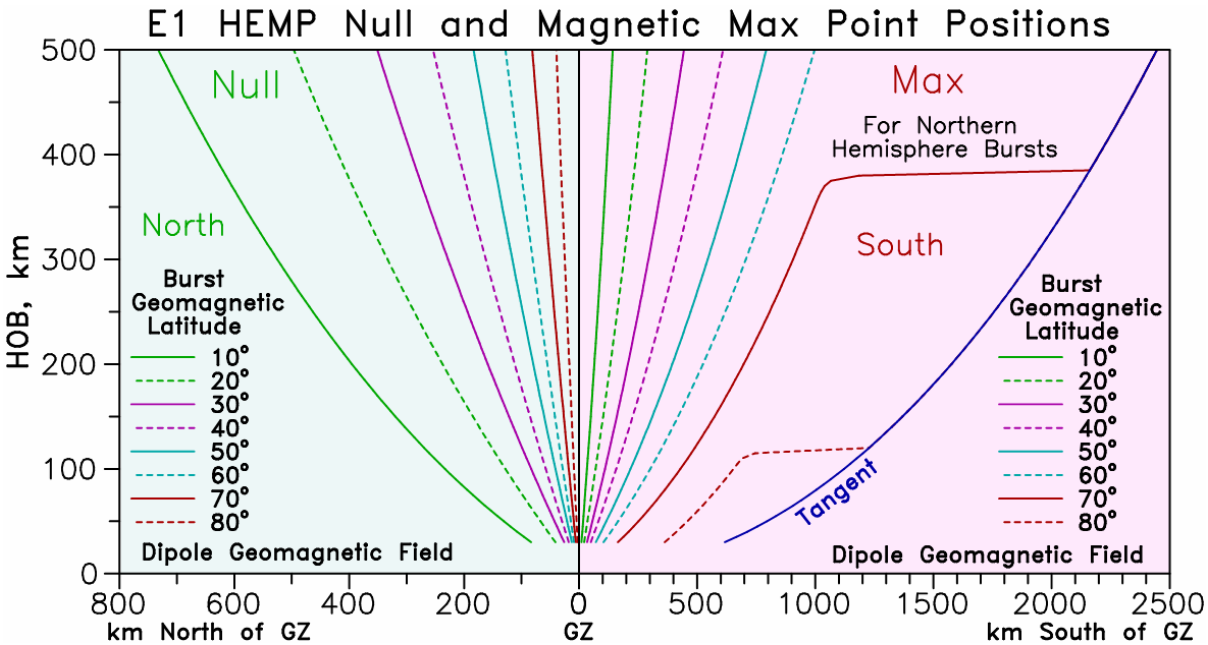

Figure 2-11. Positions of two special E1 HEMP points versus burst height. The position of the null point is on the left side of plot, and the geomagnetic max point is on the right side of plot (different x axis scalings are used in the two sides). This is for an ideal dipole model of the Earth's geomagnetic field. The lines are for 10° increments in geomagnetic latitude (solid green for 10° above the equator, up to dashed red for 80°, which is 10° from the magnetic pole).

2.9 Incident and Total E1 HEMP Environments

Traditionally HEMP is given as the E field in the pulse that is traveling down to the Earth – the incident E field. Some effects are ignored, such as the elevation of the Earth surface at the observation point (the local topography), or small observer heights off the ground. (For aircraft at high altitudes, it is easy to account for the 1/r fall-off in E field to go back to an observer point that is far off the ground). A simple spherical Earth is generally assumed, and the incident field at sea level is given.

Also, very localized conditions are not accounted for in smile diagrams and typical HEMP calculations. For example, for points near the tangent, the shadowing effect of being in a deep canyon is not included. And there could be reflection effects, such as being near the side of a very large metal building. Also, long conductors – power lines, fences, railroad rails – can collect EM energy, and so enhance the HEMP for observers nearby. These are all ignored, generally because they are considered highly variable, or too random to include in a large area display such as a smile diagram. They are considered in performing detailed localized coupling calculations.

Some effects can be calculated, if the HEMP environment is known. For example, to go a step beyond the typical calculation of the HEMP, the reflection off the Earth surface can be accounted for. Consider an incident E1 HEMP, as shown in Figure 2-12. The plane perpendicular to the incident ray is shown (it tilts forward, as required by the downward angle of the ray). The E1 E field (and H field) must be in this plane – we have separated the E field into two terms, also in this plane. The transverse electric "TE" term is horizontal, the transverse magnetic "TM" term is normal to this, and "upward" – but it has a forward tilt corresponding to the plane's tilt. Figure 2-13 shows a side view of this, for an observer position that is a small distance "h" above the ground. The incident wave is on the left, and the reflected on the right. Note that the horizontal terms (TE and TM_{Horz}) change signs on reflecting, while the vertical term (TM_{Vert}) does not.

At the observer point the incident pulse will be seen, and then that pulse will go down to the surface and then back up, so that the observer will also see a reflected pulse. (We ignore the very slight difference in horizontal positions that goes with these two pulses – E1 HEMP does not vary over such small horizontal distances.) However, because of the signs of the reflections for each component, the reflected vertical component will add to the incident pulse, while the other components (horizontal) will tend to cancel the incident pulse. The time delay for the reflection is

$$\Delta = \frac{2h}{c}\cos\theta$$

where "c" is the speed of light, "h" is the observer height above the ground, and θ is the incident ray angle from vertical. For several meter heights this offset time may be on the order of 10 nanoseconds (with large variation, depending on height and ground range from ground zero). Typical E1 HEMP pulses are tens of nanoseconds wide, so the reflection pulse comes back well within the time that the incident pulse is still present. The shorter the offset time (smaller observer height or closer to the tangent of the

exposed region), the more the total field seen is that of doubling the incident vertical field and canceling (zeroing out) the horizontal field.

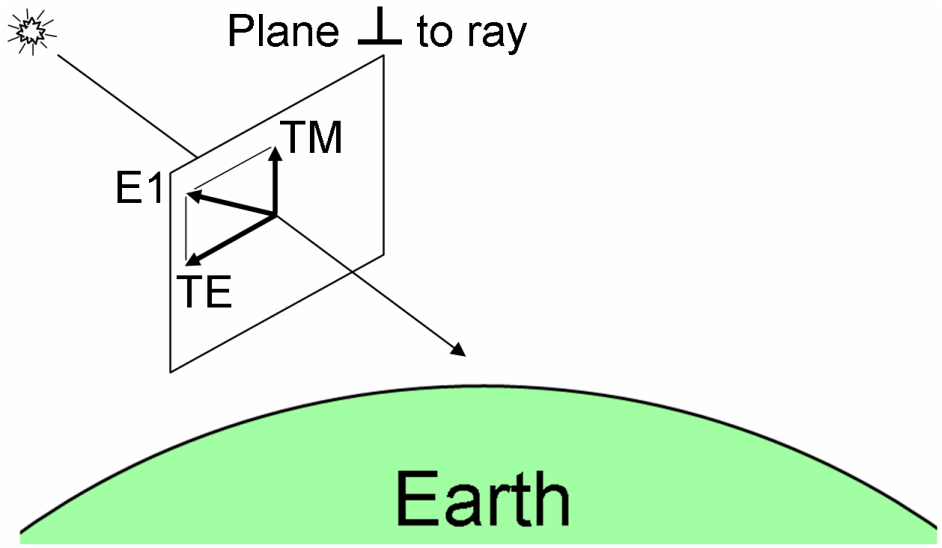

Figure 2-12. Decomposing an incident E1 HEMP into two E field terms for reflection. E1 can be decomposed into the part with the E field horizontal and to the side (TE), and the other part (TM), which is upward in the plane perpendicular to the burst-observer ray. (This field orientation is appropriate for a westward ray.)

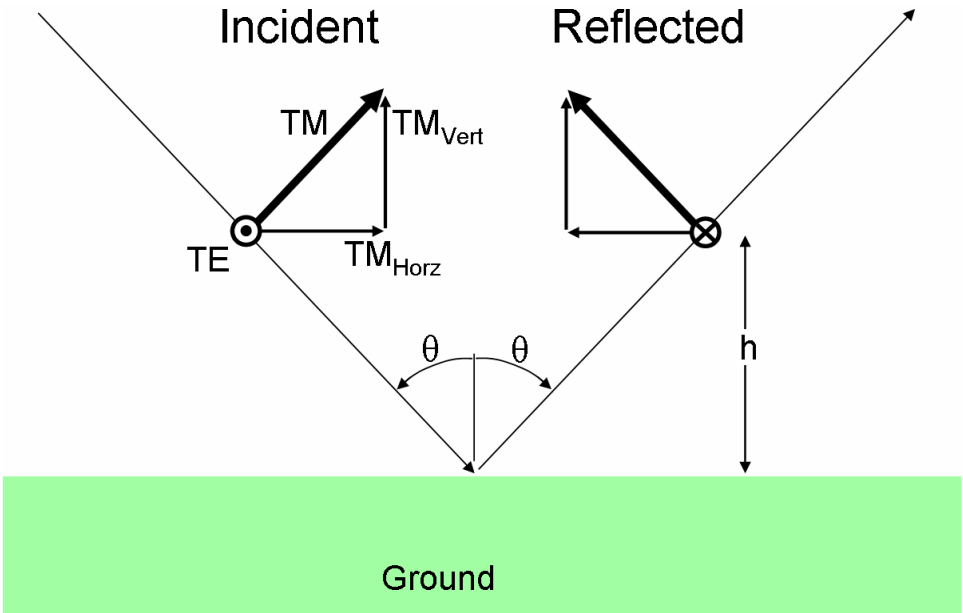

Figure 2-13. E1 HEMP Earth reflection. In this example the Earth is considered to be a perfect conductor.

The previous discussion was for a perfect conductor, while the real Earth is not perfect. The higher the conductivity, the more perfect it is. The calculation of reflections for imperfect ground is straight forward, but more complex. The reflection coefficients for the three terms all become functions of frequency, and an E1 HEMP's frequency content is very wide. As an approximation for picturing this, we can think of skin depth, defined as

$$\delta = \sqrt{\frac{1}{\pi \sigma f \mu}} \quad .$$

In simple terms, this is the distance that an EM wave of frequency "f" penetrates into a ground of conductivity "σ" (and permeability "μ", but this typically does not vary much from place to place). We can think of the reflection point not being at the Earth's surface, but further down into the ground, as given by the skin depth. Note however that the lower the frequency component, the further down the reflection surface is. Thus, the total field is very complex. (This skin depth effect is also why E1 reflections deal mostly with the soil near the Earth's surface, while the E3 HEMP is concerned with the conductivity much deeper into the Earth.)

As noted, E1 HEMP has a very wide range of frequencies (this will be shown shortly). The parameters that govern the EM response of soil tend to also vary significantly with frequency. As frequency increases, the conductivity increases, and the permittivity decreases. This further complicates the reflection process. To account for this there has to be data available for the frequency dependence of soil, and we would expect this to vary with soil type. Another complication is that for many soils, the water content has a very significant effect on its parameter values, so it may depend upon what the recent weather has been. For some EMP studies a "universal soil" model has often been used, in which the water content is a single variable that roughly determines the soil frequency variations.

Besides the reflection from a flat, homogeneous ground surface, there may be other objects that cause reflections, or other electromagnetic effects that might affect the total E1 HEMP signal seen at a point. This includes reflection from nearby buildings, for example. Also, long conductors can be important (a fence, railroad, or power line) if nearby, because the E1 HEMP can cause large currents to flow, and there are EM fields associated with such large coupled currents.

2.10 Generic E1 HEMP Environment

A given set of input parameters, including time waveforms for the burst outputs, will produce a specific E1 HEMP waveform. Typically such waveforms rise up quickly, and then fall somewhat slower. Many such E1 HEMP waveforms that have been calculated from computer models, and many generic E1 HEMP standard waveforms have been created. They are attempts to capture the characteristics of E1 HEMP waveforms, in general, in a convenient analytic form. Besides the waveform used, they generally also specify the signal amplitude. Because of "saturation" (the fact that induced air conductivity limits the growth in the E1 HEMP amplitude) it makes some sense to have a single amplitude level. However, this can also be done because the specified waveform is typically meant to be worse case – the highest peak signal that is likely to be observed. We have also mentioned that the waveshape is faster and narrower near ground zero, and becomes slower and wider out near the tangent. Thus, one waveform cannot represent such a range of shapes, and some compromise must be applied. Several approaches may

be used. Since the highest peaks are associated with close-in observers, the fast pulse might be emphasized. Or the rise time may be set by the fast pulse, and the width set by the slow pulse. This might be considered as "drawing an envelope around all possible pulses".

Often an E1 HEMP specification also gives a frequency spectrum (Fourier transform). This might simply be the transform of the given waveform. However, again there is some variation in spectra – with near-in points going farther out to higher frequencies, but points farther out toward the tangent having more low frequency energy. So another approach is to have a frequency specification that is unconnected to the given waveform – one approach is to use an envelope of all possible spectra.

Most generic E1 HEMP waveforms use one of these two forms

$$e^{-\beta t} - e^{-\alpha t}$$

or

$$\frac{1}{e^{\beta t} + e^{-\alpha t}}$$

with an appropriate provision for when to start the waveform. The first equation naturally starts at zero time, where it has the value of zero. The second equation never goes to zero, and we have to pick some arbitrary time point at which we say the E1 HEMP waveform starts. The α sets the pulse rise, and β the fall.

One generic waveform is given by the IEC ("Electromagnetic compatibility (EMC) – Part 2: Environment – Section 9: Description of HEMP environment – Radiated disturbance, Basic EMC publication", IEC 61000-2-9, February 1996, International Electrotechnical Commission, Geneva, Switzerland):

$$E_1(t) = \begin{cases} 0 & t \le 0 \\ E_{01} k_1 \left(e^{-b_1 t} - e^{-a_1 t} \right) & t > 0 \end{cases}$$

$$E_{01} = 50{,}000 \text{ V/m}$$

$$k_1 = \left(\frac{a_1}{a_1 - b_1} \right) \left(\frac{a_1}{b_1} \right)^{\left(\frac{b_1}{a_1 - b_1} \right)} = 1.3$$

$$a_1 = 6 \times 10^8 \text{ s}^{-1}$$

$$b_1 = 4 \times 10^7 \text{ s}^{-1}$$

with spectrum

$$E_1(\omega) = \int_{-\infty}^{+\infty} E_1(t) e^{-j\omega t} dt = E_{01} k_1 \frac{a_1 - b_1}{(a_1 + j\omega)(b_1 + j\omega)} \quad .$$

We will shortly show plots of these.

Table 2-4 summarizes some characteristics of this generic E1 HEMP signal. By construction, is has a peak of 50 kV/m. The peak power is very high, but the total energy (approximately peak power times pulse width) is modest. The pulse rises in a few nanoseconds, and has a pulse width of about 23 nanoseconds. The spectrum extends well above 100 MHz.

Table 2-4. Characteristics of the IEC E1 HEMP waveform.

IEC E1 HEMP Waveform Properties	
Characteristic	Value
Waveform peak	$E_{peak} = 50{,}000\,V/m$
Spectrum peak	$E_{low\ freq} = 0.00152\,V/m/Hz$
Waveform peak power	$P_{peak} = 6.64\times10^{6}\ W/m^2$
Spectrum peak power	$P_{low\ freq} = 6.11\times10^{-9}\ W/m^2/Hz$
Total energy	$W_{total} = 0.115\,J/m^2$
Time of peak	$t_{peak} = 4.84$ ns
Rise time, 10% to 90% of peak	$t_{10-90} = 2.47$ ns
Pulse width, full width at half maximum	FWHM = 23.0 ns
Pulse width, total energy over peak power	$W_{total}/P_{peak} = 17.3$ ns
Spectrum width, total energy over peak spectrum power	$W_{total}/P_{low\ freq} = 18.8$ MHz

To get a feeling for this E1 HEMP signal, consider another EM signal – a FM radio transmission at 100 MHz. Assume the transmitted power is 10,000 watts (RMS), and we are receiving the signal close by, at a distance of 1 mile (1.61 km). For a crude estimate, assume a transmitting antenna gain of $\sqrt{2}$ (2 in power). Then the peak power at the 1 mile range is 1.23 mW/m^2, and the peak electric field is 0.68 V/m. Thus, this signal is smaller than the E1 HEMP electric field peak by a factor of 73,500 – or a factor of 5.4×10^9 in power (97.3 dB). Figure 2-14 shows the IEC E1 HEMP waveform, compared to the FM radio signal – scaled up to the same amplitude. We can also see that the rise of the E1 pulse is similar to the rise of a cycle of the FM signal, and so we can see that the E1 HEMP does have signal content up to 100 MHz. Figure 2-15 shows the actual spectrum of the E1 HEMP waveform.

Certainly the E1 HEMP signal is much larger than the FM radio signal. However, the E1 HEMP energy density is modest - 0.114 Joules/m^2. By contrast, about every 3.1 minutes the FM radio signal delivers the same amount of energy density (of course the E1 HEMP delivers its energy in a few tens of nanoseconds, and over a much larger area). This is an energy density – the amount of energy going by through an area of a square meter. In general it would also be about the amount of energy picked up by a wire antenna about a meter long. Coupling collection areas can vary quite a bit, of course. For example, a long wire could collect significantly more than 0.114 Joules.

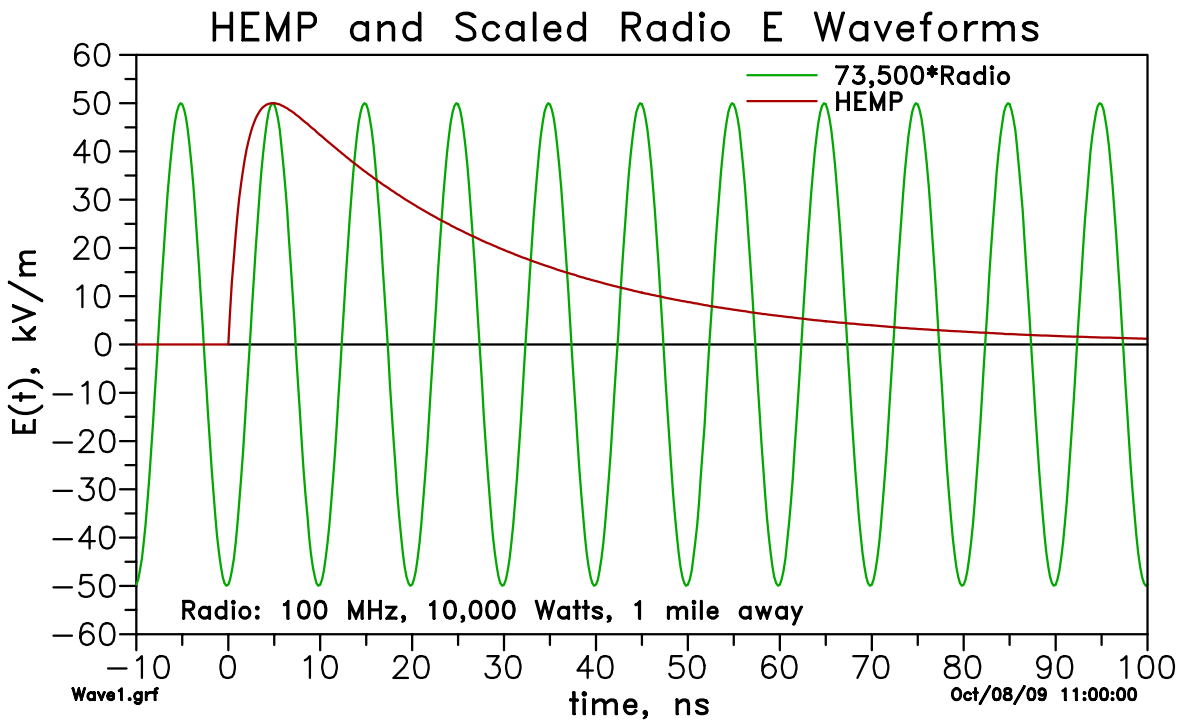

Figure 2-14. Sample E field signals for E1 HEMP and FM radio. The parameters for the FM radio signal are listed in the figure. Note, however, that the FM signal has been multiplied by 73,500, to get it up to the same amplitude as the HEMP signal. The FM signals goes on forever (essentially), while the E1 HEMP signal is transient, and very short-lived.

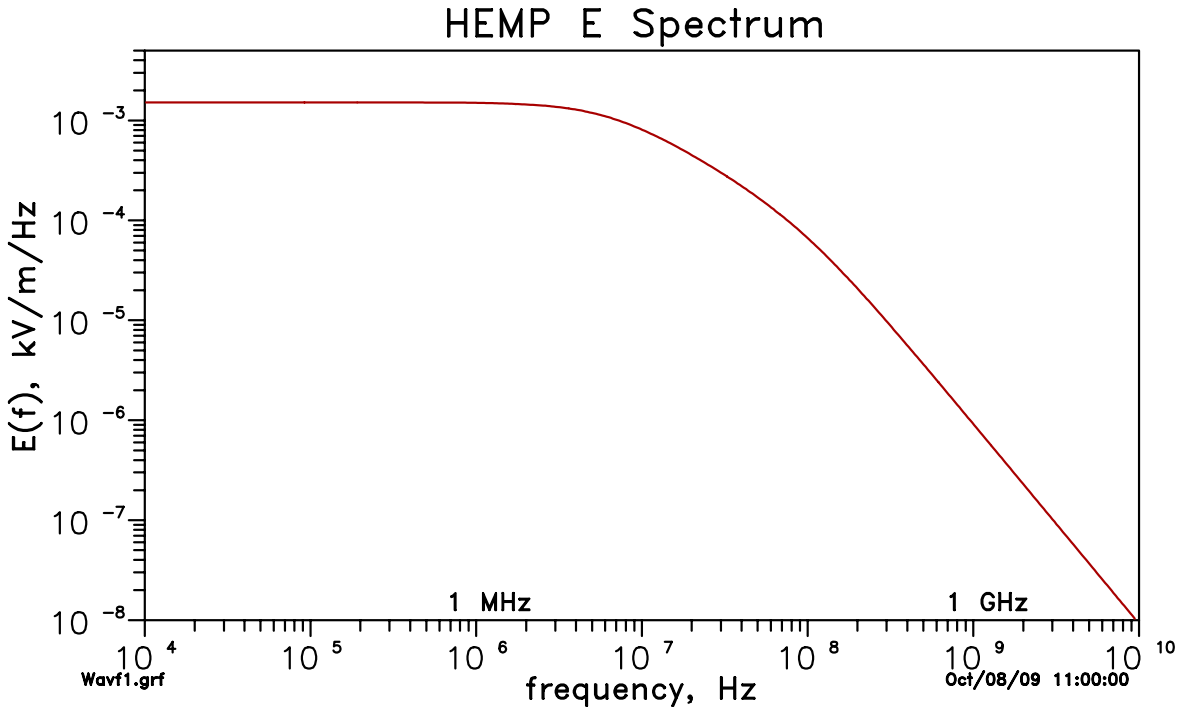

Figure 2-15. Spectrum of the idealized E1 HEMP E field signal. This is the spectrum (magnitude of the Fourier transform) for the signal shown in Figure 2-14. This sample E1 HEMP pulse is flat up to about 10 MHz, and then it starts falling for higher frequencies.

2.11 Energy Conservation Check

It might be that no one thinks about questioning the strength of E1 HEMP. After all, it is produced by a nuclear weapon, which everyone knows has vast energy (destructive power). However, let us look at the energy in the E1 HEMP. Remember that E1 is generated from the gammas, which typically carry away only a small fraction (typically less than 1%) of the burst's energy.

We shudder at the immense destructive power of a nuclear explosion – a full town destroyed by one weapon (of course, some of the total destruction can also come after the burst, from fires ignited by the explosion.) But with EMP there could be damage over a whole continent – can there really be so much destructive power in the E1 HEMP? The following very crude calculation verifies that the amount of energy calculated for E1 HEMP is reasonable, and is actually only a small fraction of the total energy from the nuclear burst. The significant feature about E1 HEMP is that its energy is released extremely quickly - it has very high power levels, while its energy levels are actually modest. E1 HEMP is important because of:

1. Its very high power levels, not usually seen, except in limited circumstances, such as very near lightning strikes, or very close to some very high power RF sources, such as large radars.
2. Its very large area coverage, exposed simultaneously.
3. Modern society's reliance on microscopic, high frequency, electronic devices.
4. E1 HEMP can trigger the destructive release of other energy stores (just as the flick of a match head can cause the match to ignite, which starts a wildfire, which then goes on to burn many homes).

Here we will look at energy, which is the time integral of power (E1 HEMP has very high power, but it also only lasts for a very short time).

Nuclear weapons are rated in terms of their "yield" – their explosive power, often expressed in kT or MT – kilotons or megatons. This refers to the initial energy release of the nuclear device – of all energy types, as discussed previously. As is well known, but it may be hard to comprehend, a "Ton" ("T") corresponds to the explosive power in a ton (2000 pounds) of TNT – such as the amount of explosives that a terrorist might put into a van or small truck. The largest conventional (chemical) bombs may be a few tons. The basic unit for nuclear devices is a kiloton – or what might be in a thousand terrorist vans. The Hiroshima and Nagasaki devices were reported to be about 10 to 20 kT. Thermonuclear devices can be measured in terms of megatons (a million times the yield of big conventional bombs), with the largest nuclear weapon being multiple ten's of megatons.

For this approximate check we will assume a 500 kT nuclear device. Converting to MKS units, the burst initial output energy, in Joules, is:

$$W_{500kT} = 500\ \text{kT} \times 4.184 \times 10^{12}\ \text{J/kT} = 2.09 \times 10^{15}\ \text{J} \quad .$$

In everyday units this is:

$$W_{500kT} = 2.09\times10^{15}\ \text{W}-\text{s}\ /\ (60\ \text{s}/\text{min}\times60\ \text{hr}/\text{min}\times1000\ \text{W}/\text{kW})$$

$$= 5.8\times10^{8}\ \text{kW}-\text{hr}\quad (\text{i.e., kilowatts}-\text{hours})$$

(using 1 Joule = 1 Watt-second). A rough estimate is that an American residence uses about 10,000 kW-hrs a year in electrical power energy, and so this 500 kT weapon represents a year's electricity need for 58,000 American homes.

E1 HEMP is produced by the gamma output of the burst. Assume a gamma efficiency of 0.1%. Then the energy into the gammas for this 500 kT weapon is:

$$W_{\gamma} = 0.001\times2.09\times10^{15}\ \text{J} = 2.09\times10^{12}\ \text{J}\ .$$

Some of the gammas simply radiate out into space, away from the Earth. Figure 2-16 gives the geometry parameters for a 75 km burst height. It shows that about 0.424 of the gammas head in a direction toward the Earth's surface (for convenience of showing the angles, we drew the figure with the HOB distorted – note that the angle at the burst is actually 81.25° and the angle at the Earth's center is 8.75°). Assuming only this fraction of the gammas contribute to E1 HEMP, the energy going into E1 generation is:

$$W_{\gamma E1} = 2.09\times10^{12}\ \text{J}\times0.424 = 8.87\times10^{11}\ \text{J}$$

$$= 2.46\times10^{5}\ \text{kW}-\text{hr}\quad (\approx 24.6\ \text{U.S. households for a year}).$$

This is still a significant amount of energy, but remember, it is spread out over an area corresponding to much of the continental U.S.

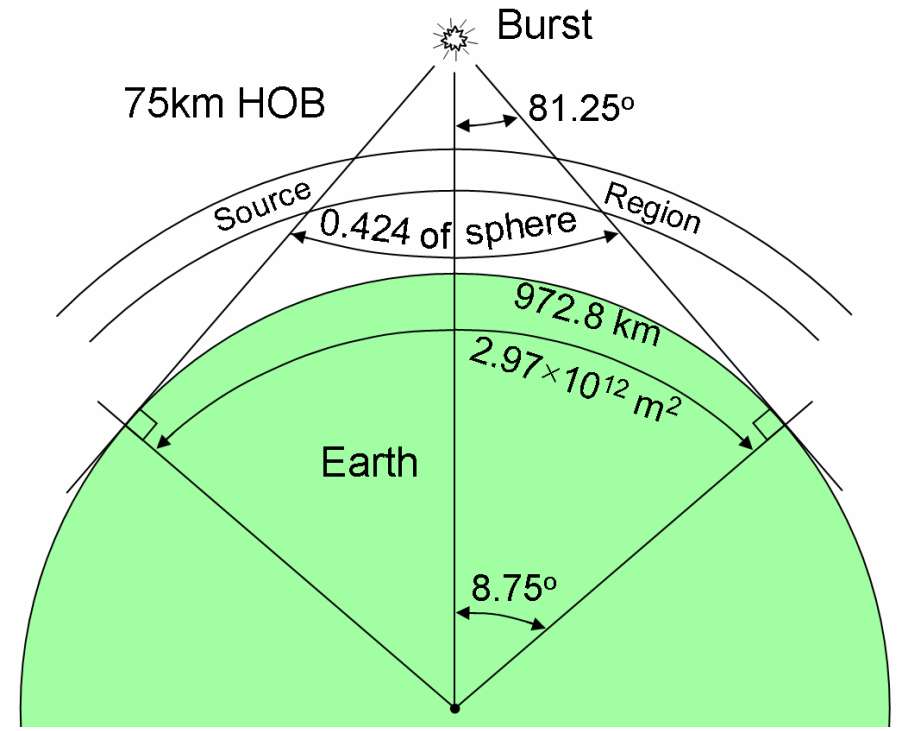

Figure 2-16. Geometry used in an energy calculation for E1 HEMP. This is for a 75 km burst height (46.6 miles, 246 thousand feet). The view shown is very distorted – the Earth is actually much larger, relative to the burst height, than represented by the drawing.

Now that we have the amount of weapon energy that can generate E1 HEMP, we will consider the total energy in the E1 HEMP. We will use the IEC E1 HEMP signal defined previously, which had a peak of 50,000 kV/m at the strongest point on the Earth, and energy density of 0.115 J/m^2. The exposed region goes out to the tangent of 972.8 km, an area of

$$A_{E1} = \pi(972.8\text{ km})^2 = 2.973\times10^{12}\text{ m}^2$$

(more accurately, accounting for the Earth's curvature, it is actually 2.967x10^{12} m^2). The 50,000 kV/m is the E1 HEMP at the maximum point; it is less elsewhere, as previously shown in Figure 2-3. Averaged over the exposed region, for this case the peak is 0.1243 of the maximum (so about 6.21 kV/m). Thus, the total energy in the E1 HEMP is

$$W_{E1} = 2.967\times10^{12}\text{ m}^2 \times 0.1145\text{ J/m}^2 \times 0.1243^2 = 5.25\times10^9\text{ J}$$
$$= 1457\text{ kW} - \text{hr}$$

(approximately 53 days of electricity for a typical U.S. household). This E1 HEMP energy is only about

$$\frac{W_{E1}}{W_\gamma} = \frac{5.25\times10^9\text{ J}}{8.87\times10^{11}\text{ J}} = 0.59\%$$

of the energy in the gammas that generate the E1 HEMP. This is also only

$$\frac{W_{E1}}{W_{500kT}} = \frac{5.25\times10^9\text{ J}}{2.09\times10^{15}\text{ J}} = 0.0000025 \quad \text{(fraction, not percent)}$$

of all the energy from the burst. Thus, the E1 HEMP total energy is only a small fraction of the energy of the burst output gammas that go into generating it. The rest of the gamma energy goes into losses, such as what ultimately ends up as heating the source region, or radiating energy away from the source region (as photons: gammas, x rays, ultraviolet, infrared, etc.). Part of the lost energy was initially converted to EM energy, but ended up being lost to heat due to the air conductivity. Again, we need to emphasize that the E1 HEMP may have a small fraction of the burst's output, but it is a coherent, high level, EM pulse that is delivered very quickly. The total peak power from of the E1 HEMP is about

$$\frac{5.25\times10^9\text{ J}}{17.25\text{ ns}} = 3.0\times10^{17}\text{ watts}.$$

Again, we note, this is an extremely high level partially due to the very short time duration of the pulse.

2.12 E1 HEMP: Instantaneous and Simultaneous

E1 HEMP has been described as instantaneously and simultaneously blanketing a continent size region. How fast is this really? We have seen that the E1 HEMP pulse is very fast – for example, the IEC waveform is 23 nanoseconds wide. And it also hits the entire exposed region essentially at once. This is because the speed of light applies – to the gammas and to the E1 HEMP signals. For a 100 km burst (62.1 miles), various time delays are:

From the burst straight down to GZ: 0.333 ms
From the burst to the farthest exposed point (tangent): 3.78 ms
From GZ out to the tangent (1122 km, or 697 miles): 3.74 ms

These can be compared to the cycle time of 16.7 ms for 60 Hz AC power. Of course, different points in the exposed region could not "know" about each other faster than the speed of light anyway, and typically cascading power failures travel at much slower speeds.

2.13 Observer Location Variation (Smile Diagram) and Observed Function

Often E1 HEMP is discussed in terms of the peak incident E field, as if no other characteristic matters. And most smile diagrams do plot this quantity. However, other quantities could also be of interest. In the following diagrams we show "smile" diagrams plotting different field quantities, all for the same E1 HEMP conditions (a 75 km HOB over the central U.S.). The figures are listed in Table 2-5 (the last three results listed in the table will be discussed in the next subsection). In general, the contour levels used are as fractions of the maximum incident field (which occurs at the white "+" inside the red contour in Figure 2-17).

Table 2-5. List of the sample "smile" diagrams. All cases are for the same burst scenario.

Sample Smile Diagrams	
Smile	Display function
Figure 2-17	Peak of incident E field
Figure 2-18	Peak of horizontal component of incident E field
Figure 2-19	Peak of north/south horizontal component of incident E field
Figure 2-20	Peak of east/west horizontal component of incident E field
Figure 2-21	Field direction of peak of horizontal component of incident E field
Figure 2-22	Peak of vertical component of incident E field
Figure 2-23	Peak of horizontal component of total E field (including reflection)
Figure 2-24	Peak of vertical component of total E field (including reflection)
Figure 2-25	Total energy density in incident E1 HEMP
Figure 2-26	Total energy denisty in 10 to 100 MHz band for incident E1 HEMP
Figure 2-30	Peak current on north/south overhead line
Figure 2-31	Peak current on east/west overhead line
Figure 2-32	Peak current on vertical wire
Parameters: Burst: 40^{o}N, 95^{o}W, 75 km. Reflected field (Figures 2-23 and 2-24): 10^{-2} S/m ground, observer 3 meters up. Coupling (Figures 2-27 – 2-29): 10^{-3} S/m ground, wire 0.2 centimeters radius. Horizontal: wire 100 meters long, 5 meters above ground. Vertical: wire 5 meters long, base on ground.	

These samples use the same case as shown in Figure 2-3, and so incident peaks in Figure 2-17 shows the same result. Figure 2-18 shows the peak of the horizontal part of the incident E1 HEMP – it is almost the same as for the peak of the total signal shown in the previous figure. In the next two figures this is separated into the peak for the north/south component (Figure 2-19) and the east/west component (Figure 2-20). Figure 2-21 repeats Figure 2-18 (peak horizontal) but also has arrows to show the direction of the horizontal field. We see that the E field looks to be azimuthal – pointing clockwise around the center. However, looking closely near the center, we see that it actually swirls around the null point, slightly above the center (ground zero, marked by a "+"). Figure 2-22 shows the peak of the incident vertical E field. This component tends to be smaller than the horizontal (and total) field, and so here we have used a different contour set than the previous plots. Note that most of the results seem to have east-west symmetry, but the vertical peak does not – this will be discussed later.

The previous results were all for the incident field. In the next two figures we have peaks for the total field, which includes reflection off the ground. We assume 10^{-2} S/m ground conductivity (in the range of soil conductivities, this would be considered toward the high end), and an observer point 3 meters off the ground. Figure 2-23 shows the horizontal peaks, and Figure 2-24 the vertical. The horizontal results show a suppression of the signal, especially as we go out toward the tangent (this gets worse as the observer point gets closer to the ground), while the vertical signal shows a slight enhancement.

For the next two figures we go to the frequency domain, for the incident E1 HEMP signal. Figure 2-25 shows the total energy density in the signal, while Figure 2-26 shows the energy density in the band of 10 to 100 MHz (toward the high frequency end). These are plotted as a fraction of the total energy density at the maximum E1 HEMP point (the max point, to the south of GZ). Note the contour set for the high frequency band had some low level contours added – this is to show how drastically the high frequencies fall off as we go to the tangent.

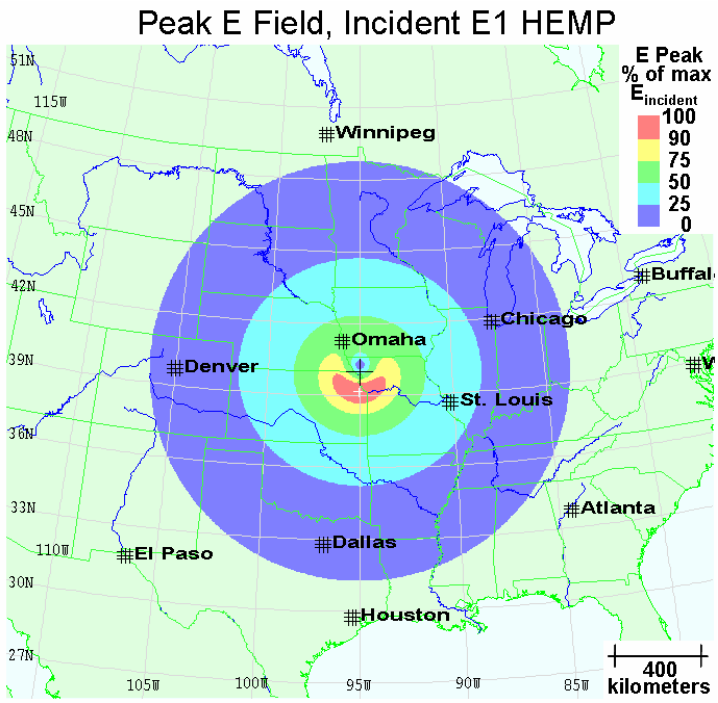

Figure 2-17. Sample E1 HEMP peak contours. This plots the peak value of the incident E field total waveform. The burst height is 75 km. The contours are as percentages of the absolute highest peak, which occurs at the point marked by the white cross hairs, south of the burst position (GZ, marked by the black cross hairs).

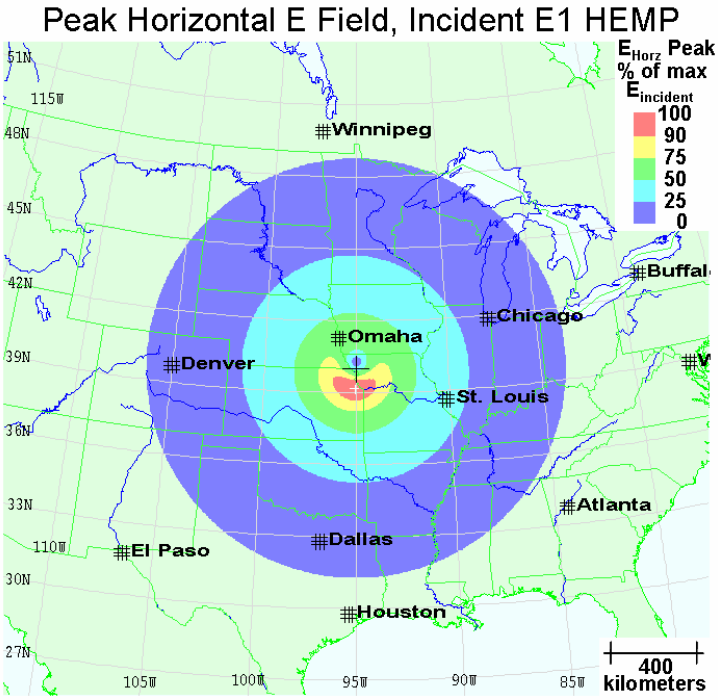

Figure 2-18. Sample E horizontal component contours. For the sample case of Figure 2-17, this gives a contour plot of the peak of the horizontal component of the incident E1 HEMP E field. The contour edges are at the same field level values as for Figure 2-17 (both use the same percents of the maximum peak magnitude of the incident field).

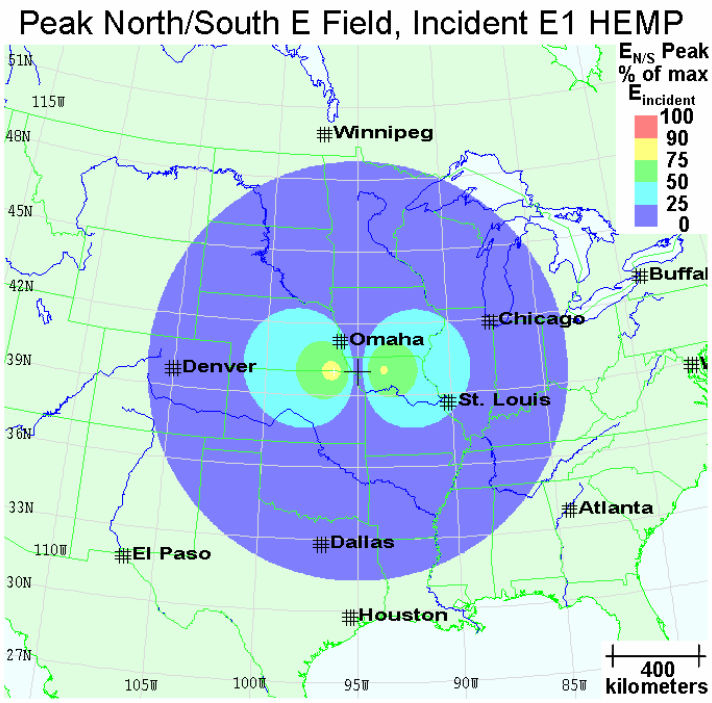

Figure 2-19. Sample E north/south horizontal component contours. This and the next figure break down the horizontal term (Figure 2-18) into two components. These contours show the North/South component of the peak E1 HEMP incident E field. (Again this uses the same E field values for edges of the contour set.)

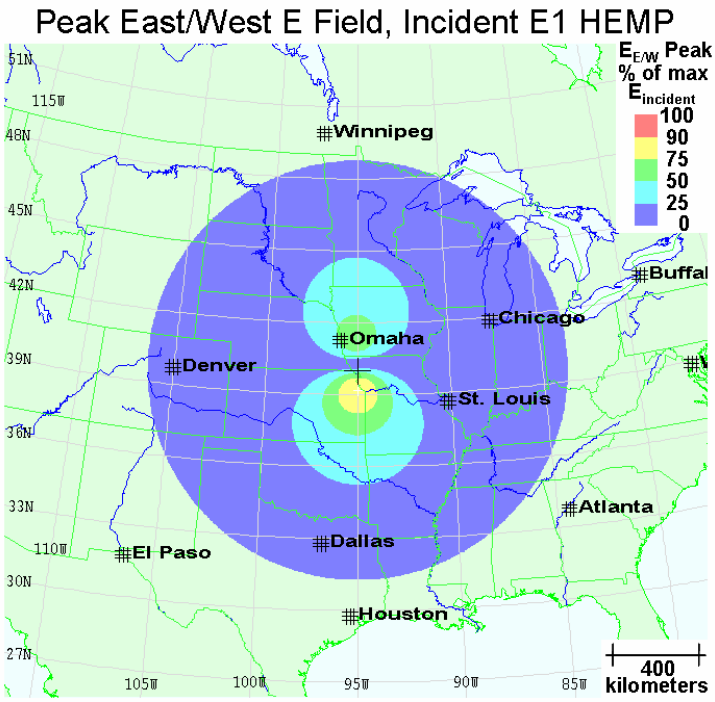

Figure 2-20. Sample E east/west horizontal component contours. This shows the other horizontal component for the E1 HEMP sample – the East/West part of the peak E field (using the same contour set values as the previous plots).

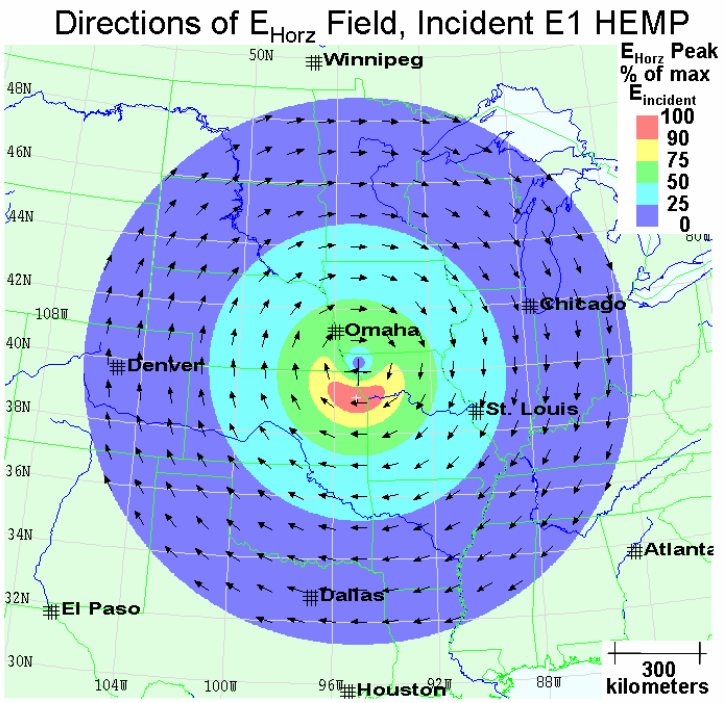

Figure 2-21. Horizontal E field direction for E1 HEMP sample. Arrows show the E field directions for the horizontal E field peak for the sample case. The contours are for the peak horizontal E field – the same as in Figure 2-18. (Here we have zoomed in a little more than for the other figures.)

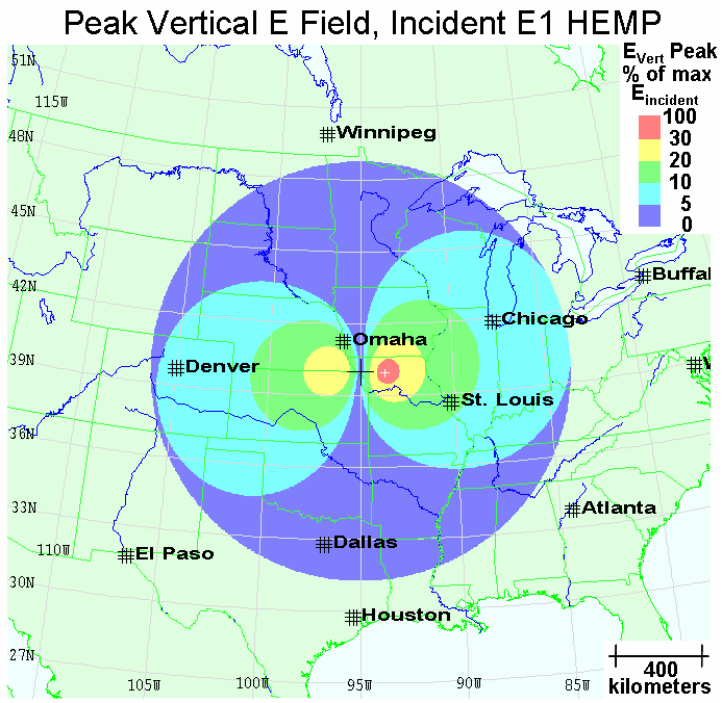

Figure 2-22. Sample E vertical component contours. This gives the peaks of the vertical component for the E1 HEMP sample. Here a different contour levels set is used, since the vertical values tend to be somewhat smaller than the horizontal values (but the contours still use percent of the maximum total incident E field value).

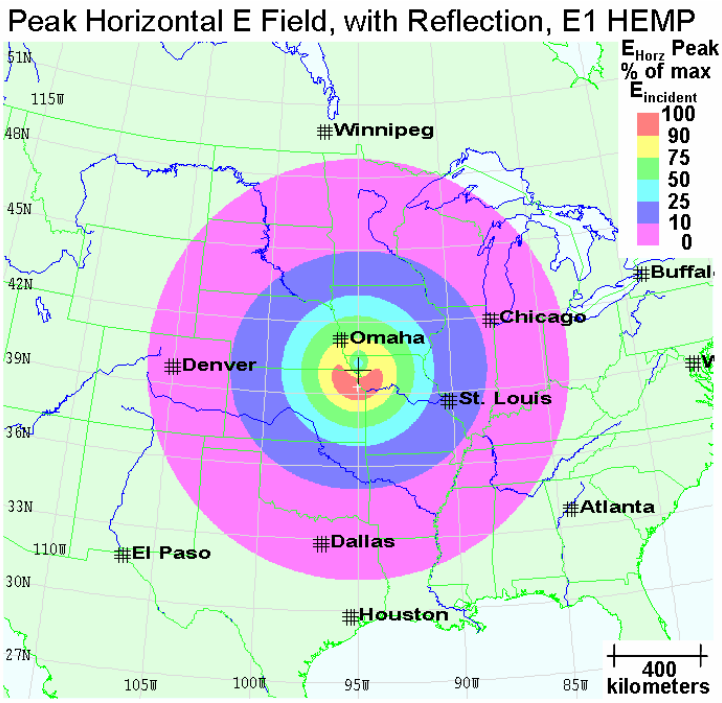

Figure 2-23. Peak horizontal E1 HEMP contours, including ground reflection. We have added a 10% contour level for this plot. (Parameters: 10^{-2} S/m ground conductivity, observer 3 meters off ground.)

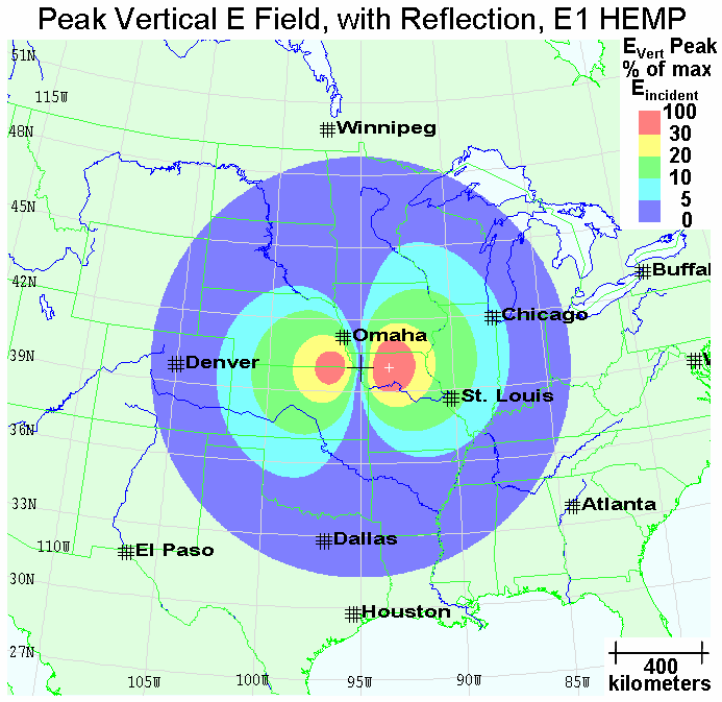

Figure 2-24. Peak vertical E1 HEMP contours, including ground reflection. (Parameters: 10^{-2} S/m ground conductivity, observer 3 meters off ground.)

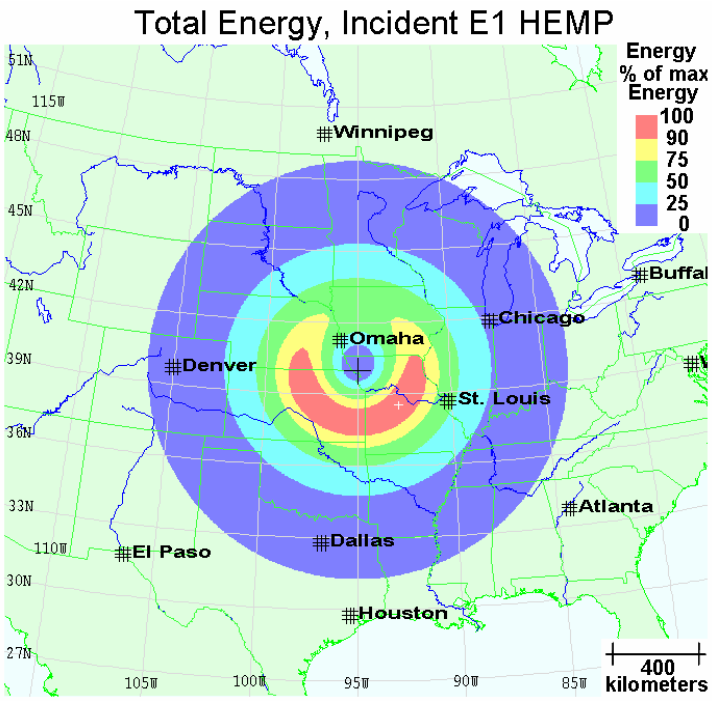

Figure 2-25. Sample E1 HEMP total energy contours. This plot shows the total electromagnetic energy in the incident E1 HEMP. The contour set uses percents of the value at the peak point.

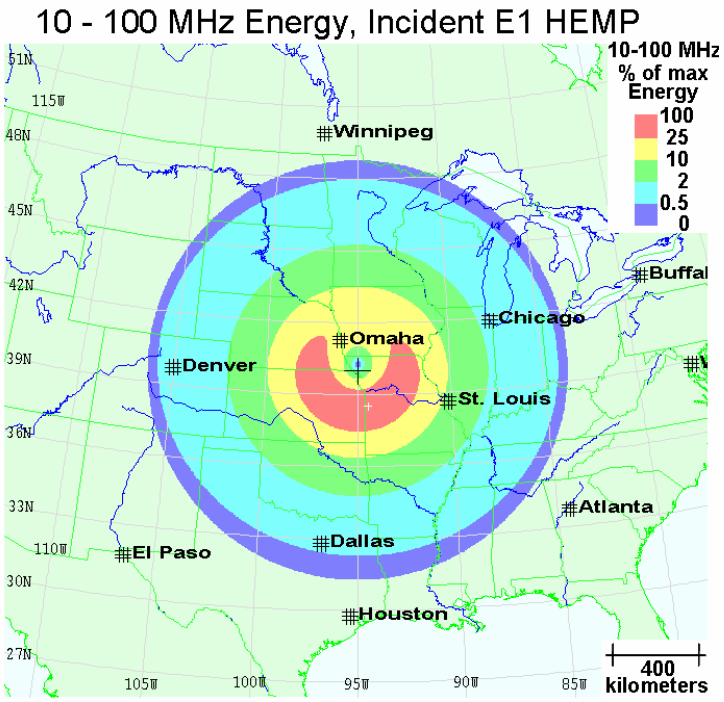

Figure 2-26. Contours of energy in the 10 to 100 MHz band. This is like the previous plot, but for only the energy in 10-100 MHz. The contour values are as percentages of the value of total energy at the maximum E1 HEMP energy point (the same normalization used for Figure 2-25).

2.14 E1 HEMP Effects on Systems

E1 HEMP peak field levels can be very high, and certainly there could be some devices within a system that have some vulnerability to such high levels. However, typically vulnerabilities involve the intermediate step of having voltages and currents generated on a conductor, and then that signal getting to the fragile device. The conductor might be deep within the system, such as wiring in the internal circuits, however a major concern is external cabling attached to the system, for two reasons. First, outside wiring can be very long, which tends to increase coupled signal levels, while internal wires are limited by the enclosure size. Secondly, the system enclosure and support structure, especially if metallic, attenuates electromagnetic fields and leads to lower coupling for internal wires.

With a peak field of 50 kV/m, even a short "antenna" 10 cm (4 inches) long can mean a voltage of about 5000 volts, and it could be much higher for longer lines. Power lines, of course, can be very long. Other possible long lines include communication lines within a facility, such as network lines and phone lines. For power substations there are also the various sensing and activation lines used for the relaying process that maintains power reliability and tries to lessen harm to the power system from faults.

With the advance of modern systems, and miniaturization of components, the normal operating voltages of systems tends to be a few volts, and so HEMP levels of thousands of volts or more cannot be good for the system. Also, the operating frequencies of systems, such as computers and various types of controllers, are such that an E1 HEMP pulse would cover many clock cycles. Thus the fact that E1 HEMP type pulses can have effects, as has been found in vulnerability tests, is not surprising.

Typically system effects are separated into two types (although finer gradation is possible):

Temporary Upset
Permanent Damage

Damage is fairly clear – something physically happens to some part of the system, such that the system no longer works. Sometimes the damage might be readily seen, such as a device "blown up", but other times there may not be any visual damage, yet the system will not work. It might be that the damage is to a small, but critical, area inside an integrated circuit (IC). With devices being microscopic, it is believable that even very small energies could be worrisome. This is why ESD (electrostatic discharge) is such a concern when handing modern electronics. Besides outright damage to a device, we can also have degradation, in which the device still operates, but its performance is not as good as before the assault by the high level pulse. Damage can also be ranked by how long it would take to repair, or how easily it could be fixed. In many cases it would involve determining that there is a problem, and what subsystem is broken, and replacing the subsystem. It might not always be obvious that there is a problem, such as for functions that are only used occasionally. For example, damage to some part of the fault protection for a power substation might not be detected until a fault happens, and the protection does not work properly. In some cases, damage that completely brings down a system might be better than subtle, less obvious, damage. It might be better to know

there is a problem, and so try to fix it, than to depend on some function working properly when needed, only to have that function fail at the critical time.

For EMP vulnerability, it can be very important whether the system is powered up or not. Certainly a HEMP coupled pulse could cause damage, whether it produces no easily seen evidence of the damage, or blows a device apart, as shown in Figure 2-27. Typically the pulse amplitude level needed to cause damage is higher for narrow pulses than wide pulses, and the susceptibility levels for E1 HEMP are higher than for some other types of effects. However, E1 HEMP coupled levels can get very high, and the coupling to long cables can produce pulses that are longer than the incident EM pulse itself. So even an un-powered system, attached to long cables, can be vulnerable.

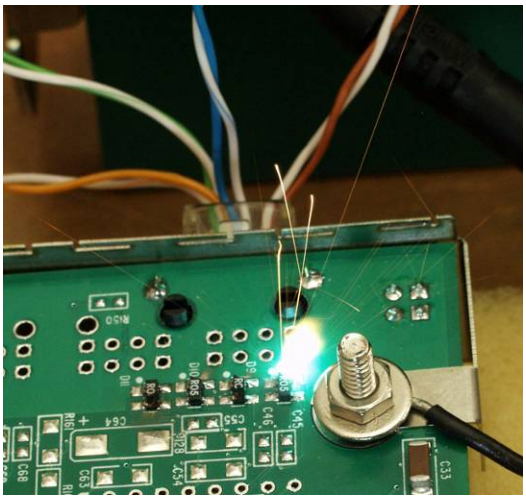

Figure 2-27. Flash and sparks from pulse damage testing. In this case the device under test (DUT) is not powered (not turned on) – the flash in only from the pulser's energy.

However, when a system is powered – actually in an operating state, there can be other vulnerabilities. Even if the incident pulse is low in energy, the system itself typically has access to the power source that runs the system, such as the AC power or a battery supply. The full system gets illuminated by E1 HEMP, so with all the many wires connected to a device are simultaneously assaulted by huge signal pulses, it is very likely the complex circuitry may respond in some abnormal ways. Are any of those responses such that, for example, a high-current arcing path gets created across the power supply – so this short circuit burns out some device along that path? Such effects are very hard to predict, and high-level laboratory tests should always be used if it is important to detect such vulnerabilities.

A classic example of this is found in the TREE discipline (transient radiation effects on electronics). Complementary designs are very common for digital circuits – two transistors are connected in series across the power supply, and the circuit design is such that only one transistor is on at a time. The output level is either high or low, depending on which transistor is on. There can be high efficiency, and little wasteful energy going into heating the wafer in this design, since current might only flow through the series of transistors during switching transients. However, a gamma or x-ray pulse hitting the

active region of the "off" transistor could switch the junction on, just as light does for a photodiode. Once on, there is then a short through the two transistors, and, being microscopic transistors on an IC, extremely little of the energy from the power supply would be needed to heat up and destroy something along the path, such as one of the transistors.

Upset is considered a disruption of the normal operation of the system. It can occur at various levels. There might be a minor glitch, from which the system quickly recovers and continues working. Or it might bring the system down, requiring a "re-boot". The effect might be immediate, or show up later. Some data could be corrupted for a control system, thus leading to improper processing steps, and ultimately some type of failure. For unmanned facilities this might take some time, and again it might not always be immediately obvious that the system is not working correctly, thus leaving the system in a crippled state. That upset could happen is completely understandable. A modern system can be very complex, with many digital signals going around – pulses of a few volts, with switching at frequencies in the megahertz range. When E1 HEMP pulses come in on all of the wires, with much higher voltage levels, lasting for many clock cycles, and with content up to high frequencies, the system could easily get confused.

Under the wrong circumstances, the confusion of an upset could lead to damage, such as if incompatible commands get issued. Such vulnerabilities are often unforeseen. Luckily the world has not experienced real E1 HEMP events that might trigger such unusual, but possibly catastrophic events, but they do occur occasionally due to "EMI/EMC" issues, such as high radar pulses causing a missile on a fighter aircraft to think it has been commanded to fire, while the fighter is on an aircraft carrier deck. Of course, careful design, and extensive testing, can help minimize such possibilities.

2.15 E1 HEMP Coupling

Electromagnetic signals, such as E1 HEMP, generate voltages and currents on conductors exposed to the fields. E1 HEMP coupling is like any other electromagnetic coupling. The EM fields encounter a conductor, and induce voltage and current signals on that conductor. Vulnerability issues occur when the conductor connects to a circuit with parts that could be destroyed or upset.

Coupling is a full electromagnetic effect, but often can be thought of in terms of individual electric (capacitive – see Figure 2-28) or magnetic (inductive – see Figure 2-29) coupling. In these figures we have a cable connected to a metal plate at both ends, such as the shields of a shielded cable that is fully bonded to the metal enclosures where it connects. The same effect applies if the cable is unshielded, except the currents and voltages signals would be seen directly by whatever circuits are attached to the cable ends (with the circuit impedances governing the exact currents and voltages). For capacitive coupling the electric field rearranges electric charges on the conductor – those charge movements are currents, and the force that moves them is a voltage. Similarly, for magnetic coupling, there is an EMF (voltage) generated in the conductive loop by the

time-rate-of-change of the total magnetic flux through the loop, and a current is driven in response.

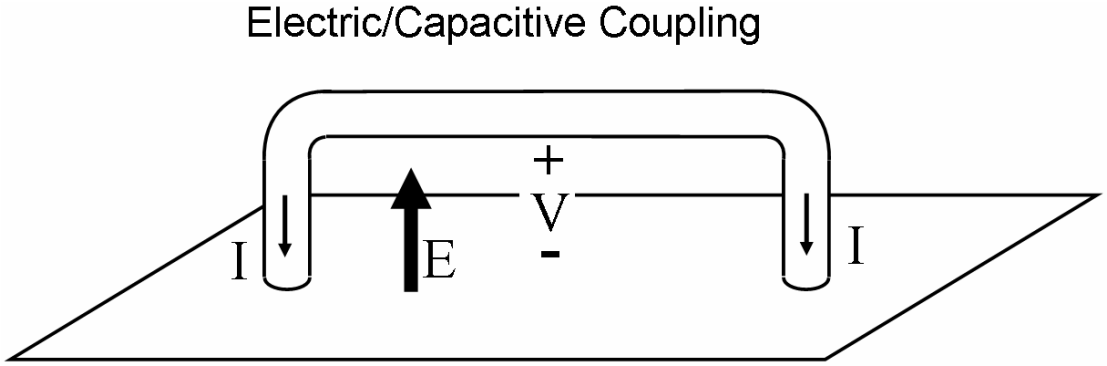

Figure 2-28. Capacitive (electric) coupling to a short cable. The electric field (E) induces the voltages and currents shown.

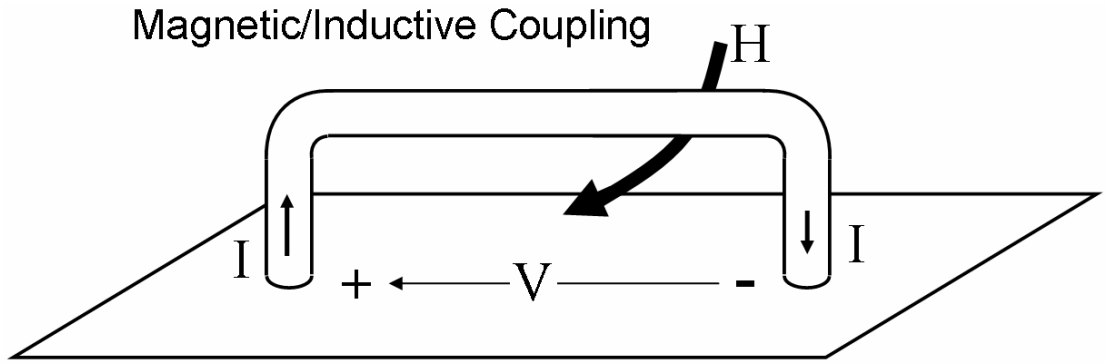

Figure 2-29. Inductance (magnetic) coupling to a short cable. The magnetic field (H) induces the voltages and currents shown.

There are also couplings that are electromagnetic in nature, such as high frequency wave coupling to long cables or antennas. This is exactly the process by which receiving antennas work – and so they will pick up E1 HEMP energy by their very nature. But any conductive object, not just antennas, would have induced signals. The process for antennas and long lines can be very complex, depending on details of exactly which way the incident EM wave is propagating, and the field polarization (which direction the E and H fields point). The E and H must be in the plane perpendicular to the propagation direction, and H must be perpendicular to E in that plane, but otherwise there is no restriction on where E points within the plane (this is the polarization of the field).

Because they can be long, and fully unshielded out in the exposed region, long cabling (lines) are important for E1 HEMP. This applies to lines such as power lines, communication lines, and control lines. In the next three diagrams we continue the pervious set of results – here we show contours of peak currents on wires exposed to the same E1 HEMP as used before. Figure 2-30 shows the peak current on a 100-meter long wire, 5 meters above the ground. This result is for a north/south alignment of the wire, and Figure 2-31 is for an east/west alignment. In Figure 2-32 a vertical wire is used (5 meters long). Current levels get up to hundreds of amps for these coupling examples.

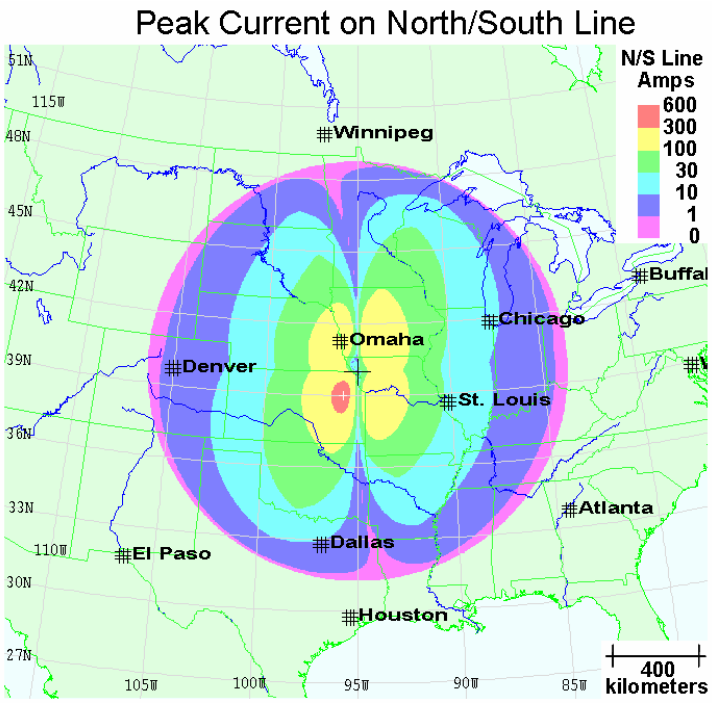

Figure 2-30. Sample contour plot of the peak current on a north/south line. This is for an overhead wire, running north and south, for the same sample E1 HEMP case as the previous contour plots. The line is moved to each observer position to get the data for the contour plot. (Parameters: 10^{-3} S/m ground conductivity, line 5 meters off ground, line 100 meters long, wire 0.2 centimeters in radius.)

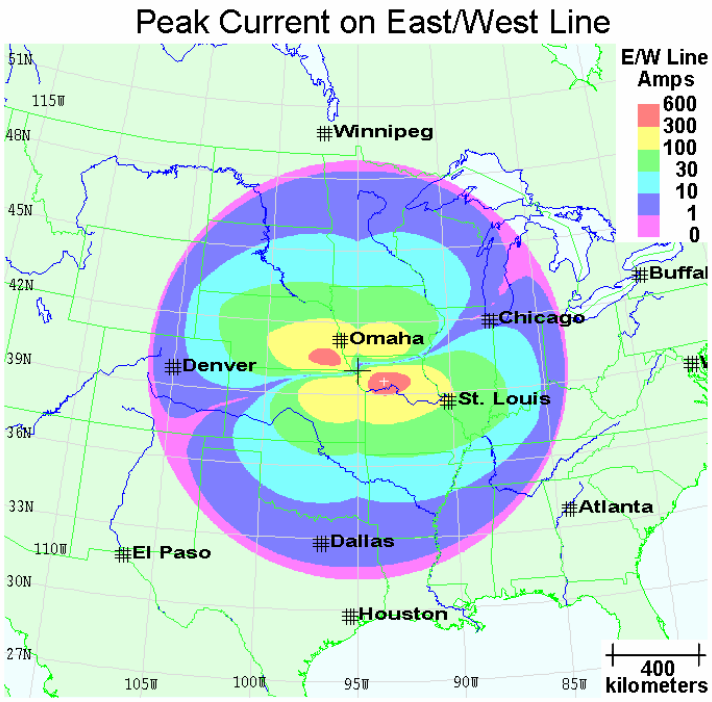

Figure 2-31. Sample contour plot of the peak current on an east/west line. This is the same as in the previous figure, but with the line going east and west. (Parameters: 10^{-3} S/m ground conductivity, line 5 meters off ground, line 100 meters long, wire 0.2 centimeters in radius.)

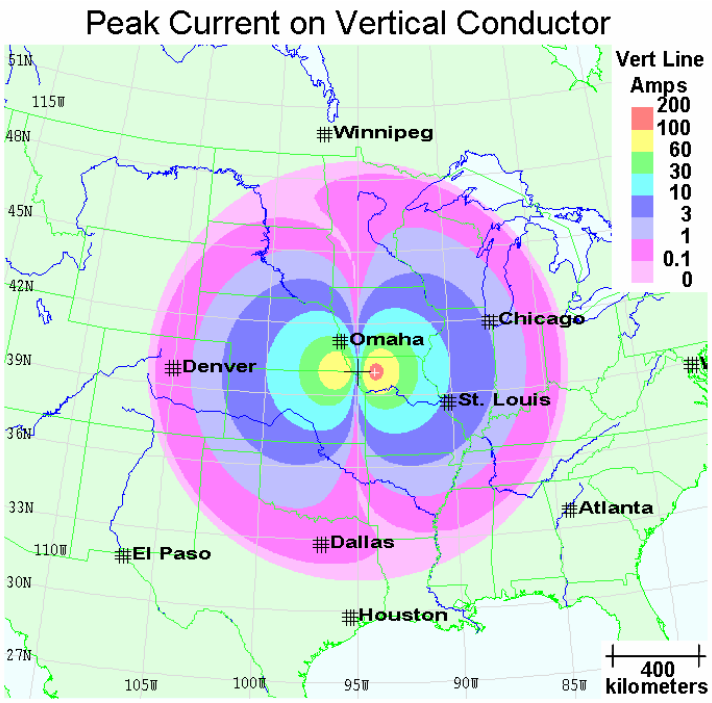

Figure 2-32. Sample contour plot of the peak current on a vertical wire. This is the same case as the previous contour samples, but with a short vertical wire. (Parameters: 10^{-3} S/m ground conductivity, wire 5 meters long, with base on ground, wire 0.2 centimeters in radius.)

2.16 E1 HEMP Penetration and Protection

Typically system vulnerabilities are due to small parts deep within the system, while the assaulting EM environment, such as E1 HEMP, is outside. There are various ways that the external energy can find its way down to the internal devices.

Often (but not always) there is some type of conductive (usually metallic) enclosure around the system. This can provide a barrier to external electromagnetic signals. In fact, a full conductive enclosure is a "Faraday cage", which shields out EM signals by "shorting out" the electric field and reflecting it. A conductive barrier is also associated with the concept of skin depth, introduced earlier:

$$\delta = \sqrt{\frac{1}{\pi \sigma f \mu}} \quad .$$

This gives an indication of penetration depth for EM signals. Higher conductivities (σ) and frequencies (f) mean better shielding. For good shielding, the enclosure thickness should be large compared to the skin depth. Besides being sure the metal is thick enough, we also need to worry about other issues, such as in the following discussions. Generally they are more of a concern than enclosure wall thickness.

The conductive case needs to totally enclose the system to be a good "Faraday cage" – any breaks ("apertures") will allow EM energy to leak in. Figure 2-33 indicates how an external electric field normally "terminates" on a conductor (with surface charge

re-arranging itself on the exterior accordingly). However, if there is an aperture, some of the lines go inside, and end on the interior walls. Thus, some of the EM signal has penetrated inside, and besides the E field, there are the associated magnetic fields, and currents from the moving surface currents. Figure 2-34 shows that magnetic fields parallel to the wall can also penetrate in through the hole and get inside the shield. Surface currents are associated with such magnetic fields, and some of the external current can flow into (and then back out of) the aperture.

Even small holes can be problems for sensitive systems. If made of separate metal plates, the plate seams might have microscopic leaks if pressed or bolted together, and the best approach is for welded seams (and even those need to be tested for leaks after welding, if very good shields are desired). Seams are especially of concern if parallel to the external magnetic field. Such magnetic field orientation implies an outside surface current perpendicular to the seam – and that surface current faces a barrier to its flow when it gets to the seam crack. In diverting that current, some current gets inside the enclosure wall (as shown in Figure 2-34).

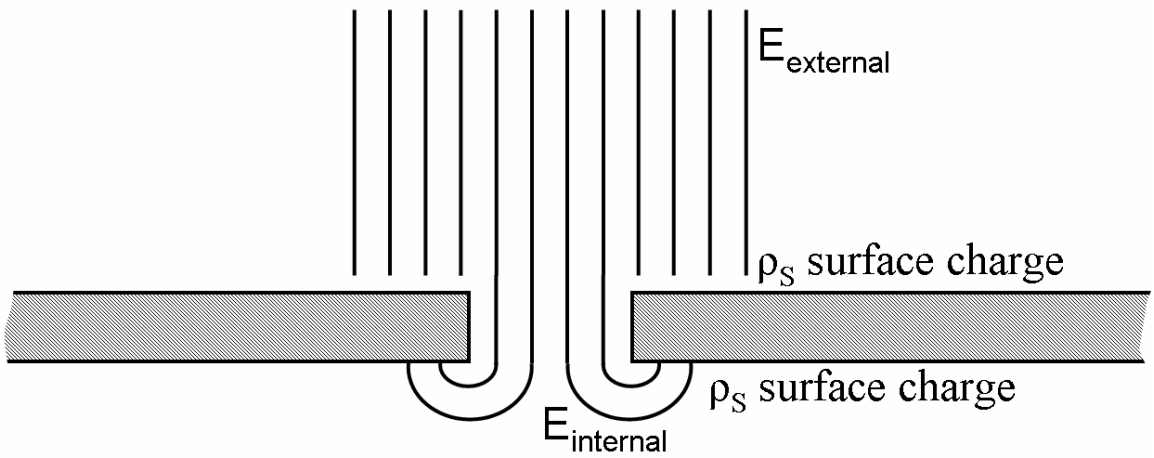

Figure 2-33. Electric leakage through an aperture.

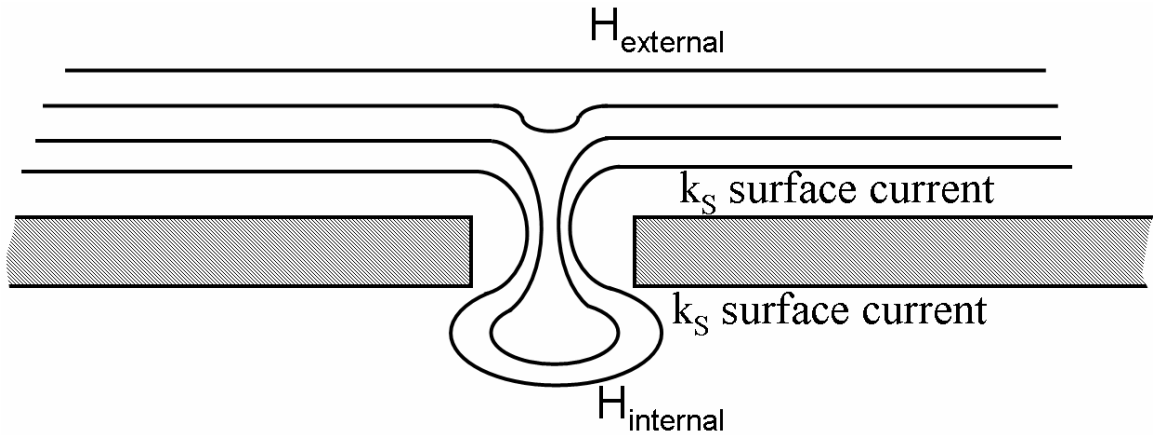

Figure 2-34. Magnetic leakage through an aperture.

Generally a system cannot have such a perfect complete metallic enclosure and still provide some useful service – the system usually must provide for some exchange of electricity and data between it and the outside world. Various types of access are needed. Access panels or doors are a special concern, and attention is given to making sure they seal well electromagnetically when closed. Generally visual windows are discouraged – or else special treatment must be used to allow optical transparency while shielding at RF frequencies (think of microwave oven doors). Air-cooling of equipment, and fresh air for manned rooms, are incompatible with a perfect barrier. For such cases, and others in which the metal case must have openings, the concept of "waveguide below cutoff" can be used. An electromagnetic signal cannot go down a hollow metal pipe (a waveguide) unless its frequency is high enough (the smaller the pipe diameter, the higher the frequency required). This is why car AM radios lose reception when they go into a tunnel. However, it is important that there not be any floating conductors (not connected to the pipe wall) going down the "waveguide" – because this introduces another mode of EM propagation, and the waveguide protection is lost (some tunnels have such a wire so that car AM radios will get reception).

Any metal conductor that needs to get inside the system may be a penetration path for EM signals. Thus, for example, a water pipe should be electrically sealed (such as welded) completely around its circumference where it enters the metal shield. However, some conductors might need to get inside, and have electrical connectivity. Often a useful system must have "ports" that external cables connect to, and connect to internal circuits. These might be for power, communications, or control, for example. They require wires going through holes in the shield. Such unavoidable penetrations can be a major vulnerability for systems. Special treatment may be used at each such penetrating wire to lessen system vulnerability. One approach is to put protective circuits (TPDs, terminal protection devices or SPDs, surge protective devices) at the entry point. These circuits are designed to let the desired signal pass without hindrance, but block unwanted, and especially possibly damaging, signals. Two approaches to this are filtering and limiting. Frequency domain filtering uses a filter (low pass, high pass, or band pass) tuned to the desired signal, and energy at all other frequencies gets blocked. A more common approach is to use non-linear devices that change state for high level signals, such as voltages or currents that are much higher than the normal signals on the lines. Such devices might either short the line to ground (low shunt impedance), or open up the line (high series impedance) in response to any high level input (of course, during such an event, the normal use of the line is disrupted, but hopefully all will be OK when the assaulting signal is gone). Another approach is to use fiber optics for signal lines in and out of the system, as they will not conduct electrical current if the line does not contain any metal.

Another approach to external cabling is to extend the enclosure shielding to include the wires too – use "shielded cables". This is very common, for cases in which it is thought that the protection is worth the added expense. However, as for water pipes, the shield should have a full "circumferential bond" – attached all 360^{o} around to the enclosure. Especially bad would be a long thin wire connecting the shield to ground, as shown in Figure 2-35. Thin long wires ("pigtails") can have high inductance, and so provide a poor connection and high impedance at the high frequencies of E1 HEMP.

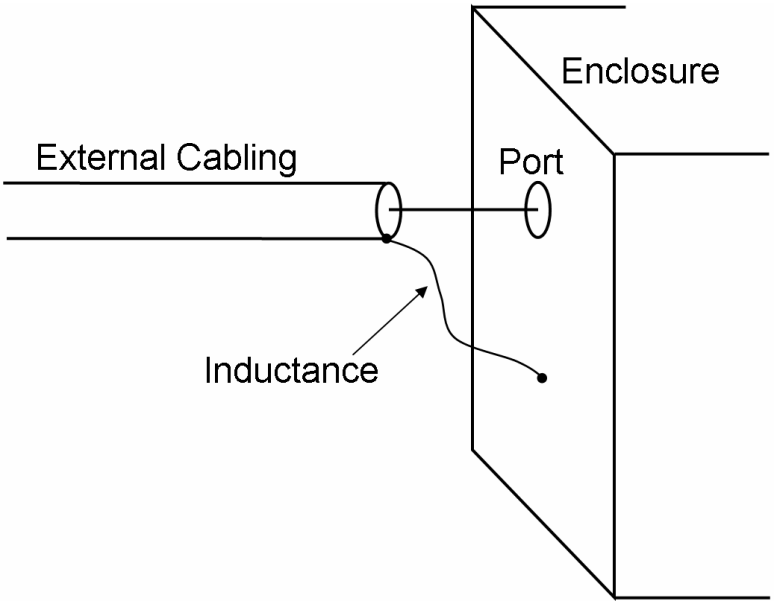

Figure 2-35. External cabling with poor termination at the subsystem.

Much effort has gone into the study of system protection, not just for EMP but also for other electromagnetic issues. This includes more common everyday issues such as considered in EMI/EMC (electromagnetic interference and electromagnetic compatibility), which have been concerns since the early days of electronics, but have become more so as there are more and more electronic devices in our lives, and they become more complex, more miniaturized, and operate at higher frequencies.

There are other approaches to providing protection for a system ("hardening" the system). The circuit design can consider the vulnerability of individual devices when doing part selection – more robust parts can be selected, especially for devices most directly connected to incoming wiring. Also, especially for upset, the functional design can be very important. The system should be able to sense bad incoming signals (such as using error detection for digital data), and should be OK with the temporary interruption of its I/O (input/output) ports. There should be ways to sense if everything is running OK. If a circuit gets stuck in a dead end state, there should be a way to sense this and force the circuit to reset (a watchdog system). It would also be useful to have automated ways to look for dead circuits within a system, instead of waiting for someone to realize that it was not responding, or worse, depending on it for protection but instead having it not correctly do its job at some critical moment.

2.17 E1 HEMP Specifications

E1 HEMP is a real concern for survivability of important military systems. E1 HEMP has a very large area of coverage, and there is no easy way to determine what effect E1 HEMP will have on any given piece of equipment. The issue is: if all my resources will be hit by E1 HEMP – what will happen to them, and what will be usable afterwards? E1 HEMP is an incomprehensible phenomenon, outside the realm of everyday experiences.

Generally, we cannot directly test the equipment - put it into the field and set off a nuclear burst to see what happens to it. Instead, we rely on indirect evaluations, involving theory, modeling, and testing. There is much variation in possible E1 HEMP environments, and damage mechanisms are not always perfectly clear. Thus, often it is not possible to specify a worse case scenario. For example, E1 tends to be higher in amplitude, but narrower in pulse width, for locations toward the center of the coverage area, compared to locations out near the edge. Is it just the peak that is important, or could a smaller, but wider pulse be more damaging? For military systems an approach has been to develop a single E1 waveform that is a composite of many possible E1 waveforms – drawn around the envelope of all possible waveforms with a high amplitude. Also, the specification might use an envelope of all the corresponding frequency spectra, with the result being that the design spectrum is not the transform of a particular waveform. Beside the specifications being "worse case", the designers of a system might also use a safety margin, to account for unknowns and to help avoid surprises when the system is finally built and tested.

2.18 Effects on Power Grid and Society

Some reasons that E1 HEMP is such a concern for the electric power grid are:

1. The power grid is so important for our modern society. It is so convenient, and yet generally taken for granted. However, as has been shown by the occasional large-area blackouts, society does not function well when there is an outage.
2. An E1 HEMP event can cover a large area at once, simultaneously illuminating the whole area with large disturbing fields.
3. The other parts of HEMP, E2 and E3, will immediately follow the E1 HEMP pulse. There may be synergistic effects due to this. Such effects can be hard to predict, and often each phase of HEMP is studied independently.
4. Other parts of the infrastructure will also be hit by the E1 HEMP. This may directly interrupt them, such as by causing problems with their control systems or causing interruptions in the power grid that might shut them down. There also could be feedback issues, such as needing those other systems to help in restoring the power grid.
5. Blackouts do not always occur at once, but often problems from various parts of the power grid cascade, sometimes slowly, eventually affecting other nearby regions. Under ideal situations, the situation can be brought under control, and the cascading blackout may be contained. However, a massive, wide area E1 HEMP attack would undoubtedly not be an ideal situation, especially if communication systems are adversely affected also.
6. Many systems do not have built-in health-sensing circuits that can detect if there is some damage, if system data has been corrupted, or if the system has been put into an unusual state. This is of concern, for example, for all the control and fault detection systems for the power grid. Would all those circuits be working perfectly when blackouts start to cascade?

7. A major concern is simply that we have not really experienced such an event yet (an E1 HEMP attack), and there is not a good way to simulate such an attack on a widely distributed network.

Some specific hardware concerns are:

1. Low voltage distribution transformers: It has been found that these transformers can suffer pin-hole damage from high level pulses.
2. Insulators on distribution lines: E1 HEMP can initiate an arc over an insulator, which then dumps the AC power to ground. Both wide area simultaneous faults due to the insulator arcs and the fact that AC power may cause damage to some insulators are important aspects of E1 HEMP vulnerability of the power system.
3. Control and sensor systems: The electric power system makes extensive use of automated controls and sensors, such as within power substations. These substations are often unmanned, but besides the local automated controls, they are also connected to manned central stations for collection of data, and to allow some outside control. (SCADA, Supervisory Control And Data Acquisition, is the general term for this.) This involves many electronic devices, such as sensors, computer-like units, and communication devices; and all generally must, by necessity, have attached cables.
4. Central Control: Likewise, the central control facilities would also typically have computers and communication units, with the associated long cabling.
5. Power Generators: The concerns of the last two items also apply to the power generation stations. There is a huge amount of energy involved, such as from burning fuel, hydro, or even nuclear, and there is the concern that E1 HEMP induced voltages might lead to problems in the control systems.

Unlike for E3 (late time HEMP), the high voltage transmission lines themselves are not of especially high concern for E1 HEMP. This is because the very long lengths of these lines do not mean extra high coupling for E1 HEMP – typically E1 coupled signals do not grow much with line length once the length gets up to a kilometer or so. Also, high tension systems tend to be hardier – they already are dealing with high voltages and currents compared to what E1 HEMP can produce. These high voltage lines also often have good lightning protection.

Section 3
A Brief History of E1 HEMP Experiences

The history of nuclear EMP experiences started early, as indicated in Table 3-1. Even before the first actual nuclear explosion, it was recognized that there would be EM effects produced from a burst. However, initially the attempts to postulate the mechanisms, and estimate the fields and effects produced, generally were not very good. HEMP is not an ordinary phenomenon, nor is it similar enough to anything seen before, and so many estimates about it were wrong. Those initial assumptions were used to setup measurement scales, but then during the real tests the HEMP effects turned out to be much stronger. Some test recordings were driven off scale, and so did not produce useful data. Tests were moved underground before all of the mechanisms were completely characterized, and so our measurements of real HEMP fields and effects are very limited, in quantity and quality.

In the 1950's it was recognized that SREMP could be a threat to systems, eventually leading to extensive efforts to harden and test military systems. (It was later that E1 HEMP was also seen to be a bigger problem.) Other countries also showed interest in EMP. The term "radioflash" was initially used for EMP by the British. Russian publications showed it was a concern to them, and they also tried to measure nuclear EMP from their aboveground nuclear tests. Besides the big effort for military systems, there were also efforts for civilian communications systems - Bell telephone, and public broadcast radio; and for the U.S. electric power grid – all spurred on by the government's concern. Gradually EMP efforts fell off in the U.S., especially with the end of the Cold War. With the fall of the Soviet Union there seemed to be less of a threat, and the extra cost of HEMP protection, even if slight, makes it difficult to consider. At the same time HEMP efforts have increased elsewhere, which has resulted in the work of the IEC in HEMP protection for civil equipment.

The early 1960's saw the U.S. and Soviets perform high altitude nuclear tests. For example, the U.S.'s 1962 Starfish test, using a 1.4 MT device at 400 km altitude, produced EMP effects on Hawaii, 1400 km (800 nautical miles) away. HEMP measurements were made, but without an adequate theory, there was difficulty in getting high quality measurements. However, the limited measurements from the tests were enough to help confirm the E1 HEMP theory that eventually was developed. Figure 3-1 shows one of those calculation/measurement comparisons for a high-altitude nuclear test. Waveform A is the E1 HEMP prediction, and "B" is the resulting prediction for what would be recorded in the test, including distortions from the measurement equipment and field distortion from the aircraft carrying the equipment. "C" is the actual measurement recording. The predicted (B) and measured (C) show very good agreement. This confirmation of the theory was done many years later, due to the need to account for the corrupting effects of the measurement systems collecting the E1 HEMP data, and the effects of metallic aircraft carrying that equipment. Once the detailed data for these two effects were collected and properly processed, the measurement results verified the calculations, for the frequency range of the measurement equipment.

Table 3-1. Early historic EMP events. (From Daniel F. Higgins and Conrad L. Longmire, "Input to the EMP Interaction Handbook", MRC-R-345, September 1977.)

EMP Events	
1945	TRINITY EVENT; electronic equipment shielded, reportedly because of Fermi's expectations of EM signals (from collapse of the geoelectric field) from a nuclear burst.
1951-1952	First deliberate EMP observations made by Shuster, Cowan, and Reines.
1952-1953	First British atomic tests; instrumentation failures attributed to "radioflash".
1954	Garwin of LASL proposes prompt gamma-produced Compton currents as primary sources of EMP.
1957	Bethe makes estimate of high-altitude EMP signals using electric dipole model (unturned Compton electrons), getting a vast under-prediction of the field.
1957	Haas makes magnetic field measurements for PLUMBBOB test series (interest in EMP possibly setting off magnetic mines).
1958	Joint British/U.S. meetings begin discussions of system EMP vulnerability and hardness issues.
1958	Kompaneets (USSR) publishes open literature paper on EMP from atomic explosion.
1959	Popham and Taylor of the U.K. present a theory of "radioflash".
1959	First interest in EMP coupling to underground cables of Minuteman missile.
1962	FISHBOWL high-altitude tests; EMP measurements driven off scale; first indications of the magnitude of the high-altitude EMP signal.
1962	Karzas and Latter publish two open literature papers on using EMP signals for detections of nuclear tests; weapon case EMP and hydromagnetic EMP considered.
1963	Open literature calls for EMP hardening of military systems begin to appear.
1963-1964	First EMP simulation experiments carried out by Air Force Weapons Laboratory.
1963-1964	Longmire gives a series of EMP lectures at AFWL; presents detailed theory of ground burst EMP and shows that the peak of the high-altitude EMP signals is explained by magnetic field turning (magnetic dipole signal).
1964	First note in the AFWL EMP notes series published.
1965	Karzas and Latter publish first open literature paper giving high-frequency approximation for the high-altitude magnetic dipole signal.
1967	Construction of the ALECS bounded-wave simulator is completed; to be used in EMP simulation on missiles.

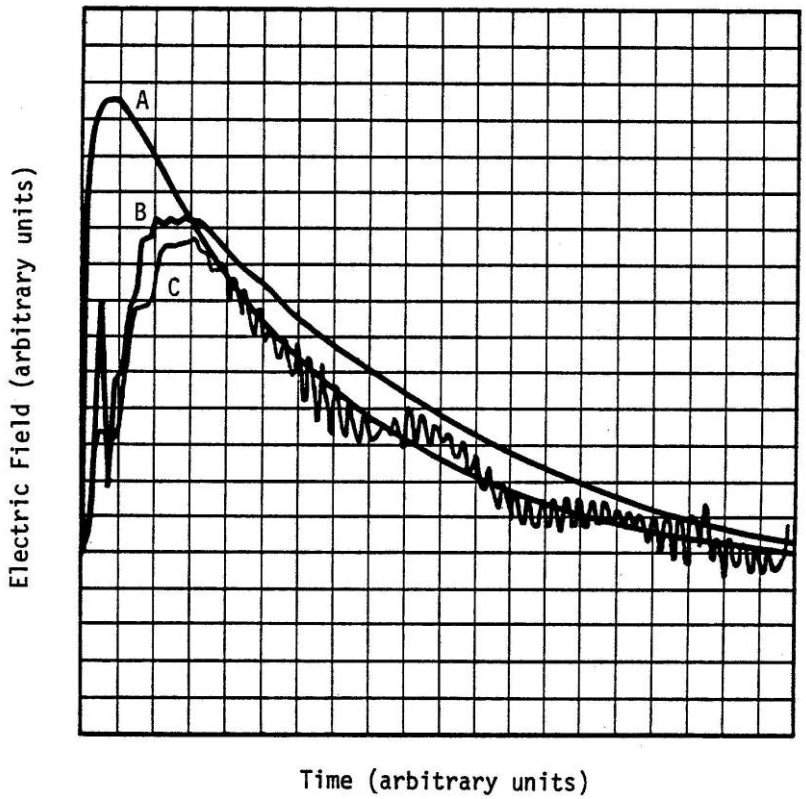

Figure 3-1. Comparison of measured and calculated E1 HEMP signal. "A" is the calculated incident field, and in "B" the effects of the measurement system's distortions are included. These distortions are from the measurement equipment and the antenna (including the metal structure on which the antenna was mounted). "C" is the actual measured E1 HEMP response. (From Daniel F. Higgins and Conrad L. Longmire, "Input to the EMP Interaction Handbook", MRC-R-345, September 1977.)

In the mid 1960s the complete theory (as now accepted) of E1 HEMP was developed, independently by William Karzas and Richard Latter, and Conrad Longmire. After that the theory was refined, and efforts were put into hardening and testing. Numerical codes were developed to calculate HEMP, and numerical fits were found for various parameters involved in the generation process. Generally, the early computer models were constrained by the existing computer resources, and were run on the "supercomputers" of the time. Analytic and numerical models were also developed, and extensively used, to account for EMP coupling to systems.

Much effort was also put into the final step of the HEMP process for system interactions: determining whether a system is disrupted (upset) or damaged by a given HEMP. However, such a system vulnerability evaluation is extremely difficult to do, and attempts at predicting vulnerability levels, and determining in advance where within the system the damage would occur, were typically very inaccurate. Generally tests must be performed instead. Thus, many HEMP simulators were constructed, and test procedures developed. For large size systems, such simulators were large and expensive, and in recent years many have been mothballed.

At the time of the aboveground nuclear tests (1962 and before), our infrastructure and technology in general was significantly different than it is now. Equipment operated at much lower frequencies, was simpler, and this was before the extensive microminiaturization we now have. Equipment generally consisted of tubes, electromechanical devices, and heavy metal cases. There was also not as much automated control of processes. Many aspects of our world today have greatly increased HEMP vulnerability when compared to the technology of the early nuclear age.

A general summary of EMP, and other nuclear effects, can be found in the official U.S. government unclassified textbook on nuclear effects (Samuel Glasstone, "The Effects of Nuclear Weapons"), which has been periodically updated. Various editions reflect the development of HEMP understanding. The 1957 edition has no mention of EMP of any kind, while the 1962 edition does include a little material on EMP. It has only the beginnings of understanding of EMP, especially for E3 HEMP and SREMP. However, some of its material is wrong, and it is very far from being complete. It also has nothing of the theory that would come to be the accepted explanation of E1 HEMP. Finally, the 1977 edition presents a better, and more complete discussion of the various types of EMP, including the accepted explanation for E1 HEMP.

E1 HEMP history contains little experience with real E1 HEMP effects, such as upset and damage to systems. And there is no experience with modern systems. The U.S.'s Starfish test over the Pacific in 1962 did cause some effects in Hawaii, a long distance away from the burst. Figure 3-2 shows the geometry of the test – it can be seen that Hawaii was near the tangent, however some effects were reported:

1. Burglar alarms and air raid sirens went off.
2. Some street lights went off, while others came on. Fuses blew out in some street lights.
3. A microwave telecom system went out.
4. A HF ionosound transmitter was damaged (part of an experiment).

Much later after the tests, analyses of failures were attempted. For street light strings that failed, the failure level was estimated to be about 14 Amps (the normal 60 Hz operating level was 6.6 Amps), while the calculated E1 HEMP coupled current was 140 Amps.

In 1994, Prof. Vladimir Loborev presented results on failures from the Soviet Union's 1962 high altitude tests. Figure 3-3 shows a slide from that presentation (annotated by William Radasky, based on the oral presentation itself) indicating failures. These included:

1. A long, radially oriented, aboveground communication line failed.
2. A buried communication line more than 600 km away from ground zero failed.
3. Power line insulators were damaged, resulting in a short circuit on the line and some lines detaching from the poles and falling to the ground.
4. Diesel generators failed.
5. Antenna systems were affected.

It was thought that later time HEMP contributed to the failures identified in numbers 1 and 2. The other effects are thought to be caused by E1 HEMP.

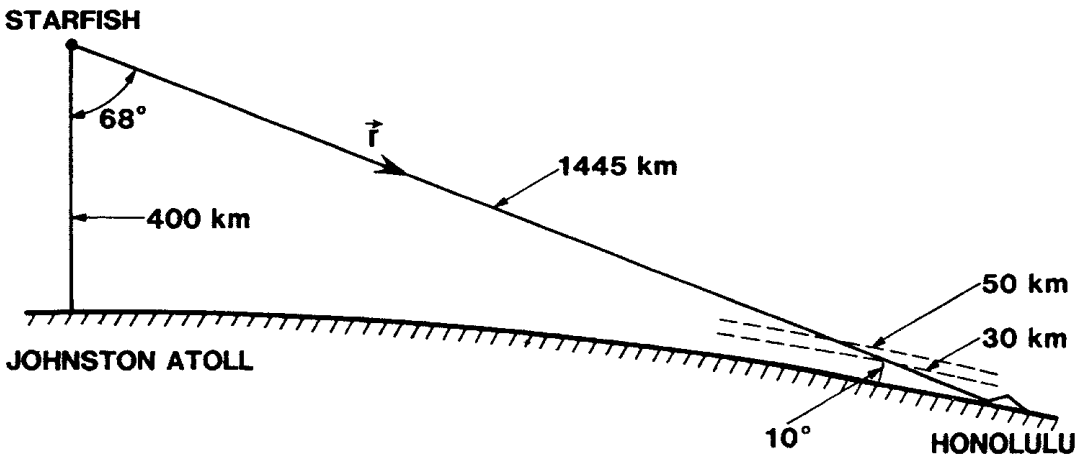

BURST 30 km SW of J.A.
AT 16° 28' N, 169° 38' W

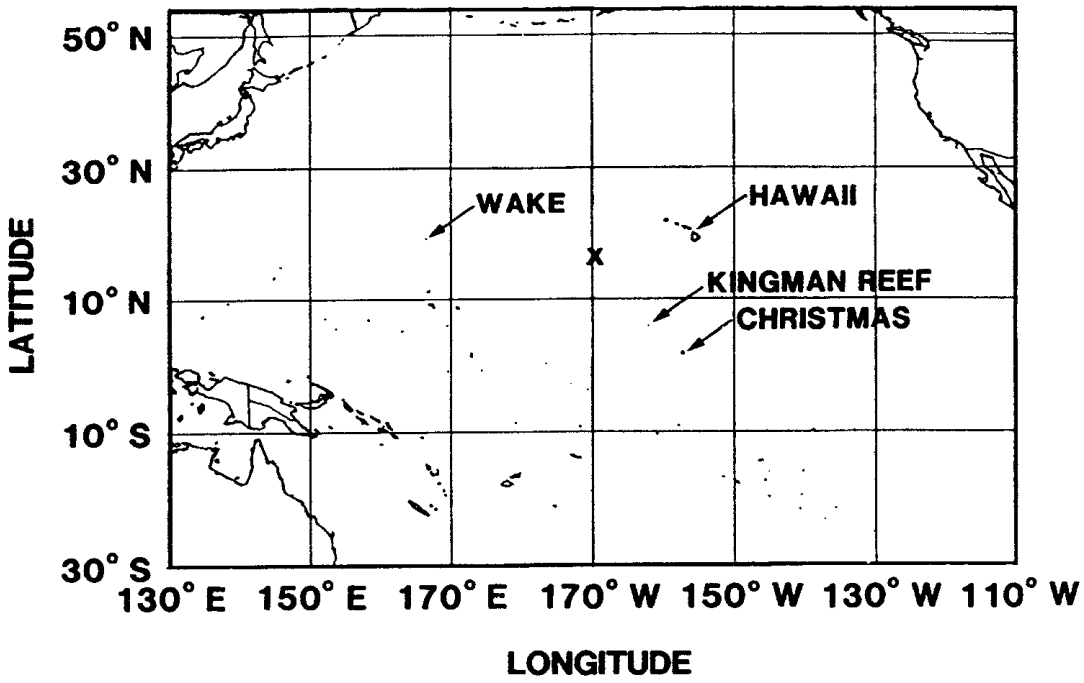

HONOLULU 21.3° N, 157.6° W

JOHNSTON ATOLL 16.6° N, 169.3° W x

Figure 3-2. Geometry of the Starfish test. The "x" shows the burst location. (From: Vittitoe, C., "Did High-Altitude EMP Cause the Hawaiian Streetlight Incident?" Sandia National Laboratories, SAND88-3341, April 1989.)

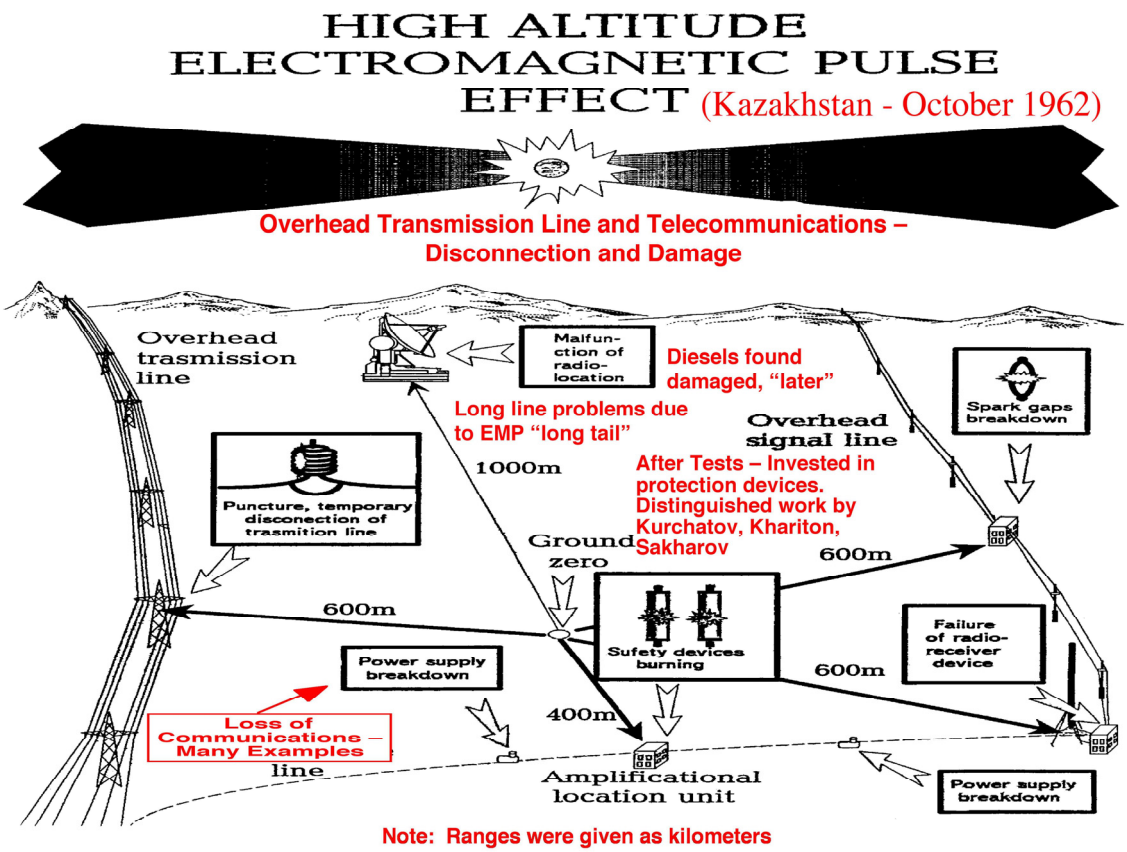

Note: Red text based on Loborev's spoken words in June 1994 as documented by Radasky

Figure 3-3. Soviet HEMP test experience. This presentation slide summarizes effects from the Soviet high altitude test bursts in 1962, as reported by the Russians. (From: "Report of the Commission to Assess the Threat to the United States from Electromagnetic Pulse (EMP) Attack," Vol. 1, Executive Report, 2004.)

Section 4
E1 HEMP Generation and Environments

In this section we present a more detailed discussion of various aspects of E1 HEMP environments. We first give more details on the generation process, and then consider the very important issue of air conductivity. Next we discuss the modeling done in typical computer codes used to calculate the E1 HEMP environments. In the fourth subsection we show a useful and enlightening decomposition of E1 HEMP fields. The fifth subsection looks at the electric field direction for E1 HEMP, and how the differences in directions for the dipole and quadrupole terms mean that there is not perfect east/west symmetry for the vector components of the fields. The final subsection introduces some simplifications made in typical E1 HEMP modeling.

4.1 E1 HEMP Generation

As noted, E1 HEMP is generated by the prompt gammas from a nuclear explosion – about 0.1% of the burst's energy. The gammas travel in an expanding spherical shell, a few meters thick, moving outward at the speed of light. As they get down to lower altitudes, where the atmosphere starts to get denser, collisions with air molecules become more common. This is mostly in the 40-20 km altitude range. These collisions, depicted by Figure 4-1, produce Compton recoil electrons. These electrons have high energy, and are forward-directed on average (away from the burst). (The region where this is happening, about 20 to 40 km in altitude, is called the "source region" for the E1 HEMP.) The forward motion represents a source current, and this results in an electric field aligned with the forward direction. This field, however, is not significant for E1 HEMP on the ground. It stays local to the source region; it does not have the correct geometry to radiate away, and so does not propagate down to the Earth's surface.

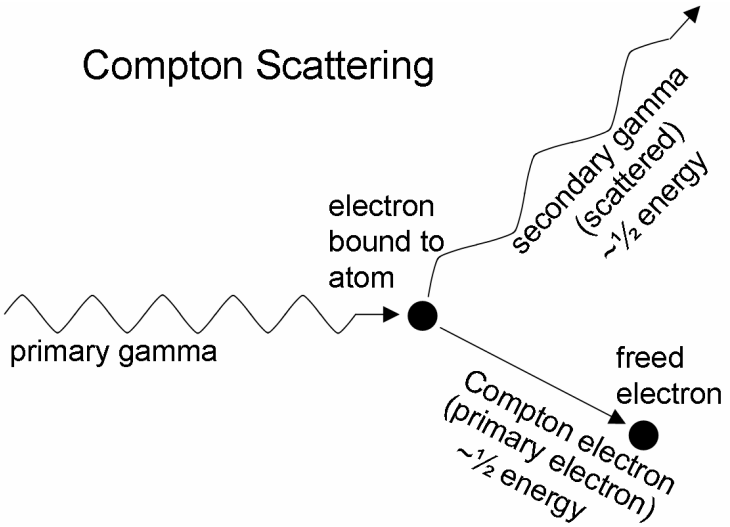

Figure 4-1. Compton scattering. The initial gamma comes in from the left, and strikes an electron in an air atom. This knocks the electron free, with about half the gamma's energy, and the exiting gamma goes off with about the other half. When all of the collisions that occur in this region are considered, the average initial direction of the Compton electrons is forward.

Electrons moving in a magnetic field (the geomagnetic field in this case) are turned coherently to curve away from their initial forward path, as shown in Figure 4-2. This is the important effect for E1 HEMP – the turned part of the electron's path generates a radiated EM field (just like the electric current driven by the transmitter on an AM station's broadcast antenna). This radiated EM field travels outward, away from the burst point – the same direction as the gammas that are traveling outward. And they both are electromagnetic radiation, and so they both travel outward at the speed of light.

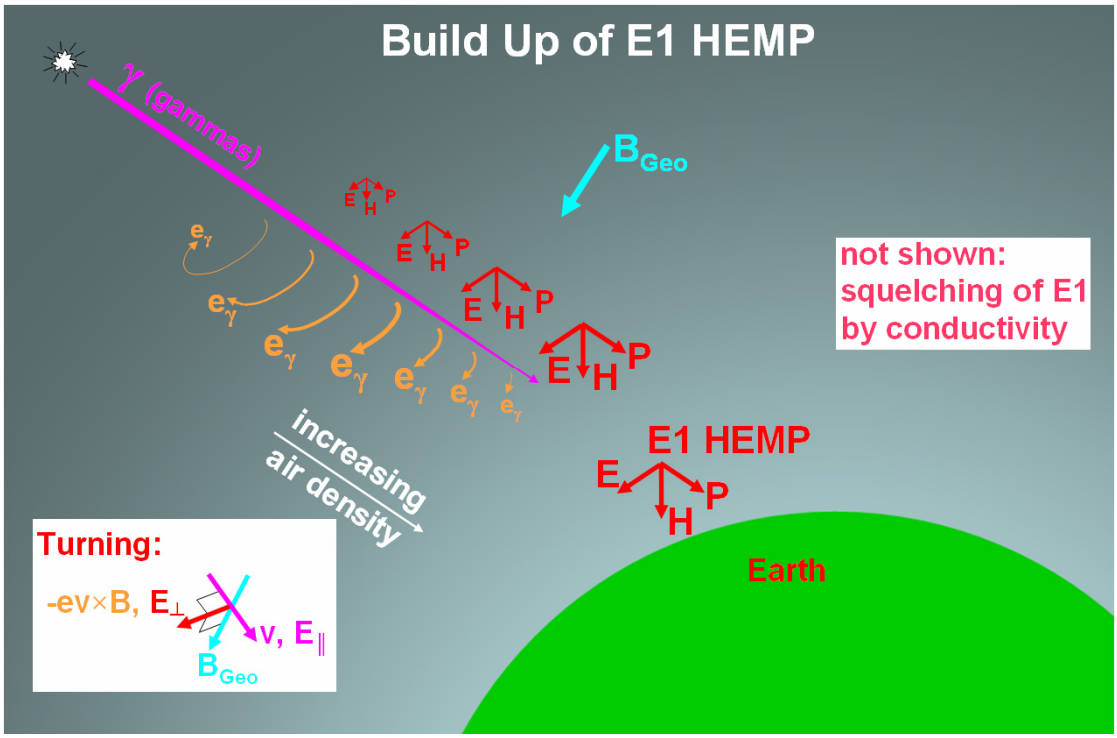

Figure 4-2. Detailed representation of the E1 HEMP generation process. Gammas speed down unaffected in the vacuum of space, until they are low enough to start scattering in the upper atmosphere. Eventually the gamma beam gradually disappears as it transverses more and more air, especially with the increase in air density with lower altitude. Along with scattering that erodes away the gammas, Compton electrons are generated, which turn in the geomagnetic field. The turned path, on average, is longer in thinner air, so there may be more of the spiral path in the higher altitudes than in the lower altitudes. The turned part of the Compton current generates a radiated EM pulse, and this builds up in strength along the burst-observer path (as the gamma beam decreases in its strength). At some altitude the gamma beam is essentially gone, the EM pulse no longer is built up any more, and the EM pulse radiates toward the Earth's surface as a free-field EM wave.

The equal speed for the gammas and E1 HEMP fields is important, because the EM field generated at a small position along the path might not be large, but there is a synchronized phasing effect. Now consider the next point along the path (the process really happens continuously along the path, not in discrete points – it is just easier to think of it in terms of discrete positions along the burst-to-observer path). At this point the process repeats, and more EM field is generated, to propagate toward the observer on Earth – and this new EM field adds onto the EM field that is already propagating by from the previous generation point. This is what is meant by "phased generation" – along 10's of kilometers of path length we have EM fields generated, and these travel down toward

the observer – each adding onto, and strengthening, the EM field that is also passing by from previous generating points along the path already traveled from the burst point. The build-up of the E1 HEMP is represented by the increasingly larger E-H-P vectors in the figure.

Eventually almost all of the gammas will have been attenuated by going through the air (especially with the ever-increasing air density further down in altitude), and there is no more generation and incremental increase of the EM signal. However, the EM signal continues on, heading toward the observer on the Earth. Just as the gammas were a spherical shell moving away from the burst point, the E1 HEMP is also a spherical shell (although, it turns out, not as thin as the few meters of the gamma shell). Air does not significantly attenuate EM fields for the frequencies of HEMP, and so this shell propagates on toward the Earth's surface with only the 1/r (for field strength) spherical divergence.

Historically this primary signal from the E1 HEMP has been called the "dipole term" (or more precisely, "magnetic dipole term") because of the spatial variation of the signal strength – variation of observer position relative to the geomagnetic field line direction.

So, in summary, the gammas generate forward-going source electrons that get turned by the geomagnetic field, producing a transverse current. This current radiates a forward-going EM wave. This occurs all along the ray path through the source region, with a little more EM field added onto the total E1 HEMP signal at each point. This is exactly the same effect as a phased array antenna (except without the frequency sensitivity of the antenna). Such an antenna has several emitting elements, with each sending out an EM wave. For the desired direction and frequency, the signals from each array element have just the right delay so that their oscillatory EM waves perfectly match up, and add together. This phased array build-up is a well-known effect in antenna theory.

Figure 4-3 pictorially shows the E1 HEMP generation process for the dipole term. The top of the left column shows the Compton scatter and forward current. This results in the forward source current and electric field shown below in that column. This E field is not the E1 HEMP (although it cannot be completely ignored in calculations, due to "self-consistency" effects, as we shall see). The next column shows the Compton electrons being turned in the geomagnetic field (represented by the blue "B" vector). This produces electron motion, and an electric field, that is perpendicular to the forward direction and to the geomagnetic field, as shown in the lower box of that column. However, there is another mechanism, and that is induced air conductivity. All the energy being dumped into the air causes a huge quantity of free electrons to eventually be produced, and those electrons then travel in the opposite direction of the electric field terms, as shown in the top of the last column. Then, as shown below that, these conduction currents are oriented in the opposite direction to the original source currents, and thus work against generation of the E1 HEMP field. The green line in Figure 4-4 represents an E1 HEMP that might result if there was no air conductivity. The blue line is a limit imposed by there really being air conductivity, and the red line shows the actual E1 HEMP for this case.

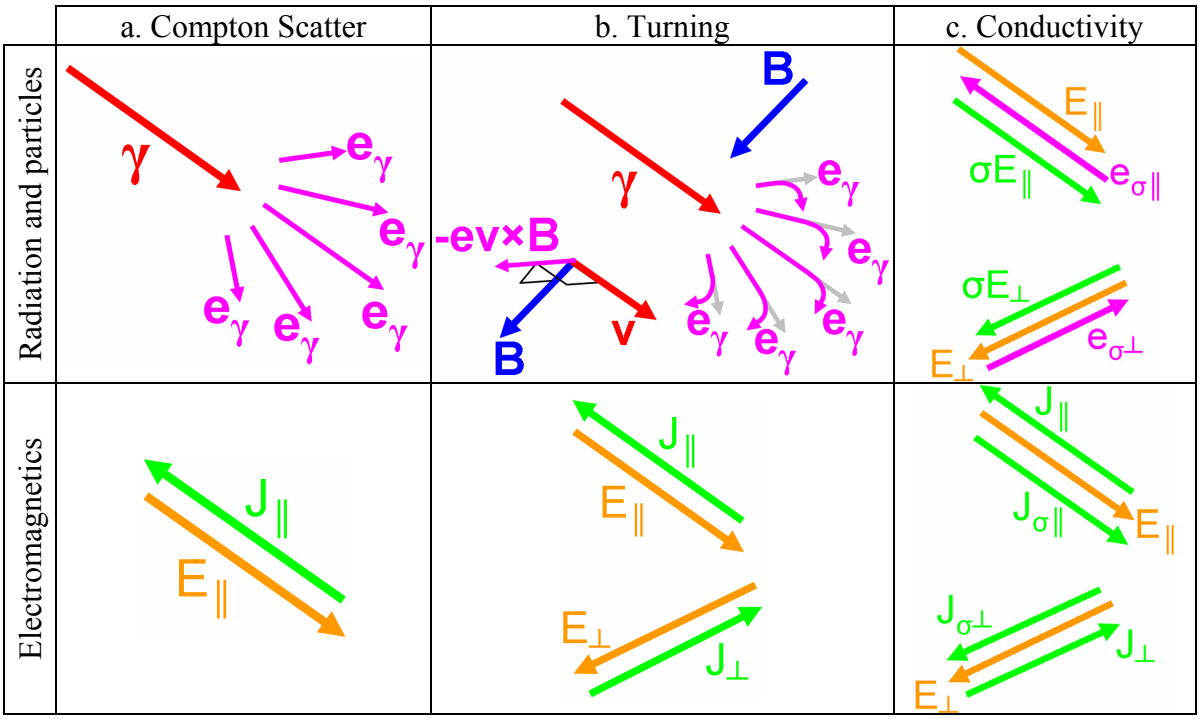

Figure 4-3. Details of the E1 HEMP generation in the source region. Drawing "a" shows the initial Compton scattering, producing a forward (on average) electric source current, which generates a local E field parallel with the burst-observer ray direction. In "b" the Compton electrons come under sideway force due to the motion of their charge in the geomagnetic field. The turning component of their motion is perpendicular to both the geomagnetic field and their forward motion. (The Earth's magnetic field points downward, at the local dip angle, in the northern hemisphere.) In column "c" we show conduction current. As a significant amount of lower energy secondary electrons are produced, air conductivity (σ) is produced, resulting in air currents (σE) directed against the source current.

Looking back at Figure 4-2 again, we show the electrons as having curved paths, not just being turned in only the transverse direction. This is a well-known effect – electrons actually tend to spiral around the B field lines. This is because the initial turned direction is, by construction, exactly perpendicular to the geomagnetic field, and so there is further turning force on the electrons. This leads to another source current term, and another electric field term. This additional term has been traditionally called the quadrupole (or more precisely, electric quadrupole) term. We will discuss this more later.

Finally, Figure 4-5 shows a hypothetical laboratory experiment that might show the E1 EMP generation process. There is a column of air, at the pressure of about the 20 km altitude, with a gamma source shining a beam from the left. We have shown a vacuum on the left, but only because it does not matter if it is air or vacuum there – we assume the air column is thick enough that all the gammas and Compton electrons cannot make it through this column. Also within the column is a magnetic field. An EM field should be emitted out the right side. However, no such test has been done – such a test is not practical – the air column would need to be much too wide to fully simulation E1 HEMP generation.

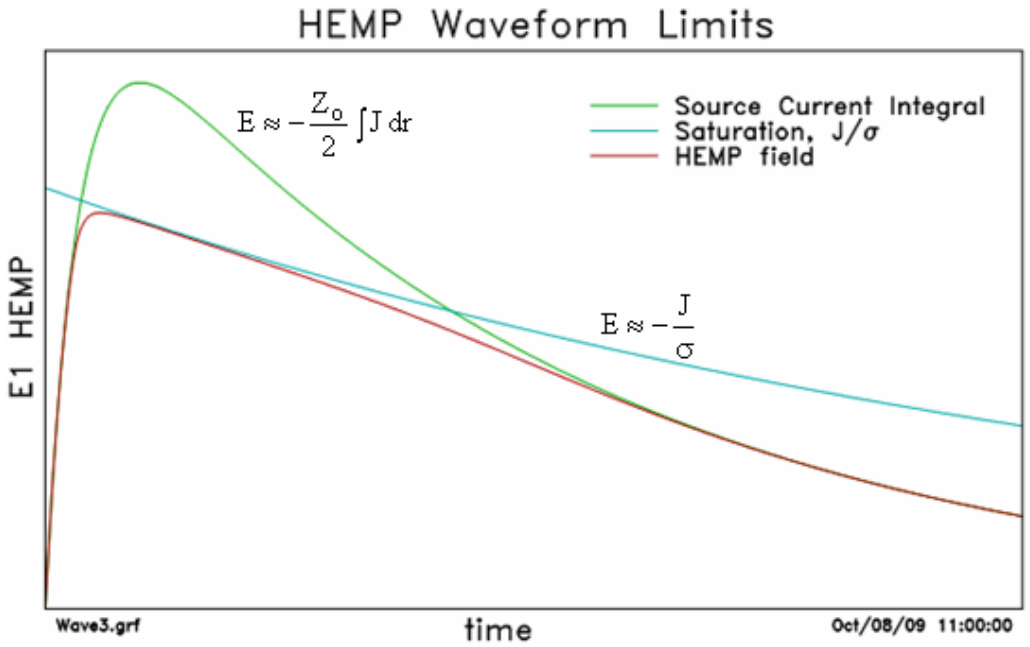

Figure 4-4. Representation of the generation of E1 HEMP. The green line, which has the shape of the incident gamma pulse, shows the electric field if no conductivity is generated. However, conductivity will be generated, and the red line shows the actual E1 electric field – it initially follows the no-conductivity field. However, as the conductivity builds up it gets limited by the saturated electric field, in blue. Later, the driven electric field (green line) has fallen below the saturated field, and starts to follow the red line again.

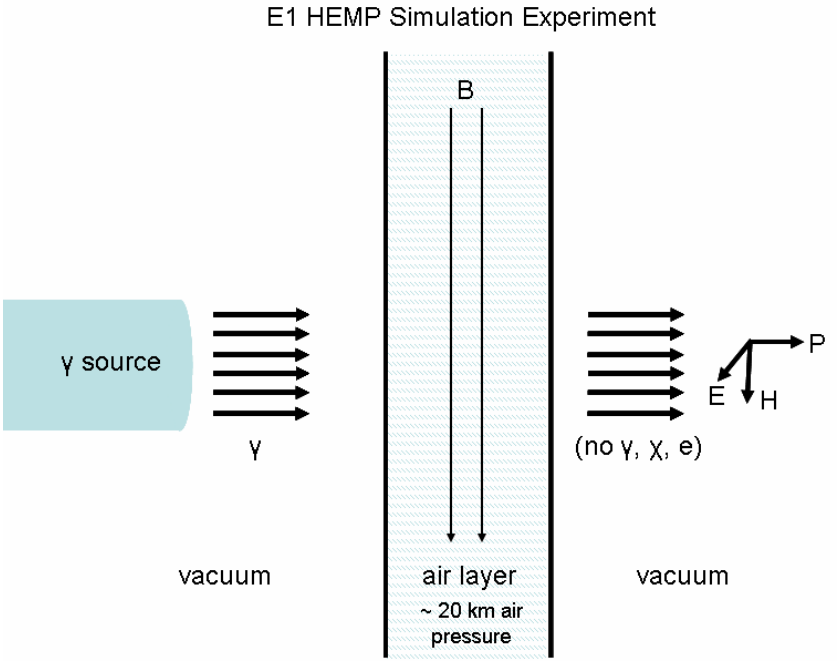

Figure 4-5. Laboratory E1 HEMP generation experiment. This shows an example of a hypothetical laboratory demonstration of the E1 HEMP generation process. A plane wave of gammas is incident on a planar sheet of air, in which there is also a static magnetic field. On the other side of the target sheet of air there is a radiated EM field (to either side of the air sheet there is vacuum, although it could also be air for the right side). Unfortunately, the gamma cross section for air is such that the sheet of air would need to be many kilometers thick to create such as laboratory demonstration.

4.2 Conductivity - Air Chemistry

E1 HEMP is so significant because of the large electromagnetic fields that can be generated. The fields could actually be even much higher, except for air conductivity. Generally air is normally NOT conductive – this allows very high voltage transmission lines as bare wires, without insulation. To be conductive, there needs to be free electrons, stripped away from the air molecules. This can happen if enough of the right type of energy is dumped into the air – resulting in electrons being freed from the molecules. Those freed electrons can move under the force of the electric field – which constitutes conduction current. This air current is in the opposite direction to the Compton current source, and so works to limit the amplitude of the E1 HEMP – the "field saturation" effect. Air conductivity is also seen in other common phenomenon – such as lightning, the air arcs of ESD, and arcing of high voltage insulators in dewy air.

As noted, there are competing effects, the Compton current generating the electric field, and the secondary electrons making conductivity that tries to quench the electric field – this leads to an effect called "saturation" – the electric field tends to be limited from getting too high. Because of the saturation effect due to air conductivity, there is not a large variation in the peak values for E1 HEMP (although, technically, other weapon parameters such as rise time and gamma ray spectrum can influence the actual saturated peak electric field). It may be counter-intuitive, but air conductivity effects lead to the E1 HEMP peak level not being very correlated with device yield. The range in yields for all nuclear bursts can be large, from few kilotons to tens of megatons, but the maximum peak E1 HEMP from all known devices might vary by only about an order of magnitude. And in some cases the peak E1 HEMP from a small yield device can be higher than peak E1 HEMP from another device with much higher yield.

The overall process is complex. Generally air conductivity involves low energy electrons. Such an electron starts accelerating in the electric field, drawing more and more energy from the electric field and getting faster, until randomly, it hits an air molecule – giving up its energy and starting again as a slow electron. However, some electrons have higher energies. The initial ionization is started by the high energy Compton electrons (which are not considered part of the air conductivity themselves) having collisions with air molecules – each such collision freeing an additional electron. These extra electrons are of lower energy, but with a distribution that includes some of high enough energies to also go on and create more ionizing collisions. Also, if the electric field is high enough and the air density low enough, the conduction electrons can accelerate (adding energy to them) enough that they can produce further ionization collisions. This is aptly called "avalanche". This all is important because the number density of freed electrons determines the air conductivity, which usually limits the peak electric field value.

Except for a countering effect, as the gamma pulse dumps more and more total energy into the air, the total number of freed electrons would continue to grow. This would build up the air conductivity to higher levels with time, "shorting out" the generated E1 HEMP field more and more, so that the E1 HEMP would get ever smaller. However, the freed

electrons do not last forever. The electrons end up attaching to a neutral molecule (leaving it a negatively charged ion), or being neutralized by combining with a positively charge molecule (ion). Ions also can move under the influence of the electric field, and so also can be part of the air conductivity. However, since they are so much more massive compared to electrons, they are not very significant until later in time, when their numbers get much higher than the number of electrons.

The term "air chemistry" is used to refer to the processes that control the number density of free electrons and ions. Electrons and positive ions are created (in equal numbers) by ionizations – from collisions of either:

1. Compton electrons.
2. The higher energy fraction of freed electrons from Compton electron collisions.
3. Freed electrons that are accelerated to high enough energy before they collide with an air molecule (called avalanche).

But the electron numbers are also decreased by attaching to a neutral (creating a negative ion) or neutralizing with positive ion (eliminating an electron and a positive ion). Also, there can be a neutralizing collision between a positive and negative ion.

In determining how strong an E1 HEMP might get, one consideration is how strong the original driving source is – the gammas from the burst. However, for E1 HEMP what might be more important is how slowly the air conductivity builds up, relative to the build up of the E1 by the Compton current. The peak of the E1 HEMP tends to be higher for faster build up of the Compton current and for anything that delays the air conductivity build up (for example, E1 HEMP tends to be higher for burst gammas that have higher photon energies).

Let us consider the air conductivity processes in more detail. The burst's downward-going gammas eventually end up being absorbed by the atmosphere. There is a lot of energy being deposited in the air, much of which ultimately ends up stripping electrons off of air molecules. Two processes are very important for the HEMP situation. First is a Compton electron, which is the result of a gamma hitting an air molecule. This electron has high energy, and constitutes the source current that generates electric fields. This is the interaction of photons (of very high energy) with air molecules. The second effect is the interaction of energetic electrons with air molecules. The Compton electron eventually hits an air molecule – such a collision results in loss of some of the original Compton electron's energy, and freeing of an additional electron (this, and additional electrons it later helps create, are called "secondary electrons") with low energy (and leaving the molecule as a positive ion). Generally the low energy freed electron has much less energy than the Compton electron, but some can have significant energy compared to the typically low energy imparted onto the freed electrons by the force of the E field (conduction energy). The freed electrons that have excess energy might continue to strike air molecules, causing further ionization. For those with extra energy (above the electric field induced energy), the additional energy continues to erode until the electron does fully become a "conduction electron" – with energy dominated by the energy from the electric field.

This is a very complex process, and much effort was put into trying to characterize it for EMP studies. A high energy Compton electron gradually loses energy as it repeatedly collides with an air molecule. Each such collision results in an additional freed electron (a secondary), and some loss of energy for the original Compton electron. Typically there is about one initial secondary electron created (one collision) for each 85 eV of energy loss from the Compton electron. Each secondary electron generally has on the order of 10's of eV of energy. However, a few do have higher energies, enough to go on and have more ionizing collisions themselves, producing more freed electrons. It has been found that, after all the higher energy electrons have lost their excess energy, the final set of freed electrons have on the order of 10 eV of energy, and there is about one of these freed electrons produced for each 34 eV of energy lost by the initial primary electron. For a 1 MeV Compton electron this is about 30,000 conduction electrons.

The exact process of the build up of freed electrons by a Compton electron is very important, since more delay generally means higher E1 HEMP levels. The initial Compton electron starts building the E1 HEMP electric field level higher as it turns in the geomagnetic field, while it randomly also starts colliding with air molecules. These collisions happen over some time frame, and involve two effects that diminish the E1 HEMP level. The collisions impede the forward motion of the Compton electron, thus reducing the source current. Also, the collisions generate secondary electrons, contributing to air conductivity, and shorting out of the electric field. The secondary electrons also, over time, lead to more electrons (about 85eV/34eV = 2.5 final electrons per each 85 eV of energy lost). There are time evolutions for these effects, and details of these processes, especially delays to the processes, affect the E1 HEMP level.

Once freed electrons are generated, the "air chemistry" processes come into play. A freed electron does not stay free forever, as there are various processes that work to remove electrons. General EMP studies (for all burst altitudes) account for free electrons, and positive and negative ions (charged air molecules). A free electron can become attached to a neutral oxygen molecule in the two-body process

$$e + O_2 \rightarrow O^- + O \qquad (\text{rate constant } k_1) \quad .$$

Here we show that there is a rate constant that governs how quickly this process can occur. The air chemistry rate constants have values that depend on the air density and electric field. The electric field is important because it affects the average velocity of the conduction electrons – the electrons move under the force of the electric field and accelerate to higher speeds with higher E field. The air density is also important – the lower the air density, the more time between collisions, and so the higher the electron velocity when it finally does collide. Air density also governs the likelihood of a collision – the more air molecules there are to hit, the more likely there is a collision. (This is even truer when it is a three-body collision, such as for SREMP; then the rate constant variation goes as the square of the air density.)

A second air chemistry reaction is dissociative recombination – a freed electron is absorbed by, and neutralizes, a positive air ion, which then splits into separate atoms

$$\begin{aligned} e + O_2^+ &\rightarrow O + O \\ e + N_2^+ &\rightarrow N + N \end{aligned} \qquad \text{(rate constant } k_2\text{)} \quad .$$

Air molecule ions are created when an electron is knocked free (making a positive ion) or when an electron attaches (making a positive ion). These ions can recombine, and neutralize, in a two-body reaction such as

$$\begin{aligned} O_2^- + O_2^+ &\rightarrow O_2 + O_2 \\ O_2^- + N_2^+ &\rightarrow O_2 + N_2 \end{aligned} \qquad \text{(rate constant } k_3\text{)} \quad .$$

Usually EMP studies use the same k_2 and k_3 rate constants for nitrogen and oxygen, since little difference has been found in their values for these two types of molecules.

The air chemistry equations account for the various reactions just discussed:

$$\frac{dN_e}{dt} = S_e + k_a N_e - k_1 N_e - k_2 N_e N_+$$

$$\frac{dN_+}{dt} = S_e + k_a N_e - k_2 N_e N_+ - k_3 N_+ N_-$$

$$\frac{dN_-}{dt} = k_1 N_e - k_3 N_+ N_-$$

where "N" are densities of the charged species (electrons and ions), "Se" is the production rate of free electrons (which drives the equations), and the "k" values are the rate constants already introduced (these are functions of electric field and air density). As noted, the free electrons generally are created with energies of tens of eVs. Once they have participated in the conductivity for a while they tend to have energies governed by the electric field level and the air density (spacing between collision targets). If the electric field is high, and the air density low enough, an electron can build up substantial energy in its travels between collisions – high enough energy to even have an ionization collision, and so generate an additional freed electron. This is, appropriately, called avalanche. It represents another source of conduction electrons besides the collision loss of energy from the primary Compton electrons. We use "k_a" for the avalanche rate constant. Its value is higher for stronger E field and lower air density. It gives the average number of ionizations per freed electron, for a unit of time.

In EMP studies, the air chemistry equations are used to account for the reactions above, including avalanche, and so to calculate the numerical value for the number density of charged species at any time and position: freed electrons, positive ions, and negative ions (as stated, ignoring whether the ions are oxygen or nitrogen). These numbers are then used to calculate air conductivity.

In Maxwell's equations the conduction current is represented by a conductivity "σ", so that the conduction current is proportional to the electric field

$$J_\sigma = \sigma E \quad .$$

The conduction current is also given by the net flow of the free electrons

$$J_\sigma = -e N_e v_e$$

where "e" is the electric charge, "N_e" is the density of free electrons, and "v_e" is their average velocity. As stated above, each electron's acceleration, and so its average velocity, is proportional to the electric field. EMP studies usually use a parameter called "mobility" to account for the process of electrons being accelerated in, and having collisions in, air. Electron mobility, μ_e, is the ratio of average velocity to driving electric field

$$\mu_e = \frac{-v_e}{E} \quad .$$

Conductivity can then be written as

$$J_\sigma = \sigma E = -e N_e v_e \quad \rightarrow \quad \sigma = \frac{-e N_e v_e}{E} = e N_e \mu_e \quad .$$

thus using number density and mobility. The same approach is used for the ions, positive and negative, so that the final air conductivity is taken to be

$$\sigma = e\left(N_e \mu_e + N_- \mu_- + N_+ \mu_+ \right)$$

where, as stated before, the mobility values are essentially the same for oxygen and nitrogen, so we combine them both into total negative (N_-) and positive (N_+) ion densities. Actually, the mobility values are about the same for both polarities of ions also, so typically the conductivity just groups all ions ("I") together, giving

$$\sigma = e\left(N_e \mu_e + N_I \mu_I\right) .$$

The air chemistry rate constants and mobilities are functions of air density and electric field. Lower air density means more acceleration time between collisions, and higher electric fields mean more acceleration force. Also, water vapor means having water molecules present in the air too, and this can have significant effects on the parameters. However, water vapor is often not considered very important for the high altitudes of E1 HEMP generation.

E1 HEMP is only concerned with very early times, and low air density. This means that typically the ions are ignored, as their levels have not yet built up enough to be significant. Thus, only the attachment and avalanche processes are considered.

Studies to characterize the air conductivity processes have been a significant part of E1 HEMP efforts. Air chemistry is especially important for predicting peak field levels, because of the competition between Compton and conduction currents. Anything that could delay the air conductivity could lead to significantly higher field levels. One process of concern involves the electrons freed when a Compton electron collides, and the fact that there is some excess energy that eventually produces more ionization (the extra ~1.5 free electrons per initial secondary). It is important to accurately account for the higher energy secondary electrons. However, in the lab we can only study them indirectly, as we do not have a good method of experimentally simulating E1 HEMP directly.

A major potential source of uncertainty for E1 HEMP calculations is due to various aspects of air conductivity. One aspect of this is that the E1 HEMP peak level depends on how fast the air conductivity turns on. This can be very critical for fast gamma pulses

– the E1 HEMP peak might be higher if the conductivity builds up slower than predicted by our models. Secondary electrons are generated as the Compton electron scatters and losses energy. These initial secondaries have higher energy than truly "free" electrons that are only under the force of the electric field. They go on to scatter and produce more electrons. Even after the scatter they may still leave the collision with more energy than would be associated with accelerating in the electric field. The process of the higher energy electrons gradually producing more electrons constitutes an important delay in the conductivity buildup. Another delay is due to conduction characteristics of the electrons that have excess energy over the average energy that comes from the acceleration of the electric field (being in equilibrium with the electric field). These "hotter" electrons have lower mobility than the average conduction electrons, and so the cooling off of the excess energy also represents a delay in the conductivity build up.

Most of the E1 HEMP calculations that have been made are based on the air chemistry described above where the mobility, and attachment and ionization rates depend on the electric field and air density. Experimental values for the functional dependence of these parameters have been determined by measurements in drift tubes, where the electron velocity distribution has reached an equilibrium with a constant electric field. However, when the electric field is rapidly changing, the assumption that the electron velocity is continually in equilibrium with the electric field is not necessarily a good one, and, for some types of threat weapons, it becomes preferable to use techniques where one does not assume an equilibrium distribution for the freed electrons.

Several more recent approaches are based on starting with the Boltzmann equation in velocity space for secondary electrons. One can take the first three velocity moments and obtain a set of equations known as the swarm model. One can then assume an appropriate form of the distribution as a function of electron energy, and only need to advance five scalar equations in time.

Another approach was taken by Russian authors (Terekhin, V.A., et al., "Development of Modern Techniques for the Calculation of HEMP Parameters Accounting for Non-Linear, Non-Stationary and Kinetic Effects," Sarov Laboratories, Final Report on Subcontract S0303-1021-03, January 2004), who modeled the secondary electron distribution as a function of time and electron velocity as

$$f(t,\vec{v}) = \frac{f_0(t,v)\sqrt{1-\gamma^2}}{1-\vec{\gamma}\cdot\frac{\vec{v}}{v}}$$

where $\vec{\gamma}$ is a measure of the anisotropy of the secondary electrons. This is called the elliptical approximation because the angular portion has the form of an ellipse, with eccentricity γ. In this approach, only the angular distribution is assumed to have a particular form, and finite differencing in scalar velocity (or, equivalently, in energy) is used. The approach is thus intermediate between swarm theory, where only three moments of the distribution are kept, and a full solution of the Boltzmann equation, which would involve differencing in both scalar velocity and angular variables. Both the swarm model and this approach allow secondary electron properties to dynamically

change instead of being in instantaneous equilibrium with the electric field, and generally produce lower air conductivity and higher E1 electric fields. Development of more general Boltzmann techniques based on multipole moments of the angular distribution is currently underway.

Sarov Laboratories recently performed a series of fast non-equilibrium air chemistry experiments using a radiation simulator with an extremely fast pulse x-ray generator, with a FWHM (pulse width – full width at half maximum) of 0.140 nanoseconds (Soldatov, A.V., et al., "Experimental Study of Air Ionization Non-Stationary Kinetics Using Short-Pulsed (0.3-4.0 ns) Gamma Radiation," Sarov Laboratories). This allowed fast air chemistry experiments to be performed at near atmospheric pressure in a small volume. The x-ray pulse is sent into a three-electrode pie-pan sensor. The central conductor is held at a potential with respect to the outer electrodes so that electric fields in opposite directions result in the two chambers of the sensor. This design causes the directional high energy electron flux to produce equal and opposite response on the two sides of the central electrode so that the measured response should be due only to the air conductivity, and not to the current produced by high energy photoelectrons. When the experiments are analyzed with the usual equilibrium air chemistry, the air conductivity rises much too rapidly, as shown in Figure 4-6 – compare the dashed lines (predicted results) to the same color solid lines (measured results). Changing to a model where the newly created secondary electrons are assumed to have a lower mobility (representing higher energy electrons) produces much better agreement, as seen in Figure 4-7. But this is an ad-hoc procedure, and shows the need for first-principle improvements in the air chemistry treatment for very rapidly rising radiation sources.

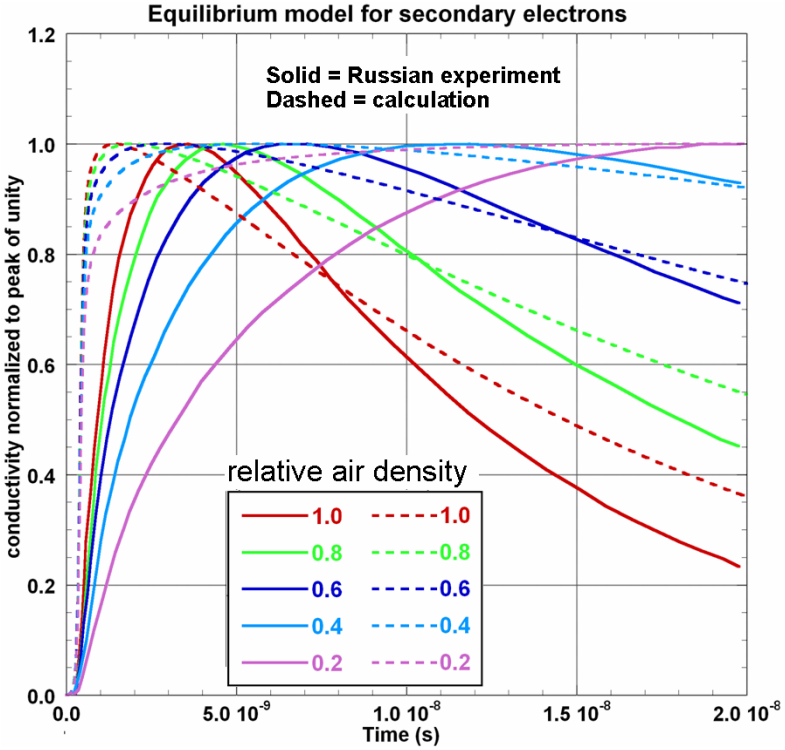

Figure 4-6. Air conductivity calculated with equilibrium secondary electron model.

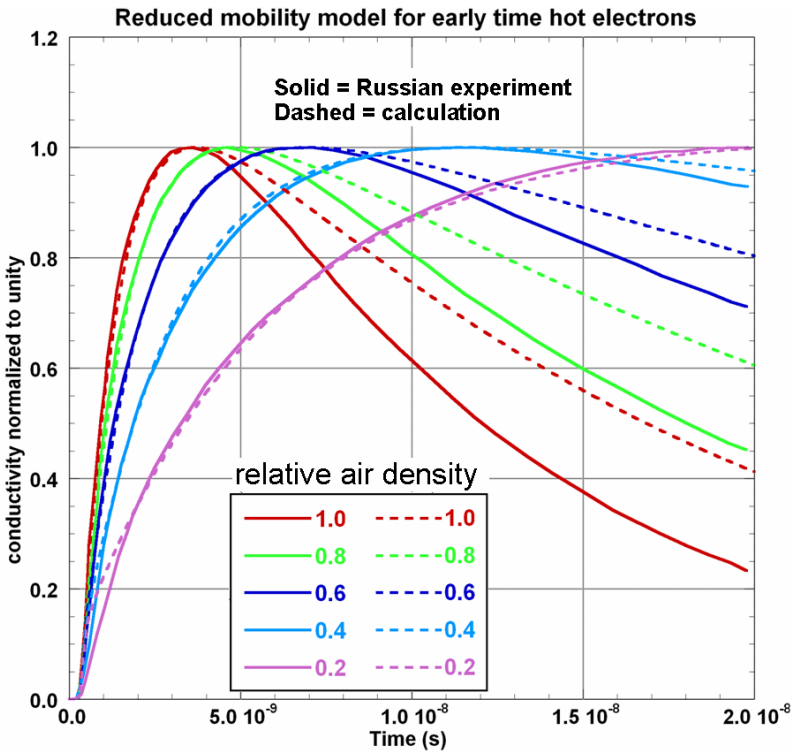

Figure 4-7. Air conductivity calculated with early-time hot secondary electron model.

4.3 E1 HEMP Modeling

The E1 HEMP generation process is complex enough that good calculations of predicted E1 HEMP fields require computer modeling. Development of such models began in the late 1960's, and the models were refined over many years. In the early days the models stretched the limits of the available computer resources, although decades later this is no longer a problem. The models used a combination of techniques to calculate the E1 HEMP field radiated toward an observer on the Earth's surface. Dynamic equations used finite differences for their differential equations (the motion of energetic electrons, electromagnetic fields, and air conductivity). Standard analytic formulas were used for some effects, such as gamma scattering and the drag force on energetic electrons. Fits were found, using experimental data, for parameters such as air chemistry rate constants. Special approximations were developed for some processes, such as accounting for the multiple scatterings of Compton electrons. Modeling was based on analytic and experimental work, but typically the computer resource limits of the time could not be ignored. The most complex parts of the E1 HEMP process are:

1. The behavior of the Compton electrons in the time varying HEMP field (for the current source and the driver for generating free electrons).
2. The behavior of the secondary electrons (for air conductivity).

For the Compton electrons a "macro-particle" approach is used today. At each time step in a finite difference implementation there would be very many Compton electrons

generated; instead we collapse them down into a small number of particles (with weighting according to how many electrons each macro-particle represents). For the secondary electrons only a single "average" electron is modeled, although with some special coding added to account for special effects.

The first three E1 HEMP codes created were at AFWL, HDL and Sandia Corporation by 1967. The work at AFWL continued (now AFRL) with HEMP and HEMP-B, and MRC developed a code known as CHAP in 1971. In 1984 Metatech extended the development of HEMP-B from AFWL and added physics improvements, including the treatment of x-ray currents and conductivities, in a code known as METAHEMP. Today the METAHEMP code is active at Metatech Corporation and some older versions of HEMP-B and CHAP are being used at LANL and LLNL national labs.

Often x rays have been ignored in E1 HEMP calculations. It is just the small fraction of the x rays that have higher energies that are of concern (the low energy ones are absorbed nearer to the burst than the source region). For E1 HEMP the x rays are like gammas, but with some differences in parameters. They scatter more readily, so they do not travel as far as gammas. Also, the electrons produced by scattering (photoelectrons) tend to scatter more in the transverse direction and not in the predominately forward direction of gamma (Compton) scatters. Thus x-ray effects tend to happen on the upper side of the source region, and not contribute much to the source current. However, they can produce significant ionization, contributing to air conductivity. How they affect the E1 HEMP signal depends on their time histories and their spectrum. Two approaches have been used to add x rays to E1 HEMP codes. A direct approach is to model them similarly to the gammas, but with parameters appropriate for their photon energies. This uses extra computer resources, but this is much less of a concern for modern computers. Another approach uses numerical fits for the ionization (air conductivity source) generated by x rays – ignoring any slight current source contribution, and any field self-consistency effects for the photoelectrons.

Figure 4-8 shows a pictorial view of the E1 HEMP process, and so indicates what needs to be modeled. The burst (on left) sends out gammas (γ) and x rays (x). We will generally confine our discussion to the gammas, which are much more important. The gammas interact with air, producing the current source (J) and air conductivity (σ). The geomagnetic field (B_{Geo}) and air density (ρ_{Atm}) affect this. J produces the electromagnetic fields (electric, E and magnetic, H), as modified by the σ. There is self-consistency (feedback) in that the fields go back to affect the source current and conductivity. Part of the electromagnetic field is just local, and part is what propagates down as the radiated field that becomes the E1 HEMP that is seen on the ground.

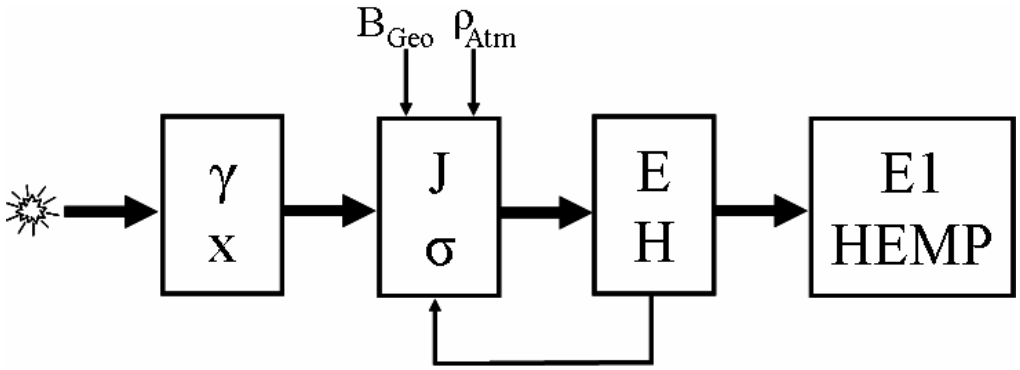

Figure 4-8. Overview of E1 HEMP generation theory terms. Gammas (and x rays, of less importance) interact with the air (with its variation of density, ρ_{Atm}, with altitude), producing source current (from the geomagnetic field, B_{Geo}, turning the Compton electrons) and conductivity. The current generates the electromagnetic field (E and H), as moderated by the conductivity. The EM field propagates away as the E1 HEMP.

Figure 4-9 shows the beginning of the process in more detail – the generation of the source current and conductivity (using just the gammas in this case). The gammas generate Compton electrons (e_γ). These are influenced by the electromagnetic fields (E, H) that are being generated and by the geomagnetic field (B_{Geo}), with air density (ρ_{Atm}) as a parameter. The net motion of all the Compton electrons gives the source current (J). Energy loss of the Compton electrons is an initial source (S_e) of secondary electrons. With some delay, more freed electrons are generated. Air density is a factor in this delay. The production of freed electrons feeds into the air chemistry model, which is concerned with the density of electrons (N_e) and positive and negative ions (N_+ and N_-). The electric field level and air density affects these processes. Separately, we also need the mobilities (μ), which also depend on the electric field level and air density. For E1 HEMP we typically ignore the ions, and only account for the free electrons. From the electron density and mobility we get the air conductivity.

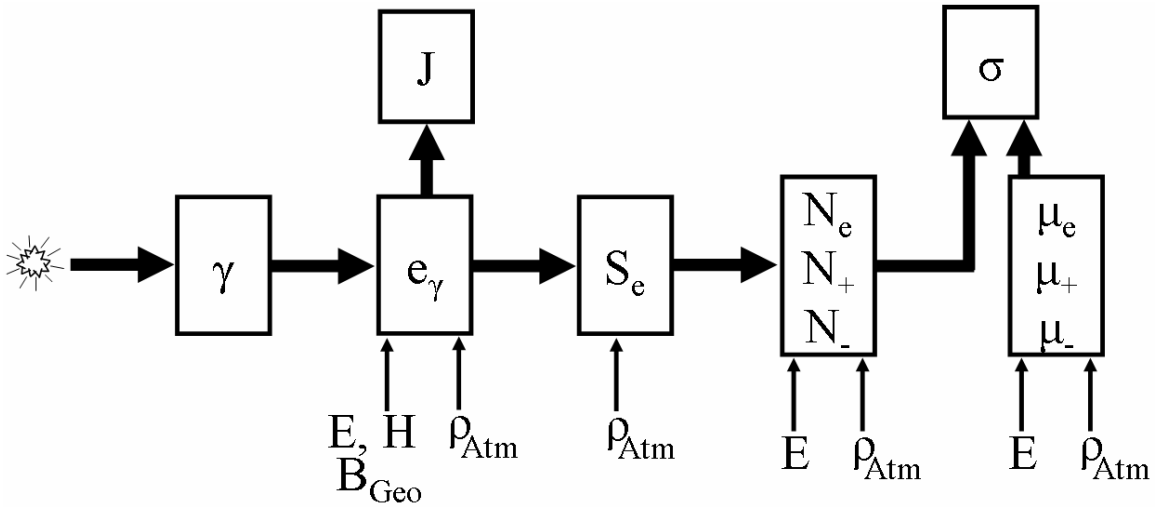

Figure 4-9. Overview of the source and conductivity terms, including air chemistry. The source current (J) and the air conductivity (σ) are the outputs. The burst gammas are the driver, with the air density (ρ_{Atm}) and geomagnetic field (B_{Geo}) as parameters. There is feedback from the generated electric (E) and magnetic (H) fields.

Computer models are needed for all the processes just discussed. Table 4-1 lists some of the modeling used for E1 HEMP codes. First we will consider the electromagnetics aspect of the generation of E1 HEMP.

Table 4-1. Summary of E1 HEMP generation modeling.

E1 HEMP Calculations		
Entity	Significance	Modeling
Gammas	Source of Compton electrons	Gamma beam intensity at each source region point: Waveform from burst output. Several energy bins for burst output spectrum. Beam attenuated by scattering. But add in extra effect for gammas from small-angle scatters (ignore most scattered gammas - large angle scatters and multiple scatters have much longer path, too far behind and too late). Klein-Nishina formula for scattering.
Compton electrons	Source current. Energy loss generates free electrons	Macro-particles: Compress all Compton electrons into fewer sample particles - several angle bins for Compton electrons in different directions. Advance in time according to forces of electric and magnetic fields. Multiple scatters lead to spread in directions, less forward range: obliquity factor or Monte Carlo simulation (average about ⅔ of extreme range). Compton current source: $J = e\sum N_C v_C$ (N_C = macro particle weight) Energy loss (Bethe formula for drag force) leads to ionization.
Free electrons	Conductivity	Every 85 eV of Bethe energy loss gives an initial conduction electron. Full ionization delayed as higher energy electrons scatter (formative time lag) – final ionization is about 2.5 electrons per 85 eV lost. Air chemistry for electrons: attachment and avalanche (using rate parameters that are a function of electric field and air density).
Electro-magnetics	Propagating E1 HEMP	Maxwell's equations. Finite difference. Retarded time. Inward and outward going waves. Source current from macro-particles and their velocity. Air conductivity from electron density (air chemistry) and electron mobility (electron mobility = function of electric field and air density).

For modeling the electromagnetics, Maxwell's equations are used. In the following we provide a standard derivation (from Conrad Longmire) of the electromagnetic essence of E1 HEMP. For simplicity, we approximate the situation as a planar geometry, as shown in Figure 4-10 (Karzas and Latter developed equivalent results using the more appropriate spherical geometry). In this case the gammas from the explosion are going straight down, and the geomagnetic field is into the page. The initial forward Compton electrons generate an E_Z (downward). The turned electrons go to the left, and generate E_X (which becomes the E1 HEMP). This E field has an associated magnetic field, H_Y (into the page).

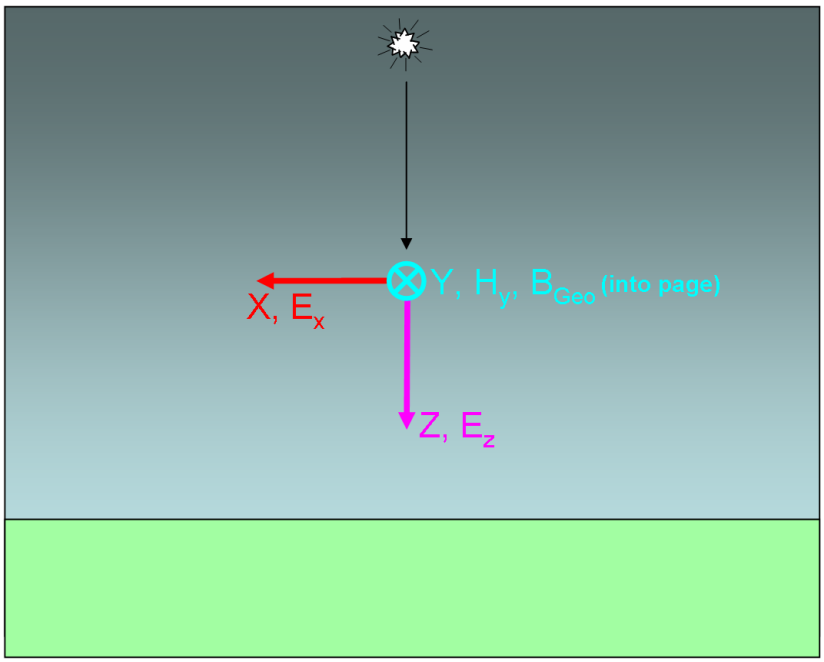

Figure 4-10. Terms and vector directions for the E1 HEMP equation derivation.

Maxwell's equations for the case are:

$$\mu_o \frac{\partial H_y}{\partial t} = -\frac{\partial E_x}{\partial z}$$

$$\varepsilon_o \frac{\partial E_x}{\partial t} + \sigma E_x + J_x^c = -\frac{\partial H_y}{\partial z}$$

$$\varepsilon_o \frac{\partial E_z}{\partial t} + \sigma E_z + J_z^c = 0 \ .$$

Besides the fields already mentioned, there is the source currents from the initial Compton electrons (J_z^c) and from their turning (J_x^c). There is also air conductivity (σ), which builds up from the energy loss of the Compton electrons.

Next some transformations of variables are used. The first is the use of "retarded time"

$$\tau = ct - z$$

which is a time scale that is synchronized with waves (the gammas and electromagnetic fields) moving downward with the speed of light. The other transformation replaces two of the field components with

$$F = E_x + Z_o H_y$$

$$G = E_x - Z_o H_y$$

where "F" is the outward (or downward) going wave, and "G" is the inward (or upward) going wave. F will become the E1 HEMP that propagates down to the Earth. The traditional fields can be reconstructed from

$$E_x = \frac{F+G}{2}.$$

$$H_y = \frac{F - G}{2 Z_o}.$$

With the retarded time transform the derivatives change as

$$\frac{1}{c}\frac{\partial}{\partial t} \rightarrow = \frac{\partial}{\partial \tau}$$

$$\frac{\partial}{\partial z} \rightarrow \frac{\partial}{\partial t} - \frac{\partial}{\partial \tau}.$$

And putting in the inward and outward waves, Maxwell's equations become:

$$\frac{\partial F}{\partial z} + \frac{\sigma Z_o F}{2} = -Z_o J_x^c - \frac{\sigma Z_o G}{2}$$

$$\frac{\partial G}{\partial \tau} + \frac{\sigma Z_o G}{4} = -\frac{1}{2}\frac{\partial G}{\partial z} - \frac{Z_o J_x^c}{2} - \frac{\sigma Z_o F}{4}$$

$$\frac{\partial E_z}{\partial tz} + \sigma Z_o E_z = -Z_o J_z^c.$$

These are exact transforms of Maxwell's equations given above – no approximation has been applied.

Note that the equations are separated into sets. The third only involves E_Z and J_Z and is independent of the first two. This is just the local electric field (with no associated magnetic field), due to the separation of charge produced by the Compton scattering knocking electrons in the forward direction. This does not propagate away from the source region. We can ignore E_Z for the rest of this discussion. It is, however, important when doing a full calculation of E1 HEMP, because of self-consistency: the electric field acts on the Compton electrons, thus affecting the source current, and also affects the average energy of conduction electrons, which in turn affects parameters in the "air chemistry" used to calculate air conductivity.

For very early time the air conductivity has not built up yet, so those terms can be dropped, and the remaining E1 HEMP equations become

$$\frac{\partial F}{\partial z} = -Z_o J_x^c$$

$$\frac{\partial G}{\partial \tau} = -\frac{1}{2}\frac{\partial G}{\partial z} - \frac{Z_o J_x^c}{2}.$$

The first one shows that the forward wave starts to build up as

$$F(z,\tau) \cong -Z_o \int_0^z J(z',\tau)\,dz' \quad .$$

As the conductivity and electric field build up, the conduction current (σE) can become significant, and if it dominates, the first equation instead is approximately

$$\frac{\partial F}{\partial z} + \frac{\sigma Z_o F}{2} = 0$$

where we have also assumed that the upward wave, G, is not significant. Under these conditions the forward wave is given by

$$F(z,\tau) \cong -\frac{2\,J(z,\tau)}{\sigma(z,\tau)} \quad .$$

This is the saturation condition. Except for very low gamma output bursts, or very far distances from the burst (such as high HOB), saturation typically does occur. It tends to limit the strength of E1 HEMP. It is also the reason that, even with more than three orders of magnitude variation in burst total yield, the values of the largest E1 HEMP field from nuclear bursts have much less variation.

Now consider the upward going wave, G. The downward wave (F), with only a spatial derivative in z (altitude), builds up over distances of about a scale height of the exponentially increasing air density (scale height is the distance over which the atmosphere density changes by an e-folding, e^{-1}, and is about 7 kilometers in the lower atmosphere). However, the outward wave (G) equation has a retarded time derivative, and this dominates. This represents a wave buildup over the retarded time width of the pulse, which is only a few meters – much shorter than the build-up distance for the F term. This means G is much smaller than F. For example, a 50 nanosecond pulse has a spatial width of 15 meters ($c\,\Delta t = 3\times10^{8} * 50\times10^{-9} = 15$ meters). With the insignificant spatial derivative removed, the G equations becomes

$$\frac{\partial G}{\partial \tau} + \frac{\sigma Z_o G}{4} = -\frac{Z_o J_x^c}{2} - \frac{\sigma Z_o F}{4} \quad .$$

Thus the upward wave is driven by the turned current and F's conduction current (the drivers on the right side of the equations), while air conductivity resists the build-up of G (just as for F; the σG on the left side). However, if there is saturation of the F term, then, as discussed above, the current and F are directly related as

$$J_x^c \cong -\frac{\sigma F}{2} \quad .$$

Then the driver term (right hand side) for G then becomes

$$\frac{Z_o J_x^c}{2} + \frac{\sigma Z_o F}{4} \cong 0$$

thus the driver for G is zero, and so this is another reason for G not getting big. Thus G does not build up to any significant level

$$G \cong 0 \quad .$$

With G zero, the transformations then give

$$F \cong 2E_x$$

$$E_x \cong Z_o H_y \quad .$$

The second equation is that of a propagating electromagnetic plane wave.

Going back to Maxwell's equation for F (with G=0) and transforming back to the electric field term, we get

$$2\frac{\partial E_x}{\partial z} + \sigma Z_o E_x = -Z_o J_x^c \quad .$$

This is the standard E1 HEMP result – it is called the outgoing-wave approximation, or the high-frequency approximation. The early time approximate solution for this is

$$E_x \cong -\frac{Z_o}{2}\int_0^z J_x \, dz' \quad .$$

(Karzas and Latter's corresponding spherical geometry result is

$$E \cong -\frac{Z_o}{2r}\int_0^r r' J \, dr' .)$$

and the saturated field approximation result is

$$E_x \cong -\frac{J_x}{\sigma} \quad .$$

These equations can be used to explain E1 HEMP, and check results, but computer code modeling of E1 HEMP usually uses the full set of Maxwell's equations. This is needed to include self-consistency – the electromagnetic field effects on the source currents and air conductivity.

Standard E1 HEMP codes use retarded time and inward/outward going waves, as shown in the initial part of the derivation above. However, usually such codes are also "self-consistent", which means:

1. The Compton electrons respond to the force of the local electric and magnetic fields generated by the nuclear output (they do not just respond to the geomagnetic field).
2. The air chemistry parameters are allowed to be functions of the electric field.

Thus, the upward going wave, which is part of the total fields in the source region, is not ignored. For computer solutions, the only approximation used for Maxwell's equation is ignoring the spatial derivatives with angle.

As mentioned before, for E1 HEMP typically the air chemistry is simplified by only accounting for the electrons (ignoring ions), so that the only air chemistry equation used is

$$\frac{dN_e}{dt} = S_e + k_a N_e - k_1 N_e \quad .$$

And then the air conductivity is calculated as

$$\sigma = e N_e \mu_e \quad .$$

Finite differencing is used for the air chemistry equation – calculating the free electron density with S_e as the producer of free electrons from energy loss of the Compton electrons; k_1 is the rate for attachment to neutral air molecules, and k_a is for avalanche. A major difficulty is determining the free electron source term, S_e.

The other difficult part is defining the source current, J. In simple terms the source is the sum of the velocity of all the Compton electrons in a unit volume, times the electron charge (a negative value). To use this, we need to account for Compton electrons. In the codes this is done by using "macroparticles". Compton electrons are sent out in all directions (although, on the average in the forward direction). The Compton electrons have different initial energies (correlated with scattering angle), and are affected differently according to their motion relative to the forces of the local electric and magnetic fields. But we cannot model each single electron. Instead we divide the scatter space into bins, and group all the Compton electrons within each bin into a single electron (a macroparticle) that represents, on average, all the electrons in that initial bin. Thus, for each time point (using finite difference), there might be 10 to 20 macroparticles that are generated. The code then follows each particle forward in time. A true electron would have random scatters through time and space, plus the acceleration/deceleration of the electric field, and turning by the magnetic field. For the macroparticles the random effects are put into an average behavior instead.

With this approach, the source current is simply

$$J = e\sum N_C v_C$$

where N_C represents the weight of each macroparticle, indicating how many Compton electrons each one represents. The weight values vary with the time waveform of the burst's gamma output, and the amplitude of the gammas that have not been scattered in getting to the position (all simple analytic calculations). However, for extra accuracy, generally there is also a factor included to help account for gammas that may have gone through small angle scatters (gammas with large scatters would be delayed too much in time to be of interest for E1 HEMP).

The macroparticles are governed by the relativistic equations of motion (using finite differencing). Also, Bethe's formula for average energy loss is used. This is a "drag force" for the motion – the particles slow down with the loss of energy associated with the Compton electrons scattering many times. Such scattering also represents some randomization in their motion, which lessens their forward motion (and so the Compton source current). This is handled by an approximate approach termed the "obliquity factor". All of this is calculated in retarded time, which requires care in setting up the equations.

The energy loss (Bethe drag) is also used to increase the electron density – as a source of one new freed electron for each 85 eV of lost energy. Although, as noted, eventually 1.5 more electrons will be freed per each initial electron. The timing of this generation of additional ionization has been studied, and a fit developed for the processing. The term "formative time lag" is associated with this. The waveform of the extra ionization has been fit to simple differential equations, so simple finite differencing may be used in the computer calculation to account for it.

The air chemistry equation for the electron density is carried forward with finite differencing. Analytic fits to experimental data are used to determined rate constants and electron mobility. From these, the air conductivity is calculated, and, with the source

current, the finite differenced Maxwell's equations can be advanced in time and space (down the ray).

4.4 E1 HEMP Decomposition

In this section we discuss E1 HEMP signals in a way that is both illustrative and useful. We derive a result that decomposes E1 HEMP so that some functional variations are readily seen. This derivation does not provide a way to calculate E1 HEMP directly, but its usefulness will become apparent. Initially we will just consider the early part of E1 HEMP, when conductivity can be ignored. Previously we showed that the field is approximately

$$\bar{E} = -\frac{Z_o}{2}\int \bar{J}\, dz \quad .$$

We will approximate the integral as the Compton current times some representative length, Δz

$$\bar{E} = -\frac{Z_o}{2}\bar{J}\,\Delta z$$

where J is the turned source current.

Now consider the turned current. The Lorentz force on an electron is given by its charge (e), velocity ($\bar{v}_0$), and the magnetic field (B – such as the geomagnetic field). This force causes acceleration of the electron (of mass "m") in the turned direction, leading to turned velocity $\bar{v}_1$

$$\bar{F}_1 = -e\left(\bar{v}_0 \times \bar{B}\right) = m\frac{d\bar{v}_1}{dt} \quad .$$

So that the turned velocity is

$$\bar{v}_1 = -\frac{e}{m}\int\left(\bar{v}_0 \times \bar{B}\right)dt$$

$$= -\frac{e}{m}\left(\bar{v}_0 \times \bar{B}\right)\Delta t$$

$$= -\frac{e}{m} v_0 B_{Geo}\,\Delta t\,\left(\hat{r} \times \hat{b}\right)$$

where we are using unit vectors (lower case, with "hats" above) to represent the direction of the various vector quantities

$$\bar{v}_0 = v_0\,\hat{r}$$

$$\bar{B} = B_{Geo}\,\hat{b}\,.$$

As before, we have simply replaced the integral by some representative time, Δt. The total turned current is given by the number of Compton electrons, N, their velocity, and the electron charge

$$\bar{J}_1 = -e\,N\,\bar{v}_1$$

$$= e\frac{e}{m} N\, v_0\, B_{Geo}\,\Delta t\,\left(\hat{r} \times \hat{b}\right).$$

Thus the turned current is proportional to the number and forward velocity of the Compton electrons, the geomagnetic field strength, and the cross product of the ray direction and B field direction. This cross product gives a direction, perpendicular to the ray and B, and an amplitude given as the sine of the angle between those two vectors.

Using this current and the form of the initial electric field from the high-frequency approximation we get

$$\bar{E}_1 = -\frac{Z_o}{2}\bar{J}_1\,\Delta z$$

$$= -\frac{Z_o}{2} e \frac{e}{m} N\, v_0\, B_{Geo}\, \Delta t\, \Delta z \left(\hat{r}\times\hat{b}\right).$$

(This is the E1 HEMP dipole term.) As a reminder, Table 4-2 shows the polarity of turned quantities: electron velocity, electric field, and source current. These are formed from the vector from the burst to the observer (the ray, direction $\hat{r}$), and the geomagnetic field in the source region (direction $\hat{b}$). Note that the Earth's north pole is the "north seeking" pole, and so is the south pole of the Earth's magnetic field. The geomagnetic field polarity is such that the field lines point from the south to the north. Using the standard "right hand rule" for the cross product gives the source current direction; the opposite direction (from the minus sign), or "left hand rule", gives the source electron and electric field direction.

Table 4-2. Vector directions for turned quantities.

Positive Directions	
$-\hat{r}\times\hat{b}$	$\hat{r}\times\hat{b}$
Left hand rule	Right hand rule
v_e, E	J
$\hat{r}$ = direction from the burst to the observer.	
$\hat{b}$ = direction of the geomagnetic field (it points down in the northern hemisphere).	

Now we will consider the same process for the second turning. Remember that the first-turn electron will also see the geomagnetic field – in fact, by construction, it is automatically fully perpendicular to the geomagnetic field. The second turning force, driven by the first turn velocity, leads to acceleration and a 2nd-turned velocity, $\bar{v}_2$

$$\bar{F}_2 = -e\left(\bar{v}_1\times\bar{B}\right) = m\frac{d\bar{v}_2}{dt} \quad .$$

Thus the velocity is

$$\bar{v}_2 = -\frac{e}{m}\int\left(\bar{v}_1\times\bar{B}\right)dt$$

$$= -\frac{e}{m}\left(\bar{v}_1\times\bar{B}\right)\Delta t$$

$$= \left(\frac{e}{m}\right)^2 v_0 B_{Geo}^2 \frac{\Delta t^2}{2} \left(\left(\hat{r}\times\hat{b}\right)\times\hat{b}\right)$$
$$= \upsilon_2 \left(\left(\hat{r}\times\hat{b}\right)\times\hat{b}\right)$$

where we have again simply used a time Δt to represent the integration (as noted, we will not use this analysis to calculate E1 HEMP). The "υ_2" represents the amplitude of all the various factors shown, and the vector function gives the direction and a geometry factor. The first turning had an amplitude factor from the cross product $\left(\left|\hat{r}\times\hat{b}\right| = \text{the sine of the angle between those two vectors}\right)$, for the second turning the amplitude of the vector $\left(\left|\left(\hat{r}\times\hat{b}\right)\times\hat{b}\right|\right)$ also equals the same sine function – the extra "$\times\hat{b}$" simply represents a change in direction.

Again we can form the source current for the second turning

$$\bar{J}_2 = -e\,N\,\bar{v}_2$$
$$= -e\left(\frac{e}{m}\right)^2 N\, v_0 B_{Geo}^2 \frac{\Delta t^2}{2} \left(\left(\hat{r}\times\hat{b}\right)\times\hat{b}\right).$$

But before going further we should note that the high-frequency approximation uses the part of the source current that is perpendicular to the ray direction. We will also show that, unlike the first turning, only part of this current is perpendicular to the ray, and some is parallel to the ray (and this part does not radiate down the ray).

In general, a vector ($\bar{v}_2$) can be separated into a two parts, relative to another vector (the burst observer ray here, $\hat{r}$)

$$\bar{v}_{2||} = \left(\hat{r}\bullet\hat{v}_2\right)\hat{r} \qquad \text{(parallel)}$$
$$\bar{v}_{2\perp} = \left(\hat{r}\times\hat{v}_2\right)\times\hat{r} \quad \text{(perpendicular)}.$$

As noted, the parallel component does not radiate as part of E1 HEMP. We will only consider the important component (perpendicular), and put in its vector direction from the results above

$$\bar{v}_{2\perp} = \left(\hat{r}\times\hat{v}_2\right)\times\hat{r}$$
$$= \upsilon_2 \left(\hat{r}\times\left\{\left(\hat{r}\times\hat{b}\right)\times\hat{b}\right\}\right)\times\hat{r}$$
$$= \upsilon_2 \left(\hat{r}\bullet\hat{b}\right)\left\{\left(\hat{r}\times\hat{b}\right)\times\hat{r}\right\}.$$

The third line is the result of vector simplification, shown in Table 4-3. We will see that, compared to the dipole (E_D) term, this means that the quadrupole (E_Q) term has two extra geometry effects: an extra amplitude scaling from $\hat{r}\bullet\hat{b}$, and an extra direction change (by 90^o) from the last $\times\hat{r}$.

This same selection of the transverse component can be applied to the second-turned source current, so that the second-turned E1 HEMP field is

$$\bar{E}_{2\perp} = -\frac{Z_o}{2}\bar{J}_{2\perp}\Delta z$$

$$= \frac{Z_o}{2} e \left(\frac{e}{m} \right)^2 N v_0 B_{Geo}^2 \frac{\Delta t^2}{2} \Delta z \left(\hat{r} \bullet \hat{b} \right) \left\{ \left(\hat{r} \times \hat{b} \right) \times \hat{r} \right\}.$$

Table 4-3. Vector simplifications for the transverse part of the second turning.

Vector Simplifications for $\left(\hat{r} \times \left\{ \left(\hat{r} \times \hat{b} \right) \times \hat{b} \right\} \right) \times \hat{r}$
A standard vector identity is $\left(\overline{A} \times \overline{B} \right) \times \overline{C} = \left(\overline{A} \bullet \overline{C} \right) \overline{B} - \left(\overline{B} \bullet \overline{C} \right) \overline{A}$ Applied to the center part of the vector term gives $\left(\hat{r} \times \hat{b} \right) \times \hat{b} = \left(\hat{r} \bullet \hat{b} \right) \hat{b} - \left(\hat{b} \bullet \hat{b} \right) \hat{r} = \left(\hat{r} \bullet \hat{b} \right) \hat{b} - \hat{r}$ where we have used $\hat{b} \bullet \hat{b} = 1$ Then putting on the initial $\hat{r} \times$ we get $\hat{r} \times \left\{ \left(\hat{r} \times \hat{b} \right) \times \hat{b} \right\} = \hat{r} \times \left\{ \left(\hat{r} \bullet \hat{b} \right) \hat{b} - \hat{r} \right\}$ $= \left(\hat{r} \bullet \hat{b} \right) \left(\hat{r} \times \hat{b} \right) - \hat{r} \times \hat{r}$ $= \left(\hat{r} \bullet \hat{b} \right) \left(\hat{r} \times \hat{b} \right)$ where we use the identity $\hat{r} \times \hat{r} = 0$ Now put on the final $\times \hat{r}$ to get $\left(\hat{r} \times \left\{ \left(\hat{r} \times \hat{b} \right) \times \hat{b} \right\} \right) \times \hat{r} = \left\{ \left(\hat{r} \bullet \hat{b} \right) \left(\hat{r} \times \hat{b} \right) \right\} \times \hat{r}$ $= \left(\hat{r} \bullet \hat{b} \right) \left\{ \left(\hat{r} \times \hat{b} \right) \times \hat{r} \right\}$

Thus, in summary, the two terms of E1 HEMP have variations that go as

$$\overline{E}_1 = -\frac{Z_o}{2} e \frac{e}{m} N v_0 B_{Geo} \Delta t \, \Delta z \left(\hat{r} \times \hat{b} \right)$$

$$\overline{E}_{2\perp} = \frac{Z_o}{2} e \left(\frac{e}{m} \right)^2 N v_0 B_{Geo}^2 \frac{\Delta t^2}{2} \Delta z \left(\hat{r} \bullet \hat{b} \right) \left\{ \left(\hat{r} \times \hat{b} \right) \times \hat{r} \right\}.$$

Remembering that $\hat{r}$ is pointed along the burst-observer ray, and $\hat{b}$ is the direction of the geomagnetic field (both are unit vectors – they show direction, but not amplitude), the vector terms can be put in terms of the angle between the two, as given by θ_M, as shown in Table 4-4. We see that the dipole term has a simple $\sin(\theta_M)$ variation, and for the quadrupole term it is $\sin(\theta_M)\cos(\theta_M)$. (Note that the turned term also has the geomagnetic field amplitude and the time extent factors as squared values.)

Thus, the functional dependences for E1 HEMP are:

1. All aspects of the weapon gamma (and x-ray) output: strength, spectrum, and waveform.
2. The separation distance from the burst to the source region and to the observer ($1/r^2$ value in energy or power).

3. The angle through the atmosphere.
4. The strength and angle of the geomagnetic field in the source region.

Knowledge of these dependencies has been used to allow quick shifting of burst and observer locations without re-running the full E1 HEMP calculation.

Table 4-4. Explanation of the two E1 HEMP terms.

E1 HEMP Dipole (E_D) and Quadrupole (E_Q) Terms		
Term	Amplitude	Direction
Dipole: $\bar{E}_1 = \bar{E}_D \approx (\hat{r} \times \hat{b})$	$\sin(\theta_M)$	$\perp$ to $\hat{b}$ and $\hat{r}$
Quadrupole: $\bar{E}_{2\perp} = \bar{E}_Q \approx (\hat{r} \bullet \hat{b})\{(\hat{r} \times \hat{b}) \times \hat{r}\}$	$\sin(\theta_M)\cos(\theta_M)$	$\perp$ to $\hat{r}$ and $\bar{E}_1$

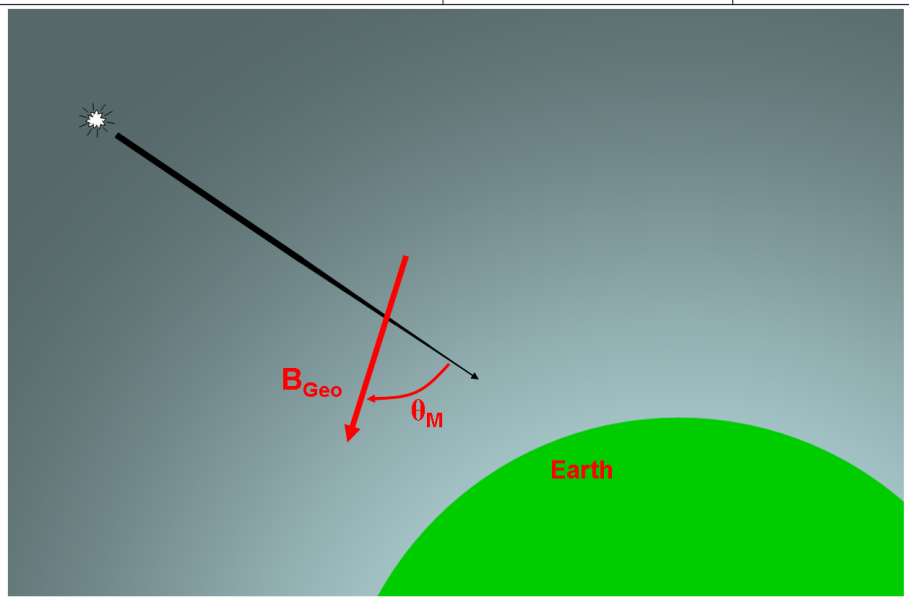

Specifically, assume a calculation has been made for a specific scenario – device, burst location, and observer location. Then if we wanted to know the E1 HEMP result at any other azimuthal position around ground zero, only item #4 changes (B_{Geo} and θ_M). Also, if we want to shift the burst and observer positions around, as a unit, again only item #4 changes. In both cases the parameters that do not change are:

1. The device.
2. The burst height.

3. The ground range (distance between ground zero and observer) – this sets the distance from the burst to the observer, and the angle through the atmosphere.

The one change is the B_{Geo} amplitude and its angle θ_M. (This all ignores differences in self consistency effects – there will be some slight differences in the total local fields in the source regions for the difference positions. However, this has been found to be a slight effect – typical errors are a few percent. This will be discussed shortly.)

Using the dependences just developed, we can write the variations for E1 HEMP as

$$\overline{E}(t) = \overline{E}_D(t) + \overline{E}_Q(t)$$

$$\overline{E}_D(t) = B_{Geo} \sin\theta_M \, \overline{\mathbf{F}}(t, \theta_R, \gamma)$$

$$\overline{E}_Q(t) = B_{Geo}^2 \sin\theta_M \cos\theta_M \, \overline{\mathbf{G}}(t, \theta_R, \gamma)$$

$$\gamma = \gamma(\text{Device}, \text{HOB}, \theta_R, t)$$

where $\overline{E}_D(t)$ is now used for the dipole term, and $\overline{E}_Q(t)$ for the quadrupole. This is shown in Figure 4-11. All the item #4 variations are explicitly shown in the B_{Geo} and θ_M variation terms. The other terms, $\overline{F}(t, \theta_R, \gamma)$ and $\overline{G}(t, \theta_R, \gamma)$, show the variation with the gamma environment (device, HOB, θ_R, and t), the angle through the atmosphere (θ_R), and time ("t"). (These **F** and **G** terms are unrelated to the F and G used in the transformations of Maxwell's equations.) Thus, from the single E1 HEMP calculation, we can extract the **F** and **G** terms, and then use them to get the E1 HEMP at other azimuth positions, and for other burst locations (for the same device, HOB, and θ_R), as indicated in Figure 4-12.

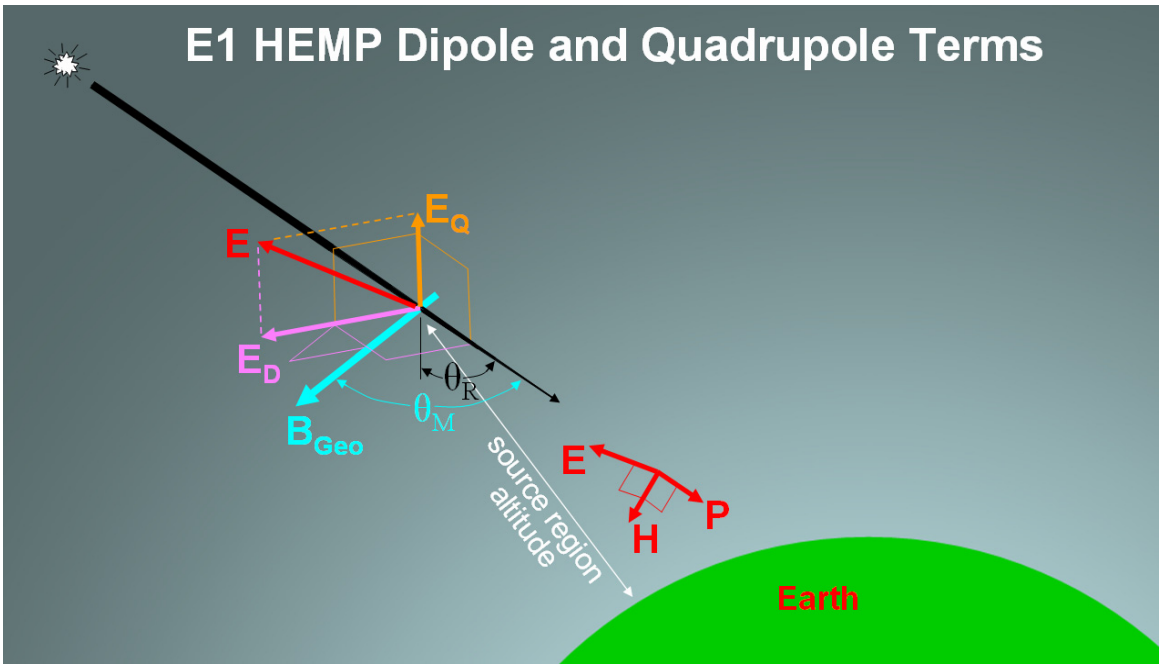

Figure 4-11. Idealization of the E1 HEMP as two terms. E1 HEMP is composed of the dipole (E_D) and quadrupole (E_Q) terms. (Vector directions are given by, for E_D: $-rxB_{Geo}$, and for E_Q: transverse part of v_2, which is in the direction of $-E_D x B_{Geo}$.)

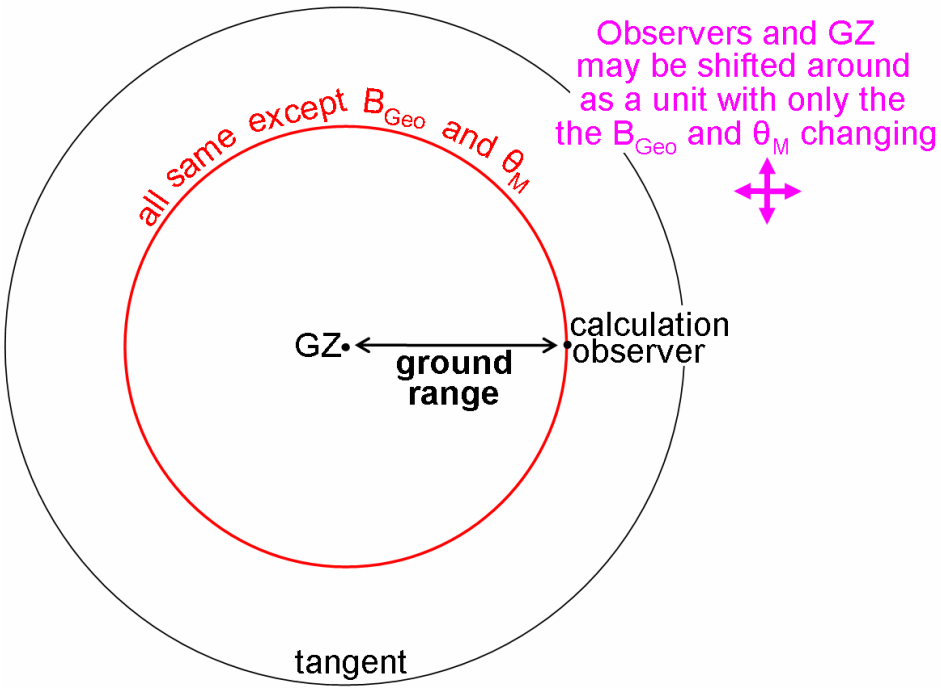

Figure 4-12. Extending one E1 HEMP calculation to other cases. An E1 HEMP calculation can be extrapolated to other observer points, and for other burst locations. A calculation at the indicated observer point has all the same parameters, except for the geomagnetic turning parameters, B_{Geo} and θ_M, as the other points at the same ground range (red circle); and the latitude and longitude positions of the whole unit may be shifted about while also only varying the geomagnetic field parameters.

Note that there are non-linear effects of the E1 HEMP: H affects the Compton turning, and E affects the motion of the Compton electrons, and the parameters that go into the air chemistry. Thus the source current (J) is affected by E and H, and the air conductivity (σ) is affected by E. However, it has been found that these nonlinear effects are slight in doing such a shifting of burst or observer position, and that there is a tradeoff of precise accuracy and computation time. Certainly any small inaccuracy in using this to greatly speed up calculations would have to be judged relative to other inaccuracies, such as possible large unknowns in the parameters of the burst. This quick calculation procedure can be used for preliminary studies, and then, if necessary, final, full, calculations can be made to confirm the results, and remove the few percent of inaccuracy that might be in the fast calculations. If nothing else, this decomposition approach provides important insight into E1 HEMP.

4.5 Field Directions, East-West Symmetry, and Special Points

Sometimes it has been stated that calculations, such as for vertical E incident as shown in Figure 2-22, must have some error, because it does not have east-west symmetry, as E1 HEMP should have. Indeed, as shown in Figure 2-17, there is such symmetry for the amplitude of the incident field. (All directions, such as east and west here, are geomagnetic, not geographic. This is generally true for all discussions of E1 HEMP – all directions should be considered geomagnetic.) However, we will see that east-west symmetry does not apply to the individual vector components of the field (here we will

use the three orthogonal components of: vertical, horizontal east/west, and horizontal north/south). Symmetry for these components is broken because of the quadrupole term. If E1 HEMP only consisted of the dipole term (by far the dominate term) then there would be symmetry in the magnitude of the three components also. Additionally, the magnitudes of the three components for the quadrupole term also have symmetry. However, the dipole and quadrupole terms have different signs for the symmetries of their components. These differences in signs for their symmetry result in the two terms being additive on one side of ground zero, and subtractive on the other side, and so east-west symmetry is broken. In this section we will discuss symmetry in E1 HEMP fields. The E1 examples used in the discussion will also give the reader a chance to see the workings of the E1 HEMP generation process. This symmetry argument is rather complex, and the reader may want to skim over it. It is here because it has not been published elsewhere, and it counters criticism of our E1 HEMP calculational models.

As a side note, we should mention that there is also another effect that breaks all east-west symmetry. However, it makes only a small difference when comparing two equivalent E1 HEMP rays, one going to the east and the corresponding one going to the west. The effect is that E1 HEMP along each ray is driven by the geomagnetic field along its ray. If we assume a dipole field for the earth's magnetic field, then the two complementary rays would see corresponding B fields. However, the earth's magnetic field has significant variations from a dipole field. The farther apart the source region positions are for the two rays (i.e., the closer to the tangent), the more likely that there are differences in the geomagnetic field values, due to the small random spatial variations in the geomagnetic field.

Let us consider the symmetry in detail. As stated above, E1 HEMP is generated by gammas producing Compton electrons, which get turned in the geomagnetic field. This occurs along the ray going from the burst point to the observer. Important parameters are how the air density varies along the ray (affecting Compton electron production, and then the histories of those energetic electrons, producing source currents, and, ultimately, conductivity). Over some distance of the downward ray's path we have the "source region" – starting where the air density starts to get high enough, and going down until the integrated amount of air mass is such that the gammas have been attenuated to a low level. Another very important factor is the geomagnetic field along the ray in this source region. The geomagnetic field varies with position around the earth, and so also varies along the ray's path. The geomagnetic field is approximately like a dipole (such as for a simple bar magnetic), with curved lines that head toward the poles (deep within the earth). Field lines concentrate as we get closer to the poles, and also the field gets stronger with lower altitude in general. However, the earth's magnetic field is known to actually have significant random variations from a simple dipole field – offsets in strength and field direction. E1 HEMP calculations can use a dipole geomagnetic field, for simplicity, in which case the results will show perfect east-west symmetry in the electric field amplitude. Higher order fits to the geomagnetic field can also be used, and then there will no longer be perfect east-west symmetry for the field amplitude. However, even with the dipole geomagnetic field, it will be found that the vertical field component (or, correspondingly, the horizontal component) does not have perfect

east/west symmetry. This is due to the Compton electrons having a polarity that governs the spiral direction of their path – the dipole and quadrupole terms each having east-west symmetry, but differing with regard to even or odd symmetry for the vertical component. The result is that the two terms add on the east side but subtract on the west side.

This lack of perfect east-west symmetry is readily seen for the vertical electric field, which is bigger on the right, as shown in Figure 2-22. There is a corresponding opposite effect in the horizontal field (Figure 2-18), which is slightly bigger on the left (but it is not really perceptible in this smile diagram). These effects are exactly the opposite of each other, such that the total field does have true east-west symmetry. However, the contour plots do not as readily show the higher field on the west side for the horizontal component. This is because the effect is not very big – the non-symmetrical differences are small compared to the total horizontal field, which is actually most of the E1 HEMP signal over the U.S.; but the non-symmetry level is more significant for the vertical field, which is smaller that the full E1 HEMP signal.

As noted above, the generation process, even under the ideal assumption of a dipole geomagnetic field, sees a slight variation of the B field along the ray path. For simplicity in the following discussion we will ignore this complication. We will assume a uniform geomagnetic field (which is equivalent to assuming the earth radius is very large, or the burst height is very low).

Furthermore, initially we will assume a perfectly vertical geomagnetic field (approximately like a burst over the north magnetic pole). For this case the null point is directly below, at ground zero. As indicated in Figure 2-11 for near-polar bursts, there is no geomagnetic max point for ground observers. The rays that go perfectly perpendicular to the geomagnetic field go out horizontally from the burst, too high to strike the ground (the geomagnetic max point goes out farther in ground range as the burst point gets closer to the pole, as shown in the figure). However, there will be a max region (and for this special case of vertical geomagnetic field it will be a circle centered on ground zero). The position of the max points (ground range to the circle) varies with each burst (nuclear device characteristics and burst altitude) – it depends on the competing effects as the observer distance goes out further in ground range: stronger geomagnetic turning but weaker source region generation (typically) for the shallower angles through the source region (and more 1/R fall-off).

With this uniform vertical geomagnetic field, and assuming that only the E1 HEMP dipole term exists, we get an azimuthal E field with cylindrical symmetry, as shown in Figure 4-13 (the fields must have cylindrical symmetry when the geomagnetic field is perfectly vertical). The E1 HEMP dipole E field is only horizontal, and tangent to the circle shown.

We now put on the next level of complexity – adding on the quadrupole term, as shown in Figure 4-14. This is produced by the v_2 motion of the Compton electrons, which is pointed radially inward. This is given by the cross product of the v_1 direction (which produces the dipole term) and the geomagnetic field. However, this term is not

automatically perpendicular to the ray (unlike the dipole driver, which is automatically perpendicular to the ray). In general, part of it will be parallel to the ray, and part perpendicular – only the later part will radiated forward and contribute to E1 HEMP. In the Figure 4-14 this is indicated by the full v_2 term being a light orange, and the transverse (perpendicular) part being dark orange. For this perfectly vertical B_{Geo} case all terms and vector components (including the total field) have east-west symmetry in amplitude.

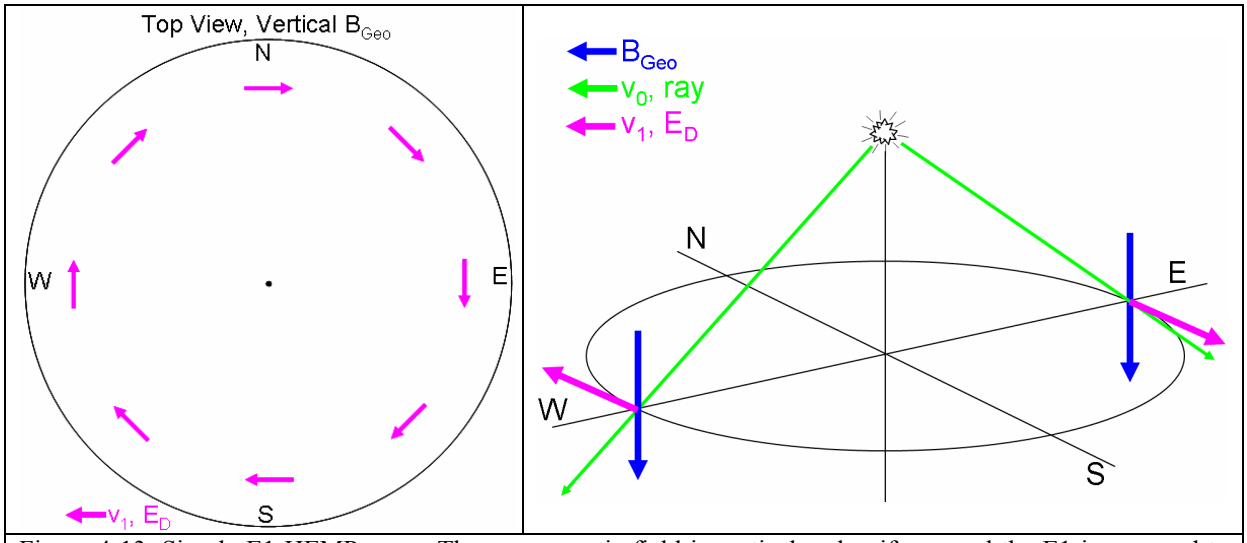

Figure 4-13. Simple E1 HEMP case. The geomagnetic field is vertical and uniform, and the E1 is assumed to only have the dipole term. The overhead view on the left shows that the electric field is azimuthal, and has cylindrical symmetry. The right view is from off to the southwest, and shows the various vectors for west and east observer points.

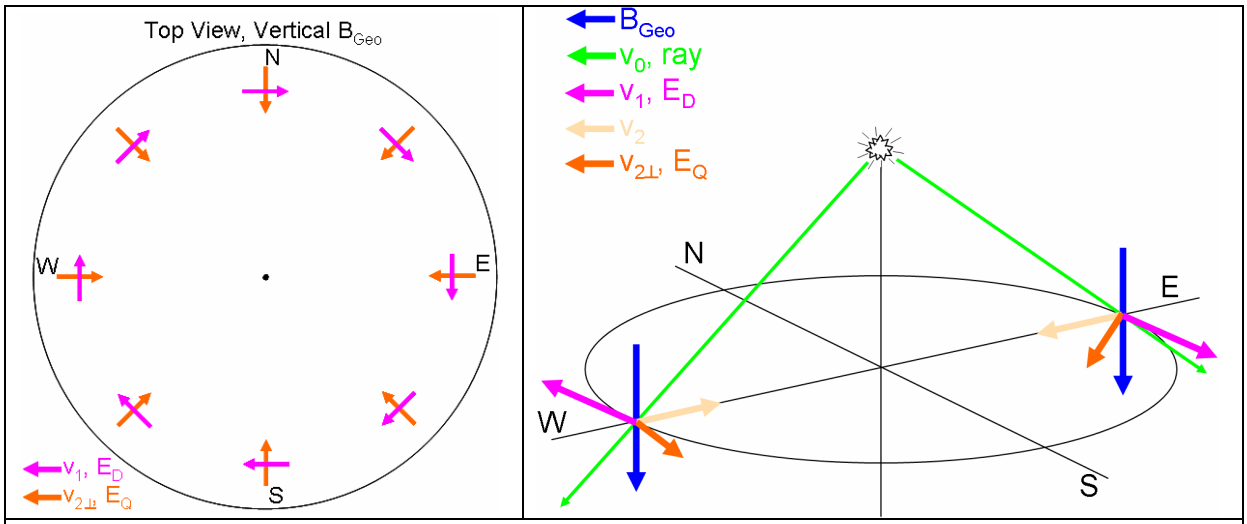

Figure 4-14. Including the quadrupole term in the simple case. This is for the same case as in Figure 4-13, but with the quadrupole term now added. This term (in orange) is radial, and also has cylindrical symmetry. The vectors in the right drawing shows the quadrupole term (dark orange) is from only part of the second turning electron motion (lighter orange) – only the transverse part of the field generated from v_2 can propagate outward along the ray. Thus, we decompose the light orange vector into a part along the green ray line (not shown) and the part that is perpendicular (dark orange – it has a vertical and radial part).

Thus, for a perfectly vertical geomagnetic field, the E1 HEMP field consists of a dipole term that is all horizontal and azimuthal, and a quadrupole term that has: radial (all horizontal and inward) and vertical (all down) components. Now consider a more realistic case. For a general case the geomagnetic field is not vertical – so in Figure 4-15 we take the B_{Geo} lines and pull the tops of the lines slightly south (for the central U.S. the dip angle is about 70^o, which we could approximate by tilting the lines by 20^o). Here we just show a small tilt – enough to demonstrate the effect: the dipole field develops vertical components. On the west side the tilt pulls the northward pointing dipole term (the violet arrow) up, while on the east side the dipole term points south, and so is pushed slightly downward for its vertical component. This tilt has little effect on the quadrupole term – v_2 is still radially inward (the tilt rotates on this axis, and so has no effect; and selection of the transverse part is related to the observer ray, not the geomagnetic field). This simple demonstration shows that for the vertical part of the incident E1 HEMP, the quadruple term is downward to the west and east, while the dipole term is downward to the east and upward on the west. Thus, for the total field, the vertical will be bigger (terms additive) on the east than on the west (terms subtractive) – and so the vertical field does not have perfect symmetry. This shows that, indeed, the lack of east-west symmetry is real.

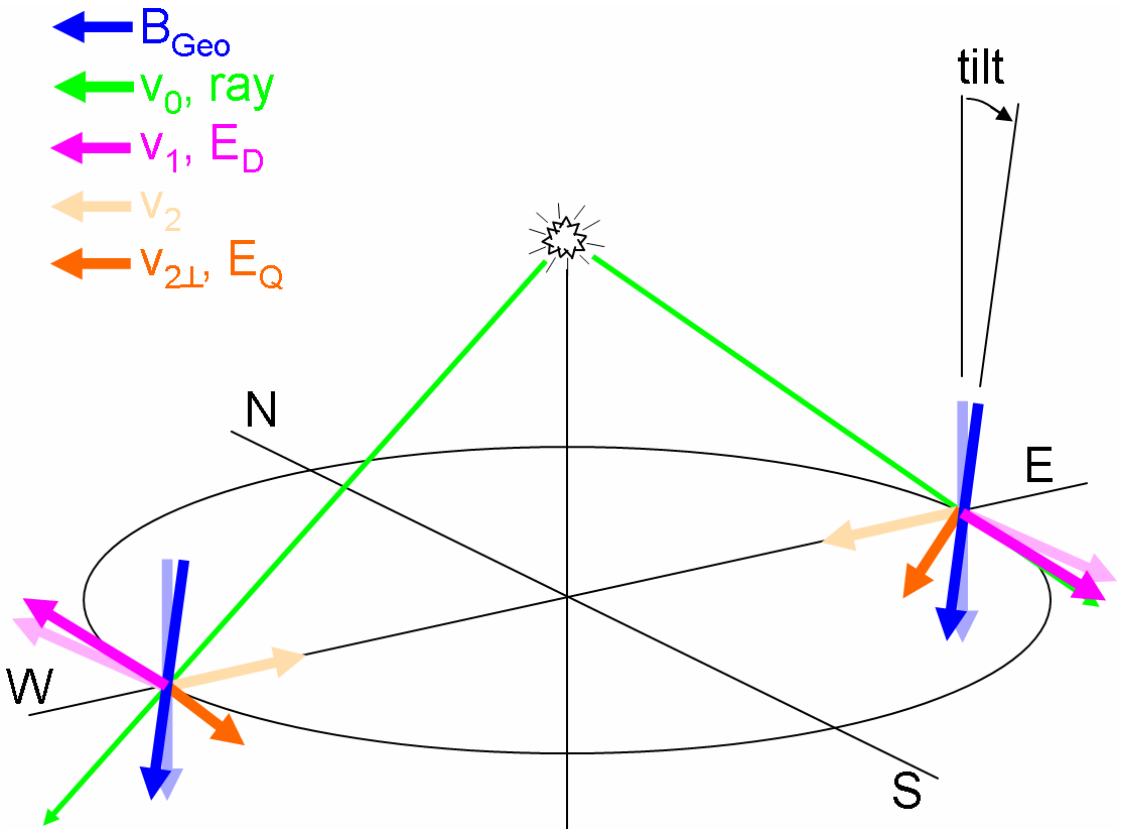

Figure 4-15. Effect of tilted (non-vertical) geomagnetic field for the simple case. This is the same as Figure 4-14, but with the geomagnetic field now tilted slightly (moving the top a little towards the south). This results in the dipole term getting a slight vertical component – up on the west side and down on the east side. Note that the quadrupole is down for both the west and east sides. Thus, the total vertical field will be higher on the east side than on the west side.

In the next few figures we show field polarities for the three components of both the dipole and quadrupole terms. These results are for a 75 km burst height. Here we are using a simple uniform geomagnetic field, with a dip angle of 60^o. (The results would be slightly different for a dipole approximation of the geomagnetic field, and using a more accurate geomagnetic field model would make the results depend on location.) Each figure has the magnetic dipole result on the left, and the electric quadrupole on the right. The red regions indicate positive direction for the field component, and the green indicates negative. Vector symbols are also given to show the direction (arrows for horizontal components). Figure 4-16 shows the east-west horizontal electric field component, and Figure 4-17 has the north-south field (so together they are the horizontal field). We saw an azimuthal field for the dipole in Figure 4-13, and this has the same form – with (because of the geomagnetic tilt) the center point being at the null point - slightly north of ground zero. The boundaries between the red and green regions are where the component changes sign (and so is also zero). For the dipole these boundary lines are where the components of the r×b are zero, as indicated. (Except at the null point, r×b itself is never zero, and these boundaries are just where the vector direction is such that a component is missing.) The vertical result is shown in Figure 4-18. We see that the dipole results are simple: odd symmetry for E_Y and E_Z, and even symmetry for E_X.

The quadrupole results on the right are more complex. All three components have a line marked "r•b=0", where there is no quadrupole term at all, and so this is a zero line for all components. For E_Y and E_Z this is a line of sign change, but for E_X it is not. This line, which goes through the max point, is where the observer ray is perfectly perpendicular to the geomagnetic field. Because of this, the turned term, v_2, will be parallel to the observer ray, and so does not have any transverse component to radiate down the ray. The other sign-change boundaries are from the transverse part of v_2 losing one of the components (as indicated by the text by the lines), and for some of the lines it may not be obvious why the lines should be as they are shown in the figures. The vertical result in Figure 4-18 has a very small "up" region between the null point and ground zero, as shown in the close-up view of Figure 4-19.

The quadrupole results, especially for the vertical component, have a complex variation along the central north-south line. Figure 4-20 shows a view along this line, with E1 HEMP vectors shown for several points. The dipole term (E_D, violet) is eastward (into the page) on the far left side, is zero at the null point, and then is westward (out of the page) for the other observer points to the south. The turned current, represented by v_2 (light orange) also has a similar variation: down for the left point, up for all the others (except zero at the null point). However, the radiated part of this (E_Q, dark orange) depends on the observer ray. For the vertical component, E_{QZ}, there is a sign change in going through GZ, due to the ray's sign change for it north-south component, and there is another sign change in going through the geomagnetic max point, due to v_2 changing which side of the ray it is on. We can also see the signs for E_{QY}, the north-south component, which has one less sign change.

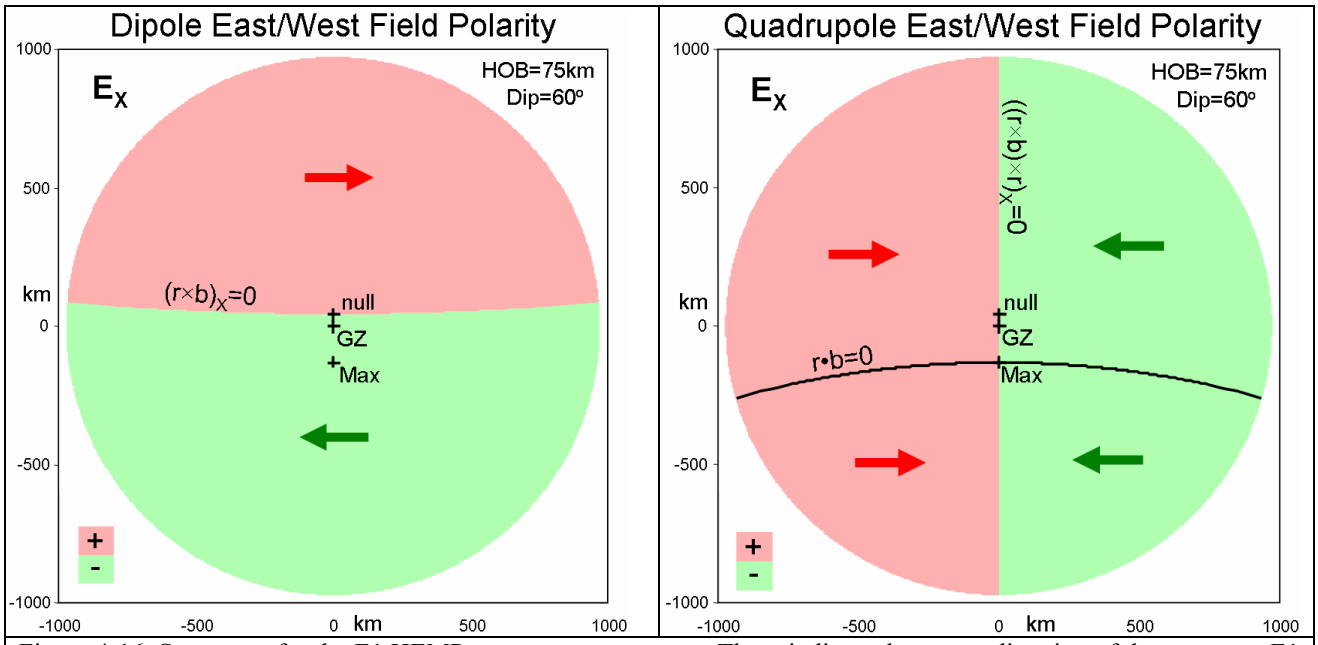

Figure 4-16. Symmetry for the E1 HEMP east-west component. These indicate the vector direction of the east-west E1 HEMP field component (E_X) for the dipole (left) and quadrupole (right) terms. These results are a uniform geomagnetic field, for a 60° dip angle (and an exposed region appropriate for a 75 km burst height).

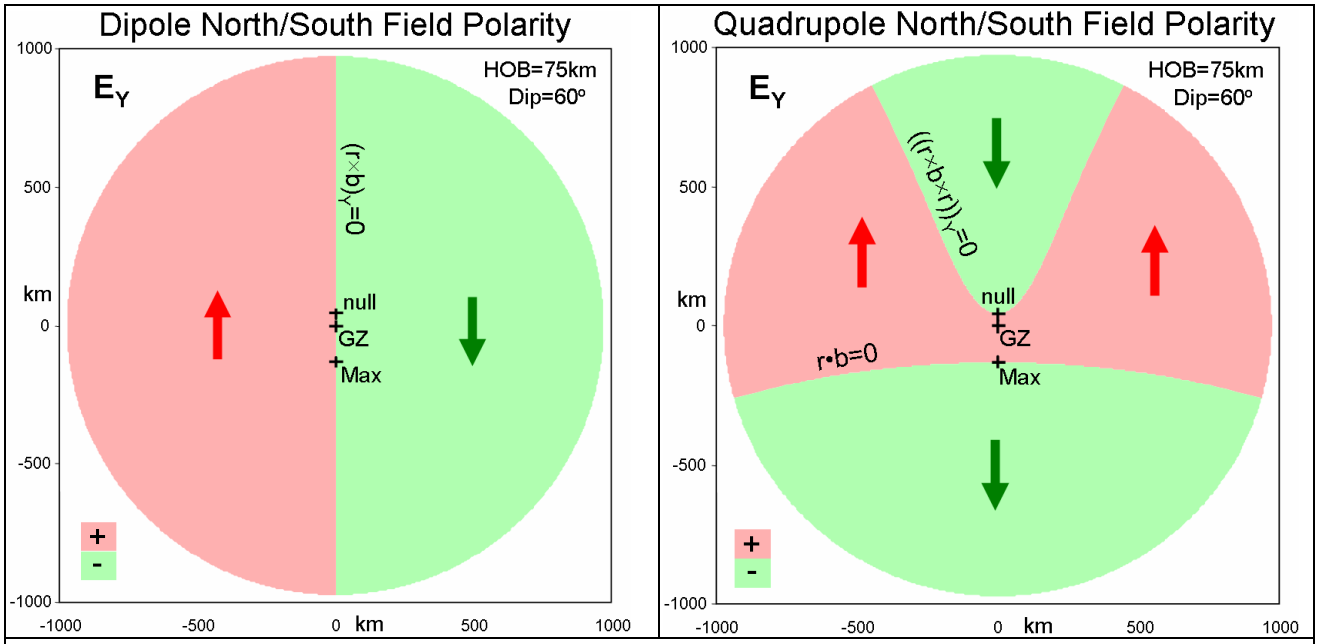

Figure 4-17. Symmetry for the E1 HEMP north-south component. These indicate the vector direction of the north-south E1 HEMP field component (E_Y) for the dipole (left) and quadrupole (right) terms. These results are a uniform geomagnetic field, for a 60° dip angle (and an exposed region appropriate for a 75 km burst height).

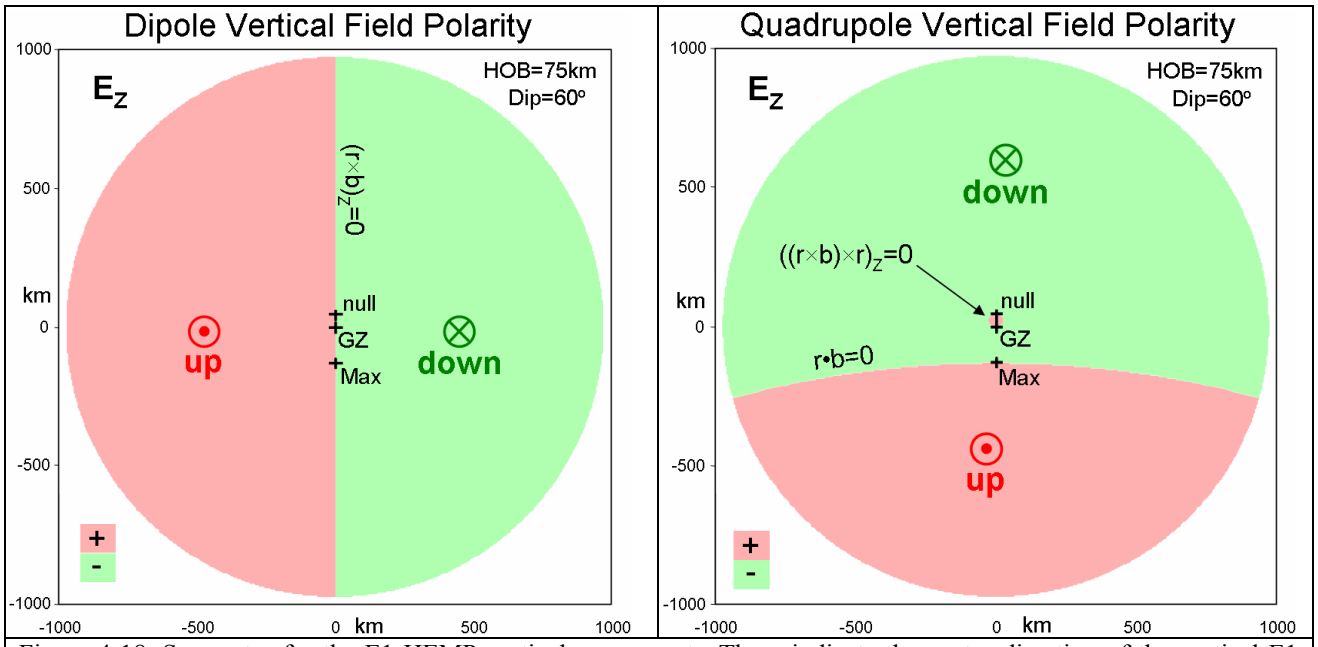

Figure 4-18. Symmetry for the E1 HEMP vertical component. These indicate the vector direction of the vertical E1 HEMP field component (E_Z) for the dipole (left) and quadrupole (right) terms. These results are a uniform geomagnetic field, for a 60° dip angle (and an exposed region appropriate for a 75 km burst height).

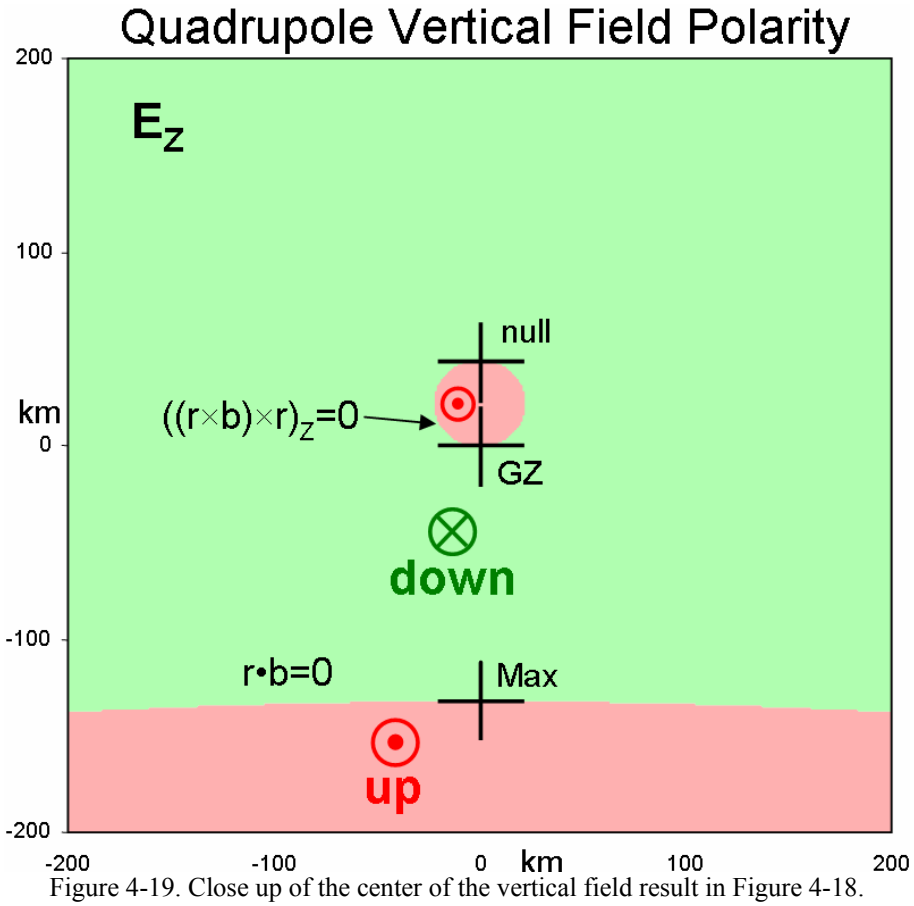

Figure 4-19. Close up of the center of the vertical field result in Figure 4-18.

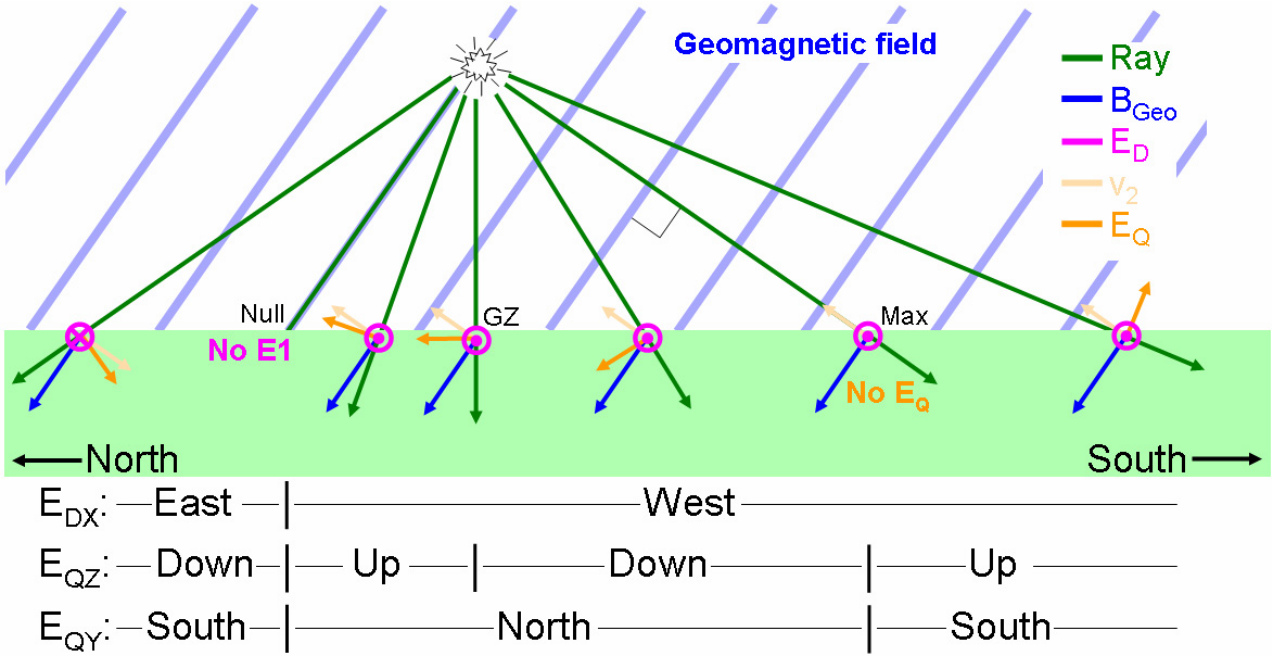

Figure 4-20. Field direction variation along a north-south central line. This shows the field direction for three of the E1 HEMP components, for a north-south line through the center of the exposed region. The vector diagrams show the components for several points along the line, and the bottom part of the figure indicates the component polarities for each region, with the three special points (the null point, ground zero, and the geomagnetic max point) as possible transition points between regions of different polarity.

Table 4-5 summaries the east-west symmetry shown in the figures. The two terms, dipole and quadrupole, have opposite symmetries for all three components. Thus, there will not be perfect east-west symmetry for any of the three vector components for the total field (except along the line where the quadrupole term is zero). Figure 4-21 shows the regions where the two terms will add, and so be larger than the corresponding points on the other side (where the terms subtract). These results do not indicate how big the effect will be, of course. Generally the quadrupole term gets more important for observers closer to the tangent, and is less important close in, where the fields tend to be higher. In general, the effect is more noticeable for the rather small vertical component (see Figure 2-22), and tends to get lost in the large horizontal components (see Figure 2-18).

From the discussions of E1 HEMP's terms, we can see that there are two sets of vectors that are perpendicular to each other, as shown in Figure 4-22 for a ray that goes straight down. The first is the set: v_1 (and E_D), v_2, and B_{Geo}, as indicated in light blue. However, v_1 (and E_D) are also perpendicular to the burst-observer ray, and this brings in the other set: v_1 (and E_D), $v_{2\perp}$, and the ray to the observer – in this set the $v_{2\perp}$ represents the quadrupole term, E_Q. These two sets vary relative to each other according to the angle between the ray and geomagnetic field; and where they themselves are at a right angle, the quadrupole term is zero.

Table 4-5. The type of east-west symmetry for E1 HEMP components. This gives the symmetry (even or odd) for each of the three components for the two terms of E1 HEMP.

Symmetry of E1 HEMP Components		
Component	Dipole	Quadrupole
E_X	Even	Odd
E_Y	Odd	Even
E_Z	Odd	Even

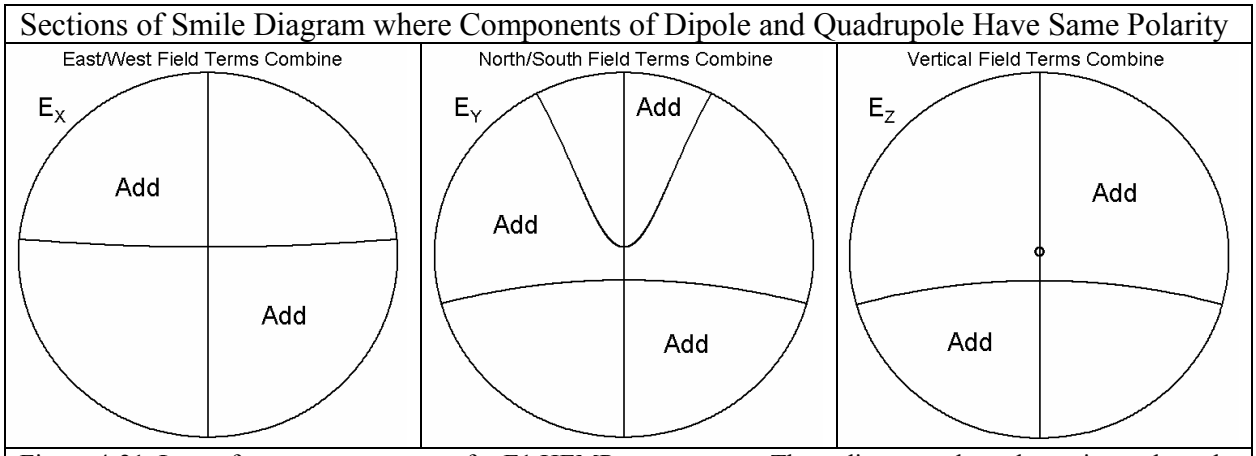

Figure 4-21. Loss of east-west symmetry for E1 HEMP components. These diagrams show the regions where the dipole and quadrupole terms add (and they subtract in the other, unmarked, regions) for the three vector components of the E1 HEMP.

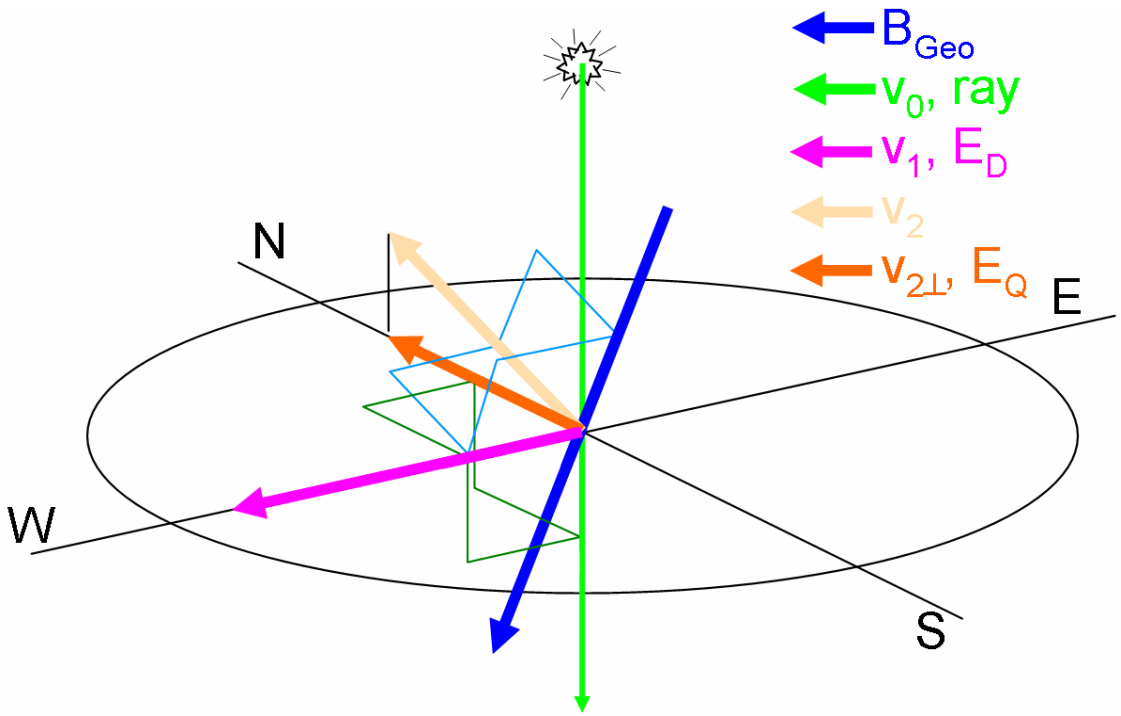

Figure 4-22. The two orthogonal systems for E1 HEMP. One (light blue) is that v_1, v_2, and B_{Geo} are all mutually perpendicular; and the second (dark green) is that v_1, $v_{2\perp}$, and v_0 are all mutually perpendicular. The connection between these two sets is that v_1 (violet arrow) is in both sets.

Now we will discuss some special locations, such as the null point, the max point, and places where there is no quadrupole term. Except at the null point, where there is no E1 HEMP, there will always be a dipole term (v_1), but there are places for which there is not any quadrupole term. There will always be a v_2 term (again, except at the null point) – by construction this is true. The v_1 vector is generated by the cross product of the ray and B_{Geo}, and so is automatically perpendicular to B_{Geo}, so that $v_1 \times B_{Geo}$, which generates v_2, will always exist when v_1 does. This is related to the Compton electrons going into spiral paths around the geomagnetic field lines (except for the electrons that go parallel to the lines, which do not produce any E1 HEMP). However, there are places where the v_2 vector is parallel to the burst-observer ray ($\mathbf{r} \cdot \mathbf{b} = 0$), and so does not have any transverse component, which means it has no radiation in the forward direction (along the ray). This occurs along a generally east-west arc that goes through the geomagnetic max point, as shown by the black arc in Figure 4-16 (and this is the same points as given by the red/green boundary in the two figures following it).

The null point probably would not actual have exactly zero E1 HEMP. There are many reasons for this

1. The geomagnetic field may vary though the extended length of the source region. The null condition cannot be exactly true over the full source path (because geomagnetic field lines curve).
2. The Compton electrons on the average go forward, but actually do have a spread in angle. There will be turning – it is just that on average the turnings will cancel out for the null point. However, can there be really perfect cancellation for the full time extent of the E1 HEMP?
3. There are also rays to either side of the null point ray, and those rays do generate E1 HEMP. Those rays will also radiate into the null point. Again, theoretically, we assume perfect cancellation for these (but it is unlikely to be perfect).
4. There may be reflections off of nearby objects, or the earth's surface.

Theoretically, the null point involves exact cancellation. It is very unlikely that cancellation would be exact for the full time extent of the pulse. Thus, there might be some slight E1 HEMP at the "null" point, but it could be very noisy – not as clean a pulse as at other points. And remember, to place a null point at a specific location would involve being able to precisely place the burst at an exact calculated position.

Besides the null point, the other specially named point is the "max point", as shown in Figure 2-10. This is the point where the E1 HEMP has its biggest peak (for a given scenario – weapon and burst location). This is geomagnetically south of GZ for a northern hemisphere burst. The exact location depends on the weapon and geometry of the burst location. There are two competing effects that control the location. First is the maximum Compton turning, where the observer ray goes through the geomagnetic field at a right angle (the geomagnetic max point). The second is the angle at which the observer ray goes through the atmosphere. The air pressure along the source ray path affects the generation of Compton current and the build-up of air conductivity. Generally the E1 HEMP is higher, and has more high frequency, for the most direct path into the atmosphere – straight down toward GZ. For tangent rays the angle into the atmosphere is very shallow, and the E1 HEMP tends to be lower, and with severely diminished high

frequencies. For lower burst heights and not too close to the poles, generally the maximum E1 HEMP will be near the point where the ray is perpendicular to the geomagnetic field. In most of this report we have used a loose definition of max point – using it to refer to the case that depends only on geometry (and not the particulars of the weapon) – it is the point where the observer ray is at right angle to the geomagnetic field, as shown in Figure 4-20 (the geomagnetic max point).

4.6 Some Simplifications

It is an approximation that the E1 HEMP only needs to be calculated along the burst-observer ray, as shown in Figure 4-23. This is the same as assuming perfect spherical symmetry all around the burst, with variations only in range (R, from the burst point) as appropriate only for the single observer point that we are currently calculating. This is a huge calculational savings. Very early in the development of the theory this assumption was checked, and it was verified that there were not significant errors in using this simplification. One check was done by Radasky and Knight in 1971 when they computed the early-time HEMP with a full 2-D Maxwell solution and compared it to the 1-D high-frequency approximation. A second check was performed by Longmire in 1974, and involved calculating additional rays, offset by small angles away from the main ray, and using those results to compute the angular derivative terms that are neglected when using the single ray approximation.

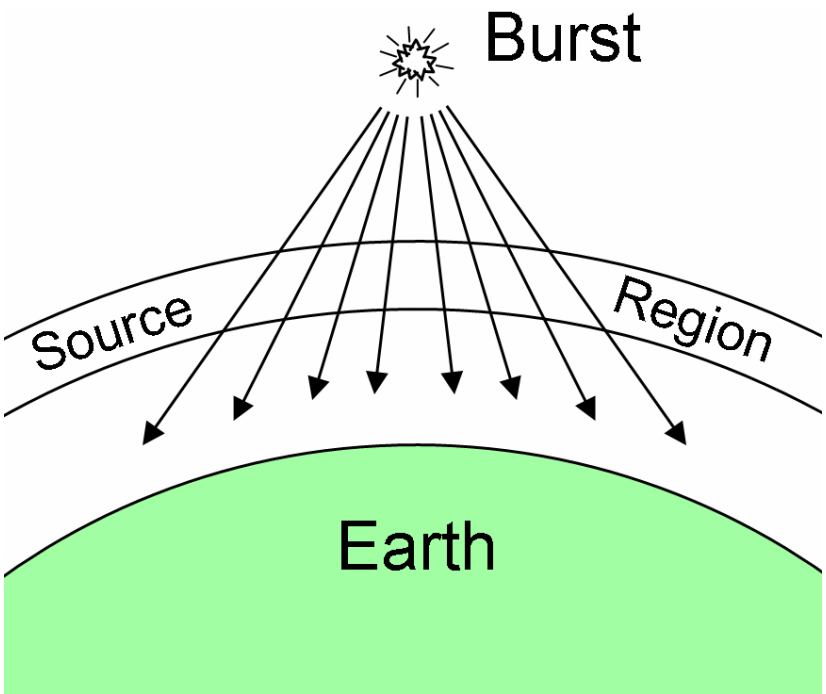

Figure 4-23. Single ray approximation. The field at each observer point on the Earth's surface is given by the generation of E1 HEMP along the ray from the burst to the observer. This is an approximation, but a very good one, for the actual fact that every point within the whole source region is a source of EM going out in all directions, and, in terms of this huge antenna (many hundreds of kilometers across), the observer point on the Earth's surface, only a few ten's of kilometers away, is in the near field.

In a similar vain, we generally assume E1 HEMP is a plane wave (not the curved wavefront of a spherical wave) for interactions – coupling to, and affecting, systems. This is also due to the slow variation over the surface of the Earth. Generally the system sizes are small – maybe up to a kilometer, while the distance to the burst point (and so the center of the spherical wave) ten, hundreds, or even thousands of kilometers. (However, we do account for the 1/R field variation, such as getting higher field values when projecting upward from the ground to high aircraft altitudes, or getting lower values when projecting past the tangent point to aircraft further out.)

In a related issue, one might ask how the E1 HEMP pulse can be a monopulse, and have DC content. It is known from antenna theory that an antenna does not radiate at DC. This is true for the far field, but for E1 HEMP we are not in the far field – note that the antenna that produced the field is really the whole source region (up to thousands of kilometers wide), and we are only about 20 km away from it. Thus, we are in much closer than what would be considered the far field.

Another simplification is shown in Figure 4-24. We assume that the E1 HEMP only has values in the exposed region – Earth surface points that are in line-of-sight of the burst point. Exactly at the tangent point is a boundary, and outside that edge the E1 HEMP is shown as zero. Of course this is not true – there will be E1 HEMP outside the tangent radius. Ground wave propagation will not allow an abrupt edge to the region that has nonzero E1 HEMP.

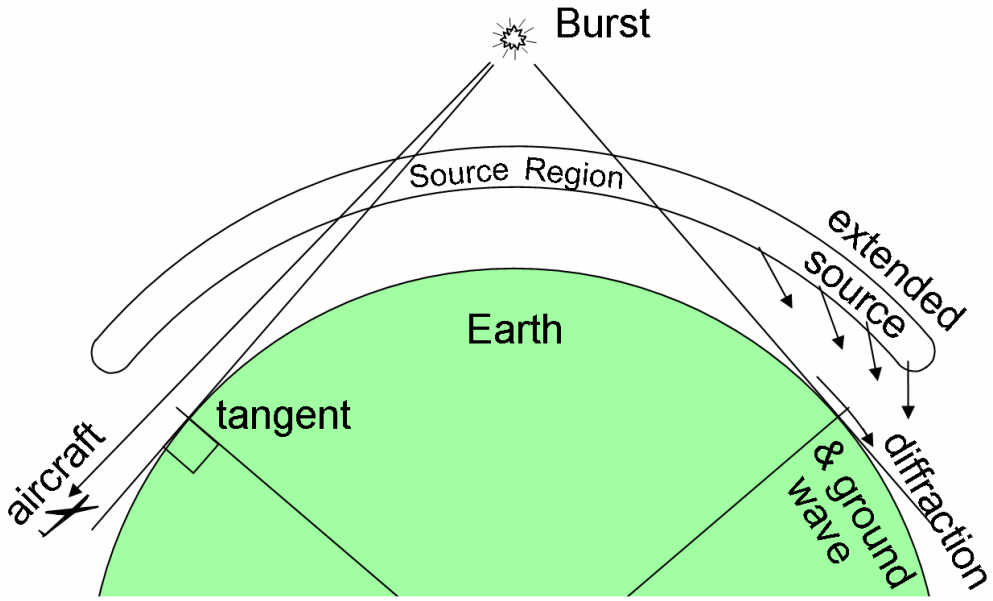

Figure 4-24. Exposed region approximation. Traditionally E1 HEMP calculations assume a sharp cutoff at the tangent point – no E1 value is calculated for points over the horizon (and so not within line of sight of the burst). The simple perfect sphere assumption does not account for the issue of topology – a mountain at a point over the horizon might still be in line of sight, while a point within a canyon in the exposed region might have its view of the burst point blocked. But even with the perfect spherical surface assumption, there would be some HEMP field over the horizon, to at least some distance. This figure shows three effects that would contribute to this: ground wave, diffraction, and the source region extending farther out than the ray that leads down to the Earth's tangent point. (In fact, the last issue would also come into play for aircraft – observers off the ground would have direct line-of-sight to the burst for points out to larger ranges than the Earth's tangent point, as shown on the left side of the figure.)

Another issue is that we have assumed a perfectly round surface for the Earth. For the tangent ray the issue of topography is important – hills and valleys can affect exactly what region will be in line-of-sight of the burst.

The issue of accurate modeling near the tangent has generally been ignored for two reasons: greater complications in the calculation, and the field levels are not very high. These complications are only important where the field levels are low. There has been a tendency in much of E1 HEMP work to worry most about the highest fields, and not to worry much about getting the best accuracy for cases where the field levels are low.

Section 5
E1 HEMP Line Coupling

In general, the most important aspect for many systems, including the electric power system, is coupling of E1 HEMP to lines (cables or wires). Voltage and current signals get generated on those lines, and these then propagate down the line and flow into circuits connected to the line. There are many factors that control the signal that is seen at the circuit on the end of the wire. Some important factors include:

1. The incident E1 HEMP waveform characteristics – amplitude and shape.
2. The geometry of the line relative to the direction that the E1 HEMP is propagating.
3. The geometry of the line relative to the E1 HEMP electric field vector direction.
4. The height of the line above (or below) the ground, and the parameters of the ground.
5. The line length.
6. The terminations (circuits and other impedances) of the line.

There are so many parameters that it is hard to provide a summary of coupling results. Some important facts to realize are:

1. It is only the component of E parallel to the line that couples to the line.
2. Generally the highest coupled levels result from good phasing – having the E1 HEMP pulse sweep along the length of the wire ("end-fire"). Just as for E1 in the source region, the coupled signal can build up from good phasing of the drive to the generated signal.
3. However, the two previous items are contradictory – for a plane wave the E field is perpendicular to the direction of propagation, so the pulse cannot sweep perfectly parallel to the wire length and also have the E field parallel to the wire.
4. Also, there tends to be a trade-off between pulse amplitude and pulse width for the coupled pulses – the best phasing (end-fire) tends to have a high level and narrow pulse; while a side illumination (broad-side) would have a low pulse level, but a wider pulse width.
5. Good phasing requires the best match between the wire propagation speed and the speed that the incident pulse sweeps down the wire. However, the wire propagation speed is always less than the speed of light ("c", in vacuum), while the incident sweep speed is always higher than c. The wire speed is slower because of the drag of the ground. The incident speed is higher because it is the incident speed relative to the wire itself (a phase velocity) – it is exactly c for perfect end-fire (but then there is no coupling), and gets faster (so poorer build-up) as it becomes more broadside – having an instantaneous incidence over the full length of the line for perfect broadside.

Generally the highest peak coupling is for slightly off end-fire – good phasing but with some fraction of the E field parallel to the wire.

The Earth's electromagnetic parameters (conductivity and permittivity) are important for two reasons. First, the total driver of the coupling is the incident E1 HEMP pulse plus its reflection off the ground. Secondly, the coupled wire signals are manifested by voltage and current pulses on the line, but really involve electromagnetic energy around the wire, including into the ground – thus the wire creates fields in the ground (which creates losses and slows down the signal speed). For both reasons the wire height and ground parameters are important. The least coupling is for buried cables; often a meter or two below ground provides significant protection from E1 HEMP fields.

Although a power line may have a long length horizontally, often we cannot ignore the vertical drop of the line at the ends. Although it may actually gradually taper down, we have to account for the fact that the power line goes down to the connected circuit. From the circuit there is also usually a connection to a ground rod in the Earth. The vertical part of the E1 HEMP couples to these vertical parts of the end terminations.

The termination circuit and the ground (ground rod and wiring) have some impedance, and these impedances control the actual voltage and current signals that get into the circuit (and so can cause damage). This is due to the standard transmission line theory. What gets into the circuit depends on how well the end impedance is matched to the line. What is not absorbed is reflected back down the line. For a short line, this reflected signal might then go back down the line and hit the circuit on the other end, providing additional incident energy that might cause damage there.

Some of the geometry of the situation is shown in a set of three figures. Figure 5-1 shows a side view, with the wire length and height. The ends have vertical runs, circuit impedances, and grounding rods. The E1 HEMP is coming in from above, at an angle that is set by the burst height and the ground range. (Two aspects of the wire are also important: the wire resistance and it radius – the last determining the wire inductance.) Figure 5-2 shows an overhead view. The observer ray angle to the wire position, α_r, helps determine the E1 HEMP that is incident, and the corresponding orientation angle for the wire, α_p, helps determine the relative horizontal angle (ϕ) between the wire and the incident E1 HEMP. This is shown more clearly in Figure 5-3, where we see that the ϕ and θ angles together determine the total angle between the two (ψ). This figure also shows the incident E1 HEMP plane, and the polarization of the E field within that plane (ρ). This and the two incident angles, determine how well the E field aligns with the line – the coupling varies as the cosine of the angle between the E vector and the line.

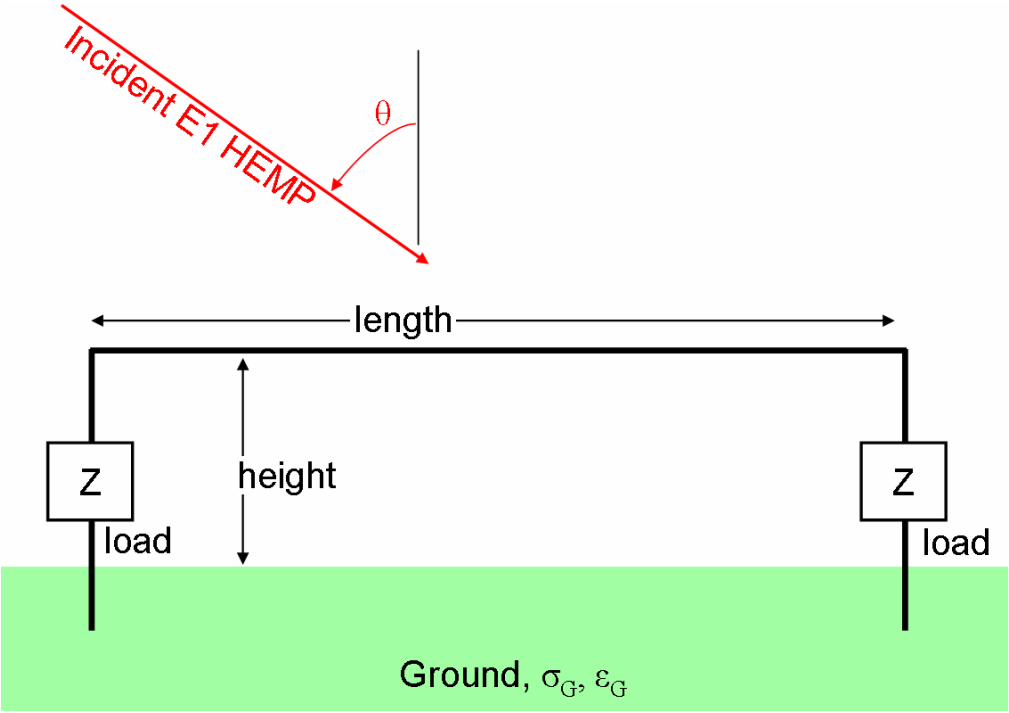

Figure 5-1. Side view of the line coupling.

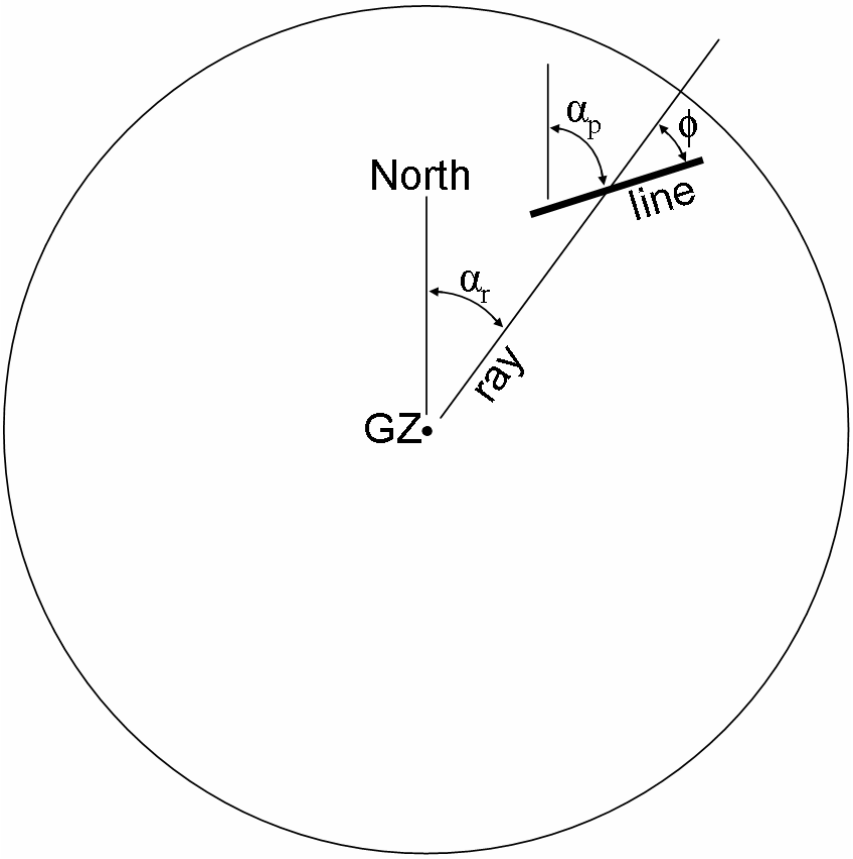

Figure 5-2. Top view of the line coupling.

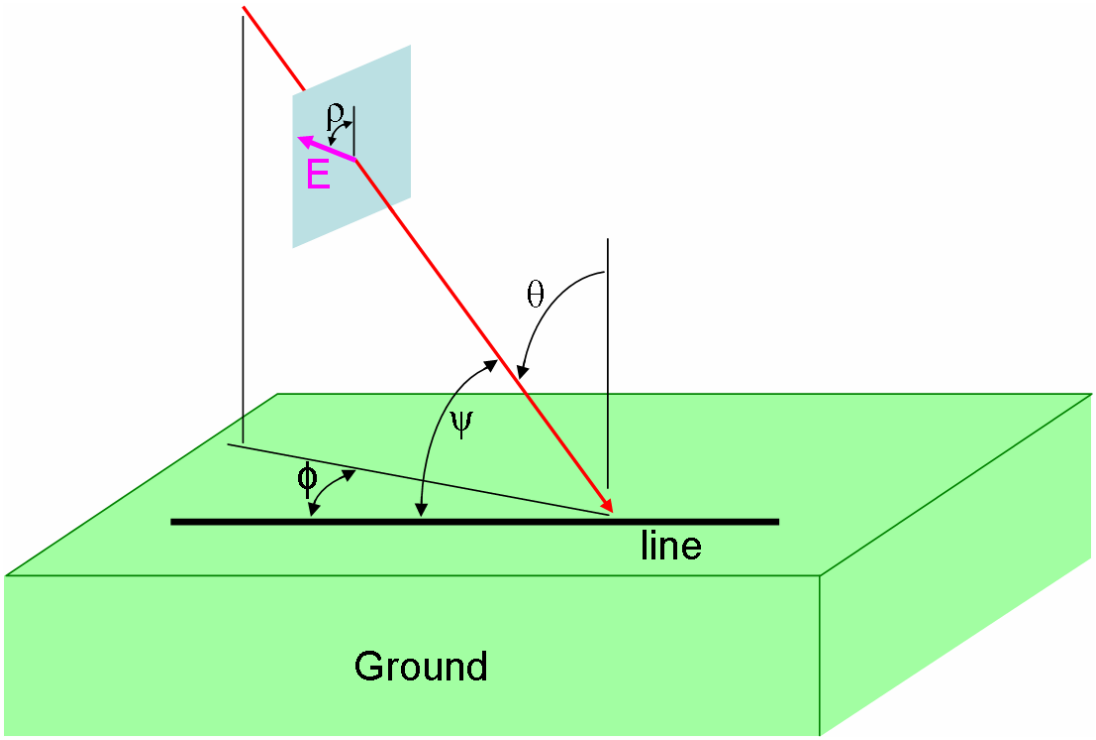

Figure 5-3. Line coupling geometry. This shows the incident plane and the electric field polarization for E1 HEMP horizontal line coupling.

Let us briefly discuss several aspects of this multifaceted problem.

1. **Coupling from E Parallel:** Only the part of the electric field that is parallel to the wire couples to the wire. The coupling varies as the cosine of the angle between the line and the E1 electric field. This is affected by all of the coupling geometry and the polarization of the electric field – the angles: ϕ , θ, and ρ (which depends on the E1 HEMP parameters).
2. **Earth Reflections:** Actually it is the total E field that couples, so the reflection from the Earth also needs to be included. The total field looks like the incident pulse, and then a delayed reflected pulse. The horizontal E field tends to decrease with reflection, and the vertical E field tends to increase. The effect is stronger with shorter reflection delay, which comes from θ being larger (closer to the tangent) and lower line height. The reflected pulse shape and amplitude depends on the ground parameters and has frequency dependence. There is even more frequency dependence if we account for the variation of the ground parameters with frequency.
3. **Wire Signal:** Signals are generated on the wire, and they propagate towards both ends (the signals in either direction are generally not the same shape or amplitude). These signals are like the TEM signals on a transmission line – the fields are in the plane perpendicular to the line, with H circling the wire and the E lines going away from the line, perpendicular to H.

4. **Wire Signal in Ground:** However, it is not a perfect TEM signal, in that some of the EM field is in the ground, which creates a drag on the propagating signal. This becomes less of a factor as the line is higher off the ground. The ground slows down the signal speed (it would be the speed of light if the ground were perfect), and also draws energy out of the signal (giving signal attenuation – and this loss is frequency dependent).
5. **Wire Orientation and Phasing:** If the wire orientation angle ψ is 90^o, then this is "broadside" and the E1 HEMP pulse excites the full line all at once. Then the pulse drains off the line on both ends, with signal amplitude that tends to be low. However, the pulse width can be very wide, due to the time for the coupled signal to propagate off the line. If there were no line losses (wire resistance, ground resistance), the pulse would tend to be a pulse that lasts the length of time for a wire signal to run the length of the wire, plus the incident pulse width. The other extreme case is end-fire, with the wire pointed towards the burst (so near the tangent, and wire radial). For perfect (parallel to the wire) end-fire conditions there is no coupling – the E field is perpendicular to the line (actually there is a little coupling, due to the ground drag on the field producing a slight horizontal component). Slightly off perfect end-fire, the E1 HEMP E field sweeps down the line, with a phase buildup to a large pulse on the far end (and the near end is much smaller, since the phasing only works in the forward direction). The highest peaks tend to be on the far end, and slightly off from end-fire. However, the pulse width also tends to be more like the width of the incident pulse, instead of having the broadside case's property of being longer for long wires.
6. **Relative Signal Speeds:** The signal speed on the wire is less than the speed of light, due to the slower speed of EM signals in ground. Several parameters control this. Lower line heights mean more signal in the ground, and so more slowing. Also, ground permittivity impacts the EM speed – the higher the relative dielectric constant, the slower the speed. However, the higher the ground conductivity, the less the fields penetrate the ground, and the less the ground speed matters. For the incident E1 HEMP pulse, as discussed in the previous item, the group (phase) velocity is always greater than the speed of light. It is c for end-fire, and infinite for broadside. With the wire speed less than c, there is no way to get a perfect phasing between the two. The best phase match is end-fire with the least amount of ground slowing as possible.

   In terms of ground parameters, the slower EM speed in the ground is due to both the permittivity (ε) and the conductivity (σ). Permeability (μ) is not an issue for most soils – it is approximately the same as for vacuum (and air). However, in terms of transmission line theory, the slower signal speed can be considered to be from increased inductance. The line signal speed is

$$v = 1/\sqrt{LC}$$

   where inductance per unit length "L" is associated with the magnetic field and permeability, and capacitance per unit length "C" is associated with the electric field and permittivity. For a wire over a perfect ground (infinite conductivity) the parameters are

$$C \approx \frac{2\pi\varepsilon}{\ln\left(h/2r\right)}$$

$$L \approx \frac{\mu}{2\pi}\ln\left(h/2r\right)$$

where "h" is the line height and "r" the wire radius. In this case the fields do not extend into the (perfect) ground, and the signal speed is that of EM waves in the air – the speed of light:

$$v = c = \frac{1}{\sqrt{LC}} = \frac{1}{\sqrt{\mu\varepsilon}}$$

and we could have perfect phase matching (for end-fire). If we pull the ground down (increase "h"), fields expand into this extra space. The inductance goes up, but the capacitance goes down proportionally, and the velocity stays c. If instead of pulling the ground down, we let the ground become imperfectly conducting, then fields also expand into the ground, and the inductance goes up because of the extra magnetic field in the ground. However, in this case, because the electric field is smaller in the ground (relative to being in air), the capacitance decrease is less than would correspond to the inductance increase, and the signal speed becomes slower than c. In general terms, looking at the equation given above for C, we can see that a decrease in C from increasing the extent of the field ("h") is partially cancelled by the increase in the permittivity (ε). Thus, in going from perfect to imperfect ground, we mostly get an increase in the inductance, and proportionally less decrease in the capacitance – and the wire signal speed decreases.

7. **Line Signal Loss:** There is signal loss (attenuation) for the wire signals from both the wire resistance and ground losses. Generally a longer wire length means more signal at the end – higher amplitude (especially end-fire) and longer pulse width (especially broadside). However, with wire attenuation there comes a point in increasing the wire length where there is little effect from having a longer length – any signal generated farther out is attenuated too much when it gets to the wire end. Thus, is it common to say, for long wires, that it is only the last part of the wire that matters. We might put some arbitrary number to this – such as we do not care about the line past about a kilometer from the end. This can be helpful in analyzing real power lines, since they tend to have branches, and change direction, which could complicate calculations. If we only care about 1 km of the length, then there is less of a chance that we would have to include such complications in our calculations.
8. **Terminations:** The coupled signals are the same as signals on a transmission line. From transmission line theory we know that at the wire ends (terminations) some of the energy gets absorbed by the loads, and some can be reflected back into a signal going back down the line. The line and load impedances determine the split of energy between the load and reflection. If the line is short (consider the previous item), then the reflected energy would eventually be incident on the other end of the line. Multiple reflections could happen, lengthening out the pulses into the loads. Total reflection of energy occurs if the load is an open circuit or short circuit. This

is significant because load protection schemes tend to be one of these – either shorting the energy to ground, or opening the line.

9. **Grounds:** However, the load circuit actually also includes the grounding resistance. The "transmission line" has a return path in currents in the ground, and the ground rod resistance is part of the circuit. Lower ground resistance comes from fatter, longer ground rods, and by having the best ground conductivity.
10. **Vertical Runs:** Besides the horizontal part of the wire, there is also the vertical run. This is, for example, the drop from the high power line pole down to a building. It also includes the line to the ground rod. The coupling to this line is similar to the horizontal line, but is driven by the vertical part of the E1 HEMP field. It has been found that this component should not be ignored. Earth reflection tends to increase the vertical electric field and lessen the horizontal component. These vertical runs do not, however, usually have much of a signal strength buildup, due to their short length.

Section 6
E1 HEMP Vulnerabilities

While it is possible that the fields themselves (E or H) might cause disturbance of some type of device, typically effects occur because of the generation of voltages and currents on conductors. This might be from EM fields leaking in through the case of a system, and then coupling to the circuits inside, or from coupling to the external cables that connect to the system, and so disruptive signals are then brought into the system at the ports connected to those cables. Certainly outside cables could be much longer than internal wiring, and so collect more EMP energy; and internal wires might have the added benefit of the shielding provided by the system enclosure. Often the external cable represents the most significant vulnerability for EMP disruption.

Several terms are used in vulnerability discussions. First, there is the distinction between "upset" and "damage". This seems simple enough: damage means some permanent, undesirable change to the system. An obvious example is a part "blowing up" – pieces flying out, with a "bang" and visual arc. Such things have been observed in pulse testing of parts. Figure 6-1 shows an example of a resistor blowing up during vulnerability pulse testing. In Figure 6-2 we see that a capacitor has disappeared, leaving just scorch marks, after pulse testing. In Figure 6-3 an IC (integrated circuit) shows that it has been destroyed since its normally flat lid is now seen to be deformed and discolored. Some damage might be more subtle – with no visual evidence – but something inside the device has changed, and it can be detected by a functional check of the device. Maybe a bonding wire inside an IC has broken, or a junction heated up too much and caused its solid-state properties to change.

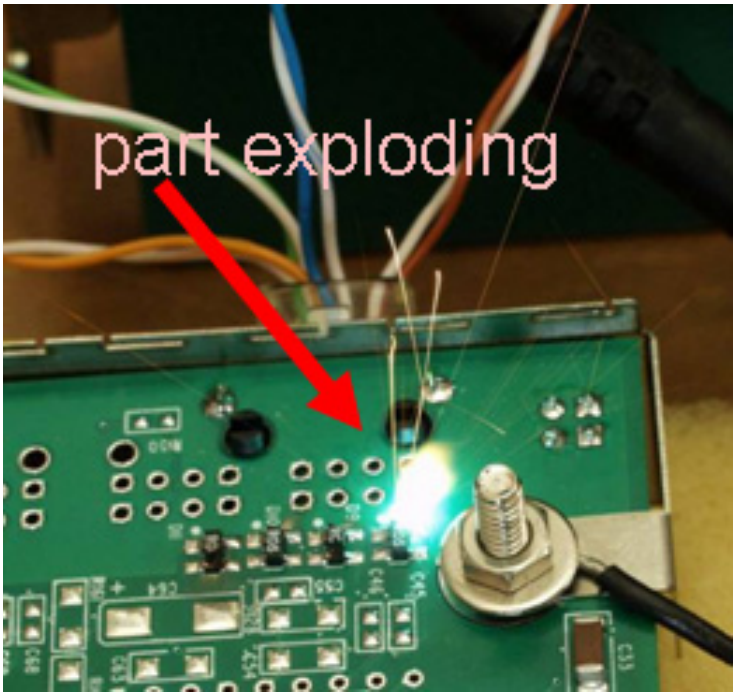

Figure 6-1. A part (a resistor) exploding under pulse testing.

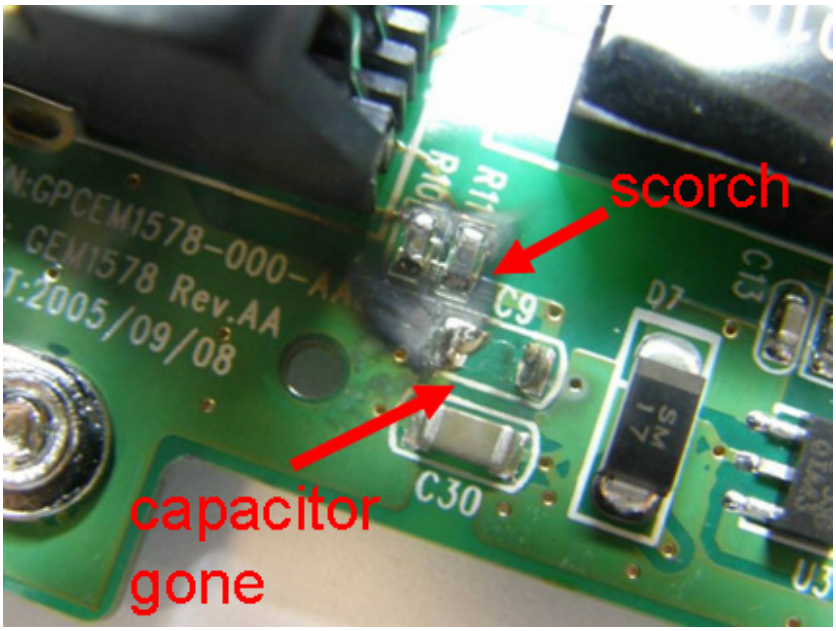

Figure 6-2. Capacitor damage from pulse testing. The capacitor (C9) is gone, and there are scorch marks (C30 shows an undamaged capacitor).

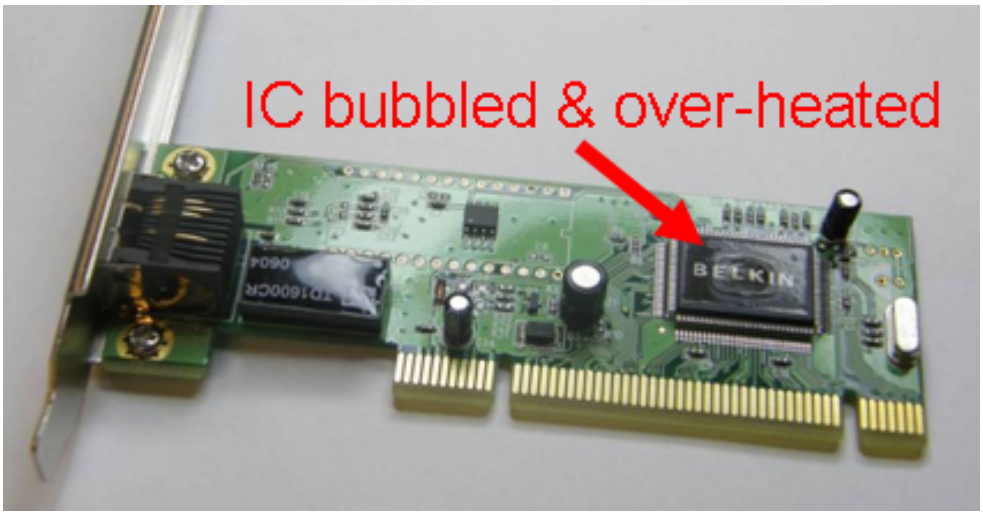

Figure 6-3. The result of pulse testing – IC damage. The IC lid, normally flat, has bubbled, and is discolored from over-heating.

Upset generally refers to functional errors that are not permanent – something that might be fixed by re-booting the system. There might be some gray area between upset and damage – such as changing the data stored in system. What if the change affects a stored program, and there is no health check that indicates the change occurred? If the program has some critical, but seldom used purpose, such as monitoring and reacting to safety issues, it might not be found until it is needed that the safety monitoring is no longer working correctly. Many functions are controlled and/or monitored by computers, and confusing those controls could have a whole spectrum of consequences, from benign to

catastrophic. If there is a control that turns the heat source on only when there is water in the boiler, and that control gets confused into thinking there is water when there isn't, that could be bad for the boiler. Or an automated crane that moves a heavy load around could cause problems if the controls that sense whether a door is open or not gets confused. Thus, upsets may cause systems to damage themselves or other systems.

Besides damage from control systems getting confused, there can be electrical damage triggered by an E1 HEMP pulse, but with the actual damage energy coming from the electrical power of the system itself. Unusual current conduction paths, or system states that never would normally be found, may "dump" system electrical power in a way that causes damage. Thus, it is always better to test for system vulnerabilities with the system powered up and operational. It also is important to try numerous pulses, since vulnerability levels might depend on exactly what state the system is in when it gets hit. This is generally recognized for upset testing, but is also true for damage.

Another issue during testing is that sometimes injection testing is used – a pulser is connected to a system port and a high level current pulse sent in. This only stresses one port at a time, while real E1 HEMP would tend to stress all ports (although not all ports would observe the same level of stress). Generally we would assume that the system might have more problems if all ports are assaulted at once.

For cables with multiple wires, another consideration for vulnerability is the drive mode. Most cables are composed of more than one wire – often there are many wires in a single "cable bundle". In this case there are many ways that the signal can appear at the system port terminals. If we consider a two terminal port, then the two drive modes are:

1. Common mode: The same signal (voltage) is applied on both terminals (the terminals are connected together), with the signal return being the system ground.
2. Differential mode: Opposite polarity voltages are put on the two terminals, with the neutral (zero voltage) being the common system ground.

Any arbitrary drive of the two terminals can be separated into these two modes, with the appropriate level for each. Generally for E1 HEMP drives, the common mode is the most significant. However, there can be vastly different circuit responses and vulnerability levels for the two modes. Often systems are weaker against differential mode assaults, but this is not always true. Often vulnerability pulse testing will separately test the two modes. Generally a prediction of E1 HEMP coupling to a cable provides the total cable bundle response – which is common mode. It can be difficult to determine what the corresponding differential drive level should be. This depends on slight differences in the exact placement of each wire within the cable bundle, and also on differences in load impedances at the ends.

There is reason to worry about our vulnerability to E1 HEMP. As the devices in our modern systems become smaller, their operating voltages get lower, and their operating frequencies get higher, E1 HEMP looks to be more of a threat. The coupled signal can easily be hundreds or thousands of volts, while electronics operate at a few volts. The E1 pulse can last for many time cycles, and also have significant energy at system operating frequencies (100's of megahertz or higher). The high density of transistors and other

devices on an integrated circuit means each is very small – so that even a small amount of energy can be very significant; the smaller the mass that absorbs a given amount of energy, the higher the mass's temperature increase from the absorbed energy.

However, recall that even if the amount of energy from the E1 HEMP pulse is relatively small, and mainly small devices are at risk for damage from the pulse, there can also be damage to more massive devices. An example is a system that is powered, and somehow the confusion from a pulse triggers a damage mode in which the system's own power is turned against the system itself. It is not 100% effective, but it is not a bad idea to turn off a system if an E1 HEMP pulse is eminent. Better still would be to also disconnect the system from long attached cables.

It certainty is unlikely that all electronics in the country, or even in any small region, would suddenly stop in the event of a high altitude explosion. Unhardened modern electronics, with long attached cables, are likely to be hard hit, and some fraction hurt. Cars and vehicles might have some failures. Newer ones do depend on a multitude of computers to work properly, but their cabling is limited in length. It is unlikely that very small systems, such as an electronic wristwatch, would experience much trouble.

One significant aspect of E1 HEMP vulnerability is that has proven to be very difficult to predict the upset and damage levels, even with very crude accuracy. A system typically is composed of many parts, and it has been hard to even estimate which part will fail, let alone get within even an order of magnitude in predicting at what level the system failure would occur. Generally testing must be done to get some idea of the vulnerability levels. For small systems we could use field illumination testing, which most accurately simulates the E1 HEMP environment, with coupling to all the various cables at once. However, sometimes the system is too big for this – especially if it has long cables. In those cases, testing must use direct drive injection into the system ports.

It should be noted that often vulnerability testing is done on a newly manufactured sample of the system, or even on a prototype. Just as we cannot predict vulnerability levels, we cannot estimate how the vulnerability might change with age and use (and abuse). Seemingly unimportant changes may have happened to the system, and gone unnoticed because they do not affect any part of the normal, day-to-day operation of the system, but the modifications could be significant for the system hardness. This is why critical hardened military systems are periodically re-tested to make sure the hardness is still intact.

There has been little success in predicting (through calculations) vulnerability levels for systems – at what levels upset and damage happen, and what part of the system fails. This is understandable, for several reasons:

1. Systems are very complex, in terms of electromagnetic coupling and circuit response.
2. The failure may be deep within the system.
3. There many be very many individual parts; even millions if we consider each device within an integrated circuit.

4. At high excitation levels there are many nonlinearities, and the system is outside the range of the normal circuit response.
5. There are many electromagnetic effects, including shielding, coupling, and re-radiating EM energy.
6. Arcing may occur, either near where the pulse enters the system, or deeper within the system.

We cannot, even with the best computers, just put together a combined electromagnetics and circuit response model of the system, including nonlinearity and arcing, and run it to find the failures (with any accuracy).

We might think that we could at least predict the damage level of a simple discrete part, such as a diode, transistor, resistor, or capacitor. Early in EMP work attempts were made to do this. The only theoretical treatment available was the Wuncsh-Bell theory. This theory had some limited success, but only for a small set of devices. It was developed for junction semiconductor devices, and had its best success with microwave diodes. Over the years electronics has moved on to many other types of semiconductors, and there is no theory for predicting their damage levels well. The Wuncsh-Bell theory mostly just has tutorial use – to indicate that our only theoretical model for failure is of very limited use, but to also indicate that we might expect damage levels to vary with pulse width, and it would not be unexpected for shorter pulses to require higher pulse levels to cause damage.

E1 HEMP has a very short pulse. For cable pickup, the coupled signal may be longer than the incident EM pulse, especially for broadside incidence on a long cable, and there may be some range in pulses widths. It is well known (Wunsch-Bell theory) that the signal damage level increases for shorter pulse widths for traditional junction semiconductors. (Other types of semiconductors would also tend to have damage level variation with pulse width, but not follow this derivation.) This theory was originally derived for the case of sending a square pulse of electrical signal into a semiconductor device. Figure 6-4 shows an example result, with the power level that causes damage plotted. In Figure 6-5 the corresponding energy levels are shown. The curves tend to have three sections. For very long pulses the damage signal level (in power) is a constant (approximately). This is the flat portion on the right side of Figure 6-4. The pulse width is long compared to the time needed for heat to diffuse away from the device's active region. For a little lower level, the device rises up to a steady state high temperature. The device is OK with this temperature, and can dissipate the heat, so the temperature does not go higher. However, turn the signal level up a little more, the temperature goes up accordingly, and that is the breaking point for the device. (This is idealized, of course.)

When a pulse initially starts, it takes some time to heat the device up to the steady state temperature that is just barely OK. This time is approximately indicated by the break in the curve (1 millisecond in this example). If the pulse turns off sooner than this, then the device will not get up to the temperature limit. Thus for shorter pulses, the device can absorb even higher amplitude pulses, and we see the damage pulse level increases for shorter pulses in the middle of this graph of damage levels for power. For very short

pulses the time frame is so short that the absorbed energy has little chance to dissipate away from the device's active region. In this limit (left edge of the graph) there is a constant energy damage level (the left side of Figure 6-5). The device is damaged by the shock of too much energy in too short a time.

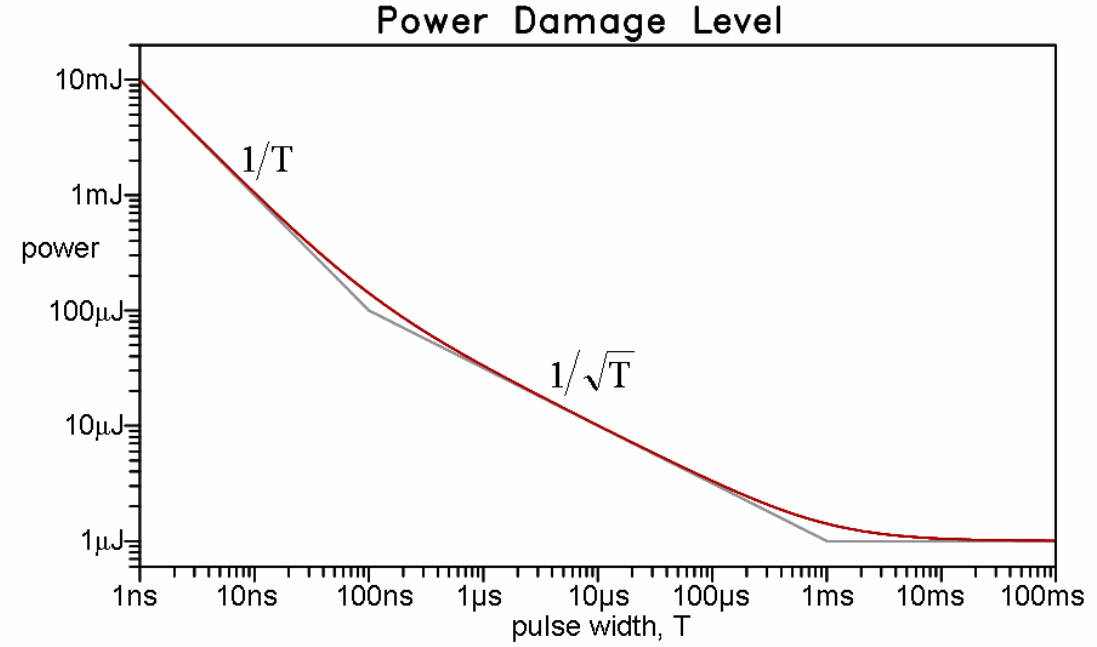

Figure 6-4. Sample Wunsch-Bell power damage levels versus signal pulse width.

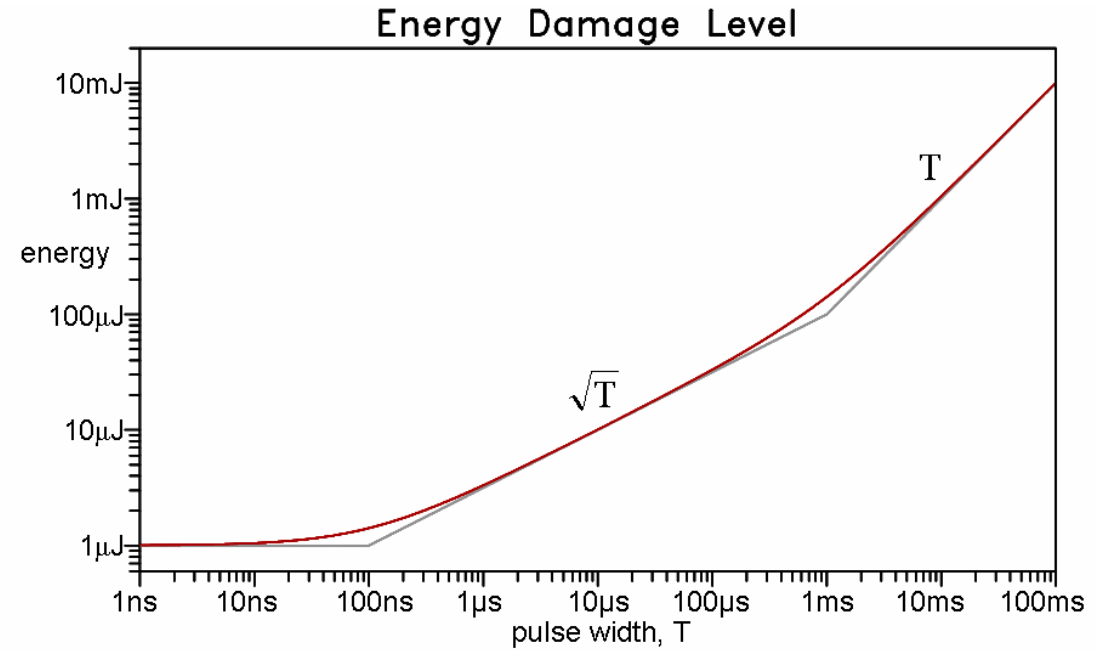

Figure 6-5. Sample Wunsch-Bell energy damage level. The damage energy levels in this plot correspond to the damage levels in Figure 6-4.

As an example of very fast delivery of energy into a device, consider a crude calculation for a silicon integrated circuit chip, for which energy is dumped in a very small region. Some properties of silicon are:

Thermal Diffusivity, D = 0.8 cm^2/sec
Heat Capacity, C = 0.7 Joule/gram-Celsius
Density, ρ = 2.33 gm/cm^3.

A point source of heat diffuses away as

$$e^{-r^2/4Dt}$$

(Charles Kittel and Herbert Kroemer, "Thermal Physics", 2nd Ed., pg 436, W. H. Freeman and Company, San Francisco, 1980). Thus, a 10-nanosecond pulse diffuses out over the distance of

$$r_I = \sqrt{4Dt} = 0.179 \times 10^{-3} \text{ cm}.$$

Assuming a cube of twice this size, its mass is

$$M = \rho (2 r_I)^3 = 1.07 \times 10^{-10} \text{ gm}.$$

Using the sample IEC E1 HEMP pulse given previously, and about a 1 m^2 collection area, then the total energy of the pulse is 0.114 Joules (as given previously). The first 10 ns of the pulse has about 45% of pulse energy, and so let us assume an absorbed energy of

$$W_I = 0.45 * 0.114 = 0.0515 \text{ J}.$$

Thus, from the energy, mass, and heat capacity, the rise in temperature rise is

$$T = \frac{W_I}{M C} = 6.9 \times 10^8 \ ^{o}\text{C}.$$

Obviously such a temperature rise could not be good for the silicon. This is only a crude estimate, but note that only a few thousand degrees is needed to get to the melting point. Damage might also be from mechanical shock from thermal expansion. The main point is that relativity small energy can be very significant if it is deposited very quickly into a very small mass.

As noted, vulnerability levels cannot really be predicted analytically – testing must be used. The most realistic tests would be illumination, such as from a very high power pulse source and antenna. The source would need to illuminate the system and its cables – possibly out to hundreds of meters of cabling length. This usually is not possible, for several reasons. This includes

1. The pulse source needs to be very high power to get up to upset and damage levels for the system, especially if the cables are very long (the antenna needs to be farther away for larger illumination areas and to provide a "plane wave" field). In addition, the source would need to be elevated to simulate illumination from above.
2. The illumination is also hitting everything else in the same area. This makes it hard to instrument the test, and there might be other auxiliary equipment that is needed to interface with the system under test. Also, there might be other equipment nearby, with no connection to the test, that would be threatened by the high level testing.

3. Such a test would only find the vulnerabilities for that one cable layout – other uses of the system might have completely different cable layouts.
4. The tests need to account for many variations, such as polarization angle and angle of incidence, to simulate the variations of E1 HEMP – it often is very impractical to fully do this.

So often the problem is separated into two issues – the coupling to the cabling, and the vulnerability of the system equipment to pulses injected at its cabling ports. It is fairly straightforward to calculate coupling to cables with simple geometries. Then pulse injection testing is used for the system port vulnerabilities. Such an approach becomes more necessary as the system size gets bigger (including cabling length).

There has been a lot of pulse injection testing of equipment – sending an electric pulse into a system port. Such testing has several deficiencies:

1. It skips the coupling step. Thus, for example, calculations need to be made of the coupled drive voltage and current, and would have to be done for each port.
2. Generic pulsers used for injection: Often standard pulsers are used for injecting disturbances into the system. There will usually be some differences from the expected E1 HEMP disturbances. Some of the issues are:
    a. Differential and common mode drive levels.
    b. Impedance of the driver.
    c. Pulse width.
    d. Waveform and frequency content, including oscillations from reflections from the other end of a line.
3. Generally pulse injection only hits a single port at a time, while for E1 HEMP all ports would be hit simultaneously.

Much more pulse injection testing has been done than the more realistic full illumination testing, which is extremely hard and expensive to do (not only because of the pulse source is more complex, and needs to have higher power levels, but the instrumentation is so much harder).

Another problem is that often it is very hard to do a full evaluation of the health of the system after each pulse – however this is actually true for any type of vulnerability testing. It would be nice if we could just pulse the system, and then its lights would stop blinking (upset) or completely go out (damage); but seldom is it so convenient. Some aspect of the system might make a mistake (upset), and this might not be noticed. Some part might be ruined, but not be noticed immediately. Modern systems are usually very complex, with many functions that can be preformed. There are very many inputs, each with many different possible histories, and the system has its complex algorithms it implements in response to those inputs. If some garbled input gets recorded for an input port, do we know that that happened? If a warning sensor or port is damaged, wouldn't the system just assume the condition that triggers a warning is OK right now? If an ADC (analog-to-digital converter) port has lost accuracy due to pulsing on that port, how would the system know that its readings are no longer accurate? Ideally there should be a test routine that runs and tests every aspect of the system. Even if there were, it is unlikely that it would be 100% effective. Upsets, especially, can easily get by without

detection. However, generally pulse testing only has very limited checks for upsets and damage. Sometimes only some aspects related to the pulsed port are checked. Of course this problem is even worse for illumination testing, since one must check the operation of an entire system, not just the section under test.

Pulse testing is still usually the best option. Vulnerability calculations are too inaccurate, and full illumination has its own problems, and generally is not practical. It just has to be understood that there is some uncertainty in vulnerability levels found by pulse injection testing. It is important to recognized, however, that obtaining vulnerability data (even with some uncertainties) will allow protection methods to be evaluated and applied.

Arcing (air breakdown) is very common in high-level pulsing of circuits. Figure 6-6 shows an example, from pulse testing of a PLC (programmable logic controller), such as used for automated controls. Air breakdown occurs at levels of about 1 kV for a 1 millimeter air gap at normal air pressure. The breakdown level may be affected by water vapor, and dust or debris that might have accumulated. The breakdown level can also be higher for very fast pulses – since some time is needed to initiate and close an arc.

Arcing can occur wherever two conductors are close together, and there is a high voltage between the two (such as produced by a high level pulse entering the system). Generally voltages would tend to be highest at the entry point into the system, and are less for points deeper into the system. Thus, often arcing is seen on the port connector itself, as shown in Figure 6-7, or where that connector first attaches to a circuit card (as in Figure 6-6). However, because there might be smaller air gaps elsewhere in the circuit, arcing might also occur deeper in the circuit, such as shown by the scorching and solder erosion in Figure 6-8.

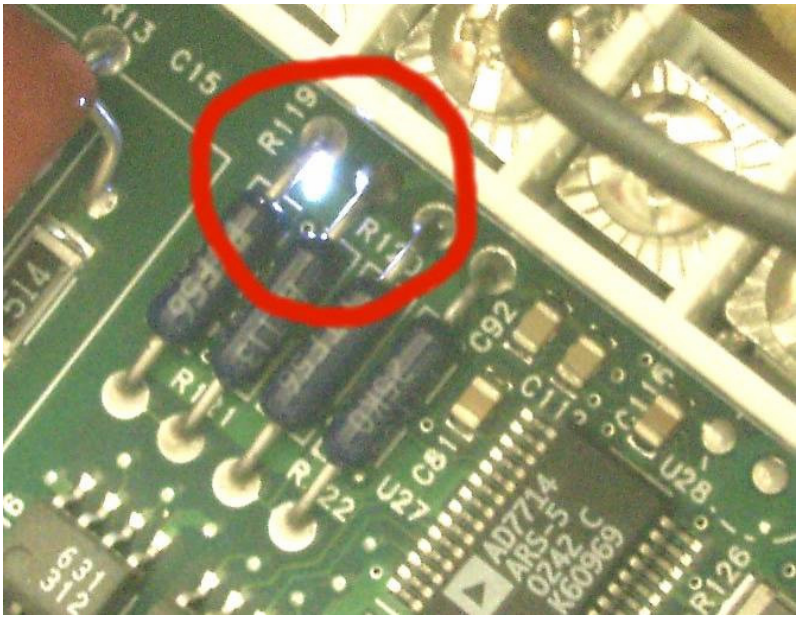

Figure 6-6. Arcing in a PLC (programmable logic controller).

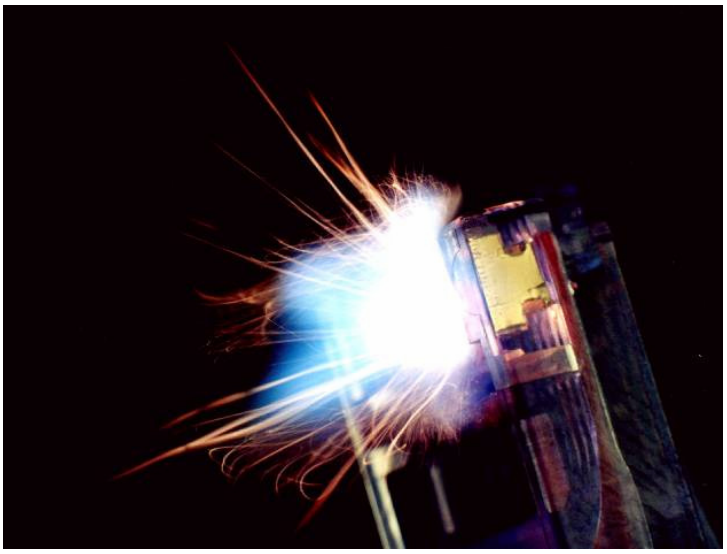

Figure 6-7. Arcing at the port to a system. This is computer network card, with the arcing in the connector where the network cable plugs in.

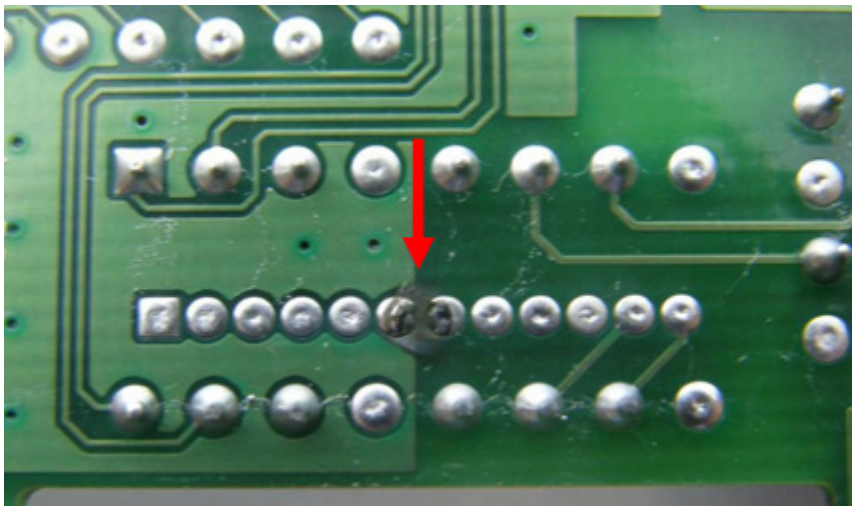

Figure 6-8. Signs of arcing between solder pads on a circuit card.

Generally it is better if the arcing is not deep within the system. The left side of Figure 6-9 indicates an arc at the entry point of the system – large currents can flow, but not through any fragile parts. However, if deeper within the system, such as in the right side of the figure, the high current might flow though a part, and damage it. The protective nature of having the arc near the entry point actually operates as a cheap protective measure, as shown in Figure 6-10. In this case each of the four input lines have a small air gap on the surface of the circuit board, so that an arc will form and short out any high voltage before it can get into the circuit and cause damage. However it would be more controllable (but a little more expensive) to use a device specifically designed to short out high voltages. There are many such devices, such as MOVs (metal oxide varistors), that can be used for protection.

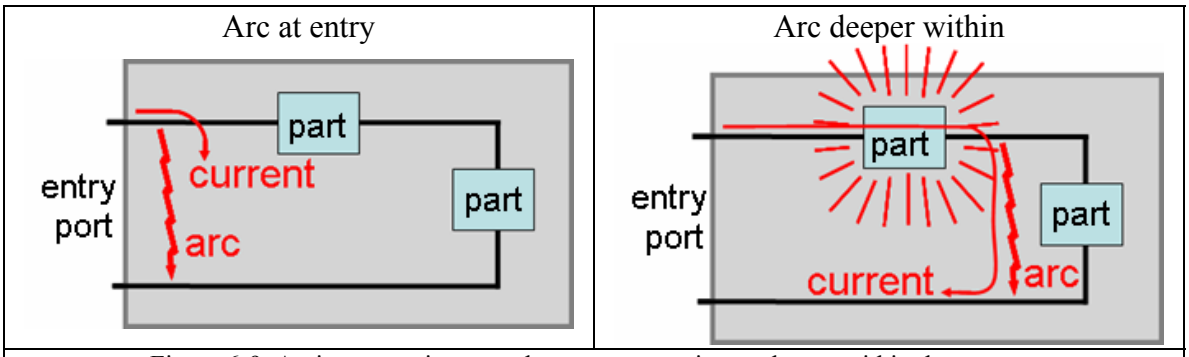

Figure 6-9. Arcing occurring near the port entry point, or deeper within the system.

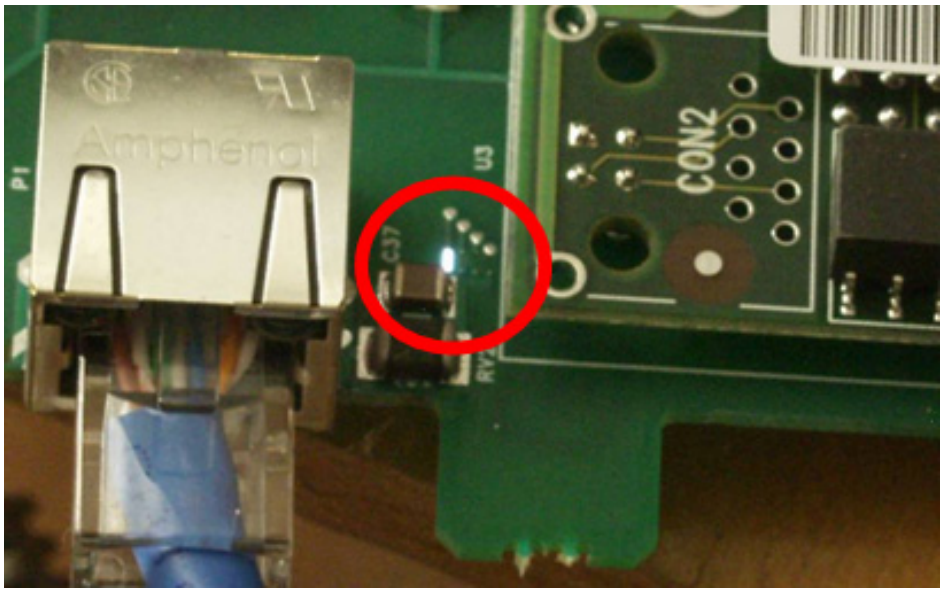

Figure 6-10. Arcing used for protection. Each of the four active input lines on this network device connected to a short air gap – one of which is arcing in this pulse test.

Section 7
Electric Power System E1 HEMP Impacts

In this section we consider the likely impacts of the E1 HEMP on various parts of the electric power system. Metatech has performed a large number of test and analysis studies dealing with the U.S. power grid and has determined that there are five main areas of concern:

1. High voltage substation controls and communications
2. Power generation facilities controls and communications
3. Power control centers communications
4. Distribution line insulators
5. Distribution transformers

It has been determined that the main pathway for the E1 HEMP to reach the electronic equipment that control the operation of the grid is through the coupling of the HEMP fields to cables and wiring, producing conducted transients that can exceed the withstand capability of the connected electronics. In addition, the distribution line insulators and transformers connect to the aboveground electric wires, and so are also influenced by the coupled HEMP fields.

Since there are common cable and wire geometries for these five cases of concern, and because some of the same electronic equipment may be found in different locations, we first present information on the statistical coupling of E1 HEMP fields to randomly oriented horizontal conductors (in the air and shallow buried), and vertical conductors (Section 7.1), and in the following section (Section 7.2) we summarize the testing of electronic control equipment that may be found in locations 1 – 3 above.

This report then proceeds through the five main areas of concern, drawing upon the information presented (Sections 7.3 – 7.7).

7.1 E1 HEMP Coupling to Randomly Oriented Lines

Generally most of the E1 HEMP concerns for the power system deal with coupling to lines – power lines or signal cabling. These calculations determine the line voltages, and the accumulated results of many calculations were processed to give probability results. The results are graphs of probability (vertical axis) that the conductor voltage will exceed the given values (horizontal axis). There are two random parameters for these distributions:

1. Line orientation: any orientation of the line is equally likely.
2. Line position: any position within the E1 HEMP exposed region is equally likely.

Calculations were performed for a nominal E1 HEMP burst, such as shown in the smile diagram of Figure 2-3. Four different burst heights over the U.S. were used:

1. 50 km
2. 75 km
3. 100 km

4. 170 km

The ground conductivity was selected as 10^{-2} S/m for all four scenario runs. For the conductor coupling there were three cases:

1. Horizontal power line: 10 meters off the ground, with results for three different line lengths: 100 m, 300 m, and 1000 m. The line has a characteristic impedance match at both ends.
2. Horizontal control/sensor lines: Essentially on the ground (or shallow buried), for lengths of: 10 m, 30 m, and 100 m. The lines were shorted on one end, and had an open circuit at the end where the voltage is computed (open circuit voltage).
3. Vertical control/sensor line: A vertical line with 4 meters length. The line was shorted at the ground, and was open at the top, where the voltage was measured.

As noted, the probability presented is for a random direction for the run of the line (this does not apply to the vertical line), and for random position within the exposed region of the HEMP burst. As noted in Figure 2-8, the exposed area varies approximately linearly with burst height.

Table 7-1 presents a summary of the assumed parameters, with an indication of where the results can be found. Consider the overhead power line (Figures 7-1 through 7-3). For all cases the lowest curve is for the 170 km burst, and then the curves go in order, with the highest levels (at the same probability value) for the 50 km burst. However, recall that the area coverage is also larger for the higher burst heights, so the probabilities are for different total areas for different HOBs. The average voltages for the 100-meter line (Figure 7-1) are about 2000 V for the 170 km HOB and 6000 V for the 50 km HOB. For the 1000-meter line (Figure 7-3), these values are about 3000 V and 7000 V – so the factor-of-ten increase in line length does not produce much gain in voltage. This is due to the build up to higher E1 HEMP voltages with longer line length being balanced by the propagation loss for signals on the line.

Table 7-1. List of results for E1 HEMP excitation of lines. This table gives some configuration parameters, and also lists the figures that plot the voltage level distributions.

Line Coupling Cases			
Line	Parameters	Length	Results
Power Line	Horizontal 10 m height Characteristic termination	100 m	Figure 7-1
		300 m	Figure 7-2
		1000 m	Figure 7-3
Control/ Sensor Line	Horizontal 0 m height Open on voltage end, short on other end	10 m	Figure 7-4
		30 m	Figure 7-5
		100 m	Figure 7-6
	Vertical Open on voltage end (top), short on bottom	4 m	Figure 7-7
Nominal E1 HEMP HOB runs: 50, 75, 100, 170 km 10^{-2} S/m ground conductivity			

For damage it is actually the high end "tails" of the curves that are important – where the voltages get into the hundreds of kilovolts that could cause insulator or transformer damage. The probability is not high for the example shown – it can get higher for some cases. However, even a low probability can be a problem because, for example, there are many insulators along a power line, and any one of them failing can result in the loss of the whole line. It should be emphasized that the single device used here is not a least or a worst-case device, so the results are representative. In particular, the worst-case E1 HEMP used by the military in MIL-STD-188-125-1 for an E1 HEMP powerline current is 5,000 amperes. The characteristic impedance for a power line is approximately 400 ohms, thus providing a peak worst-case voltage level of 2 MV.

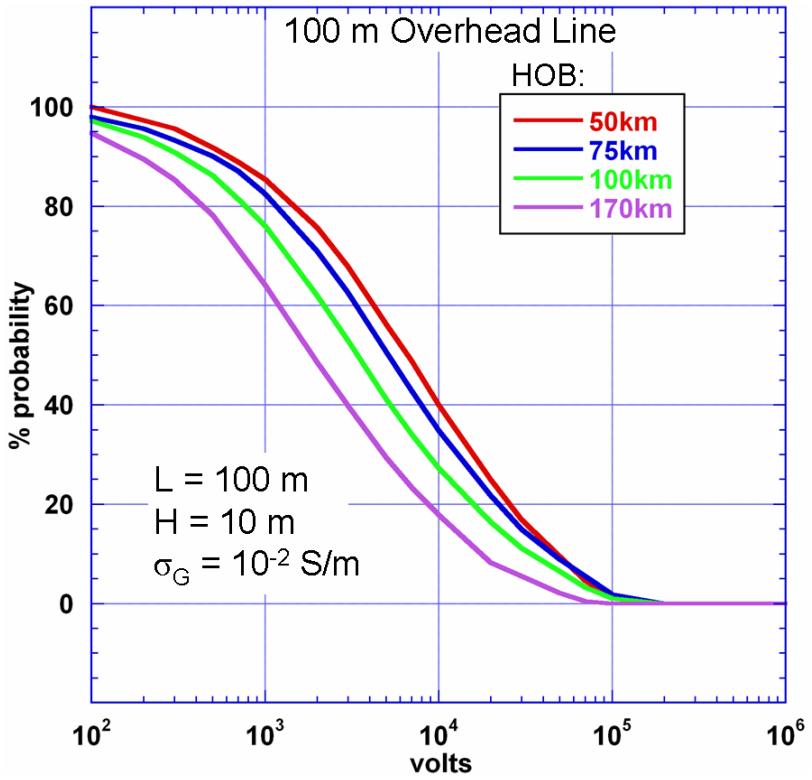

Figure 7-1. Voltage distribution for a 100-meter long horizontal power line. The results are for a typical burst, for four burst heights over the U.S. The power line is 10 meters over 10^{-2} S/m ground.

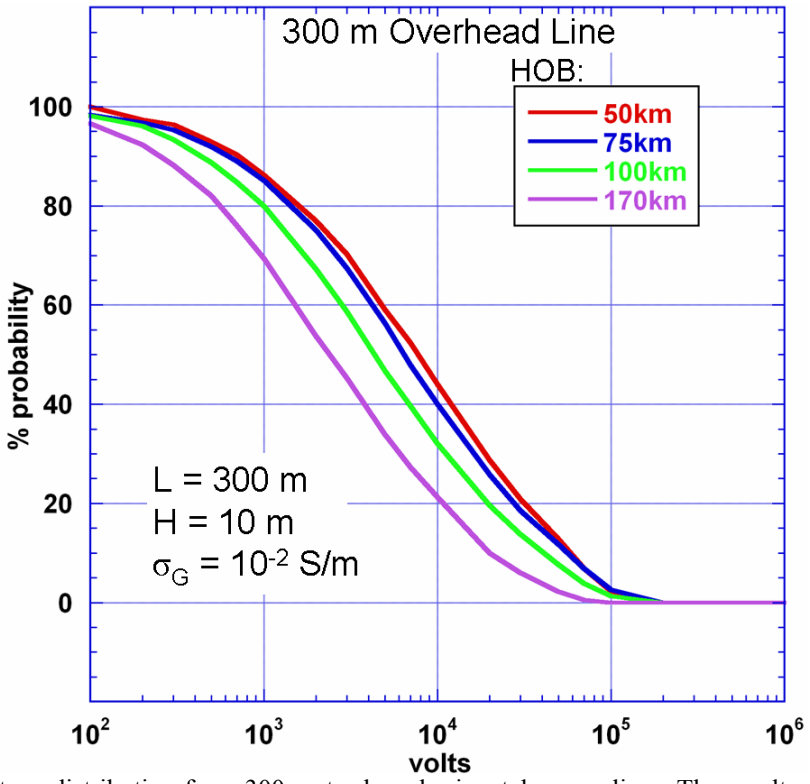

Figure 7-2. Voltage distribution for a 300-meter long horizontal power line. The results are for a typical burst, for four burst heights over the U.S. The power line is 10 meters over 10^{-2} S/m ground.

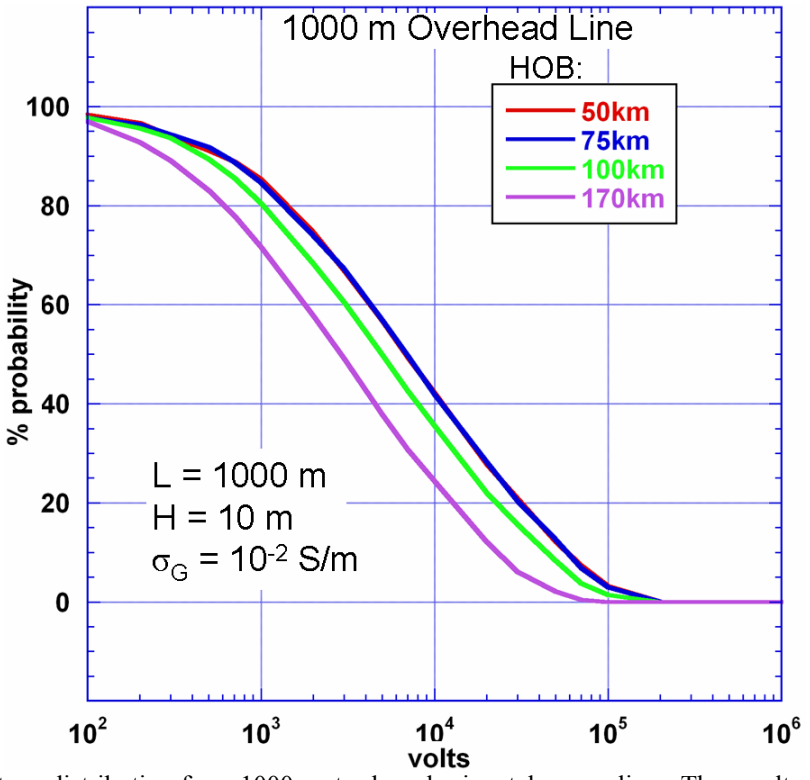

Figure 7-3. Voltage distribution for a 1000-meter long horizontal power line. The results are for a typical burst, for four burst heights over the U.S. The power line is 10 meters over 10^{-2} S/m ground.

Additional calculations are also presented for lines near the surface of the earth (on or slightly below), as these might represent control and sensor lines in a power substation. Shorter line lengths were used: 10, 30, and 100 meters. The next three figures (Figures 7-4 to 7-6) show these results – note that the voltage axis has lower values than for the power line. This is because the earth has the effect of reducing the propagation of the coupled HEMP voltages. For these cases the 75 km HOB does better than 50 km, but the 170 km case is still the result most to the left. The average voltages (50%) for the 10-meter length (Figure 7-4) are 130 V for 170 km and 350 V for 75 km. For the 100 m line length (Figure 7-6) the averages are 380 V for 170 km and 780 V for 75 km. These are less than the results for the 100 m overhead line because the line is closer to the ground. However, note that the distribution also shows that a fair fraction of the lines would have voltages up to thousands of volts. Also, these results are for lines run near the ground – coupling would be even stronger if the line runs are higher off the ground.

The last result (Figure 7-7) is for a vertical control/sensor line or feeder line that is only 4 meters long. However, the results are higher than the longer horizontal lines. The average voltage is 1200 V for the 170 km HOB, and 4000 V for the 50 km HOB. The higher values are due to the vertical field not being shorted out by the ground – it can actually be enhanced by ground reflection.

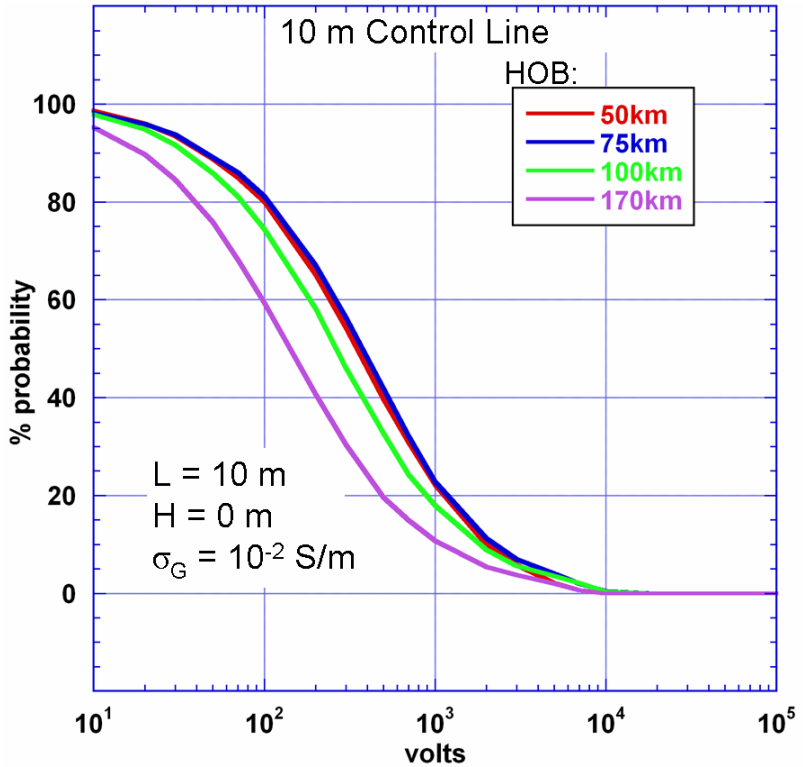

Figure 7-4. Voltage distribution for a 10-meter long horizontal control/sensor line. The results are for a typical burst, for four burst heights over the U.S. The line is lying on the surface of 10^{-2} S/m ground.

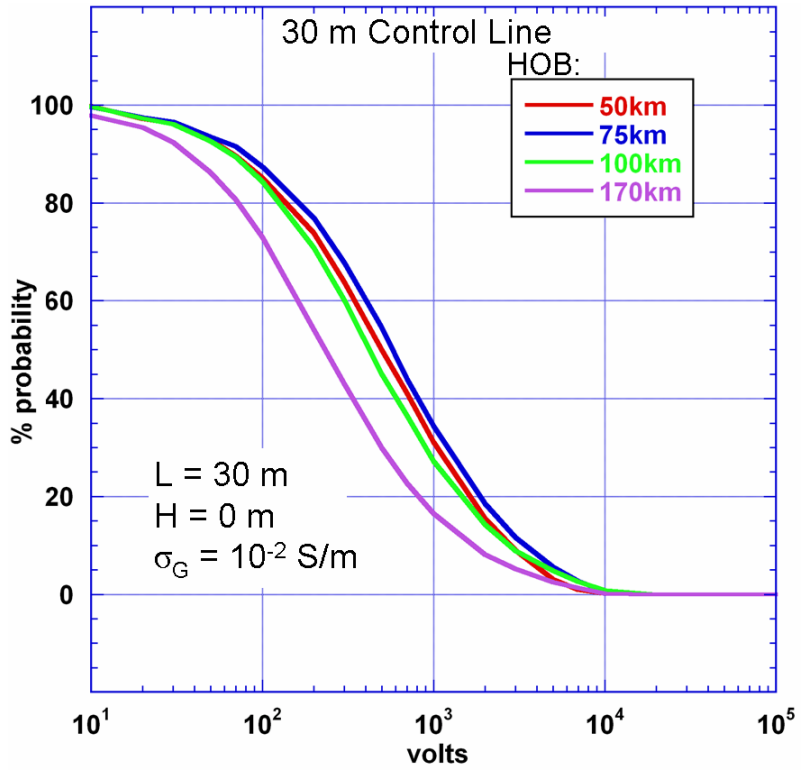

Figure 7-5. Voltage distribution for a 30-meter long horizontal control/sensor line. The results are for a typical burst, for four burst heights over the U.S. The line is lying on the surface of 10^{-2} S/m ground.

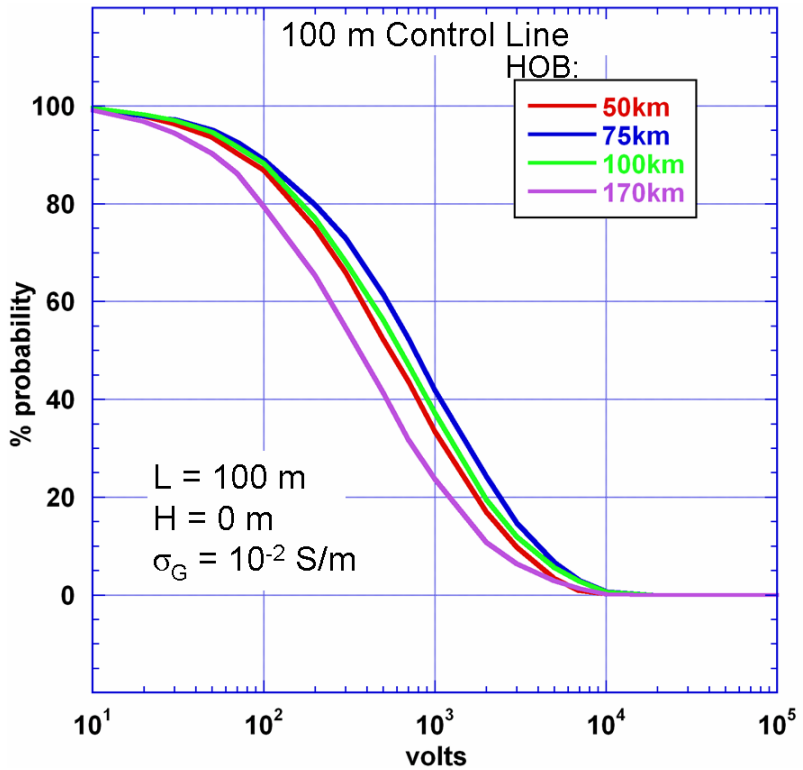

Figure 7-6. Voltage distribution for a 100-meter long horizontal control/sensor line. The results are for a typical burst, for four burst heights over the U.S. The line is lying on the surface of 10^{-2} S/m ground.

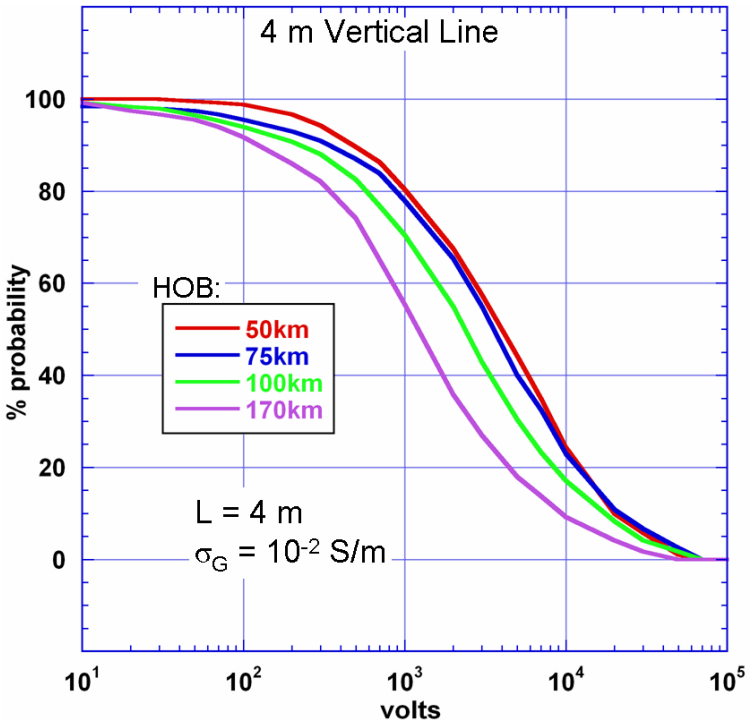

Figure 7-7. Voltage distribution for a 4-meter long vertical control/sensor line. The results are for a typical burst, for four burst heights over the U.S. The line extends upward from the 10^{-2} S/m ground.

7.2 Susceptibility of Power System Equipment

There have been various studies of the power grid vulnerability to E1 HEMP in the past, such as those listed in Table 7-2. Insulator flashover is a major vulnerability studied. Damage to distribution transformers has also been considered. Another concern is the ubiquitous use of electronic devices to control processes, including power substations, control centers, and generation stations.

In Section 7.1 calculations indicated that control/sensor/communication wires can have coupled E1 HEMP peak voltages of thousands of volts. Normally such lines transmit signals of a few volts, and so E1 HEMP pulses could certainly be disruptive. There are many electronic devices that are located in a power substation, central control facility, or generator station that would also have attached cables. These include:

1. Computers, of various kinds.
2. PLCs – programmable logic controllers – basically computers, but specialized with I/O ports, such as A/D and D/A converters (A= analog, D= digital) so that they can be process controllers.
3. Communication devices – modems, routers, switches, etc.
4. Solid-state safety relays (increasingly used as replacements for the older electromechanical power relays).
5. SCADA systems (Supervisory Control And Data Acquisition) – this involves communication of data and controls between unmanned substations and manned control centers.

Table 7-2. Some previous studies of the response of the power grid to E1 HEMP.

Power Grid E1 HEMP Studies					
Study	Main Focus	HEMP Environment	Failure Mechanisms Studied	Conclusions	Comments
ORNL HEMP Assessment Program 1983-1992	Interconnected power grid.	Early-time fixed peak field waveforms.	Component damage, multiple flashovers, excessive load flows, and system instability.	Early time HEMP may cause some local outages.	Test data collected for 500 ns pulses. Shorter duration pulse data are needed for more realistic HEMP waveforms.
First LLNL Study 1993	Interconnected power grid.	Early-time enhanced threats with fixed peak field waveforms.	Multiple flashovers resulting in excessive loss of load.	Multiple HEMP events could cause major power outages.	Flashover assessment was based on the ORNL flashover data.
Second LLNL Study 1995	Interconnected power grid.	Early-time enhanced threats with fixed peak field waveforms.	Suppressed bus voltages caused by multiple flashovers resulting in system instability.	HEMP could cause stability problems on power networks.	Flashover analysis was based on data collected from one insulator. The power line model used is not representative of U.S. 12 kV power lines.
Metatech Quick Study (EMP Commission) 2002	Interconnected U.S. distribution power grid.	Realistic early-time HEMP environments from specific weapon design categories. HEMP coupling preformed for a real distribution grid.	System instability due to multiple flashovers that result in excessive current or power flows beyond designed limits.	Regional outages are possible for some threat conditions due to stability problems in power networks. Control systems may also be vulnerable. More data on short-duration pulse insulator flashovers are needed.	A parametric study of flashover probability has been conducted. The probable impacts based on power system limits have been assessed.

Such devices can be vulnerable to either upset or damage from E1 HEMP pulses coming in on the connected wiring. (As mentioned before, there is always the possibility that some functional upsets might actually lead to damage of other equipment, particularly for devices controlling moving structures or burning of fuels, for example.)

There has recently been some susceptibility testing of samples of such devices, especially using pulse injection testing. There have been many tests of common systems, such as PC computers, and their associated devices. General pulse width variation is as expected, with the wider pulses more easily producing damage. Often there is much variation in

results, depending on the model and manufacturer of the device. Typically damage has been found at levels of several thousand volts. Some damage has been at levels less than 1000 volts, and sometimes no damage is found up to the highest typical pulse levels (about 5 kV is typical for most test equipment). Typical upset levels are generally lower than typical damage levels, but often there is not a huge difference for a given device. Susceptibility is usually found by slowly increasing the pulse level on successive pulses, until an effect is found (upset or damage), and sometimes damage occurs without any upset being noted at lower pulse levels. The following information summarizes an extensive set of testing performed by Metatech Corporation.

Pulse testing of representative substation equipment was done for the EMP Commission in a relatively rapid test program. NERC (North American Electric Reliability Council) provided the EMP Commission with a priority list of power system equipment that should be tested. In these tests, the DUT (device under test) was pulsed with an E1 HEMP relatable waveform into a single port for each shot, with the device running during the test. After each shot there was a quick check for upset or damage. The pulser drive level was gradually increased in steps, to try to resolve the level of failure, if any occurred. A full set of tests was done using a standard fast pulse waveform (5 ns rise, 50 ns wide), and there were also some tests using wider pulses – 50 microseconds wide. Here we will show a few results. Pulsing was also done for both polarities of pulses. Also, when there were multiple ports of the same type, each individual port was tested. We can never assume that polarity does not matter, or that all ports of the same type will behave in the same manner.

In the past, substation power control used big electromechanical relays, and there are many such devices still in use. Figure 7-8 shows an overcurrent relay, and Figure 7-9 shows a distance relay. Pulse testing was done on both devices, up to the 8 kV level, and no failures were noted (although there was some minor arcing).

Newer relays are now electronic (solid state), such as shown in Figure 7-10, with an inside view in Figure 7-11. This device is well built, with protection on most of the ports. This shows up in the system not suffering any damage up to the highest pulse level available, as indicated in the chart of Table 7-3. The table also includes the results for SCADA units (Figure 7-12) that are made by the same company, and also appear to have good protection against pulses. The SEL 311L relay did have upset, however, and it was repeatable and affected several aspects of the unit besides just the port that was pulsed. This was at a pulse level of 3.2 kV going into a serial port. The relay had to be turned off and then back on to get it to work properly again.

Table 7-4 shows results for wider pulses for some of the ports. The protection worked well for this wide pulse too, but in this case we did get damage, on three ports. The IRIG ports for both the SEL 331L and SEL 2032 were broken at a level of a few hundred volts (600 volts open circuit). The Ethernet connection on the SCADA unit was also damaged at a low level (1.2 kV open circuit). In this case we heard a “bang” associated with the damage, and further testing showed that a resistor on the circuit board was blown up (as seen in Figure 6-1).

In Figure 7-13 we show a sample oscilloscope recording from a shot on the SEL 311L relay. During pulse testing there may be thousands of shots, and the current and voltage signals are recorded for each. This helps look for unusual behavior (often the occurrence of arcing can be seen in the waveforms), but it also is useful if there happens to be damage – it helps characterize the parameters of damage (and once damaged, the sample unit cannot be tested again, at least not on the same port, so we cannot go back and try to make measurements afterwards). In this case the pulse was negative. Vulnerability should be checked with both positive and negative pulse drive – sometimes effects will occur at a lower level for one polarity than for the other. These results for a protected port show common results. The width of the current waveform is similar to that of the incident pulse; the voltage is much shorter. This is because the protection device (MOV – metal oxide varistor) suddenly becomes very conductive when the voltage gets too high, and shorts out the pulse. This MOV turn-on is indicated by the voltage suddenly going to a low value (and shown by the violet arrow).

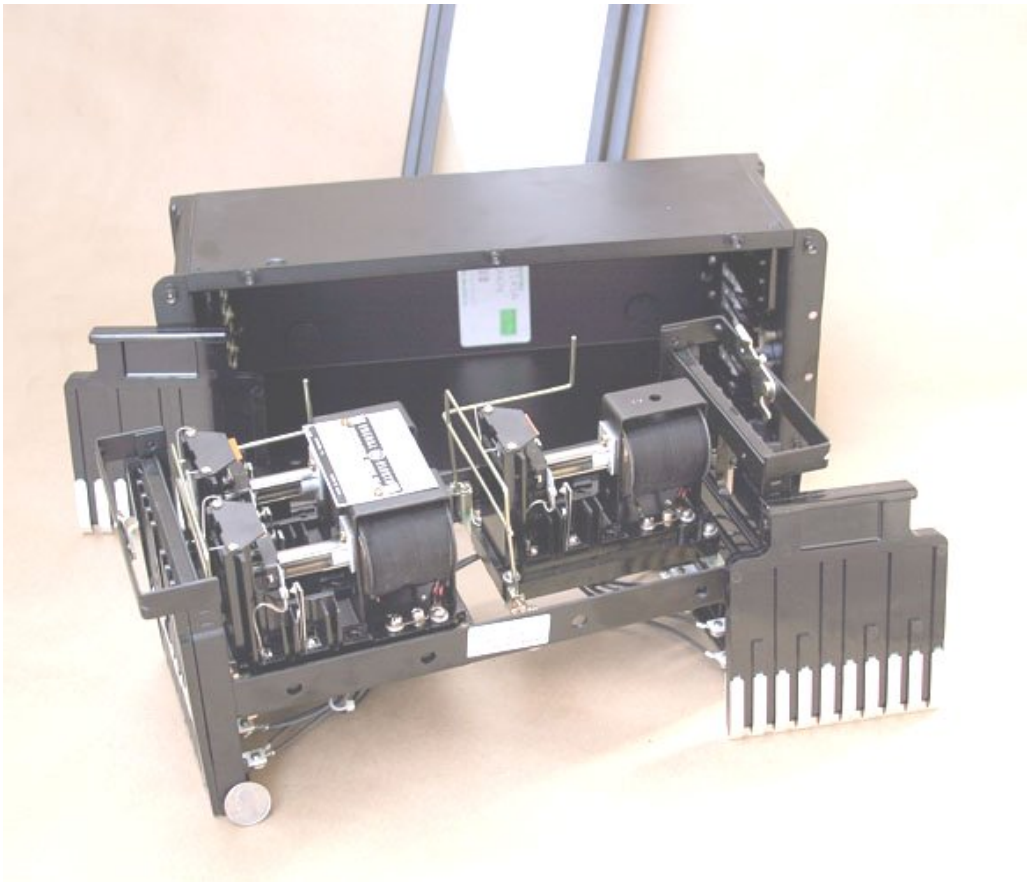

Figure 7-8. GE-PJC electromechanical overcurrent relay.

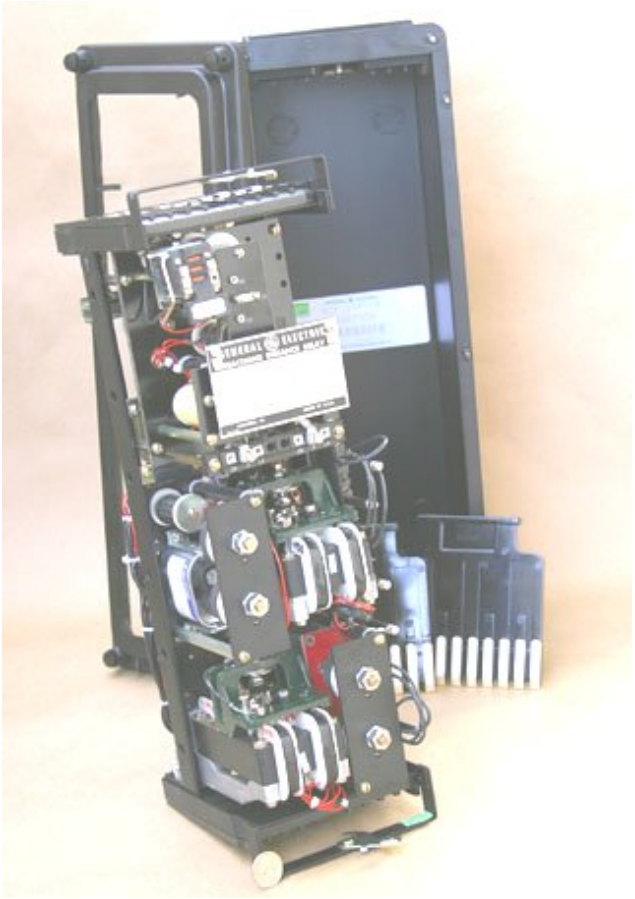

Figure 7-9. GE-GCX electromechanical distance relay.

Figure 7-10. Modern relay unit. This is the SEL-311L (front view on top, back view on the bottom).

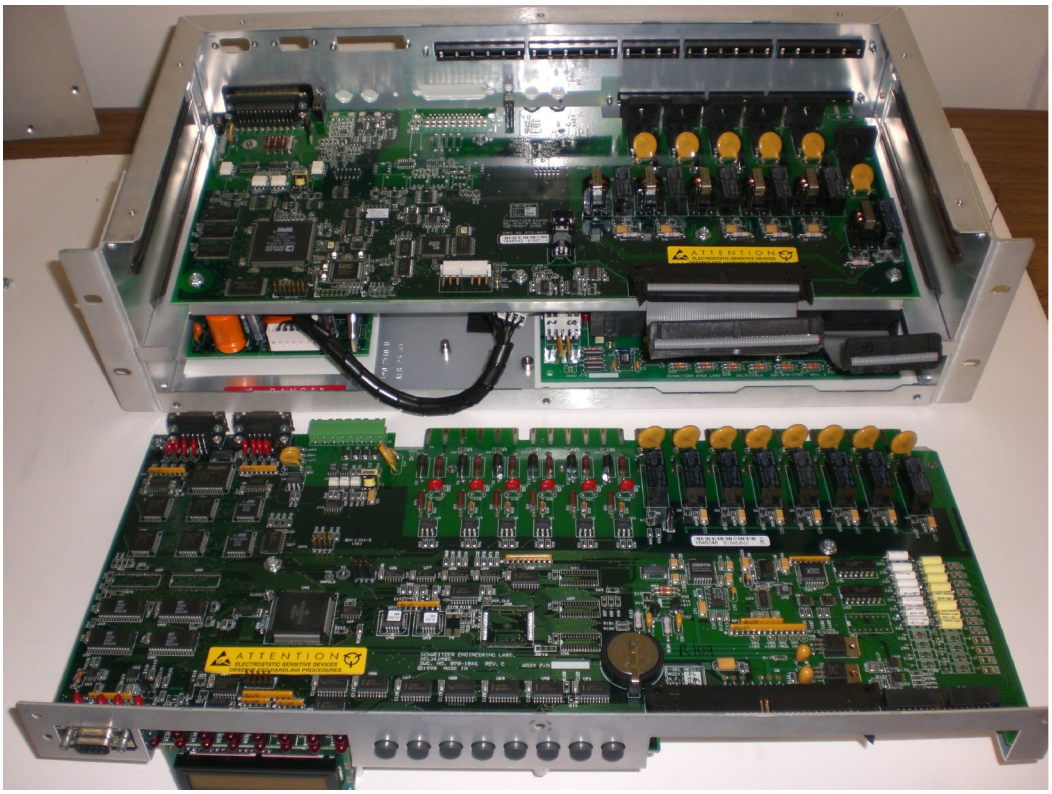

Figure 7-11. Inside the SEL-311L electronic relay unit.

Figure 7-12. Modern SCADA unit. This is the SEL-2032 (front view on top, back view on the bottom).

Table 7-3. Fast pulse results for relay and SCADA equipment. This gives the pulse test results for the Schweitzer Engineering Laboratories relay (SEL-311L) and SCADA unit (SEL-2032). The entries show the test level – for example, 5.5/3.2 means the pulser open-circuit level was 5.5 kV, but the peak voltage was 3.2 kV for the shot (due to loading). The columns show: "No Effect" means no failures up to the level shown (usually the pulser limit), "Upset" means an upset was found, and "Damage" indicates permanent physical damage and failure of the system. The cell color is used to indicate the breadth of the effect – just the pulsed port (yellow), other ports of the same type also affected (orange), or also effects on other system functions (red).

Schweitzer Electronic Relays					
DUT		Drive	Voltage Level: Charge/Load, kV		
Unit	Port		No Effect	Upset	Damage
SEL 311L Relay	Discrete In	Differential	8.0/7.9	-	-
	Discrete Out	Differential	8.0/4.0	-	-
	Analog In, V	Differential	8.0/5.8	-	-
	Analog In, I	Differential	8.0/5.5	-	-
	Serial Port	Differential	-	5.5/3.2	-
	IRIG In	Differential	8.0/4.3	-	-
	Power In	Differential	8.0/4.7	-	-
SEL 2032 Comm. Unit	Discrete In	Differential	8.0/8.0	-	-
	Discrete Out	Differential	8.0/4.8	-	-
	Serial Port	Differential	8.0/4.1	-	-
	IRIG Out	Differential	8.0/5.0	-	-
	Ethernet	Common	8.0/4.5	-	-
		Differential	8.0/4.1	-	-
	Power In	Differential	8.0/4.9	-	-
SEL 9310 Power Supply	Power Out	Differential	8.0/4.0	-	-
	AC In	Differential	8.0/4.8	-	-
SEL 9502 Arc Supp.	Contact	Differential	8.0/4.2	-	-
	I Sensor	Differential	8.0/5.0	-	-
Breadth of Effect:	Pulsed Port	Associated Ports	System Wide		

Table 7-4. Slow pulse test results for the SEL units.

Schweitzer Electronic Relays, CWG Pulse					
DUT		Drive	Voltage Level: Charge/Load, kV		
Unit	Port		No Effect	Upset	Damage
SEL 311L Relay	Discrete In	Differential	4.3/4.4	-	-
	Discrete Out	Differential	4.3/4.1	-	-
	Analog In, V	Differential	4.3/4.7	-	-
	Analog In, I	Differential	4.3/0.2	-	-
	Serial Port	Differential	4.3/0.1	-	-
	IRIG In	Differential	-	-	0.6/0.14
	Power In	Differential	4.3/1.0	-	-
SEL 2032 Comm. Unit	Discrete In	Differential	4.3/4.4	-	-
	Discrete Out	Differential	4.3/0.7	-	-
	Serial Port	Differential	4.3/0.1	-	-
	IRIG Out	Common	4.3/0.01	-	-
		Differential	-	-	0.6/0.2
	Ethernet	Common	-	-	1.2/0.1
SEL 9310 Power Supply	Power Out	Differential	4.3/0.4	-	-
Breadth of Effect:	Pulsed Port	Associated Ports	System Wide		

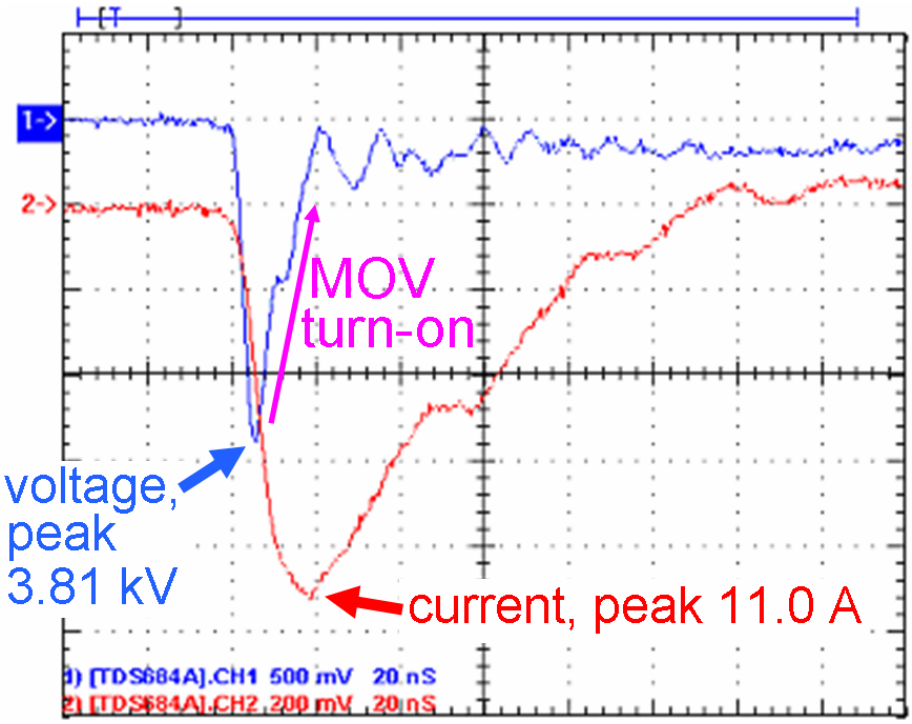

Figure 7-13. Sample pulse test shot result. This shows the recording of the voltage (blue) and current (red) at a protected port of the SEL 311L. (The horizontal axis is 20 ns per major division.)

The next results are for two types of PLCs (programmable logic controllers). They are used as the "brains" of automated controls of processes. These devices do simple computing, working with their many I/O (input/output) ports of various types. There are analog-to-digital and digital-to-analog converters. These are for sensors and controls that work on continuous ranges of voltages or currents. There are also binary I/O ports – with just two possible states, either on or off. These PLCs generally might need to occasionally send status information and receive instructions from elsewhere (and they need to be programmed), so they also have communications ports, either serial or Ethernet (or both).

These devices are much cheaper than the SEL equipment just discussed, and it shows in the hardiness of the units. The ports are not well protected (and the cases are plastic, so there is no Faraday cage around the devices).

Figure 7-14 shows the Fisher ROC809 unit (showing how it is configurable – one of the optional cards is pulled out). It also has a separate power supply, not shown. Table 7-5 gives the fast pulse results. Two types of ports did not have effects, but the rest had either upset or damage (or both). The effects ranged from some that were localized to the port that was pulsed, up to effects occurring on other parts of the device. Damage was as low as 1 kV for the analog out port. The "analog out" card damage was subtle at first – its output was more and more inaccurate as the pulse level was increased, until finally (at 1 kV) the level was too high, and it no longer would work.

The serial port results were interesting. The ROC809 has a plastic case, and no "ground". This can be challenging when trying to do common-mode pulse tests. For the serial port tests the power supply ground was used as the ground. For the higher level pulses a clicking noise was heard in the power supply. Furthermore, a completely separate card ended up being damaged – the "analog input" (ADC) card. It was suspected that this was due to there not being a clean return path of the current pulse sent into the serial port – finding a path back to the ground in the power supply might have involved some of the current going through the ADC card.

The Ethernet port was upset at 3 kV, and damaged at 4.5 kV. In this case, negative pulses had these effects, but positive pulses did not. Note that Ethernet cables can be fairly long, and so will have large E1 HEMP pickup.

The Allen-Bradley MicroLogix 1000 PLC, shown in Figure 7-15, is a similar unit. It is not configurable, as the ROC809 is, but it does have similar ports: analog input and output, binary input and output, and a serial port for programming and communications. For Ethernet communications there is a separate unit (shown on the left) that connects to the serial port.

The MicroLogix 1000 fast pulse results, shown in Table 7-6, also have a similar range of results, with ports that show: no effects, upsets, and damage. For breadth-of-effect there is the full range of affecting only the pulsed port, up to having effects on other parts of the device. As for many cases in these tests, upset generally required re-booting the

device (power off/on cycle). For some upsets the program had to be re-inserted into the PLC to get it to work again. For damage to the analog input, it was noticed that some bits of the ADC were permanently stuck, so that accuracy was compromised. For this unit we also damaged the Ethernet port – at the 7 kV level.

Some slow pulse testing was also done, with the results shown in Table 7-7. The analog out (DAC) died at a low pulse level, 600 volts. This killed all of the analog out ports – as they all share the same converter circuit.

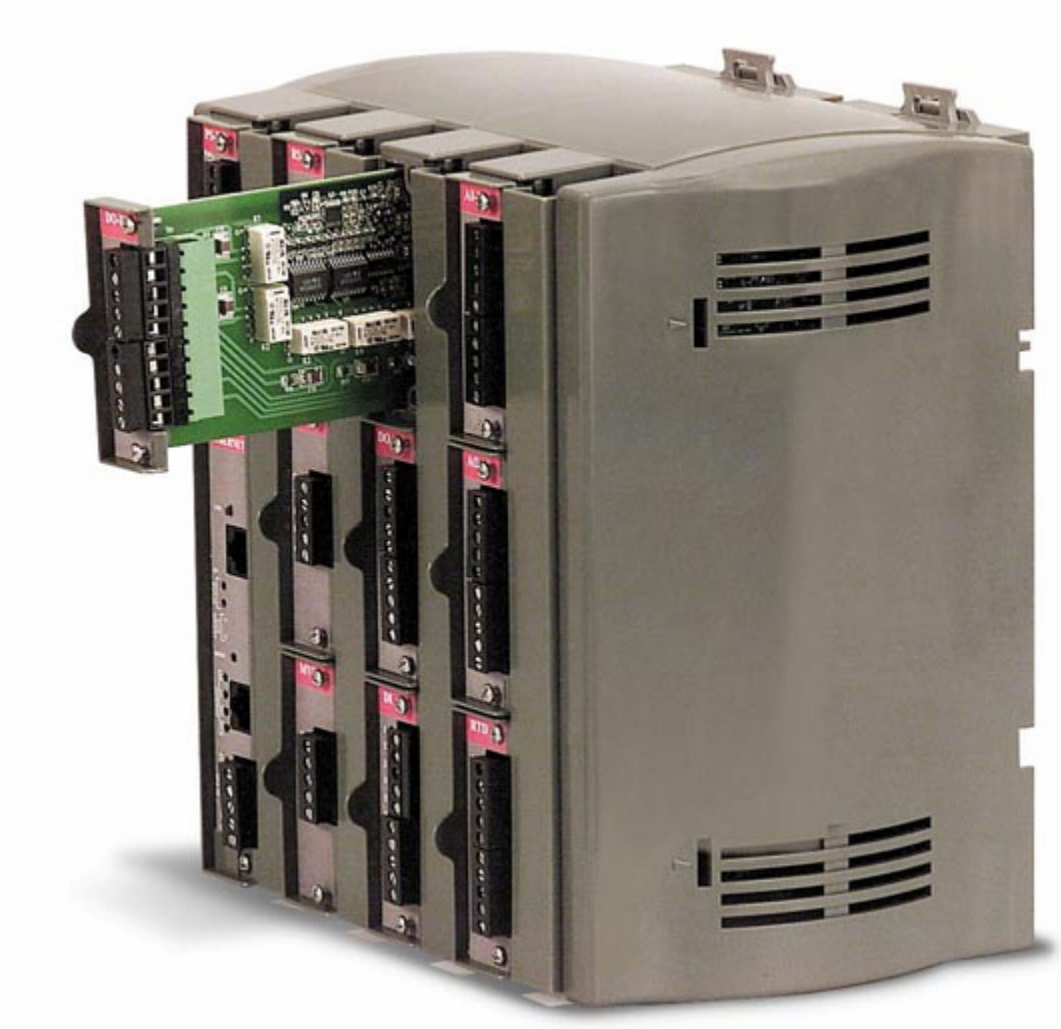

Figure 7-14. The Fisher ROC809 Remote Operations Controller. This is a PLC, such as might be used for remote controlling of a pipeline. It has a computer, and then may be configured with various I/O units: analog, binary, and communications.

Table 7-5. Fast pulse results for the Fisher ROC809 unit.

Fisher ROC809 Remote Operations Controller					
DUT		Drive	Voltage Level: Charge/Load, kV		
Unit	Port		No Effect	Upset	Damage
ROC809	Discrete In	Differential	-	3.0/3.4	-
	Discrete Out	Differential	-	8.0/5.2	
	Analog In	Differential	8.0/4.5	-	-
	Analog Out	Differential	-	-	1.0/0.6
	Serial Port	Common	-	-	2.5/2.1
	Ethernet	Common	-	3.0/3.0	4.5/4.7
Power Supply	AC In	Differential	8.0/5.1	-	-
Breadth of Effect:		Pulsed Port	Associated Ports		System Wide

Figure 7-15. The Allen-Bradley MicroLogix 1000 PLC. The PLC, the unit on the right, has analog and binary I/O ports. Its communications is handled by the 1761-NET-ENI unit shown on the left.

Table 7-6. Fast pulse results for the Allen-Bradley MicroLogix 1000 PLC.

Allen-Bradley MicroLogix 1000 PLC					
DUT		Drive	Voltage Level: Charge/Load, kV		
Unit	Port		No Effect	Upset	Damage
MicroLogix 1000 PLC	Discrete In AC	Differential	8.0/7.1	-	-
	Discrete In DC	Differential	-	8.0/6.2	-
		Common	-	4.5/1.6	-
	Discrete Out	Differential	8.0/6.1	-	-
	Analog In, V	Differential	-	-	3.5/3.3
	Analog In, I	Differential	-	2.5/1.7	-
	Analog Out, V	Differential	4.5/2.0	-	-
	Serial Port	Common	-	7.0/5.9	-
	AC power	Differential	8.0/5.0	-	-
ENI	Ethernet	Common	-	4.5/3.9	2*3.5/4.0
Breadth of Effect:		Pulsed Port	Associated Ports		System Wide

Table 7-7. Slow pulse results for the Allen-Bradley MicroLogix 1000 PLC. (Only a few ports were tested.)

Allen-Bradley MicroLogix 1000 PLC, CWG Pulse					
DUT		Drive	Voltage Level: Charge/Load, kV		
Unit	Port		No Effect	Upset	Damage
MicroLogix 1000 PLC	Discrete In AC	Differential	-	-	4.0/4.0
	Analog Out, V	Differential	-	-	0.6/0.6
Breadth of Effect:		Pulsed Port	Associated Ports		System Wide

A computer was also tested. This was a standard PC, matched with a simple Ethernet switch. Table 7-8 gives the results for the fast pulse. The Ethernet switch was upset (stopped working) at the 2.0 – 2.5 kV level. The full 8-port unit stopped communicating, although the pulse was sent into only one port. A power reset restored the device. Two different network circuits were tried for the computer – one on the motherboard and the other an expansion card. These upset at the 4.5 – 5.0 kV level, and worked again after a re-boot. The serial port on the computer died at a very low level – 750 volts. This occurred for both the built-in serial port and an expansion card serial port. The phone modem had no failure up to the 8 kV maximum, and the AC power plugs also had no problems.

Table 7-8. Fast pulse results for a typical PC and network switch.

Compaq PC					
DUT		Drive	Voltage Level: Charge/Load, kV		
Unit	Port		No Effect	Upset	Damage
Network Switch	Downlinks	Common	-	2.5/2.3	-
	Uplink	Common	-	2.0/2.0	-
	AC Power	Differential	8.0/6.8	-	-
PC	LAN PC Card	Common	-	4.5/3.8	-
	Onboard LAN	Common	-	5.0/2.4	-
	Modem	Common	8.0/4.3	-	-
	Serial Port	Common	-	-	0.75/0.5
	AC power	Differential	8.0/5.1	-	-
Breadth of Effect:		Pulsed Port	Associated Ports	System Wide	

Given the vulnerability levels for such equipment, and the levels of coupled signal that E1 HEMP can produce, it can be seen that the "brains" and communication systems of any modern power facility could be vulnerable to E1 HEMP. This applies to power substations, control centers, and power generation facilities. However, there can be a large range of variation, which depends significantly on the particular layout of each facility.

The equipment susceptibility data summarized in this section will be applied in the following sections of this report with respect to particular power grid impacts of concern.

7.3 High Voltage Substation Controls and Communications

It is important to evaluate the E1 HEMP threat to high voltage power networks throughout the world, and to develop protection methods to deal with the threat. High voltage power substations are especially at risk as they are usually operating without on-site personnel, and many substations will be exposed with high-frequency electromagnetic fields from one high-altitude nuclear burst, as shown in Figures 7-16 and 7-17.

Figure 7-16. Exposure area for E1 HEMP burst at 170 km over Ohio.

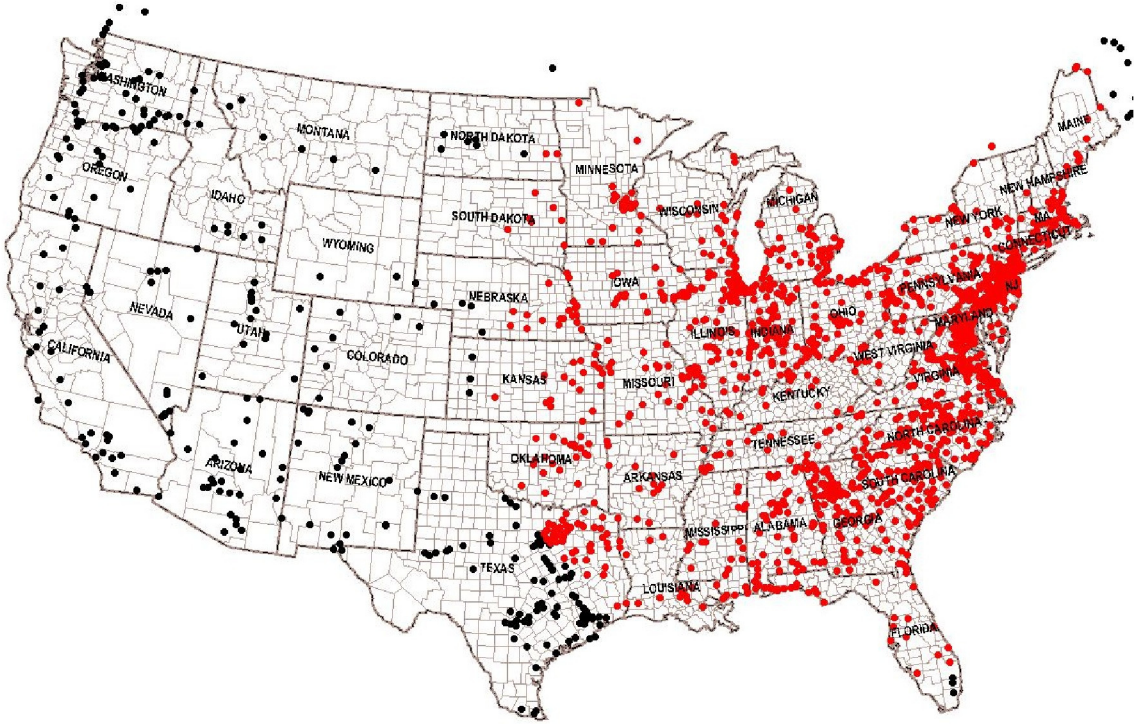

Figure 7-17. EHV substations in the exposed region shown in Figure 7-16. There are 1765 EHV substations exposed (red dots), about 83% of such substations for the country. (EHV indicates 345 kV or higher.)

The biggest E1 HEMP concern within a high voltage substation is not the high voltage transmission lines and transformers, but rather the low voltage sensor and control lines that extend from the transformer yard to the relays and other control electronics in the control building. While these cables are in conduits above ground (shown in Figure 7-18), these conduits are not effective electromagnetic shields at high frequencies. Currents and voltages coupled to an external conduit are likely to leak into the internal cable at the joints and at connection points to sensors and the controls.

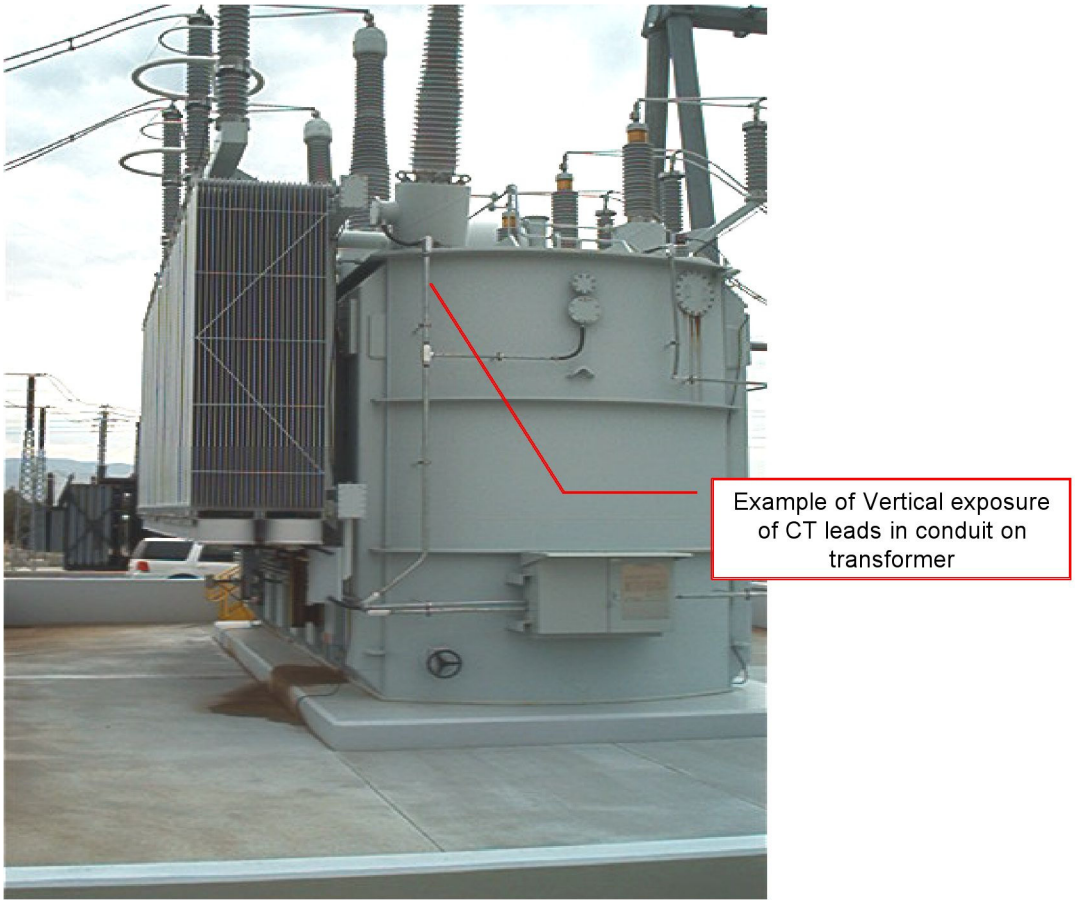

Figure 7-18. Exposure of cable conduits on transformers.

In Figures 7-19 and 7-20 the sensor and control cables are seen to run slightly below ground in trenways that are "buried" in the gravel in the transformer yard. The length of these cables and the poor electromagnetic shielding of the trenway and the gravel at high frequencies will allow the penetration and coupling of high frequency fields to the cables and the subsequent propagation of these currents and voltages to the control building.

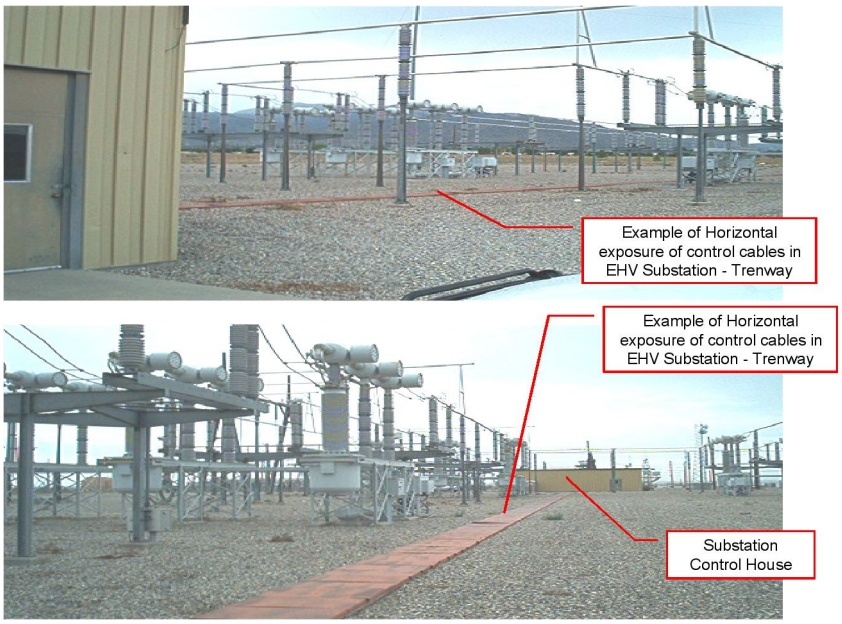

Figure 7-19. Long runs of "buried" cables in low conductivity gravel.

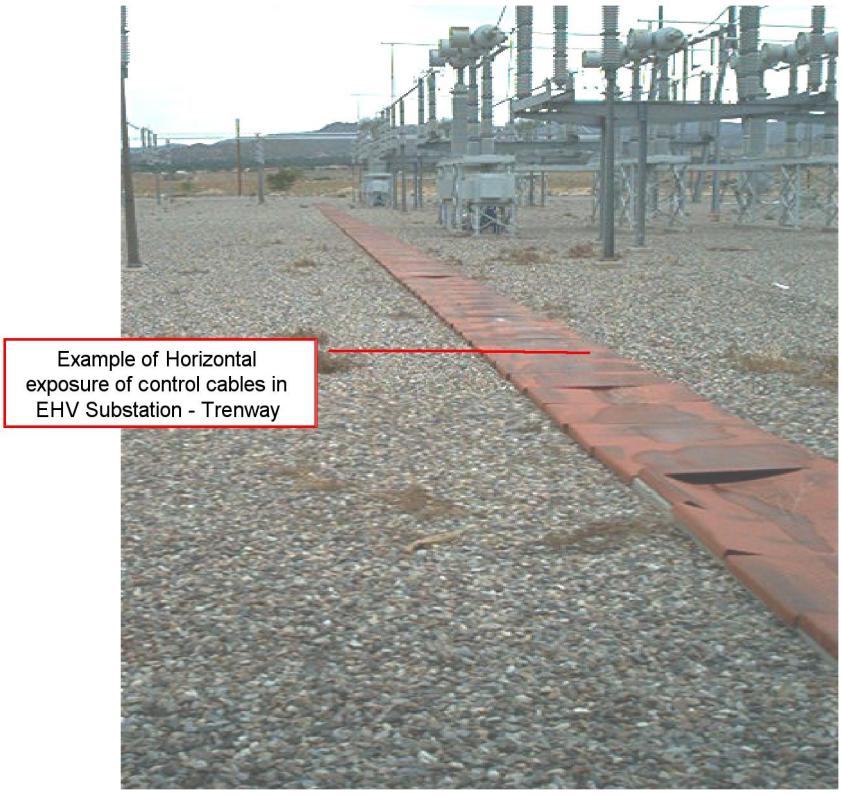

Figure 7-20. Second view of cable trenway.

In Figure 7-21 the cables are seen to be buried at a shallow depth. Under the cable insulation there is a metal external "shield", however the optical coverage of most of these braided shields is not usually very high, and generally does not provide significant shielding of the inner conductor at frequencies above 10 MHz.

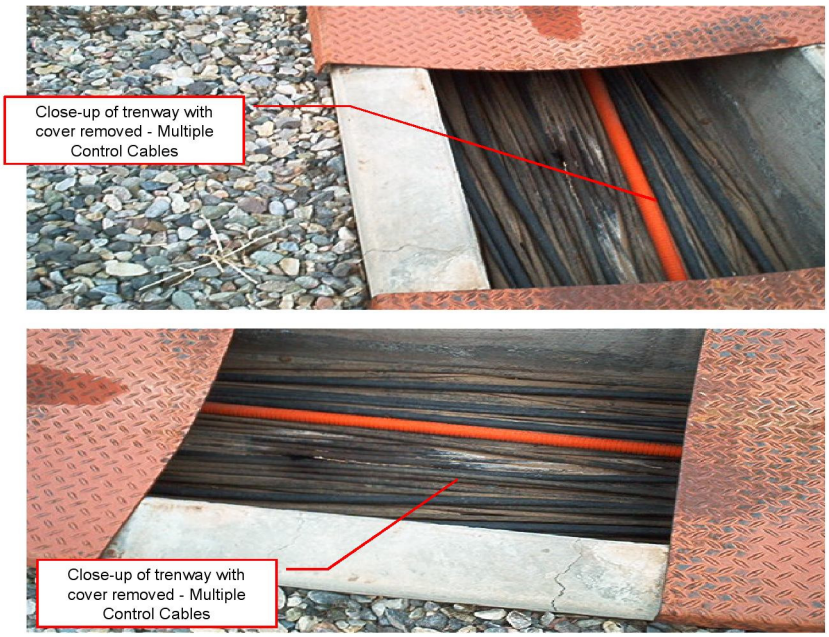

Figure 7-21. Control cables in trenway.

In Figure 7-22 the control cables have their insulation stripped back and the shields are connected to ground cables. It is noted that the ground cables are on the order of 30 cm long (or longer), which provides a high impedance at high frequencies. While this is sufficient for lightning frequencies (typically below 1 MHz), this will enable a significant portion of the high-frequency E1 HEMP transients to continue to propagate on the signal wires inside the control facility instead of being directed to ground.

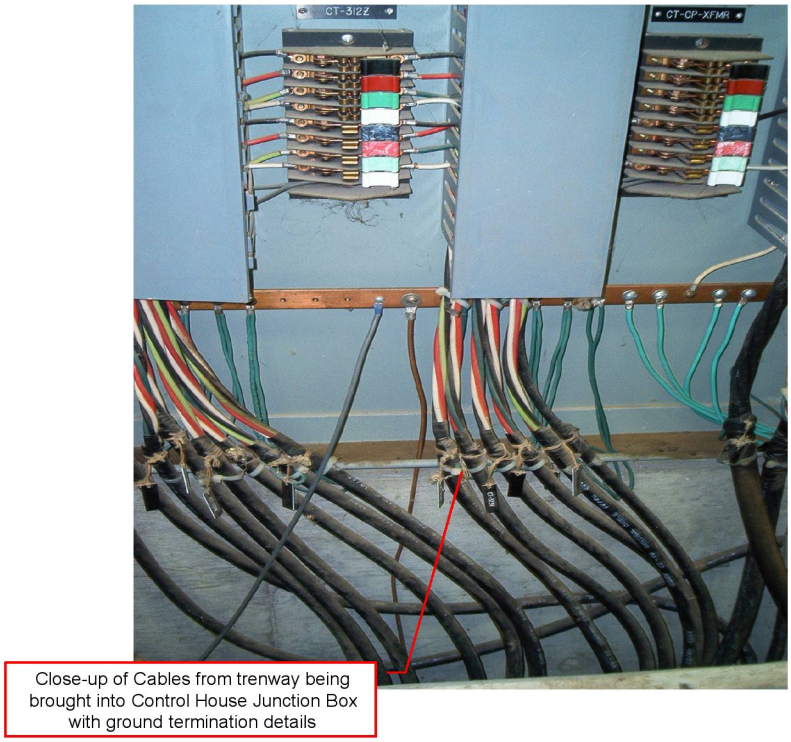

Figure 7-22. Grounding of control cable shields and j-boxes in control building.

In Figure 7-23 cables extend from the j-boxes to the individual racks of equipment. These cables will carry any remaining high-frequency transients that were coupled to the cables outside, and they will also be coupled to by the electromagnetic fields that propagate through the walls of the building. It is important to note that the direct coupling of fields inside the building is strongly influenced by the construction type of the building. There are strong variations for the penetrating electric fields at frequencies above 10 MHz due to whether the building is made of concrete (with or without reinforced bars), bolted metal, or wood.

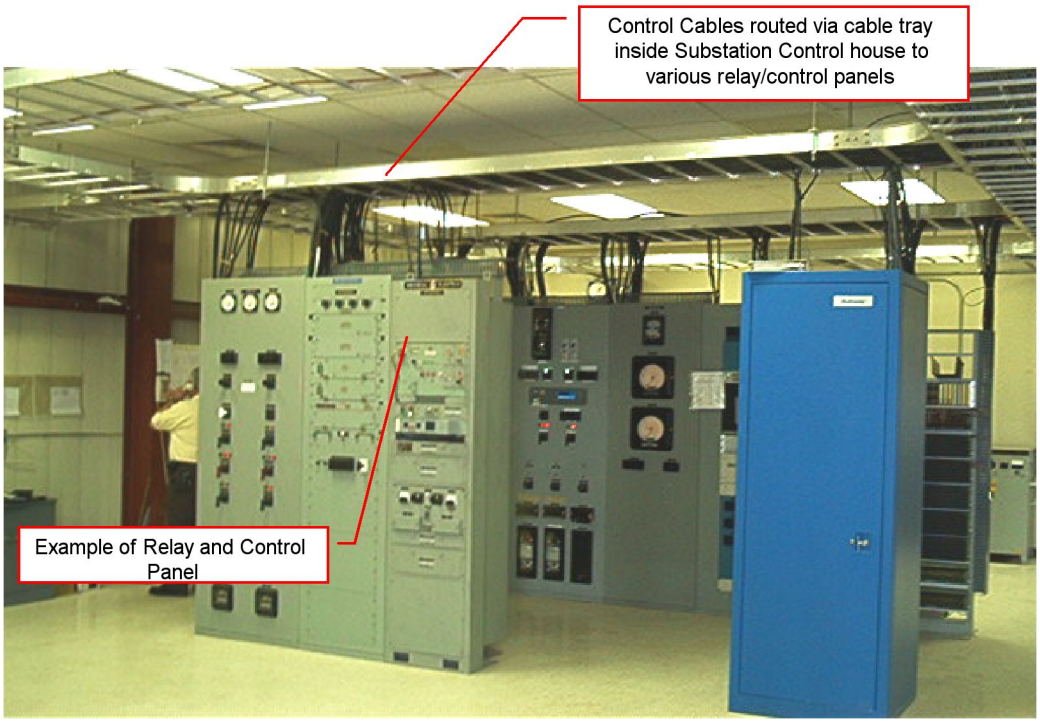

Figure 7-23. Distribution of control cables within building to cabinets.

While these figures are provided to give an indication of the scope of the problem, it will be necessary to evaluate many factors that are common or different in various power substations in order to determine the seriousness of the E1 HEMP threat and to recommend protection techniques that are cost effective.

Upon examination of Figures 7-4, 7-5 and 7-6, it appears that maximum levels of approximately 10 kV may be coupled to horizontal buried lines in a substation yard (top 1%). In Figure 7-7 levels of 70 kV may be induced on a vertical conduit. While the amount of these voltages that could propagate to the relays and other electronic control equipment is extremely variable, the fact that upsets on relays begin at 3.2 kV and damage to PLCs and PCs begin at approximately 0.5 kV, indicates a serious concern for the continued operation of a portion of the substations. When it is recognized that all of these substations shown in Figure 7-17 are exposed simultaneously (within one power cycle) it is clear that this threat is serious.

A second problem not discussed in detail indicates that even if the cable penetrations to the control building are protected, there is still the problem of the penetration of the E1 HEMP fields inside and coupling to the cables just above the electronic cabinets. The level of the field penetrating the building is completely dependent on the type of wall and ceiling construction; however, tests performed in the past on telephone switching centers indicated that voltage levels between 1 and 10 kV could be induced on cables. Depending on the way that the cables enter the cabinets (whether the shields are bonded or not) will determine if these voltages reach the electronic equipment ports inside.

7.4 Power Generation Facilities

Power generator facilities are similar to industrial processing plants in that they use PLCs to control the flow of fuel and other aspects of the power generation process. As indicated in Tables 7-5 and 7-6, damage may occur for E1-like pulses at levels as low as 0.6 kV, although only one manufacturer's equipment failed at that level. The other failed at 3.3 kV. Since power generators are manned, the impact of upset may not be as important as damage; however the damage levels indicated are quite low. In addition, it is not expected that the cabling within the generator facility will be better protected than in a substation, so again levels of induced voltages as high as 70 kV are likely to be coupled to vertical cables in a small portion of the generators.

7.5 Power Control Centers

Power control centers can be described as distributed computer facilities with many communications lines entering and leaving the facility. Since these facilities do not deal directly with high voltage transformers nearby, most of the computer equipment is not afforded the same basic level of immunity as those found in substations, or in power generation facilities for that matter. Equipment like the PC (see Table 7-8) will fail its communications port due to E1 HEMP at 0.5 kV, and other test data indicates that Ethernet ports are generally vulnerable at low levels. Given that ordinary building protection levels will typically allow 1 to 10 kV to be coupled to internal cables, this indicates a potential problem.

An important factor to consider is the location and type of wall construction of control centers. A control center built below the surface of the Earth has much better natural shielding than one built above grade in a high-rise building.

7.6 Distribution Line Insulators

Approximately 78% of all electric power delivery to end-users is delivered via 15 kV class distribution lines, as highlighted in Table 7-9. Figure 7-24 also illustrates a typical distribution feeder geometry that indicates the variation of the orientation of the lines for a single feeder. This shows that the likelihood for an optimum exposure of a segment of the line is high, and that at some point along the feeder the maximum E1 HEMP voltage will be induced, creating a possible insulator flashover.

Table 7-9. Summary of the distribution systems for the U.S. power grid.

U.S. Power Distribution

• Distribution systems in the U.S.
  ○ 5, 15, 25 and 35 kV
  ○ 15 kV is 77.5% of all load
  ○ 35,000 to 40,000 distribution substations
  ○ Substation size varies from ~1 - 100 MVA with an average of 20 MVA
 	
• Multiple feeders leave the substations
  ○ 4 to 14 feeders per substation
  ○ Typically 300 line segments per feeder
  ○ 60 fault protection and isolation devices per feeder
  ○ Average 3 phase feeder length is 10.8 miles
  ○ 93% of all U.S. feeders are of overhead construction
 	
• End users supplied by feeders
  ○ 13.0% industrial load
  ○ 18.4% supply urban/commercial load
  ○ 11.9% rural load
  ○ 55.7% suburban load

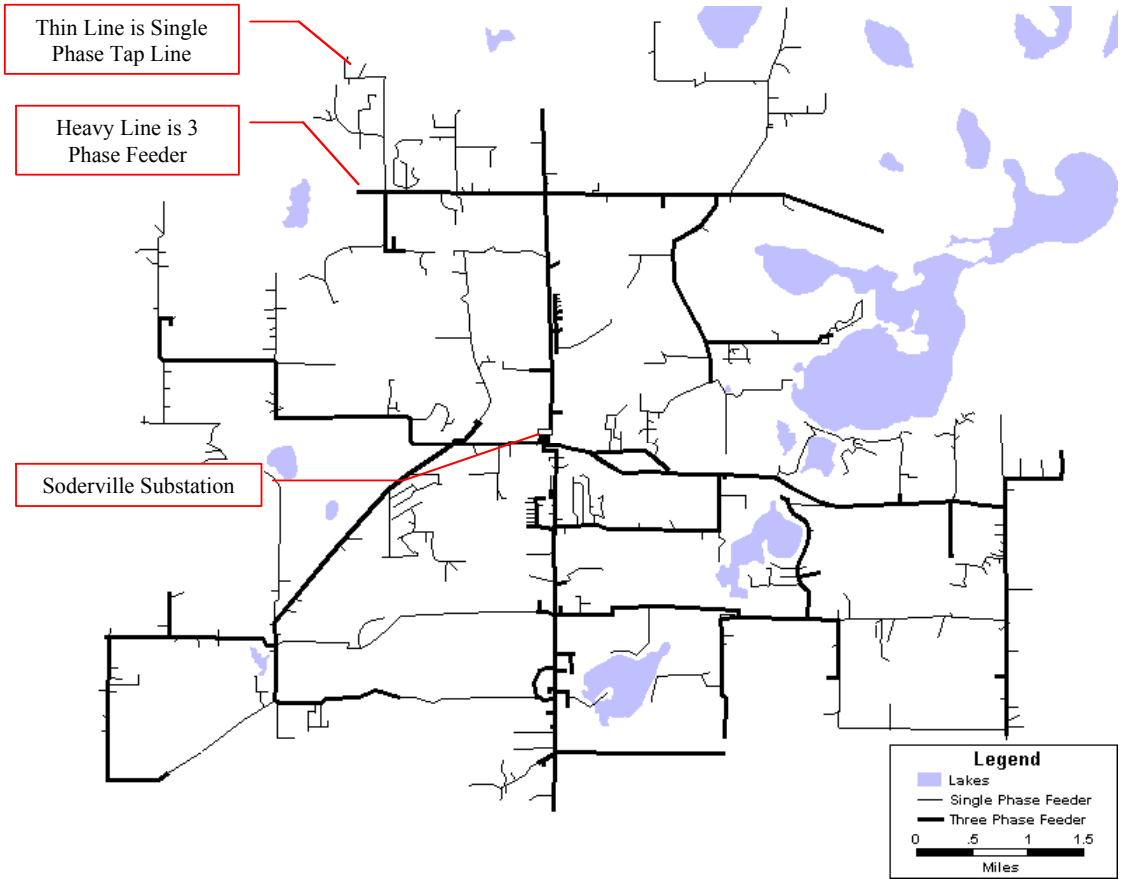

Figure 7-24. A typical above ground 15 kV distribution geometry in the U.S.

At present, considerable uncertainty exists as to whether the typical insulation capability of these distribution assets will be sufficient to withstand the induced overvoltages due to the E1 environment of a HEMP threat. Prior analysis of the E1 threat by Metatech indicated that induced overvoltages ranging from 200 kV to over 400 kV (depending on the scenario) can occur on these distribution lines over geographically widespread regions, and that if large scale distribution line insulator failure or flashover occurs, the impacted regions will likely experience power grid collapse.

Typical insulation design for distribution feeders usually are based upon the withstand (BIL, basic insulation level) of a 1.2 μs rise time impulse due to lightning (with a 50 μs pulse width). For these lightning impulses, typical pin insulator withstand generally starts at ~100 kV. It has generally been observed that the shorter duration pulse widths of the E1 HEMP threat will increase the level of the flashover voltage for these insulators, but the amount of increase was not well substantiated until further testing was performed.

Two sets of experiments and results are summarized here. The first is work done by Dr. Stan Gryzbowski from Mississippi State University (MSU), using standard insulator test techniques and testing of a wide variety of insulators found in the U.S. power grid. He also examined variations due to polarity of the impulse and other factors such as wet insulators. All of the testing was performed without power on the insulator, which is the usual method for testing insulators in the United States.

A second set of experiments and results are presented here for a set of Russian glass and porcelain insulators. The main emphasis for these experiments was the fact that the tests were performed both with no power on the insulators and also with the insulators energized with a portion of an AC waveform – up to 1,000 amperes.

7.6.1 Insulator Testing at MSU

A series of high voltage power lab tests were performed to establish the insulator performance for the steep front/short duration pulses environments typical from the E1 HEMP event. The High Voltage Laboratory at Mississippi State University (MSU) has had experience in generating pulses and conducting tests of insulators for these steep front/short duration pulses. The MSU lab can provide a test setup that will produce a ~50-60 ns pulse rise time while reaching pulse voltage peaks of as much as 900 kV. While the rise time is a bit slower than the expected E1 HEMP pulse rise time, the voltage peak levels and pulse width meet the test environment requirements fully. It is also believed that the pulse width of the E1 waveform is the critical parameter in understanding the peak voltage levels of flashover relative to the much wider lightning impulse tests.

The test plan of this project had the objective to determine the critical flashover (CFO) voltage, withstand voltage level and V-t characteristics for both major types of 15 kV insulators used in the U.S. – porcelain and polymer. (The CFO is the level with 50% probability of insulator arcing – and so possible disruption or damage to the power system.)

While porcelain insulators are the most common insulator type in use on the 15 kV U.S. distribution network, the application of polymer type insulators is more commonly used for new construction and/or for insulator replacements on existing distribution lines. The tested insulators are of pin type as well as suspension insulators. The evaluation of the CFO voltage and the V-t characteristics were conducted under dry and wet conditions for positive and negative polarity of the applied pulses.

Evaluation of the CFO voltage and V-t characteristics under steep front/short duration pulses (E1 type pulse) was performed on the following insulators (photo in Figure 7-25):

- porcelain pin type insulators: ANSI CLASS 55 - 4 and ANSI CLASS 55 – 3.
- porcelain suspension insulators: ANSI CLASS 52 - 1 and ANSI CLASS 52 – 9.
- 15 kV polymer suspension insulator, arcing distance 6.5 inch.

Figure 7-25. Insulators tested. This has two views of tested insulators, from the left: Pin type: ANSI 55-4, ANSI 55-3; Suspension type: ANSI 52-1, ANSI 52-9; 15 kV Polymer.

Test results are summarized in Tables 7-10, 7-11 and 7-12, showing both the peak CFO levels for the standard lightning tests, the steep front waveforms, and the ratio of those results. It is noted that in most cases the E1 HEMP related tests indicate that the peak HEMP voltage required is often less than a factor of 2 higher than the lightning BIL tests, and with negative polarity it is only about 10% higher. The polymer suspension insulator appears to be more robust to E1 HEMP waveforms. It is also recognized that apparently peak CFO voltages of much less than 200 kV are a concern for flashover.

Table 7-10. Insulator lightning results. This lists the peak CFO voltage, for both polarities, of the tested insulators under standard lightning impulse, in kV.

Configuration	Typical Application Line Voltage	POSITIVE POLARITY		NEGATIVE POLARITY	
		DRY	WET	DRY	WET
ANSI 55-4	13.2 kV	105	-	130	-
ANSI 55-3	11.5 kV	90	-	110	-
ANSI 52-1	13.2 kV	100	-	100	-
ANSI 52-9	13.2 kV	100	-	90	-
Polymer Suspension	<=15 kV	140	-	160	-

Table 7-11. Insulator fast pulse results. This gives the peak CFO voltage of the tested insulators under steep front, short duration pulses, in kV. Results are given for both pulse polarities, and wet and dry conditions.

Configuration	Typical Application Line Voltage	POSITIVE POLARITY		NEGATIVE POLARITY	
		DRY	WET	DRY	WET
ANSI 55-4	13.2 kV	282	201	135	133
ANSI 55-3	11.5 kV	153	160	117	127
ANSI 52-1	13.2 kV	119	131	132	141
ANSI 52-9	13.2 kV	126	132	122	130
Polymer Suspension	<=15 kV	358	299	308	371

Table 7-12. Effect of pulse type for insulator CFO voltage. This gives the ratio of peak CFO voltage at steep front, short duration pulse to the voltage for the lightning impulse.

Configuration	Typical Application Line Voltage	POSITIVE POLARITY		NEGATIVE POLARITY	
		DRY	WET	DRY	WET
ANSI 55-4	13.2 kV	2.7	-	1.04	-
ANSI 55-3	11.5 kV	1.7	-	1.06	-
ANSI 52-1	13.2 kV	1.2	-	1.32	-
ANSI 52-9	13.2 kV	1.3	-	1.36	-
Polymer Suspension	<=15 kV	2.6	-	1.93	-

7.6.2 Insulator Testing in Russia

Due to the fact that the Soviet Union indicated that some distribution insulators were damaged (resulting in power lines dropping to ground) during their high-altitude tests in 1962, they developed the capability to perform power-on tests on power line insulators. This testing is very difficult, but it was decided by the EMP Commission that such testing should be done and Metatech Corporation was the prime contractor for this test program.

The parameters used for the Russian testing included a fast pulser that could vary the rise time of the fast pulse between 20 and 40 ns with pulse widths of up to 100 ns. Peak voltages of slightly greater than 400 kV were also available. The tests included both porcelain and glass suspension insulators used on Russian 10 kV class power lines. Figure 7-26 is a photo of the glass insulator type tested. There was some examination of dry vs. wet vs. polluted insulator surfaces in the study, but the main interest was in the power-off vs. power-on test results.

Figure 7-26. Suspension glass insulator for 10 kV power line.

For the power-off tests, Table 7-13 illustrates the peak voltage for "overlap", which is the Russian term for flashover, for multiple tests on 4 different insulators. It is clearly observed that the variation in the flashover voltage is within measurement error. It is also interesting to see that there is not much variability between the 4 insulators tested.

Table 7-13. Peak levels of voltage for multiple tests (power off).

Insulator number	***Overlapping voltage, kV***			Notes
	First overlap	Second overlap	Third overlap	
1	360	380	370	-
2	380	400	400	-
3	400	370	390	-
4	390	380	400	-

Table 7-14 shows the variation of the characteristics of the insulators after flashover, as measured with "static" tests (these measurements look for insulator damage). There is also not much variation shown for insulator number 1 from Table 7-13.

Table 7-14. Characteristics of insulator number 1 after repeated flashovers (power off).

Measured parameter	Initial values	Value of parameter after overlapping		
		First overlap	Second overlap	Third overlap
Tangent of an angle of dielectric losses, %	2.9	2.8	3.2	2.9
Capacity, pF	56	55.5	57	56
Resistance, MOhm	7500	7400	7500	7400
Leakage current, μA	0.2	0.2	0.2	0.2

Comparable tests were then performed for the same types of insulators for a normal operational voltage of 14 kV and with a peak current of 1.8 kA available as follow current when an insulator flashed over. Several tests indicated that after a single flashover, the operating characteristics of nearly all of the insulators were degraded. In addition, it was found that the peak voltage level required for subsequent pulses were lower. Most dramatically, one of the six insulators tested was destroyed. Table 7-15 illustrates this behavior. Table 7-16 illustrates the degradation of the characteristics of insulator number 1, showing degradation in most of the measured parameters.

Table 7-15. Peak voltage of flashover for insulators under operational voltage.

Number of insulator	Voltage of overlapping, kV			Notes
	First overlap	Second overlap	Third overlap	
1	370	360	340	-
2	400	390	360	-
3	360	360	330	Destroyed after third test
4	370	320	280	-
5	380	360	330	-
6	390	380	340	-

Table 7-16. Characteristics of insulator number 1 after repeated flashovers (power on).

Measured parameter	Initial value	Values after overlapping		
		First overlap	Second overlap	Third overlap
Tangent of angle of dielectric losses, %	2.9	7.3	9.7	10.9
Capacity, pF	56.0	55.0	57.0	56.0
Resistance, Mohm	7500	6400	5500	3400
Leakage current, μA	0.2	0.4	0.5	0.7

For the case of insulator destruction, high-speed movies were taken in several cases. Figure 7-27 illustrates the fact that after the flashover occurs due to the fast voltage pulse, the power-follow provides the energy to destroy the insulator. Note that this did not happen in all cases, but it is likely that the mechanism for destruction has to do with small defects in the manufacture of the insulators. The Russian experimental team tried to determine whether these defects were present before the testing, but they were not able to find a simple way to evaluate this aspect.

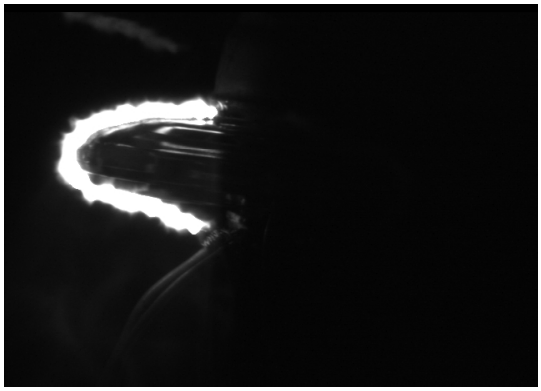

a. 0.5 ms

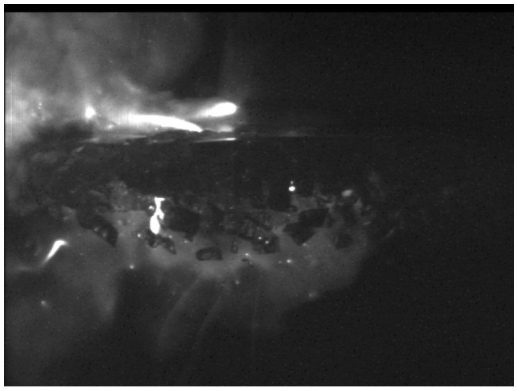

c. 10 ms

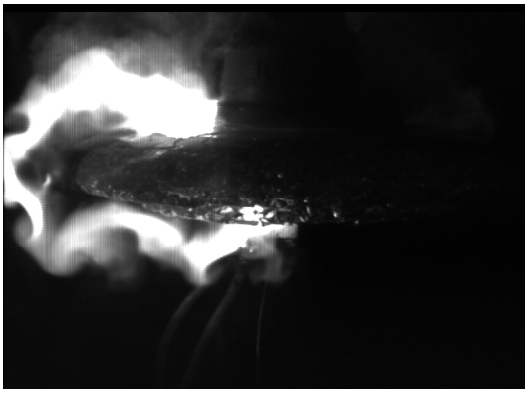

b. 2 ms

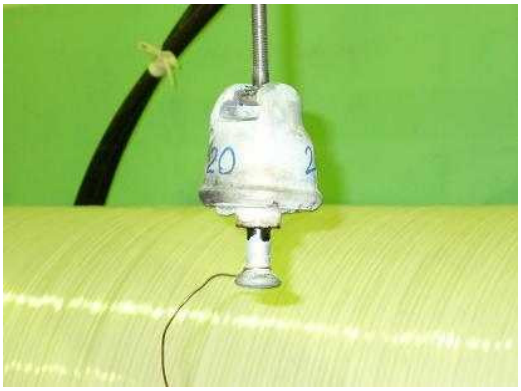

d. afterwards

Figure 7-27. Snapshots from an insulator test shot, with damage due to power follow. The frames are at times of 0.5 ms (a), 2 ms (b), and 10 ms (c); and after power is removed (d).

An important aspect of the multiple flashover testing under power is that while we do not expect large numbers of pulses to expose the U.S. power grid, lightning pulses are likely to occur in many locations in the U.S. and could therefore expose many insulators to previous impulses without causing noticeable failures. Thus a future E1 HEMP pulse could be the second or third pulse that some insulators will observe.

While this Russian test data is very dramatic, it is noted that the tests were performed on Russian insulators and statistical damage data were not obtained due to limitations in test time and funding. More work is needed to determine whether the damage aspect is a real concern in the U.S., and if so, with which types of insulator designs. It is clear however, that flashovers of U.S. insulators can occur at E1 HEMP voltage levels much lower than previously thought, and therefore some consideration of mitigation measures are needed, especially near the substations where the follow current will be high.

7.7 Distribution Transformers

During the ORNL power system studies in the 1980s, tests were performed to examine the possibility of E1 HEMP damage to distribution step-down transformers that can be found in the U.S. power grid. This testing included 19 samples of 7.2 kV/25 kVA power distribution transformers, using E1 HEMP like pulses. Damage that occurred was usually from dielectric breakdown within the windings – pinhole damage. The results of that testing are summarized in Table 7-17.

Table 7-17. 7.2 kV/25 kVA transformer failure testing for fast pulses.

XFMR	Shots #@kV	Peak Voltage (kV)	Time to Peak (ns)	Surge Arrester	Notes	Result
ZS1						Pulser calibration
ZS2	1@400	264	618	No	(1)	T-T failure
ZS3	2@400	288	668	No	(2)	HV-LV failure
ZS4	2@400	280	600	No	(1)	L-L failure
ZS5	1@400	272	550	No	(2)	HV-LV failure
ZS6	2@400	290	643	No	(1)	No damage
ZV1	1@400	296	601	No	(1)	No damage
ZV2	1@400	304	592	No	(2)	HV-LV failure
ZV3	2@400	110	100	Yes	(3)	No damage
ZV4	2@500	110	100	Yes	(3)	No damage
ZV4	2@780	116	110	Yes	(3)	No damage
XV1	1@400	272	500	No	(2)	HV-LV failure
XV2	2@400	115	110	Yes	(3)	No damage
ZW1	2@400	292	552	No	(1)	No damage
ZW2	2@400	16	Oscillatory	No	(4)	No damage
ZW3	2@780	100	110	Yes	(3)	No damage
ZW4	2@1000	112	105	Yes	(3)	No damage
ZD1	2@400	120	550	No	(5)	No damage
ZD2	2@400	20	Oscillatory	No	(4)	No damage
ZE1	2@1000	95	100	Yes	(6)	No damage
ZE2	6@780	95	100	Yes	(6)	No damage

(1) External flashover on HV bushing: T-T failure denotes turn-to-turn failure; L-L failure denotes line-to-line failure
(2) No external flashover; HV-LV failure denotes a high-voltage winding flashover to the low-voltage winding
(3) Surge arrester operation and no external flashover
(4) Surge applied to the low-voltage bushings with no external flashover
(5) Surge applied common mode to both HV bushings with external flashover
(6) Surge applied common mode to both bushings, and both arresters operated

It is noted in the test results that failures occurred when the peak fast pulse voltage was between 264 and 304 kV. No damage occurred for peak pulses of 290 and 296 kV, so there appears to be some variability within the group of 19 transformers, although the variation is not that great. When lightning surge arresters were added to the transformers, no damage was noted up to the capability of the pulser (which was 1000 kV). The conclusion reached by the test team, however, indicated that standard surge arresters mounting procedures often include a long wire lead to the transformer, and this method of mounting might not allow for the lightning surge arrester to protect the transformer from fast pulses. Also, not all areas of the U.S. use lightning protection on distribution transformers (e.g. coastal California).

Section 8
Impacts on Society of E1 HEMP Power System Failures

The EMP Commission specifically was tasked to look at the impacts on general society from an EMP assault on the U.S. It noted that this is not just a power system issue – all of the other important legs of the infrastructure are also intertwined with each other and the power system, with the power grid probably being the most significant. Note also that E1 HEMP often cannot be isolated from other effects. E2 and E3 are also important, and possibly would have worse effects than E1 for some parts of the infrastructure, such as the effect of E3 on the power transmission system. Also there can be synergistic effects, such as E1 setting up a system to be further damaged by the following E2 or E3 pulse. And there are also other possible similar EM threats to the infrastructures, such as geomagnetic storms (with similarities to E3) and IEMI (intentional electromagnetic interference). IEMI has similarities to E1 HEMP in regard to the vulnerability of control, sensor, and communication lines. However, IEMI is unlikely to be a threat for power distribution insulators and transformers – for the simple fact that the high height and the inability to provide a plane wave source over 100 meters means that IEMI emitters will not be effective in coupling large voltages to long power lines.

Several issues were evaluated by the EMP commission:

1. Electronic controls are being used more and more in all aspects of our lives. This is especially true of any large-scale processing system, such as in all types of factories, but also in many aspects of our infrastructures. Certainty this is true for any unmanned station. There are controllers (such as PLCs), communication devices, and sensors. Power substations and pipelines make extensive use of these devices, which are susceptible to E1 HEMP effects.
2. EM assaults can interfere with control systems. This has been shown to be true by many experiences, and is why EMC/EMI (electromagnetic compatibility, electromagnetic interference) is so important in our modern world. For example, on July 29, 1967, an armed missile was launched from a fighter aircraft on the deck of the aircraft carrier Forrestal, causing extensive damage and killing 134 sailors. This was thought to be due to two problems, a malfunction of a connector on the missile system and a failure of a safety device, with a radar signal being the trigger of the mishap. Another problem, described in Figure 8-1, is a breakdown in the control of a water pipeline in San Diego, which was due to interference from a radar 25 miles offshore.
3. Outages have occurred in the past – large ones infrequently. Geomagnetic storms have caused some (and so, similarly, E3 is a threat to the grid). It might not be perfectly clear what caused some of the others, but none are believed to be caused by effects similar to E1 HEMP. But confusion and lack of good data of the state of all aspects of the vast power system has contributed to outage growth (the August 14, 2003 outage). With E1 HEMP simultaneously hitting a large area, distorting and interrupting communications, and damaging devices in the SCADA system, similar, or worse, could be expected.
4. The EMP Commission emphasized the interdependence of the various legs of the infrastructures. So much of modern society depends on the electric power system,

and often there is, at best, very limited back-up power. The issues include the need for communication to try to minimize the spread of an outage, and the need for many aspects of the infrastructure to recover from outages. In all, communications is an important issue, possibly secondary to the power system itself. There are also pipelines that transport fuels, such as natural gas and oil that might be needed to run a power station. Also, getting repair people out to fix HEMP damage involves communication, and fueling vehicles, while gas stations often shut down when electric power is out.

In November 1999, San Diego County Water Authority and San Diego Gas and Electric companies experienced severe electromagnetic interference to their SCADA wireless networks. Both companies found themselves unable to actuate critical valve openings and closings under remote control of the SCADA electronic systems. This inability necessitated sending technicians to remote locations to manually open and close water and gas valves, averting, in the words of a subsequent letter of complaint by the San Diego County Water Authority to the Federal Communications Commission, a potential "catastrophic failure" of the aqueduct system. The potential consequences of a failure of this 825 million gallon per day flow rate system ranged from "spilling vents at thousands of gallons per minute to aqueduct rupture with ensuing disruption of service, severe flooding, and related damage to private and public property." The source of the SCADA failure was later determined to be radar operated on a ship 25 miles off the coast of San Diego.

Figure 8-1. An example of the failure of an infrastructure system due to EM assault.

It should be noted that besides determining what damage might happen, it is also important to evaluate the recovery process. How long would it take to do the repairs, especially when so many other parts of the infrastructures might also be out of service? For E1 HEMP effects, most of the damage would be to smaller type devices – such as those that fail randomly now and then. Technicians will need to search to find what is damaged, and replace or repair it. Of course, this could be a formidable task if there is much damage over a large region. An E1 HEMP attack is unlikely to cause damage to very large transformers, such as is suspected that E3 could do – damage that could take years to repair. Probably the only way E1 HEMP would cause that level of long term massive damage would be if confusion of controls triggered the power system to destroy itself, which is certainly possible, but very unpredictable.

As a final note, the bottom line for predicting E1 HEMP effects is that our modern world has never experienced such as assault. We can try to predict effects and draw upon similar effects and experimentation, but there is always the possibility of some surprise. Often even somewhat minor issues have lead to extensive problems in the past, which would not have been predicted. It is also not known how American society in general would react if massive infrastructure failures occur over a large region and for a long time.

Section 9
Bibliography of E1 HEMP References

9.1 General E1 HEMP References

Air Force Weapons Laboratory, "EMP Interaction: Principles, Techniques, and Reference Data", AFWL-TR-80-402 (EMP Interaction 2-1), Dikewood Industries, Inc., December 1980.

Baum, C.E., "Electron Thermalization and Mobility in Air", Theoretical Note 12, July 1965.

Bridgeman, Charles J., *Introduction to the Physics of Nuclear Weapons Effects*, Defense Threat Reduction Agency, July 2001 (limited distribution).

Burke, P., and H. Fowles, "Pulsed Current Injection Testing with Short Duration (E1-Like) Pulses", MRC/ABQ-R-1315, Mission Research Corporation, Volumes I and II, May 1990.

Butler, C., et al., "EMP Penetration Handbook for Apertures, Cable Shields, Connectors, Skin Panels", AFWL-TR-77-149, Air Force Weapons Laboratory (The Dikewood Corporation), December 1977.

Davies, D., and P. Chantry, "Air Chemistry Measurements I", DC-TN-2030.301-1, Dikewood Division of Kaman Sciences Corporation, November 1982.

Defense Threat Reduction Agency, "EM-1, Capabilities of Nuclear Weapons" (unpublished).

Defense Threat Reduction Agency, "Reaction Rate Handbook", DNA 1948H, March 1972.

DoD-STD-2169A, "Military Standard - High Altitude Electromagnetic Pulse (HEMP) Environment", December 1987 (unpublished).

General Electric Company – TEMPO, "DNA EMP (Electromagnetic Pulse) Handbook", July 1979 (downgraded, limited distribution).
"Volume 1 – Design Principles", DNA 2114H-1,
"Volume 2 – Coupling Analysis", DNA 2114H-2,
"Volume 3 – Component Response and Test Methods", DNA 2114H-3,
"Volume 4 – Environment and Applications", DNA 2114H-4,
"Volume 5 – Resources", DNA 2114H-5,
"Volume 6 – Computer Codes", DNA 2114H-6.

Ghose, Rabindra N., *EMP Environment and System Hardness Design*, Don White Consultants, Inc., 1984.

Glasstone, Samuel, and Philip J. Dolan, *The Effects of Nuclear Weapons*, U.S. Departments of Defense and Energy, 1977 (1st edition: 57, 2nd edition 1962).

Grzybowski, Dr. S., and Yang Song, “Investigation on the Electrical Strength of the Distribution Line Elements Under Steep Front, Short Duration Pulses”, Mississippi State University, January 2004.

Karzas, W.J., and R. Latter, "Electromagnetic Radiation from a Nuclear Explosion in Space”, *Physical Review,* Vol. 126, June 1962.

Karzas, W.J., and R. Latter, "The Electromagnetic Signal Due to the Interactions of Nuclear Explosions with the Earth's Magnetic Field”, *Journal of Geophysical Research,* Vol. 67, November 1962.

Karzas, W.J., and R. Latter, “EMP from High-Altitude Nuclear Explosions”, Report No. RM-4194, Rand Corporation, March 1965 (unpublished).

Karzas, W.J., and R. Latter, "Detection of Electromagnetic Radiation from Nuclear Explosions in Space”, *Physical Review,* Vol. 137, March 1965.

Kompaneets, A.S., "Radio Emission From an Atomic Explosion”, *Soviet Physics JETP,* December 1958.

Longmire, C.L., "On the Electromagnetic Pulse Produced by Nuclear Explosions", *IEEE Trans. Ant. & Prop.,* Vol. AP-26, No. 1, January 1978.

Longmire, C.L., "Introduction to EMP Generation Theory", *Journal of Defense Research,* Special Issue 84-1, May 1985, pp. 91-95 (unpublished).

Longmire, C.L., and J. Koppel, “Formative Time Lag of Secondary Ionization”, MRC-R-88, Mission Research Corporation, January 1974.

Messenger, G. C. and M. S. Ash, *The Effects of Radiation on Electronic Systems*, Van Nostrand Reinhold Company, 1986.

Miller, D.B., “Experimental Investigation of Steep-Front Short Duration (SFSD) Surge Effects on Power System Components”, ORNL/Sub/87-92345, Oak Ridge National Laboratory, May 1992.

MIL-HDBK-423, “High-Altitude Electromagnetic Pulse (HEMP) Protection for Fixed and Transportable Ground-Based Facilities, Volume I Fixed Facilities”, 15 May 1993.

MIL-STD-188-125-1, “Department of Defense Interface Standard. High-Altitude Electromagnetic Pulse (HEMP) Protection for Ground-Based C4I Facilities Performing Critical, Time-Urgent Missions, Part 1 Fixed Facilities”, 17 July 1998.

Northrop, John, *Handbook of Nuclear Weapon Effects, Calculational Tools Abstracted from DSWA’s Effects Manual One (EM-1)*, Defense Threat Reduction Agency, September, 1996 (limited distribution).

Parfenov, Y., “Research of Physical Laws of the Flashover and Damage of Power Line Insulators due to Fast Voltage Pulses with Power On and Power Off is Important Problem”, Institute for High Energy Densities, January 25, 2004.

Radasky, W. A. and R. L. Knight, HAPS — A Two Dimensional High Altitude EMP Environment Code, Air Force Weapons Laboratory, EMP TN 125, November 1971.

Radasky, W. A., W. J. Karzas, G. K. Schlegel and C. W. Jones, High Altitude Electromagnetic Pulse — Theory and Calculations, Defense Nuclear Agency, DNA TR 88 123, 3 October 1988.

Radasky, W. A., "High-altitude EMP (HEMP) Environments and Effects," NBC Report, Spring/Summer 2002, pp. 24-29.

Radasky, W. A., "High-Altitude Electromagnetic Pulse (HEMP): A Threat to Our Way of Life," IEEE USA Today's Engineer, September 2007.

Radasky, W., "Approach for Protection of HV Power Grid Network Control Electronics from Intentional Electromagnetic Interference (IEMI)", CIGRE SC C4 2009 Kushiro Colloquium, June 2009.

Rickets, L. W., *Fundamentals of Nuclear Hardening of Electronic Equipment*, Wiley & Sons, Inc., 1972.

Rickets, L. W., J. E. Bridges, and J. Miletta, *EMP Radiation and Protective Techniques*, Wiley & Sons, Inc., 1976.

Rudie, Norman J., *Principles and Techniques of Radiation Hardening*, 2nd ed., 1976:
"Volume 1: Interaction of Radiation with Matter and Material Effects",
"Volume 2: Transient Radiation Effects in Electronics (TREE)",
"Volume 3: Electromagnetic Pulse (EMP) and System Generated EMP".

Sandia Laboratories, "Electromagnetic Pulse Handbook for Missiles and Aircraft in Flight", SC-M-71 0346, AFWL TR 73-68, EMP Interaction Note 1-1, September, 1972.

Schaefer, R.R., "Defense Special Weapons Agency ELECTRA Program Technical Review Group Test Objects 1, 2, and 3", LRDA-TR-211-7221-3001-001, Logicon R&D Associates, January 1997 (unpublished).

Schaefer, R.R., F.C. Dumont, and C.R. Grain, "High-Altitude Electromagnetic Pulse (HEMP) Hardness Maintenance/Hardness Surveillance for Fixed, Ground-Based C4I Facilities, Volumes 1-3", DNA-TR-93-186-V1 through V3, April 1995.

Schlegel, G.K., M.A. Messier, W.A. Radasky, and W.C. Hart, "EMP Environment Handbook", AFWL EMP Phenomenology 1-1, January 1972 (unpublished).

Sherman, R., et al., *EMP Engineering and Design Principles*, Bell Telephone Laboratories Report, 1975.

9.2 IEC HEMP References

IEC, "Electromagnetic compatibility (EMC) - Part 1-3: General - The effects of high-altitude EMP (HEMP) on civil equipment and systems", IEC 61000-1-3, International Electrotechnical Commission, Geneva, Switzerland

IEC, “Electromagnetic compatibility (EMC) - Part 1-5: General - High power electromagnetic (HPEM) effects on civil systems”, IEC 61000-1-5, International Electrotechnical Commission, Geneva, Switzerland

IEC, “Electromagnetic compatibility (EMC) - Part 2: Environment - Section 3: Description of the environment - Radiated and non-network-frequency-related conducted phenomena”, IEC 61000-2-3, International Electrotechnical Commission, Geneva, Switzerland

IEC, “Electromagnetic compatibility (EMC) - Part 2: Environment - Section 5: Classification of electromagnetic environments. Basic EMC publication”, IEC 61000-2-5, International Electrotechnical Commission, Geneva, Switzerland

IEC, “Electromagnetic compatibility (EMC) - Part 2: Environment - Section 9: Description of HEMP environment - Radiated disturbance. Basic EMC publication”, IEC 61000-2-9, International Electrotechnical Commission, Geneva, Switzerland

IEC, “Electromagnetic compatibility (EMC) - Part 2-10: Environment - Description of HEMP environment - Conducted disturbance”, IEC 61000-2-10, International Electrotechnical Commission, Geneva, Switzerland

IEC, “Electromagnetic compatibility (EMC) - Part 2-11: Environment - Classification of HEMP environments”, IEC 61000-2-11, International Electrotechnical Commission, Geneva, Switzerland

IEC, “Electromagnetic compatibility (EMC) - Part 2-13: Environment - High-power electromagnetic (HPEM) environments - Radiated and conducted”, IEC 61000-2-13, International Electrotechnical Commission, Geneva, Switzerland

IEC, “Electromagnetic compatibility (EMC) - Part 4-1: Testing and measurement techniques - Overview of IEC 61000-4 series”, IEC 61000-4-1, International Electrotechnical Commission, Geneva, Switzerland

IEC, “Electromagnetic compatibility (EMC)- Part 4-2: Testing and measurement techniques - Electrostatic discharge immunity test”, IEC 61000-4-2, International Electrotechnical Commission, Geneva, Switzerland

IEC, “Electromagnetic compatibility (EMC) - Part 4-3 : Testing and measurement techniques - Radiated, radio-frequency, electromagnetic field immunity test”, IEC 61000-4-3, International Electrotechnical Commission, Geneva, Switzerland

IEC, “Electromagnetic compatibility (EMC) - Part 4-4: Testing and measurement techniques - Electrical fast transient/burst immunity test”, IEC 61000-4-4, International Electrotechnical Commission, Geneva, Switzerland

IEC, “Electromagnetic compatibility (EMC) - Part 4-5: Testing and measurement techniques - Surge immunity test”, IEC 61000-4-5, International Electrotechnical Commission, Geneva, Switzerland

IEC, “Electromagnetic compatibility (EMC) - Part 4-6: Testing and measurement techniques - Immunity to conducted disturbances, induced by radio-frequency fields”, IEC 61000-4-6, International Electrotechnical Commission, Geneva, Switzerland

IEC, “Electromagnetic compatibility (EMC) - Part 4-12: Testing and measurement techniques - Ring wave immunity test”, IEC 61000-4-12, International Electrotechnical Commission, Geneva, Switzerland

IEC, “Electromagnetic compatibility (EMC) - Part 4-18: Testing and measurement techniques - Damped oscillatory wave immunity test”, IEC 61000-4-18, International Electrotechnical Commission, Geneva, Switzerland

IEC, “Electromagnetic compatibility (EMC) - Part 4-20: Testing and measurement techniques - Emission and immunity testing in transverse electromagnetic (TEM) waveguides”, IEC 61000-4-20, International Electrotechnical Commission, Geneva, Switzerland

IEC, “Electromagnetic compatibility (EMC) - Part 4-21: Testing and measurement techniques - Reverberation chamber test methods”, IEC 61000-4-21, International Electrotechnical Commission, Geneva, Switzerland

IEC, “Electromagnetic compatibility (EMC) - Part 4-23: Testing and measurement techniques - Test methods for protective devices for HEMP and other radiated disturbances”, IEC 61000-4-23, International Electrotechnical Commission, Geneva, Switzerland

IEC, “Electromagnetic compatibility (EMC) - Part 4-24: Testing and measurement techniques - Section 24: Test methods for protective devices for HEMP conducted disturbance - Basic EMC Publication”, IEC 61000-4-24, International Electrotechnical Commission, Geneva, Switzerland

IEC, “Electromagnetic compatibility (EMC) - Part 4-25: Testing and measurement techniques - HEMP immunity test methods for equipment and systems”, IEC 61000-4-25, International Electrotechnical Commission, Geneva, Switzerland

IEC, “Electromagnetic compatibility (EMC) - Part 4-32: Testing and measurement techniques - High-altitude electromagnetic pulse (HEMP) simulator compendium”, IEC 61000-4-32, International Electrotechnical Commission, Geneva, Switzerland

IEC, “Electromagnetic compatibility (EMC) - Part 4-33: Testing and measurement techniques - Measurement methods for high-power transient parameters”, IEC 61000-4-33, International Electrotechnical Commission, Geneva, Switzerland

IEC, “Electromagnetic compatibility (EMC) - Part 4-35: Testing and measurement techniques - HPEM simulator compendium”, IEC 61000-4-35, International Electrotechnical Commission, Geneva, Switzerland

IEC, “Electromagnetic compatibility (EMC) - Part 5: Installation and mitigation guidelines - Section 1: General considerations - Basic EMC publication”, IEC 61000-5-1, International Electrotechnical Commission, Geneva, Switzerland

IEC, “Electromagnetic compatibility (EMC) - Part 5: Installation and mitigation guidelines - Section 2: Earthing and cabling”, IEC 61000-5-2, International Electrotechnical Commission, Geneva, Switzerland

IEC, “Electromagnetic compatibility (EMC) - Part 5-3: Installation and mitigation guidelines - HEMP protection concepts”, IEC 61000-5-3, International Electrotechnical Commission, Geneva, Switzerland

IEC, “Electromagnetic compatibility (EMC) - Part 5: Installation and mitigation guidelines - Section 4: Immunity to HEMP - Specifications for protective devices against HEMP radiated disturbance. Basic EMC Publication”, IEC 61000-5-4, International Electrotechnical Commission, Geneva, Switzerland

IEC, “Electromagnetic compatibility (EMC) - Part 5: Installation and mitigation guidelines - Section 5: Specification of protective devices for HEMP conducted disturbance. Basic EMC Publication”, IEC 61000-5-5, International Electrotechnical Commission, Geneva, Switzerland

IEC, “Electromagnetic compatibility (EMC) - Part 5-6: Installation and mitigation guidelines - Mitigation of external EM influences”, IEC 61000-5-6, International Electrotechnical Commission, Geneva, Switzerland

IEC, “Electromagnetic compatibility (EMC) - Part 5-7: Installation and mitigation guidelines - Degrees of protection provided by enclosures against electromagnetic disturbances (EM code)”, IEC 61000-5-7, International Electrotechnical Commission, Geneva, Switzerland

IEC, “Electromagnetic compatibility (EMC) - Part 5-8: Installation and mitigation guidelines - HEMP protection methods for the distributed infrastructure”, IEC 61000-5-8, International Electrotechnical Commission, Geneva, Switzerland

IEC, “Electromagnetic compatibility (EMC) - Part 5-9: Installation and mitigation guidelines - System-level susceptibility assessments for HEMP and HPEM”, IEC 61000-5-9, International Electrotechnical Commission, Geneva, Switzerland

IEC, “Electromagnetic compatibility (EMC) - Part 6-1: Generic standards - Immunity for residential, commercial and light-industrial environments”, IEC 61000-6-1, International Electrotechnical Commission, Geneva, Switzerland

IEC, “Electromagnetic compatibility (EMC) - Part 6-2: Generic standards - Immunity for industrial environments”, IEC 61000-6-2, International Electrotechnical Commission, Geneva, Switzerland

IEC, “Electromagnetic compatibility (EMC) - Part 6-5: Generic standards - Immunity for power station and substation environments”, IEC 61000-6-5, International Electrotechnical Commission, Geneva, Switzerland

IEC, “Electromagnetic compatibility (EMC) - Part 6-6: Generic standards - HEMP immunity for indoor equipment”, IEC 61000-6-6, International Electrotechnical Commission, Geneva, Switzerland

9.3 EMP Commission and Related References

Dr. John S. Foster, Jr., et al., "Report of the Commission to Assess the Threat to the United States from Electromagnetic Pulse (EMP) Attack, Volume 1: Executive Report", 2004.

Dr. John S. Foster, Jr., et al., "Report of the Commission to Assess the Threat to the United States from Electromagnetic Pulse (EMP) Attack, Critical National Infrastructures", April 2008.

J.G. Kappenman, W.A. Radasky and J.L. Gilbert, "Evaluation of the Vulnerability of the NGC Power Transmission Grid to the Effects of Geomagnetic Storms", May 8, 1998, Meta-R-144.

J.G. Kappenman, "Evaluation of the Vulnerability of the CEPCO Transmission Network to the Effects of Geomagnetic Storms", March 2001, Meta-R-182.

J.G. Kappenman, J.J. Patrick, J.L. Gilbert, E.B. Savage and W. A. Radasky, "An Expedited Geomagnetic Storm and Late-Time HEMP Threat Analysis Study to Assess the Vulnerability of the U.S. Power Grid", Prepared for the EMP Commission, December 31, 2002, Meta-R-208.

W.A. Radasky, J.L. Gilbert, E.B. Savage, J.G. Kappenman, J.J. Patrick, M.A. Messier and P.R. Barnes, "An Expedited early-Time HEMP Threat Analysis Study to Assess the Vulnerability of the U.S. Power Grid", Prepared for the EMP Commission, December 31, 2002, Meta-R-209.

W.A. Radasky, J.L. Gilbert and E.B. Savage, "The Use of the Russian HEMP E3 Measurements for Model Verification", Meta-R-218.

J.G. Kappenman, J.J. Patrick, J.L. Gilbert, W.A. Radasky and E.B. Savage, "Power Grid Restoration Report: Analysis of Power Grid Restoration Concerns Due to Large E3-Initiated Power Grid Collapses", Prepared for the EMP Commission, November 2003, Meta-R-222.

E.B. Savage, W.A. Radasky, J.G. Kappenman, J.L. Gilbert, K.S. Smith and M.J. Madrid, "HEMP Impulse Injection Testing of Power System Electronics and Electrical Components", Prepared for the EMP Commission, December 29, 2003, Meta-R-225.

W.A. Radasky, J.G. Kappenman, E.B. Savage and J.L. Gilbert, "Metatech Recommendations to the EMP Commission", Prepared for the EMP Commission, December 31, 2003, Meta-R-226.

Gilbert J.L, W.A. Radasky, J.G. Kappenman, E.B. Savage, K.S. Smith and M.J. Madrid, "Final Report of Scenario Results Volume 2: E1 HEMP Effects", Prepared for the EMP Commission, January 16, 2004, Meta-R-227.

J.G. Kappenman, J.J. Patrick, J.L. Gilbert, E.B. Savage and W.A. Radasky, "Initial Report on Outage and Restoration Concerns for the U.S. Power Grid Due to HEMP Threats", Prepared for the EMP Commission, June 1, 2003, Meta-R-229.

J.G. Kappenman, J.J. Patrick, J.L. Gilbert, E.B. Savage and W.A. Radasky, "Interim Report on Outage and Restoration Concerns for the U.S. Power Grid Due to Late-Time HEMP Threats (Deliverable 2)", Prepared for the EMP Commission, July 15, 2003, Meta-R-230.

J.G. Kappenman, J.J. Patrick, W.A. Radasky and E.B. Savage, "Detailed Test Plan Including Ordered Equipment" Prepared for the EMP Commission, September 18, 2003, Meta-R-231.

J.G. Kappenman, J.J. Patrick, J.L. Gilbert, E.B. Savage and W.A. Radasky, "Final Outage and Restoration Results (Deliverable 3) An Overview of Major International Power System Blackouts and System Restorations", Prepared for the EMP Commission, September 8, 2003, Meta-R-232.

W.A. Radasky, "Russian Research Activities Work Plan for Research", Prepared for the EMP Commission, October 3, 2003, Meta-R-233.

E.B. Savage, J.L. Gilbert, K.S. Smith, M.J. Madrid and W.A. Radasky, "Preliminary Test Results: Fast Pulse Testing of Allen Bradley MicroLogix 1000 PLC (Programmable Logic Controller)", Prepared for the EMP Commission, October 30, 2003, Meta-R-234.

W.A. Radasky, "Russian Research Activities Preliminary Results", Prepared for the EMP Commission, January 16, 2004, Meta-R-235.

W.A. Radasky, "Russian Research Activities Summary of Washington, DC Meeting Held on 9 December 2003 at IDA", Prepared for the EMP Commission, Meta-R-236.

J.G. Kappenman, J.J. Patrick, W.A. Radasky, E.B. Savage, J.L. Gilbert, K.S. Smith and M.J. Madrid "Draft Research Report: Metatech Work for the EMP Commission", Prepared for the EMP Commission, January 30, 2004, Meta-R-237.

W.A. Radasky, J.G. Kappenman and P. Warner "Report on Evaluation of Harmonics Data from SARA Field Tests" October 1, 2006, Meta-R-271.

W.A. Radasky, "The Threat of High-Altitude Electromagnetic Pulse (HEMP) on the U.S. Power Infrastructure (Deliverable 4.2.1a) December 18, 2006, Meta-R-274.

W.A. Radasky and J.G. Kappenman, "The Threat of a 100 Year Geomagnetic Superstorm to the U.S. Power Infrastructure" 25 January 2007, Meta-R-280R2.

J.G. Kappenman, P. Warner and W.A. Radasky. "TEST REPORT: Report on Evaluation of UPS Performance, Complex Load Recommendations and Harmonic Propagation and Modeling Analysis to Support Additional SARA Field Tests" Meta-R-282, 26 March 2007, Meta-R-282.

J.G. Kappenman, P. Warner and W.A. Radasky. " TEST REPORT: Report on Task 2a Modeling Analysis to Support Additional SARA Field Tests", May 11, 2007, Meta-R-284.

F.M. Tesche, "HEMP Field Penetration into Poorly Shielded Enclosures and Coupling to Internal Conductors", June 4, 2007, Meta-R-287.

W.A. Radasky, “The Threat of Non-Nuclear EMP on the U.S. Infrastructure (Deliverable 4.3)” September 30, 2007, Meta-R-294.

J.G. Kappenman, “An Assessment of the Threat Potential to the U.S. Electric Power Grids from Extreme Space Weather Storms – Analysis of U.S. Power System Impacts from Large Geomagnetic Storm Events (Task A-C)” October 1, 2007, Meta-R-295.

J.G. Kappenman and P. Warner, “An Assessment of the Threat Potential to the U.S. Electric Power Grids from Extreme Space Weather Storms – Analysis of U.S. Power System Impacts from Large Geomagnetic Storm Events (Deliverable 4.6 – Part 1 of 3)” October 24, 2007, Meta-R-297.

J.G. Kappenman and P. Warner, “An Assessment of the Threat Potential to the U.S. Electric Power Grids from Extreme Space Weather Storms – Analysis of U.S. Power System Impacts from Large Geomagnetic Storm Events (Deliverable 4.6 – Part 2 of 3)” October 24, 2007, Meta-R-298.

J.G. Kappenman and P. Warner, “An Assessment of the Threat Potential to the U.S. Electric Power Grids from Extreme Space Weather Storms – Analysis of U.S. Power System Impacts from Large Geomagnetic Storm Events–U.S. West (Deliverable 4.6 – Part 3 of 3)” November 19, 2007, Meta-R-299.

J.G. Kappenman, P. Warner and W.A. Radasky. “Analysis of U.S. Power Grid Hardening Options Due to E3 HEMP” November 14, 2008, Meta-R-307.

W.A. Radasky, J.G. Kappenman, J.L. Gilbert and E.B. Savage, “Recommendations for the Protection of the Oahu High Voltage Power Network from High-Altitude Electromagnetic Pulse (HEMP)” July 13, 2009, Meta-R-314.

Appendix
E1 HEMP Myths

Much of the literature on HEMP is either classified or not easily accessible. Probably because of this, some of what is openly available tends to vary in accuracy – some, especially from the Internet, has major inaccuracies. Some discussions of HEMP have the right words and concepts, but do not quite have them put together right, or have inaccurate interpretations. Here we will discuss some common misunderstandings. HEMP has also appeared in some movies, and there are on-line discussions about possible errors in their depiction of HEMP. Here we will be concerned with E1 HEMP, and ignore misunderstandings about other types of EMP.

Extremists: Some general emphasis of comments fall into either "the world as we know it will come to an end" if there is a high altitude nuclear burst, or the other extreme: "it's not a big deal, nothing much will happen". Since we really have never had a nuclear burst over anything like our current modern infrastructure, no one really knows for sure what would happen, but both extremes are not very believable.

Yield: There appears to be an assumption that yield is important – it is not for E1. The assumption that E1 is an issue only for cold war type situations, but not for terrorists or rogue nations, is false. Very big bombs might have better area coverage of high fields by going to higher burst heights, but for peak fields the burst yield is only a very minor consideration.

1962 experience: Some point to the Starfish event, and the rather minor HEMP effects produced at Hawaii by it. However, there are many problems with extrapolating that experience:

1. That was about half a century ago. Since then the use of electronics has increased greatly, and the type of sensitive electronics we currently use did not really exist back then.
2. The burst was fairly far away from Hawaii, and the incident E1 HEMP was much less than worse case.
3. The island is small – if over the continental U.S., long transmission lines would be exposed (especially an issue for late-time HEMP). In addition, widely separated substations would have been exposed, although with electromechanical relays (not solid state).

Also the yield argument has been used – Starfish was a very big weapon, yet it did very little – see the previous item, yield is not really very significant.

Cars dying: Some say that all vehicles traveling will come to a halt, with all modern vehicles damaged because of their use of modern electronics (and one movie even had a bulk, non-electronic part dying). Most likely there will be some vehicles affected, but probably just a small fraction of them (although this could create traffic jams in large cities). A car does not have very long cabling to act as antennas, and there is some protection from metallic construction. As non-metallic materials are used more and more

in the future to decrease weight and increase fuel efficiency, this advantage may disappear.

Wristwatch dying: One movie critic pointed out that electronics in a helicopter were affected, but not the star's electronic watch. A watch is much too small for HEMP to affect it.

Electrons present: One critic, with some awareness of the generation process, said that HEMP could not be present unless there were also energetic electrons present. This is true when one is within the source region, which exists for all types of EMP – there are energetic electrons present. However for the HEMP, the radiation and energetic electrons are present at altitudes of 20 to 40 km, not at the ground.

Turn equipment off: There is truth to this recommendation (if there were a way to know that a burst was about to happen). Equipment is more vulnerable if it is operating, because some failure modes involving E1 HEMP trigger the system's energy to damage itself. However, damage can also happen, but not as easily, to systems that are turned off.

Maximum conductor length: There is a suggestion that equipment will be OK if all connected conductors are less than a specific length. Certainly shorter lengths are generally better, but there is no magic length value, with shorter always being better and longer not. Coupling is much too complex for such a blanket statement – instead it should be "the shorter the better, in general". (There can be exceptions, such as resonance effects, which depend on line lengths.)

Stay away from metal: There is a recommendation to be some distance away from any metal when a HEMP event occurs (assuming there was warning), because very high voltages could be generated. Metal can collect E1 HEMP energy, and easily generate high voltages. However, the "skin effect" (a term not really derived from the skin of humans or any other animal) means that if a human were touching a large "antenna" during an E1 HEMP event, any current flow would not penetrate into the body. Generally E1 HEMP is considered harmless for human bodies.